

**UNIVERSIDADE FEDERAL DE MINAS GERAIS**  
**Instituto de Ciências Biológicas**  
**Programa de Pós-graduação em Parasitologia**

Sérvio Pontes Ribeiro

**Ecologia do Adoecimento Aplicada às Interações Parasitárias**

Belo Horizonte  
2023

Sérvio Pontes Ribeiro

## **Ecologia do Adoecimento Aplicada às Interações Parasitárias**

Tese apresentada ao Programa de Pós-graduação em Parasitologia da Universidade Federal de Minas Gerais como requisito parcial para obtenção do título de Doutor em Parasitologia

Orientador: Nelder de Figueiredo Gontijo

Co-orientadores: Marcos Horácio Pereira  
Alexandre Barbosa Reis

Belo Horizonte

2023

043

Ribeiro, Sérgio Pontes.

Ecologia do adoecimento aplicada às interações parasitárias [manuscrito] / Sérgio Pontes Ribeiro. – 2023.

153 f. : il. ; 29,5 cm.

Orientador: Nelder de Figueiredo Gontijo. Co-orientadores: Marcos Horácio Pereira; Alexandre Barbosa Reis.

Tese (doutorado) – Universidade Federal de Minas Gerais, Instituto de Ciências Biológicas. Programa de Pós-Graduação em Parasitologia.

1. Parasitologia. 2. Pandemia. 3. Leishmaniose Visceral. 4. Insetos Vetores. 5. Vírus da SARS. 6. Psychodidae. I. Gontijo, Nelder de Figueiredo. II. Pereira, Marcos Horácio. III. Reis, Alexandre Barbosa. IV. Universidade Federal de Minas Gerais. Instituto de Ciências Biológicas. V. Título.

CDU: 576.88/.89



UNIVERSIDADE FEDERAL DE MINAS GERAIS  
INSTITUTO DE CIÊNCIAS BIOLÓGICAS  
PROGRAMA DE PÓS-GRADUAÇÃO EM PARASITOLOGIA

**FOLHA DE APROVAÇÃO**

**TESE 346/2023/09 - DEFESA DIRETA**

**TÍTULO DA TESE:** " ECOLOGIA DO ADOECIMENTO APLICADA ÀS INTERAÇÕES PARASITÁRIAS"

**ALUNO:** SÉRVIO PONTES RIBEIRO

ÁREA DE CONCENTRAÇÃO: ENTOMOLOGIA

Tese de Doutorado defendida e aprovada, no dia **vinte e quatro de agosto de 2023**, pela Banca Examinadora designada pelo Colegiado do Programa de Pós-Graduação Parasitologia da Universidade Federal de Minas Gerais constituída pelos seguintes Doutores:

**Álvaro Gil Araújo Ferreira**

Membro externo - IRR/FIOCRUZ

**Carlos Eduardo de Viveiros Grelle**

Membro externo - UFRJ

**Márcia Chame dos Santos**

Membro interno - IOC/FIOCRUZ

**Reginaldo Peçanha Brazil**

Membro interno - IOC/FIOCRUZ

**Alexandre Barbosa Reis**

Coorientador - UFOP

**Nelder de Figueiredo Gontijo**

Orientador - UFMG

Belo Horizonte, 24 de agosto de 2023.



Documento assinado eletronicamente por **Nelder de Figueiredo Gontijo**, Professor do Magistério Superior, em 30/08/2023, às 15:23, conforme horário oficial de Brasília, com fundamento no art. 5º do [Decreto nº 10.543, de 13 de novembro de 2020](#).



Documento assinado eletronicamente por **Márcia Chame dos Santos**, Usuário Externo, em 01/09/2023, às 13:49, conforme horário oficial de Brasília, com fundamento no art. 5º do [Decreto nº 10.543, de 13 de novembro de 2020](#).



Documento assinado eletronicamente por **Alexandre Barbosa Reis**, Usuário Externo, em 03/09/2023, às 07:28, conforme horário oficial de Brasília, com fundamento no art. 5º do [Decreto nº 10.543, de 13 de novembro de 2020](#).



Documento assinado eletronicamente por **Reginaldo Peçanha Brazil**, Usuário Externo, em 13/09/2023, às 17:55, conforme horário oficial de Brasília, com fundamento no art. 5º do [Decreto nº 10.543, de 13 de novembro de 2020](#).



Documento assinado eletronicamente por **Alvaro Gil Araujo Ferreira**, Usuário Externo, em 14/09/2023, às 09:56, conforme horário oficial de Brasília, com fundamento no art. 5º do [Decreto nº 10.543, de 13 de novembro de 2020](#).



Documento assinado eletronicamente por **Carlos Eduardo Viveiros Grelle**, Usuário Externo, em 25/09/2023, às 13:37, conforme horário oficial de Brasília, com fundamento no art. 5º do [Decreto nº 10.543, de 13 de novembro de 2020](#).



A autenticidade deste documento pode ser conferida no site [https://sei.ufmg.br/sei/controlador\\_externo.php?acao=documento\\_conferir&id\\_orgao\\_acesso\\_externo=0](https://sei.ufmg.br/sei/controlador_externo.php?acao=documento_conferir&id_orgao_acesso_externo=0), informando o código verificador **2519686** e o código CRC **DBA494EC**.

Dedico essa Tese a todos os descendentes dos povos Tupi-Guarani, em especial os mantenedores de sua cultura, ciência e Terras. Terras essas suas há pelo menos 4.000 anos, e toda transformação que eles, docemente, nelas impuseram

## AGRADECIMENTOS

Academicamente,

Agradeço a todos meus orientadores de minha jornada científica, desde o Hécio Pimenta na graduação (Biologia-UFMG), Geraldo W. Fernandes no mestrado (ECMVS-UFMG), Valerie K. Brown e William Hamilton no primeiro doutorado (Ecology-Imperial College), e agora, Nelder F. Gontijo, Marcos H. Pereira e Alexandre B. Reis nesse doutorado. Em especial, a Nelder, que se tornou um amigo sem deixar de ser orientador, e o mais cuidadoso e atencioso dos orientadores. Um parceiro que tem em si o que eu vim buscar ao fazer um segundo doutorado: o retorno à real ciência, à paixão por perguntas profundas em Biologia, a prioridade máxima e inegociável de ser cientista.

Também a todos que de certa forma me levaram a descer das árvores onde contava insetos herbívoros e herbivoria, para estudar ecologia de doenças parasitárias humanas. Primeiro e de novo, Bill Hamilton, que me fascinou com a profundidade de sua teoria sobre a evolução de sexo como resposta à pressão seletiva causada por doenças, e sua leitura brilhante e inspiradora na interface das sociedades, Sociobiologia, e o Ultradarwinismo, do qual ele é o principal pilar. Meu colega André Talvani que um dia me leva a Michelle Pedrosa com sua vontade de estudar *Aedes* nas matas de Ouro Preto, e anos depois, me indicou a uma repórter da BBC para que eu falasse sobre a epidemia de febre amarela no médio Rio Doce e sua possível relação com o desastre da Samarco, evento que acordou vários interesses em mim. Aos “formigões” Frederico Neves, Wesley Dáttilo e Ricardo Solar, que em discussões leves me levaram a indagar sobre o papel da pimenta no controle das epidemias de Salmonela na América conquistada, uma discussão e posterior leitura que levou à paixão pelas pandemias. Aos meus colegas Alexandre Reis e Wendel C. Vital, que me trouxeram para o fascinante sistema da Leishmaniose Visceral e do Ecohealth, pela confiança e tantas cartas brancas nesse processo! E Geraldinho, que sempre deixou claro que as barreiras entre áreas do conhecimento são fictícias. Aos grandes parceiros de antes, durante e sempre desde a pandemia, Alcides V Silva, Wesley Dáttilo, Aristoteles Góes-Neto, Debmalya Bart, Luiz Alcântara, e em destaque, meu grande amigo Vasco A. C. Azevedo. Em Governador Valadares, também em grande destaque, minha parceria com Hernani. C Santana, e de forma especial e com muito carinho, minha amiga Renata B. Campos, pela criação do LEAS, Laboratório de Ecologia do Adoecimento e Saúde dos Territórios, na UNIVALE. E à toda a administração daquela universidade.

Aos meus colegas de pós do LFIH, Laboratório de Fisiologia de Insetos Hematófagos, que a todos agradeço o tempo de alegria e coleguismo na UFMG, em especial ao Luccas Malta.

Aos professores parceiros desse laboratório e seu imprescindível e tão dedicado técnico, César Nonato.

Aos membros da banca, pelo seu tempo e contribuições, Reginaldo P. Brazil, Márcia Chame, Carlos Eduardo V. Grelle, José Dilermando A. Filho, Álvaro Ferreira, Daniela Bartholomeu. À coordenação e ao Colegiado da PPG em Parasitologia da UFMG. À Administração da UFOP, em especial às Diretoras do ICEB, Roberta Froes, Patrícia Abreu, ao chefe do DEBIO, Fábio Augusto R. Silva, e à coordenadora do NUPEB, Isabela N. de Almeida, e todas as Pró-Reitorias Adjuntas e secretários (que cumprimento no nome do Rubens G. Modesto) que sempre me salvaram no mundo cruel da burocracia!

Claro, e de enorme importância, mas sem citar um nome para não resultar em injustiças, a todos os meus orientandos do LEAF, Laboratório de Ecologia do Adoecimento e Florestas, em especial alguns: 1) aqueles que orientei nesse período sabático, que muito sofreram com minha ausência; 2) às mulheres, 60% da força de trabalho do lab ao longo de toda minha carreira, sempre as mais dedicadas, cuidadosas e nem sempre as mais valorizadas; 2) independente de sexo, aos pretos, pardos e de famílias humildes, que sempre foram os mais dedicados, os mais urgentes com a qualidade e seu desenvolvimento, e os mais brilhantes desde sua entrada no laboratório. Obrigado em especial pela confiança que depositaram em mim para contribuir com uma transformação em suas vidas pela ciência.

Na esfera pessoal,

Aos meus pais e meus irmãos, meu primeiro lar, que sempre me levou a buscar descobrir.

Às minhas filhas, Laura Maria Marques Pontes Ribeiro e Gabriela Maria Marques Pontes ribeiro (em ordem etária), pelas alegrias sem fim, pela vontade que me dão de salvar o mundo para elas viverem bem, seguras e felizes, pelos momentos mais felizes de minha vida, pelo amor que sempre fizeram brotar de meu coração, pela forma como amaciam esse velho mal-humorado.

E à minha mulher, meu amor, companheira, defensora sem limites, apoiadora em tudo, Cassiana Severiano de Sousa. Pela forma com que me olha, com que me acolhe, com que me empurra, pelo Yoga que me traz, o amor que faz, a paz que me causou. Por tudo que ainda vamos viver, e pelo que me ajudou a conseguir viver. Meu eterno e sem palavras, amor.

*The History of an Obsession, and the Obsession is Evolution*  
*William D. Hamilton 2001*



## RESUMO

A primeira parte desta Tese tratou de doenças evoluídas em associação com humanos e apresenta ecossistemas humanos degradados, com foco na pandemia de dengue e *Aedes aegypti*. Concluimos discutindo uma série de artigos de nosso grupo, nos quais modelamos a pandemia de SARS-CoV-2. O efeito dos ambientes humanos sobre o *Aedes aegypti* nas fronteiras de sua distribuição climática e ecológica - Descrevemos o efeito de resíduos de metais pesados na distribuição de insetos, com foco em uma mata ciliar altamente contaminada em uma cidade no meio do vale. Além disso, discutimos a já documentada invasão de *Ae. aegypti* para os municípios montanhosos desta bacia hidrográfica, em resposta ao aumento da temperatura ao longo das últimas décadas.

A segunda parte desta Tese investiga um cenário evolutivo hipotético para *Lutzomyia longipalpis* e leishmaniose visceral: adaptação de *L. longipalpis* à matéria orgânica rica em ferro como um mecanismo ecológico para uma interação especializada com ambientes antigos modificados pelo homem. O homem do Holoceno e espécies de canídeos oportunistas ou devidamente domesticados, produziram grandes quantidades de matéria orgânica previsível, desde que os humanos se estabeleceram em locais permanentes. Fezes de canídeos, carcaças de presas em decomposição, cadáveres e restos de comida compõem montes e descartes laterais em assentamentos humanos do Holoceno. Propomos uma hipótese sobre como o nicho de *L. longipalpis* evoluiu em torno de recursos produzidos pelo homem, e como isso pode ser uma pré-adaptação a ambientes urbanos degradados.

A terceira parte desta Tese é composta por uma série de artigos já publicados, nos quais aplicamos princípios ecológicos para explorar a pandemia de SARS-CoV-2 e outros riscos do coronavírus. Nesta série de artigos sobre ecoepidemiologia da pandemia, primeiro investigamos quais eram as condições ecológicas nos locais onde foram encontradas todas as espécies de Orthocoronavirinae depositadas no GenBank (Ribeiro et al. 2022). Com relação à dinâmica da pandemia, exploramos a disseminação do vírus no mundo (Ribeiro et al. 2020a) e no Brasil (Ribeiro et al. 2020b), com base na teoria ecológica neutra e modelos algébricos (SIR – Susceptíveis-Infetados-Recuperados + metapopulacionais) e estatísticos. Por fim, exploramos a transmissão comunitária, com foco especial na cidade de Manaus (Ribeiro et al. 2021; Silva et al. 2022).

Palavras-chave: Leishmaniose visceral, Ecologia de doenças, Insetos vetores, *Lutzomyia longipalpis*, canídeos, SARS-CoV-2, pandemia

# EVOLUTIONARY ECOLOGY OF HOST-PARASITE INTERACTIONS APPLIED TO HUMAN-EVOLVED DISEASES

## ABSTRACT

The first part of this Thesis dealt with human-evolved diseases and present degrading human ecosystems, exploring overall scenarios, and the case of dengue pandemic and *Aedes aegypti*. We explore the patterns of disease outbreaks and further dissemination to the level of pandemic events. We conclude discussing a series of articles from our group, in which we modelled the SARS-CoV-2 pandemic. The effect of human environments on *Aedes aegypti* in the borders of its climatic and ecological distribution - We describe the effect of heavy metal residuals in the insect distribution, focusing on a highly contaminated riparian forest in a mid-valley city. Also, we discuss the already documented invasion of *Ae. aegypti* into the montane towns in this river basin, in response to temperature increase along the last decades. The second part of this Thesis investigate a hypothetical evolutionary scenario for *Lutzomyia longipalpis* and visceral leishmaniasis. Ancient humans along with opportunistic, or properly domesticated, canid species, have produced large amounts of predictable organic matters, since humans settled in permanent locations. Canid feces, prey decaying carcasses, corpses and food remaining compose mounds and side disposals in human settlements from early and late Holocene. In central South America, the early Holocene settlements were around caves and the coast and the late, after Tupi-Guarani migrations, also in savanna wetlands, intensively managed. All these ecosystems are present-days habitats of *L. longipalpis*. We propose a hypothesis on how the *L. longipalpis* niche evolved around resources produced by humans, and how this might be a pre-adaptation to degraded urban environments.

The third part of this Thesis is composed of a series of already published articles, in which we applied ecological principles to explore the SARS-CoV-2 pandemic and other coronavirus risks. In this series of articles on eco-epidemiology of the pandemic, we first investigated what where the ecological conditions in places where all Orthocoronavirinae species deposited in the GenBank were found (Ribeiro et al. 2022). Concerning the pandemic dynamic, we explored the virus dissemination worldwide (Ribeiro et al. 2020a) and inside Brazil (Ribeiro et al. 2020b) based on neutral ecological theory and algebraic (SIR – Susceptible-Infected-Recovered + metapopulation models) and statistical models. Finally, we explored the community transmission, with a special focus on Manaus city (Ribeiro et al. 2021; Silva et al. 2022).

Key-words: Visceral leishmaniasis, Disease Ecology, Insect Vectors, *Lutzomyia longipalpis*, canids, SARS-CoV-2, pandemic

## SUMÁRIO

<b>1 INTRODUCTION .....</b>	<b>16</b>
<b>1.1 From the selective pressure from parasitism to the evolution of human diseases into a fast-changing world .....</b>	<b>16</b>
<b>1.2 Human-evolved diseases .....</b>	<b>17</b>
<b>2 PART 1 – HUMAN-EVOLVED DISEASES AND THE DENGUE PANDEMIC .....</b>	<b>20</b>
<b>2.1 Emergence of new parasitic diseases or increasing human pathogen outbreaks? Anthropomorphic ecosystems and population growth to be blamed. ....</b>	<b>20</b>
<b>2.2 Dengue pandemic and <i>Aedes aegypti</i>: how the speciation around home water reservoirs in the Holocene became a pre-adaptation to a worldwide polluted and warm planet .....</b>	<b>26</b>
<b>2.3 References .....</b>	<b>29</b>
<b>3 PART 2 - ADAPTATIONS OF <i>Lutzomyia longipalpis</i> TO NATIVE CANID DENS AND BLOOD-RICH ORGANIC MATTERS: A SOUTH AMERICAN INDIGENOUS MEN-FOX-SANDFLY NICHE INVADED POSTERIORLY BY <i>Leishmania infantum</i>? .....</b>	<b>35</b>
<b>3.1 Preface .....</b>	<b>35</b>
<b>3.2 Evolutionary Ecology of <i>Lutzomyia longipalpis</i>: from Human and Canid-Inhabited Caves to Primary Vector of <i>Leishmania infantum</i> in South America.....</b>	<b>37</b>
3.2.1 <i>Abstract</i> .....	37
3.2.2 <i>Introduction</i> .....	38
3.2.3 <i>Methodology</i> .....	43
3.2.3.1 <i>Experimental designs</i> .....	44
3.2.3.1.1 <i>Female oviposition choices</i> .....	44
3.2.3.1.2 <i>Oviposition group behaviour: avoidance of fungi hyphae entanglement or collective choice of suitable sites?</i> .....	46
3.2.3.1.3 <i>Larval survival analysis and substrate choices</i> .....	48
A) <i>1<sup>st</sup> Experiment - Hatching and first instar choice of substrate and survival</i> .....	48
B) <i>2<sup>nd</sup> Experiment - Last instars survival and pupae in contrasting substrates</i> .....	49
3.2.3.2 <i>Ferritin phylogeny and differentiation among Diptera</i>	

<i>specie</i> .....	49
3.2.3.3 <i>Biogeographic overlap between Holocene humans, L. longipalpis, foxes and cave-rich ecosystems</i> .....	51
3.2.4 <i>Results</i> .....	53
3.2.4.1 <i>Experimental designs</i> .....	53
3.2.4.1.1 <i>Female oviposition choices</i> .....	53
3.2.4.1.2 <i>Oviposition group behaviour: avoidance of fungi hyphae entanglement or collective choice of suitable sites?</i> .....	55
3.2.4.1.3 <i>Larval survival analysis and substrate choices</i> .....	56
A) <i>1<sup>st</sup> Experiment - Hatching and first instar choice of substrate and survival</i> .....	56
B) <i>2<sup>nd</sup> Experiment - Last instars survival and pupae in contrasting substrates</i> .....	57
3.2.4.2 <i>Ferritin phylogeny and differentiation among Diptera species</i> .....	57
3.2.4.3 <i>Biogeographic overlap of Holocene humans, Lutzomyia longipalpis and foxes distribution to cave-rich ecosystems</i> .....	62
3.2.5 <i>Discussion</i> .....	65
3.2.5.1 <i>Wetlands with late Holocene indigenous' mounds as new habitat for foxes- L. longipalpis: revisiting the classical Lainson 's hypothesis on AVL evolution from foxes to dogs</i> .....	68
3.2.5.2 <i>The adaptation of L. longipalpis to a long extinct fox-human habitat in caves as a pre-condition to invade modern suburbs and habitats exposed to swage and dog waste</i> .....	70
3.2.5.3 <i>Was human-foxes-L. longipalpis interaction system a vacant niche for a European introduced Leishmania infantum?</i> .....	72
3.2.6 <i>Conclusions</i> .....	72
3.2.7 <i>References</i> .....	73

<b>4 PART 3 - THE SARS-COV-2 PANDEMIC: MOST FAVOURABLE ENVIRONMENT FOR ORTHOCORONAVIRINAE SPILLOVERS AND ECOLOGICAL MECHANISMS BEHIND DISSEMINATION</b> .....	<b>83</b>
<b>4.1 Preface</b> .....	<b>83</b>
<b>4.2 Long-term unsustainable patterns of development rather than recent deforestation caused the emergence of Ortochoronavirinae species</b> .....	<b>86</b>

<b>4.3 Severe airport sanitarian control could slow down the spreading of COVID-19 pandemics in Brazil .....</b>	<b>97</b>
<b>4.4 Worldwide COVID-19 spreading explained: traveling numbers as primary driver for pandemic .....</b>	<b>113</b>
<b>4.5 From Spanish Flu to Syndemic COVID-19: longstanding sanitarian vulnerability of Manaus, warnings from the Brazilian rainforest gateway .....</b>	<b>123</b>
<b>4.6 Succesive Pandemic Waves with Different Virulent Strains and Effects of Vaccination for SARS-CoV-2 .....</b>	<b>137</b>
<b>5 CONCLUSION .....</b>	<b>153</b>

## 1 INTRODUCTION

Concerning the Thesis structure, this Introduction intent to organize a rationale which defines the main theme of this work, and the cohesion of such a vast range of subjects within Host-Parasite theory. After, the Thesis is organized in three Parts. The Part 1 deepen up the evolutionary ecology of human-adapted diseases, exploring recent changes in epidemiological worldwide scenarios for infectious diseases outbreaks. The Part 2 investigates the adaptation of *Lutzomyia longipalpis* (vector of *Leishmania infantum*, cause of Visceral Leishmaniasis) to metal-rich organic matter as an evolutionary adaptation to human-canids environments. Finally, the Part 3 is composed of a series of already published articles, in which we applied ecological principles to explore the SARS-CoV-2 pandemic and other coronavirus emergent risks, and a General Conclusions.

### 1.1 From the selective pressure of parasitism to the evolution of human diseases into a fast-changing world

Parasites, as any infectious pathogens, cause a selective pressure onto the host population, depending on density and frequency of susceptible genotypes, which is known as soft-selection (Hamilton 1988; 1990). An immediate consequence of the soft-selection at the host population level is an increasing genetic variability, as the dominant genotypes become a favourable niche for those parasites better fit to infect them, due to, among other things, the chances of encounter and infection (Silva et al. 2022). In other words, abundant and similar individuals become better recognizable as host than rare genotypes, decreasing gradually the frequency of those dominant and increasing those which are rare, causing genetic variability (Hamilton 1988; 1990). Such selective pressure may be so powerful that is considered an evolutionary driver for the quasi-universal strategy of sexual reproduction. Sex is the most effective mechanism to produce intrapopulation genetic variability, thus, likely to cope with the much faster life cycle and evolutionary rates of parasites (Hamilton 1988; 1990).

Genetically homogenous populations may only prevail in habitats or abiotic conditions that prevent the accumulation of parasites and so compensate the pressure on a few dominant host genotypes. Climatic unpredictability may produce such scenario for long living organisms, as trees, since the unpredictable conditions are less favourable for the insect herbivores and not for the host tree, as Ribeiro & Brown (1999; 2006) showed for *Tabebuia aurea* (Bignoniaceae) in the Brazilian Pantanal. Without strong herbivory, even in the tropics, the

predominant selective pressure on this tree species was to grow faster and overcome the extreme flooding events, recurrent at unexpected time interval of one to two decades (Ribeiro & Brown 2002). Hence, a selection for fast growth, without enough herbivory to produce soft-selection, resulted in a genetically homogenous and very large tree population, consisting of one of the largest and most stable tree monodominant stand in the tropics (Ribeiro & Brown 2006).

The strict causal relation of diseases, density and genetic frequency of rare genotypes, as postulated by Hamilton (1990), was rarely applied to human populations, and hardly was investigated beyond classic evolutionary literature (but see Low 1994). Still, the conditions demonstrated mathematically by Bill Hamilton in his late works, and confirmed for tropical tree species by Ribeiro and Brown, suggest that several human civilization collapses could be explained by the way we evolved and how our behaviour and population densities favoured some particular diseases. Our behavioural tendency to aggregate is well described (Zuckerman et al. 2013) and may have roots in the advantages of surviving predation, cold and starvation. However, such advantages might disappear in front of the accumulation of pathogens well adapted to our populations, or to the spillover of zoonotic and highly virulent emergent pathogens. The demise of most of human populations in the Holocene are still not fully understood, and parasites and diseases start to be investigated as likely causes, but by very few researchers (Saldanha et al. 2022).

Concerning human parasites, the adaptation for the most predictable, dominant genotypes must have been boosted by some level of sedentarism, since the Holocene. First, the occupation of caves in several parts of the world, due to climatic unpredictability, must have improved the ecological conditions for respiratory diseases to thrive, based on droplets and direct contact. These inside-dwelling contagious is still important among civilized societies now-a-days, and results in the so-called “crowd diseases” (Lewis Jr. et al. 2023). Further, with the improvement of agricultural skills and animal domestication, zoonotic diseases might have found the most beneficial opportunities to spillover to humans inside our settlements (Talavaara et al. 2018; Lewis Jr. et al. 2023).

## **1.2 Human-evolved diseases**

Loss of food diversity adds to crowd diseases a components of host prediction and stress, namely, more susceptibility due to low quality nutrition (Zuckrman et al. 2013 and Lewis Jr. et al. 2023). It is discussed that such conditions could have dominated several populations in the late Holocene, related to agriculture and increasing human group sizes along with

sedentarisation (O'Hagan et al. 2019; Silva et al. 2021). A likely similar scenario may still be a reality in modern suburb communities experiencing poverty, added to some environmental novel deteriorating traits, as drug resistance and habitat pollution and intoxication. Hence, human-degraded environments, caused by agriculture and crowding settlements, shaped our very existence in this planet from quite a long time ago. Such conditions evolved worldwide in late Holocene and made us vulnerable to diseases. Still, that was a worthy trade-off in front of a safer live, less vulnerable to predation or other tribe/human enemies, or climatic unpredictability and periods of starvation.

In any case, the human-modified environments become ideal for those few parasites and pathogens species adapted to us as hosts. Actually, human-adapted pathogens compose a small proportion of pathogens in an ecological community. Dunn et al. (2010) demonstrated that from any pathogen community worldwide (mostly sylvatic and zoonotic pathogens of birds and mammals), a much lower species proportion become prevalent among humans, even where the highest pathogen diversity occurs, which is caused by the richness of mammals and bird species. Nevertheless, Keesing & Ostfeld (2021) emphasises how biodiversity loss may boost zoonotic diseases spillovers, as those pathogens capable to infect humans are more likely to be found among ruderal animals, thus capable to cope with polluted and simplified human habitats.

Talavaara et al. (2018) made clear as pathogen stress have a strong regulation effect on hunter-gatherer human populations. Pathogen stress causes a threshold in the benefits of increasing biodiversity and net productivity on tribe sizes. Thus, from a certain degree of ecosystem productivity on, there might be more diseases than food surplus. By looking at the most common human pathogens, Cashdan (2014) showed clear biogeographic diversity and prevalence distribution patterns, in response to classical ecological factors (latitude, altitude, seasonality and humidity). Still, no more than seven human pathogens were considered relevant for this pattern. Fincher et al. (2008) defines a relevant prevalence of only nine pathogen guilds which are detrimental to human reproductive fitness: leishmanias, trypanosomes, malaria, schistosomes, filariae, leprosy, dengue, typhus and tuberculosis, considering the 93 geopolitical regions worldwide, and this is also accepted by WHO. Karesh et al (2012) presented a broader list including the most relevant emergent zoonoses species and guilds, but these reach only 14 groups. To note, these so called "disease groups" combine individual species with classical ecological guilds, i.e., group of species using similar resources or of similar taxonomic origin, thus defining a similar ecological role (for instance, all type A influenzas or all cutaneous leishmaniases, are guilds of a groups of similar species), but rarely the term "guild" is applied in Parasitology.



From an evolutionary perspective, it is a bit of a paradox why only few pathogen species or guilds are capable of causing human population disruption, being humans the most widespread and habitat modifier species in the Planet. Whatever is the reason for this limited number of pathogen guild outbreaks along the history of civilization, and despite the progress in medicine, this number might be actually increasing in the recent times. The ecological crisis resulted from demographic explosion and global warming could be facilitating new pathogens and parasites to get definitively incorporated into our lives as endemic diseases. Besides causing better conditions for crowd diseases, the sedentary human habits that resulted in habitat simplification and degradation have an immense positive effect on insect vectors of diseases, especially for those arthropod species long adapted to us and our civilizations.

## **2 PART 1 – HUMAN-EVOLVED DISEASES AND THE DENGUE PANDEMIC**

### **2.1 Emergence of new parasitic diseases or increasing human pathogen outbreaks? Anthropomorphic ecosystems and population growth to be blamed.**

Humanity is affected by two very distinct group of diseases: emergent zoonotic infections, that spillover to humans in contact with a new pathogen originated from another animal species; human-evolved diseases, that remerge in different societies worldwide, due to human migration and other ecological dissemination processes. Both may result in outbreaks and epidemics time to time. However, to distinguish between these groups is not always straightforward, due to lack of data on disease origins, or on eco-epidemiological dynamics. Some of these human diseases, as the Plague, caused by *Yersinia pestis*, now are known to relates to us much earlier than the first record plague pandemic (Justinian plague, 541-549 AD). Based on next-generation sequencing methods applied to ancient teeth DNA, Rasmussen et al. (2015) were able to date these bacteria as endemic to humans in Eurasia from 3,000 years before a first historical record of the plague disease, and it might have passed directly from people to people, before been transmitted by flees.

Although a quite large number of pathogens might have evolved to infect exclusively humans, or to survive around us in our modified, anthropomorphic environments, only a few species were capable to produce substantial outbreaks in human populations. Along with those, new emergent pathogens, due to badly evolutionary adjustments, have increased the number of detectable infectious disease outbreaks in humankind. New pathogens may take two likely epidemiological paths: 1) to be excessively virulent, cutting down transmission and dying out as a parasite of concern in a few generations; 2) to spread out quickly and undetectable due to a large amount of tolerant, thus asymptomatic, individual hosts. In the latter, a parasitic pathogen causes a substantial number of deadly infections on more vulnerable individuals, causing a detectable outbreak with populational consequences (May & Anderson 1983; Volpato et al. 2020). Even though emergent diseases tend to evolve gradually towards decreasing virulence (May & Anderson 1983; Silva et al. 2022), before that, they tend to result in dramatic pandemic events, as the H1N1 in 1918 (Spanish Flu) or now, the SARS-CoV-2 in 2019 (Ribeiro et al. 2021; Silva et al. 2022).

Nevertheless, only recently, due to next-generation sequencing and all progress in molecular surveillance and phylogenetic studies, one may properly separate new from recurrent pandemics, sensu zoonotic spillover versus human-evolved diseases. It is crucial for mankind

to better explore the causes of each outbreak origin, as well the likelihood of becoming a new pandemic. It must be a key aspect to separate two key ecological niches for pathogens. First, those causing silent human infections, that constantly transmit to humans with no detectable consequences. Some pathogens might be likely endemic in regions where local communities evolved resistance to them, but suddenly spread towards outsiders and cause a more severe outbreak. This is a situation that should concern governments of regions under ecotourism management, in especial caves, as in Vietnam, for instance. Second, actual new diseases that are indeed getting in contact with humans for the first time, and rapidly become a public health problem by effective pathogen invasive capability. Curiously, by 2012, new detected zoonoses were mostly emerging diseases identified in the previous 70 years, but were consider rare, of no populational relevance, as they were well-known endemic zoonoses (Karesh et al. 2012). One of the challenges in designing a global preventive scenario may lay in our inability to early detect what is the ecological igniting cause behind a pandemic progressing from a punctual pathogen emergence.

The general wisdom in the literature relates new emergence of diseases of relevance with environmental destruction (Murray et al. 2015; Nava et al. 2017), climatic unpredictability, global warming (Carlson et al. 2020; OHHLEP 2022) and human exposition to habitat disturbances. Concerning the latter, a strong perception that human presence in environments under severe transformation (deforestation frontiers, for instance) may expose us to new emergent diseases, came from a few striking examples. A very famous case is the Nipah virus spilling over to domestic pigs after fruit bats seek refuge in orchards, escaping from a deforestation in Asia. That event resulted in more than 100 people killed and thousands of pigs sacrificed, in 1998 (Pulliam et al. 2012). Likewise, hunting wild animals for consumption was a clear origin of several foodborne diseases (Karesh et al. 2012; Ribeiro et al. 2022), among them, HIV is the most famous one (Sharp & Hahn 2011).

Nevertheless, these scenarios of catastrophic destructions are not necessarily the only source of risks. For instance, Ribeiro et al. (2022) demonstrated the existence of a greater chance to find a new Orthocoronavirinae in old human-modified environments, as largely transformed urban landscapes, as found in the Southeast Chinese and American coasts, where continuous urbanized ecosystem extent for miles, and relate to densely occupied human populations, elevated CO<sub>2</sub> emissions, and consumerism that can boost animal trafficking. Hence, new coronavirus might appear in our anthropomorphic ecosystems more likely than spilling over from animals in some wilderness we are destroying! Remaining of native, however

heavily impacted, natural ecosystems could be a source of several diseases which exists among us for decades, close to old cities and farmlands.

The key aspect is whether such pathogens will become a public health problem, due to its ecological capability to overcome populational immune responses and thus cause outbreaks or epidemics of concern. Beyond the argument of better tools for pathogen identification, the diversity of diseases causing detectable outbreaks of public relevance has increased substantially, from early XIX to late XX Century (Figure 1). This trend refrained just after SARS-CoV-2 pandemic, eventually due to the measures to contain this virus, that might have decelerated the spread of other infectious diseases as well.

We explored the progression of outbreaks of national relevance worldwide, recording events large enough to be listed in global database, public health surveillance sources or even in non-scientific news (Table 1). We recorded outbreaks of relevance from 1800 to the present times (organized per decades), and tested the occurrence of such events against CO2 emissions (<https://github.com/owid/co2-data>), and worldwide population size (<https://www.statista.com/statistics/997040/world-population-by-continent-1950-2020/>). As it is usual to have pandemic events related to worldwide wars (movement of soldiers can be a driver of infection dissemination from places already under humanitarian crisis – Barry 2004), we also tested the number of cross-nations conflicts along this same period, summed up from three global databases (Table 1). We tested using a multiple regression analysis with Poisson distribution logit, and model selection by AIC, in R v. 4.2.3.

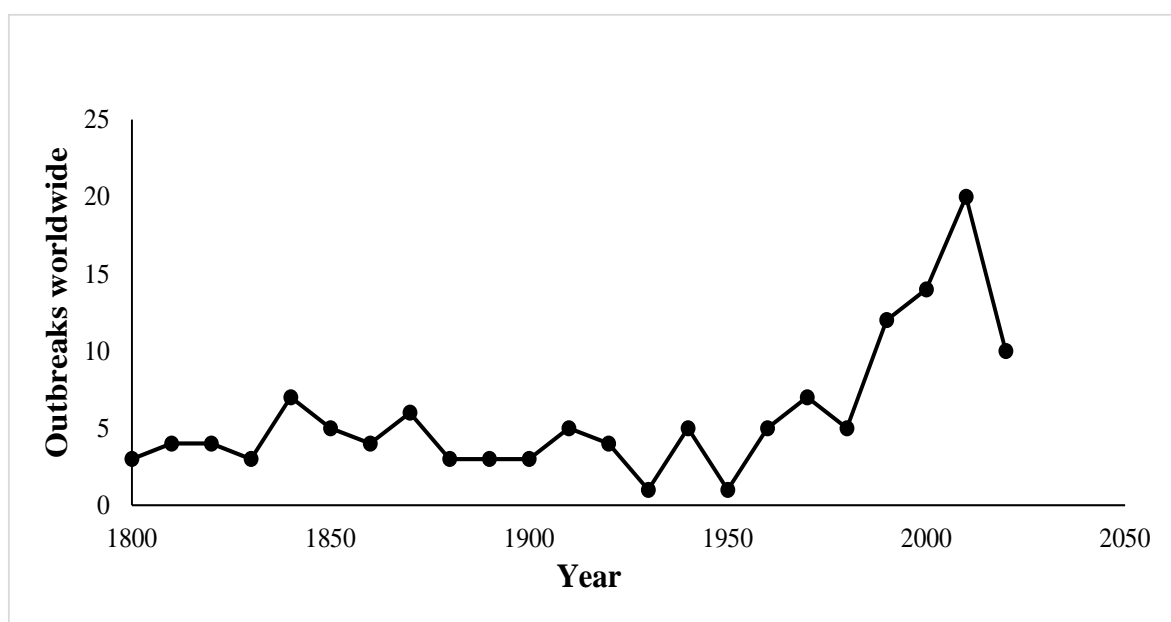


Figure 1 - Number of outbreaks from 1800 to 2020, Worldwide. Each outbreak is a detectable event at populational consequences, somewhere in the Planet.

Along the 22 decades from 1800 to 2020, 48 different diseases caused some sort of disruptive outbreaks in humanity, among classical human diseases and emergent zoonotic diseases recently spilled over to us (Table 2). In the XIX Century, only 13 pathogens caused detectable outbreaks, but most were recurrent, as typhus, plague, cholera, yellow fever and smallpox. In the XX Century, 19 new emergent diseases added up, and 16 new ones only in the first two decades of the XXI Century (eight new pathogens per decade against 1.9 in the previous Century). This is a substantial increase in diversity, even though there might have some underestimation in number of pathogens from XIX and early XX Centuries. For instance, several different bacteria species that may cause dysentery and virus species causing flu are unlikely to be properly identified from that time. Even though, and most importantly, not just the number of new pathogen species are raising, but the number of outbreaks per decade as well.

Table 1 – Accessed database for explanatory factors.

Wars	<a href="https://ourworldindata.org/grapher/deaths-in-conflicts-by-source?time=1945..1989">https://ourworldindata.org/grapher/deaths-in-conflicts-by-source?time=1945..1989</a> <a href="https://www.iwm.org.uk/history/timeline-of-20th-and-21st-century-wars">https://www.iwm.org.uk/history/timeline-of-20th-and-21st-century-wars</a> <a href="https://en.wikipedia.org/wiki/List_of_wars:_1800%E2%80%931899">https://en.wikipedia.org/wiki/List_of_wars:_1800%E2%80%931899</a>
pandemic	<a href="https://www.oecd.org/futures/globalprospects/37944611.pdf">https://www.oecd.org/futures/globalprospects/37944611.pdf</a> <a href="https://www.statista.com/">https://www.statista.com/</a>
CO2	<a href="https://github.com/owid/co2-data">https://github.com/owid/co2-data</a>

Our analysis showed that the number of outbreaks were explained by population growth and interaction between population and number of conflicts per decades (Figure 2). Increase in CO2 emissions was highly correlated to increase in population size at a Planetary scale (0.996), and then was used as a proxy to population+emissions effect. Thus, Population/emissions was determinant of 34% of variance in data, showing a significant and positive effect on the number of outbreaks ( $p < 0.0001$ ). The number of conflicts worldwide during the first 30 years of the XX Century were immense, thus resulting in a negative effect of number of conflicts on the number of outbreaks, but depending on population size (significant factors interaction: deviance = 5.3,  $p < 0.02$ ). Hence, less conflicts were associated with higher number of outbreaks only more recently, quite likely due to a larger worldwide population and the present times greater importance of ordinary people movement versus disruptive migrations, while a similarly

low number of conflicts in the past did not affect at all the number of disease outbreaks. However, the most relevant effect of wars might be in the intensity of one or few outbreaks, and not in the total number.

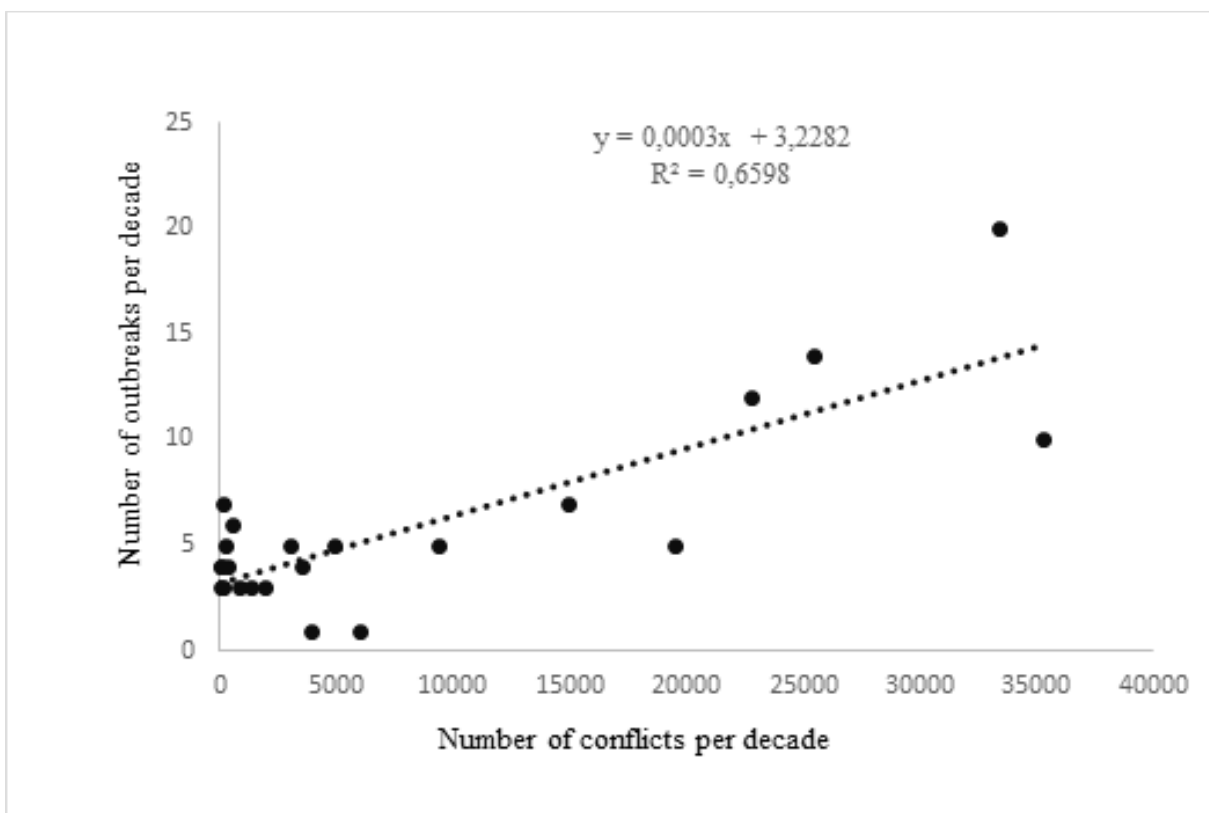
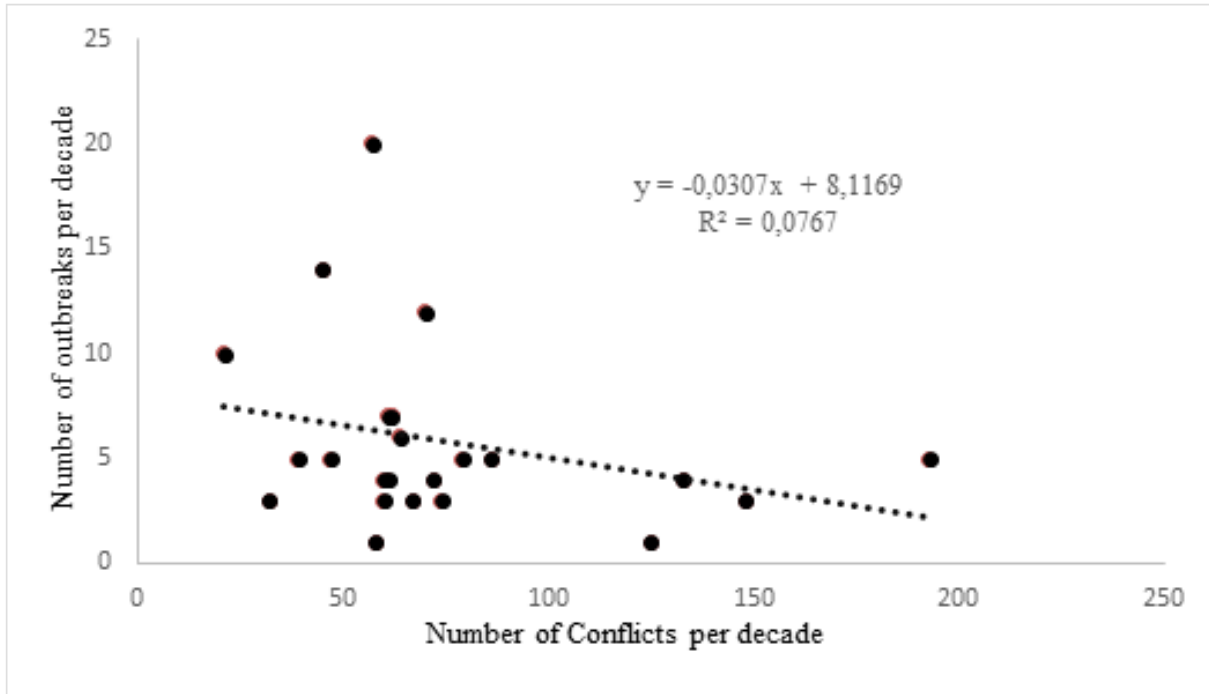


Figure 2 - Effect of conflicts on number of outbreaks was affected by the population size at each decade, resulting in a significant interaction of factors in the multiple linear regression

Table 2 – Number of outbreaks per pathogen guilds/species, and per decades when they happened, from 1800 to 2020, Worldwide. Each outbreak is a detectable event at populational consequences, somewhere in the Planet.

<b>Pathogen Guild/Species</b>	<b>Number of outbreaks</b>	<b>Decade</b>
dysentery	1	1840
scarlet fever	1	1870
kuru	1	1900
encephalitis	1	1910
psittacosis	1	1920
relapsing fever	1	1940
Marburg	1	1960
anthrax	1	1970
Hendra	1	1990
mad cow disease	1	1990
jakob disease	1	1990
Q-fever	1	2000
rift valley	1	2000
SARS-CoV-1	1	2000
H7N9 Bird Flu	1	2010
japanese encephalitis	1	2010
lassa	1	2010
legionnaires	1	2010
MERS	1	2010
New Delhi enterobacteriaceae	1	2010
adenovirus hepatitis	1	2020
black fungus	1	2020
monkey pox	1	2020
whooping cough	1	1840 -
H5N1 Bird Flu	1	1990 - 2000
SARS-CoV-2	2	2010 - 2020
H2N2	2	1950 -1960
H3N2	2	1960 - 1970
HIV	2	1980 - 1990
marburg	2	1990 - 2000
meningitis	2	1990 - 2000
nipah	2	1990 - 2010
HFM disease	2	2000 - 2020
chicungunha	2	2010 - 2020
unspecified Flu	3	1840 - 1850 - 1890
hepatitis	3	1980 - 2000 - 2010
zika	3	2000 - 2010 - 2020
malaria	4	1820 - 1900 - 1940 - 2000
measles	4	1840 - 1860 - 1870 - 2010
poliomyelitis	4	1910 - 1930 - 1940 - 1970
H1N1	4	1910 - 1970 - 2000 - 2010
ebola	5	1970 - 1990 - 2000 - 2010 - 2020
dengue	5	1980 - 1990 - 2000 - 2010 - 2020
typhus	6	1810 -1840 - 1860 -1910 - 1920
smallpox	8	1820 - 1830 - 1850 - 1860 - 1870 - 1880 - 1920 - 1970
plague	12	1800 - 1810 - 1830 - 1850 - 1870 - 1890 - 1900 - 1910 - 1920 - 1980 - 1990 - 2010
YF	12	1800 - 1840 - 1850 - 1870 - 1940 - 1960 - 1980 - 2010 - 2020
cholera	14	1810 - 1820 - 1830 - 1840 - 1850 - 1860 -1880 - 1890 - 1940 - 1960 - 1970 - 1990 -

\* - some pathogens caused more than one outbreak within a same decade

As neither a precise estimation on number of deaths per conflicts nor per outbreaks are likely to be obtained, in this analysis we explored only the number of events, and an important confounding resulted from not having the dimension of this conflicts. The great number of conflicts in early XX Century culminated in the World War I, the same period of the Spanish Flu, the deadliest pandemic of modern times. By having both one war and one pandemic at such planetary dimension eclipsed any chance to detect an effect of multiple conflicts on multiple disease outbreaks. Historical analysis clearly shows the relevant role to social disturbance in the occurrence of epidemic or pandemic events (Barry 2004).

Considering a combination of frequency and intensity of outbreaks, which are increasing now-a-days, all facts point towards a high expectation of a new pandemic at the same scale of SARS-CoV-2 to occur, whatsoever a human-evolved or a new-born emergent disease. The climate unpredictability might quite contribute for such probability as well. As a warmer and disturbing climate may favour opportunistic insects, a consequential pandemic of arbovirus is a real treat. We review the Dengue ongoing pandemic, likely origins, evolutionary ecology behind its adaptation to humans, and response to the interaction between climate change and environmental disturbance. For such, we present a study case of *Aedes aegypti* and dengue distribution in a highly human-modified biogeographic regions in South-east Brazil.

## **2.2 Dengue pandemic and *Aedes aegypti*: how the speciation around home water reservoirs in the Holocene became a pre-adaptation to a worldwide polluted and warm planet**

Dengue is a Flavivirus, as Yellow fever, both transmitted by the same Tribe of mosquitos, the Aedini (Culicidae family), and particularly by *Ae. aegypti*. The first likely cases of human dengue were reported in Chin Dynasty (2,300 BP). The disease is supposed to have first spread to the Western tropical colonies in America and to Europe thru the slavery trade from the XV to the XIX Centuries, as *Ae. Aegypti* supported well the long boat trips (Saeed & Asif 2020). Nevertheless, the four present strains of dengue were first recorded in different places: DENV1 in Japan and French Polynesia from 1943, DENV2 in Papua New Guinea and Indonesia from 1944, DENV3 in Philippines and Thailand from 1953, and finally DENV4 in Philippines, Thailand, Indonesia and Sri Lanka from 1953, all likely spread towards East from the Americas (Brown et al. 2014; Saeed & Asif 2020). Dengue is considered the first pandemic of arbovirus (Brady & Hay 2019).

The disease has not developed a sylvatic cycle in the Americas and has also lost continuity from the sylvatic to the human cycle in Africa (Weaver & Vasilakis 2009; Powell &



Tabachnick 2013). All four dominant strains evolved endemic human sub-lineages, now-a-days mostly predominant in comparison with ancestral sylvatic lineages (Weaver & Vasilakis 2009). Brown et al. (2014) further investigated the possibility that a sub-species of *Ae. aegypti*, which evolved in association to humans (*Ae. aegypti aegypti*, now on only *Ae. aegypti* for sake of simplification), became more competent to transmit dengue to humans. More precisely, they discuss the adaptation of the virus to this particular human-adapted mosquito, making dengue a truly human disease (Powell & Tabachnick 2013; Brown et al. 2014; Brady & Hay 2019).

The subspecies *Ae. aegypti aegypti* most likely evolved in North Africa, by surviving around human houses and cities from 4,000 to 6,000 BP, when Sahara Desert was expanding, and most predictable water supply would be found around human inhabitations (Powell & Tabachnick 2013). DNA sequencing left not much room for doubts about the routes of the planetary invasion of this mosquito: New World populations came from the *Ae. aegypti aegypti* population from North Africa, and the Southeast Asia and Pacific present day's populations came from those established in the Americas (Brown et al. 2014). As the dengue pandemic spread through populations of a highly domesticated mosquito, it is not expected that the disease could invade natural, well-preserved ecosystems, even though South America forests have a substantial diversity of Aedini mosquito species. On the other hand, the danger of a new urban cycle of another Flavivirus species, the Yellow Fever Virus (YF), has also little probability to happen, for the same reason: *Ae. aegypti* is unlikely to invade the forests where YF is endemic, and so unlikely to transmit it back to humans in nearby urban habitats. Nevertheless, such assumption of ecological barriers between forest and urban diseases stands only while forests are well preserved, which, in many cases, particularly around developed regions, is not the truth.

Our group have been studying *Ae. aegypti* ecology and distribution in the capital of Minas Gerais State, Belo Horizonte City, Brazil, as well as in cities and riparian forests along the Doce river valley. As this is a montane region, the effects of global warming are relatively easy to detect in the higher altitudes. In the Doce river valley, we described the first *Ae. aegypti* populations established in the montane town of Ouro Preto, around 1,150 metres above sea level (Pedrosa et al. 2020). The abundance of both eggs and adults in the town centre were enough to characterize a well-established population, but with less individuals than Mariana, the closest town at a slightly lower altitude, 750 metres a.s.l. We sampled in 2009 and 2012, finding a consistent pattern which suggested a recent invasion in Ouro Preto. From 2012 on, dengue became an endemic disease in this town. Our unpublished survey in 2022, showed that the difference in *Ae. aegypti* abundance between these towns were still similar 10 years later, although numbers in Ouro Preto did not vary significantly, while Mariana had a greater

population than before, which might explain the recent outbreaks of dengue disease in that town from 2022 to 2023 (ANOVA,  $p < 0.05$ ).

The altitudinal gradient still holds as an important driver for the *Ae. aegypti* abundance along the doce river valley. When comparing these two montane towns to Governador Valadares city, at 200 a.s.l., using a same sampling protocol as in Pedrosa et al. (2020), we found that Valadares had twice more eggs laid than Mariana and 5.7 times more than Ouro Preto (Figure 3). Apart from that, and regardless altitude, when comparing the mosquitos' abundances within these urban centres, we found that *Ae. aegypti* decreased significantly from densely constructed urban biotopes towards urban green areas (Pedrosa et al. 2020). Hence, we confirmed the well described pattern of *Ae. aegypti* not been able to colonize native vegetations.

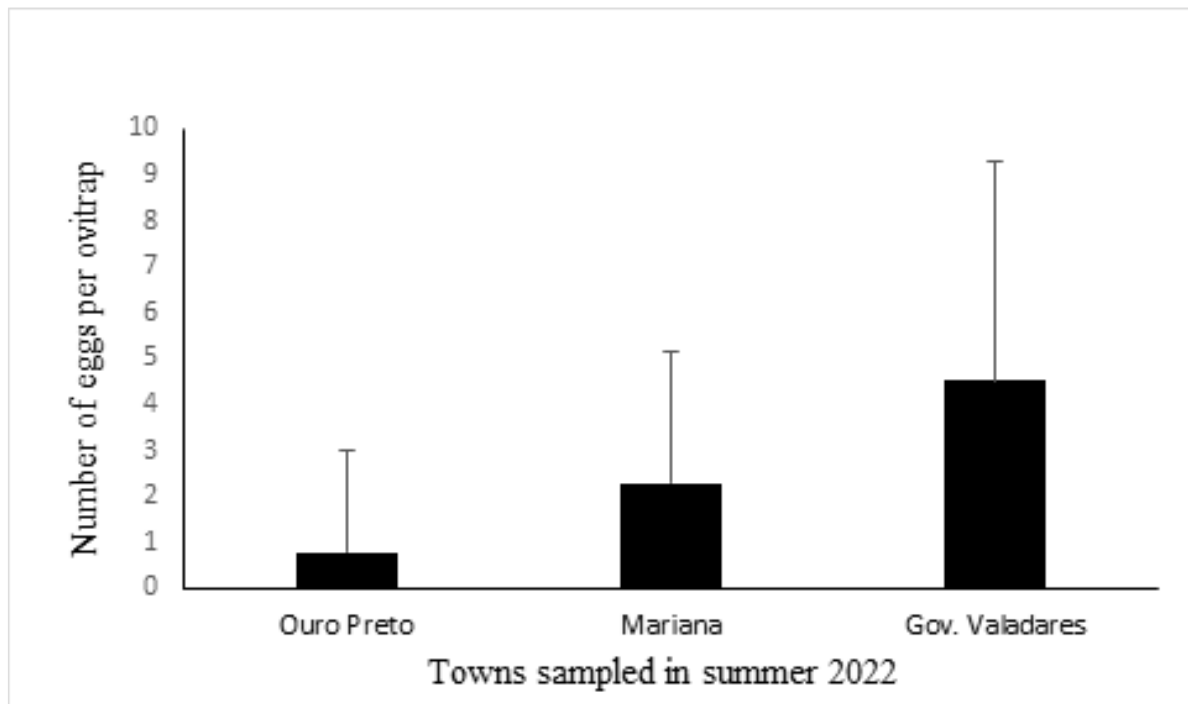


Figure 3 – *Aedes aegypti* oviposition per city, taken from ovitrap network in each city, following a same sampling design, and sampled at the same week.

Then, we sampled the riparian forests within the most important towns from the high altitude to the mid-valley Doce river, at 200 metres a.s.l., in 2020 and 2021. *Aedes aegypti* always was absent of any preserved forest, with one exception. In the Governador Valadares city, we sampled a riparian forest which had its understorey vegetation ripped off and replaced by the mud from a 2016 iron mine dam disaster. The mud released from that disaster accumulated in a large volume along the river (Fernandes et al. 2016), and in this particular forest fragment, it covered completely the soil. Although the trees survived, and the canopy

cover was retained intact, the understory habitats were completely modified. Ovitrap samples in this degraded forest showed an almost exclusive presence of *Ae. aegypti* (98% of 311 sampled eggs collected in 90 ovitraps), in a much higher density than even sampled in the streets nearby.

The event of *Ae. aegypti* in a heavily contaminated riparian forest is cause of concern. Perez & Noriega (2014) have shown that immatures of *Ae. aegypti* are relatively resistant to metal contamination in the waters where they grow. A special aspect of this contamination brings a special attention to the toxicity in other urban habitats: the high concentration of heavy metals in sewers. Sadly, the modern technological civilization left a planet highly contaminated by heavy metals (Alloway 2013). Several terrestrial food webs are contaminated (Gall et al. 2015). Linear sources of heavy metal contamination, as sewage-contaminated rivers and roads, spread this kind of pollution across the habitats where they bypass through (Gan et al. 2023).

If a hematophagous invasive species as *Ae. aegypti*, have evolved the ability to cope with high concentrations of chemical elements which are becoming extremely common around human ecosystems, that must be a key aspect of their success among us. Biotic barriers, such as competition and predation, seem to prevent *Ae. aegypti* to invade preserved forests. More extensively, we have shown that urban arboreal biotopes decrease the cases of dengue, even in vulnerable communities (Cunha et al. 2021). However, if *Ae. aegypti*'s natural enemies cannot bare high levels of heavy metals, a forest contaminated become favourable to the dengue insect vector as any other urban habitat.

Due to this mine disaster, another species might have been taking the advantage of an environment extremely heavy metal contaminated, the *Lutzomyia longipalpis*, the sandfly vector of the visceral leishmaniasis. In the Part 2 of this Thesis, we show for the first time that this is a species adapted to develop in organic matters that are naturally rich in heavy metals, especially iron: corpses and carnivore feces. As such, this native species could have a pre-adaptation to the present days' highly contaminated human ecosystems.

### 2.3 References

- Alloway, B.J. 2013. Sources of Heavy Metals and Metalloids in Soils. In Alloway, B.J. (ed.), Heavy Metals in Soils: Trace Metals and Metalloids in Soils and their Bioavailability, Environ. Pollut. 22, DOI 10.1007/978-94-007-4470-72.
- Barry, J.M. 2004. A Grande Gripe. Ed. Intrínseca, RJ.

- Brady, O.J., Hay, S.I. 2019. The Global Expansion of Dengue: How *Aedes aegypti* Mosquitoes Enabled the First Pandemic Arbovirus. *Annu. Rev. Entomol.* 65:9.1–9.18.
- Brown, J.E., Evans, B.R., Zheng, W., Obas, V., Barrera-Martinez, L., Egizi, A., Zhau, H., Caccone, A., Powell, J.R. 2014. Human impacts have shaped historical and recent evolution in *Aedes aegypti*, the dengue and yellow fever mosquito. *Evolution* 68: 514-525.
- Carlson, C. J. et al. 2020. Climate change increases cross-species viral transmission risk. *Nature* <https://doi.org/10.1038/s41586-022-04788-w>.
- Cashdan, E. 2014. Biogeography of human infectious diseases: A global historical analysis. *PLoS One* 9: 1–11. doi: 10.1371/journal.pone.0106752.
- Cunha, M.C.M., Ju, Y., Morais, M.H.F., Dronova, I., Ribeiro, S.P., Bruhn, F.R.P., Lima, L.L., Sales, D.M., Schultes, O.L., Rodriguez, D.A., Caiaffa, W.T. 2021. Disentangling associations between vegetation greenness and dengue in a Latin American city: Findings and challenges. *Landscape Urban Plan.* 216: 104255.
- Dunn, R.R., Davies, T.J., Harris, N.C., Gavin, M.C. 2010. Global drivers of human pathogen richness and prevalence. *Proc. R. Soc. B Biol. Sci.* 277: 2587–2595. doi: 10.1098/rspb.2010.0340.
- Fernandes, G.W.; Goulart, F.F.; Ranieri, B.D., et al. 2016. Deep into the mud: ecological and socio-economic impacts of the dam breach in Mariana, Brazil. *Natureza Conserv* 14: 35 – 45.
- Fincher, C.L., Thornhill, R., Murray, D.R., Schaller, M. 2008. Pathogen prevalence predicts human cross-cultural variability in individualism/collectivism. *Proc. R. Soc. B* 275: 1279–1285. doi:10.1098/rspb.2008.0094
- Gall, J.E., Boyd, R.S., Rajakaruna, N. 2015. Transfer of heavy metals through terrestrial food webs: a review. *Environ Monit Assess* 187:201-221.
- Gan, W., Zhang, Y., Xu, J., Yang, R., Xiao, A., Hu, X. 2023. Distribution of Soil Heavy Metal Concentrations in Road-Neighboring Areas Using UAV-Based Hyperspectral Remote Sensing and GIS Technology. *Sustainability* 15: 10043. <https://doi.org/10.3390/su151310043>.

Hamilton, W.D., Axelrod, R., Tanese, R. 1990. Sexual reproduction as an adaptation to resist parasites (A Review). *Proc. Natl. Acad. Sci. USA* 87: 3566-3573.

Karesh, W., Dobson, A., Lloyd-Smith, J.O., Lubroth, J., Dixon, M.A., Bennet, M., Aldrich, S., Harrington, T., Formenty, P., Loh, E.H., Machalaba, C.C., Thomas, M.J., Heymann, D.L. 2012. Ecology of zoonoses: natural and unnatural histories. *Lancet* 380: 1936–45.

Keesing, F., and Ostfeld, R.S. 2021. Impacts of biodiversity and biodiversity loss on zoonotic diseases. *Proc. Natl. Acad. Sci. USA* 118: 1–8. doi: 10.1073/PNAS.2023540118.

Lewis, C.M., Akinyi, M.Y., DeWitte, S.N., Stone, A.C. 2023. Ancient pathogens provide a window into health and well-being. *Proc. Natl. Acad. Sci. USA*. 120: 1–8. doi: 10.1073/pnas.2209476119.

Low, B.S. 1994. Pathogen Intensity Cross-Culturally. *World Cultures* 8: 1-9.

May, R.M., Anderson R.M. 1983. Epidemiologic and genetics in the coevolution of parasites and hosts. *Proc. R. Soc. Lond. B* 219: 281-313.

Murray, K.A, Preston, N., Allen, T., Zambrana-Torrel, C., Hosseini, P.R., Daszak, P. 2015. Global biogeography of human infectious diseases. *PNAS* 112: 12746-12751. doi/10.1073/pnas.1507442112.

Nava, A., Shimabukuro, S., Chmura, A.A., Luz, S.L.B. 2017. The Impact of Global Environmental Changes on Infectious Disease Emergence with a Focus on Risks for Brazil. *ILAR J* 58: 393–400.

O'Hagan, Z., Chousou-Polydouri, N., Michael, L. 2019. Phylogenetic classification supports a Northeastern Amazonian Proto-Tupí-Guaraní homeland. *LIAMES* 19: 1-29, e019018.

One Health High-Level Expert Panel (OHHLEP), Adisasmito, W.B., Almuhairi, S., Behraves, C.B., Bilivogui, P., Bukachi, S.A., et al. 2022. One Health: A new definition for a sustainable and healthy future. *PLoS Pathog* 18:e1010537. <https://doi.org/10.1371/journal.ppat.1010537>.

Pedrosa, M.C., Borges, M.A.Z., Eiras, Á.E., Caldas, Sérgio, C.A.B., Brito, M.F., Ribeiro, S.P. 2020. Invasion of Tropical Montane Cities by *Aedes aegypti* and *Aedes albopictus* (Diptera: Culicidae) Depends on Continuous Warm Winters and Suitable Urban Biotopes. *J Medical Entom* 58: 333 - 342.

Perez, M.H., Noriega, F.G. 2014. Sublethal metal stress response of larvae of *Aedes aegypti*. *Physiol Entomol* 39: 111-119. DOI: 10.1111/phen.12054.

Powell, J.R., Tabachnick, W.J. 2013. History of domestication and spread of *Aedes aegypti* - A Review. *Mem Inst Oswaldo Cruz* 108: 11-17.

Pulliam, J.R.C., Epstein, J.H., Dushoff, J., Henipavirus Ecology Research Group (HERG), et al. 2012. Agricultural intensification, priming for persistence and the emergence of Nipah virus: a lethal bat-borne zoonosis. *J R Soc Interface* 9: 89–101.

Rasmussen, S. et al. 2015. Early Divergent Strains of *Yersinia pestis* in Eurasia 5,000 Years Ago. *Cell* 163: 571–582.

Ribeiro, S.P., Brown, V.K. 2006. Prevalence of monodominant vigorous tree populations in the tropics: herbivory pressure on species in very different habitats. *J Ecol* 94: 932 – 941.

Ribeiro, S.P., Brown, V.K. 1999. Insect Herbivory In Tree Crowns of *Tabebuia Aurea* and *T. Ochracea* (Bignoniaceae): Contrasting The Brazilian Cerrado with the Wetland Pantanal Matogrossense. *Selbyana* 20: 159 – 170.

Ribeiro, S.P.; Brown, V.K. 2002. Tree species monodominance or species-rich savannas: the influence of abiotic factors in designing plant communities of the Brazilian cerrado and the Pantanal matogrossense - a review. *Ecotropica* 8: 31 - 45.

Ribeiro, S.P., Barh, D., Andrade, B.S., Silva, R.J.S., Costa-Rezende, D.H., Fonseca, P.L.C., Tiwari, S., Giovanetti M., Alcantara L.C.J., Azevedo V., Ghosh, P., Filizola-Filho, J.A.D., Loyola, R., Brito, M.F., Goes-Neto, A. 2022. Long-term unsustainable patterns of development rather than recent deforestation caused the emergence of Orthocoronavirinae species.

Environmental Microbiology 10: 4714-4724.brown

Saeed, O., Asif, A. 2020. Dengue virus disease; the Origins. In Qureshi, A.I., Saeed, O. (eds) Dengue Virus Disease From Origin to Outbreak. Pp 9-16

Saldanha, B.M., Chame, M., Nunes, G.K.M., Sianto, L., Leles, D. 2022. Parasites of the Brazilian Rock Cavy, *Kerodon rupestris*: Revealing Their History in the Brazilian Semiarid Region. J Parasitol 108: 395,

Sharp, P.M., Hahn, B.H. 2011. Origins of HIV and the AIDS pandemic. Cold Spring Harb Perspect Med 1:a006841.

Silva, M.A.C., Ferraz, T., Couto-Silca, C.M., Lemes, R.B., Nunes, K., Comas, D., Hunemeier, T. 2021. Population Histories and Genomic Diversity of South American Natives. Mol. Biol. Evol. 39:msab339 doi:10.1093/molbev/msab339

Silva, A.C., Bernardes, A.T., Barbosa, E.A.G., Chagas, I.A.S., Dáttillo, W., Reis, A.B., Ribeiro, S.P. 2022. Successive pandemic waves with different virulent strains, and 2 the effects of vaccination for SARS-CoV-2. Vaccines 10: 343 - 360.

Tallavaara, M., Eronen, J.T., Luoto, M. 2018. Productivity, biodiversity, and pathogens influence the global hunter-gatherer population density. Proc. Natl. Acad. Sci. USA 115: 1232–1237. doi: 10.1073/pnas.1715638115.

Volpato, G., Fontefrancesco, M.F., Gruppuso, P., Zocchi, D.M., Pieroni, A., 2020. Baby pangolins on my plate: Possible lessons to learn from the COVID-19 pandemic. J Ethnobiol Ethnomed <https://doi.org/10.1186/s13002-020-00366-4>.

Weaver, S.C., Vasilakis, N. 2009. Molecular Evolution of Dengue Viruses: Contributions of Phylogenetics to Understanding the History and Epidemiology of the Preeminent Arboviral Disease. Infect Genet Evol 9: 523–540. doi:10.1016/j.meegid.2009.02.003.

Zuckerman, M.K., Harper, K.N., Barrett, R., Armelagos, G.J. 2014. The evolution of disease: Anthropological perspectives on epidemiologic transitions. *Glob. Health Action* 7: 1–8. doi: 10.3402/gha.v7.23303.



### **3 PART 2 - ADAPTATIONS OF *Lutzomyia longipalpis* TO NATIVE CANID DENS AND BLOOD-RICH ORGANIC MATTERS: A SOUTH AMERICAN INDIGENOUS MEN-FOX-SANDFLY NICHE INVADED POSTERIORLY BY *Leishmania infantum*?**

#### **3.1 Preface**

Classic parasitological literature has posed the likely sylvatic origin of South American visceral leishmaniasis (AVL), caused by *Leishmania infantum*. The natural infection of crab-eating fox (*Cerdocyon thous*) was put as an evidence (Lainson & Shaw 1987; Lainson & Rangel 2005). However, the lack of *L. infantum* genetic markers in support of the existence of enough time of isolation between populations from the New and Old world, provides supports to the hypothesis of a European (Portuguese) introduction of the disease, by infected domestic dogs (Leblois et al. 2011). In the next part of this Thesis, we tested the hypothesis that females of the sandfly which is AVL vector, *Lutzomyia longipalpis*, can identify blood-rich organic matter related to canid dens, and that newly hatched immatures would be able to choose between contrasting organic matter substrates. The preference was by rotten carcasses and fresh faeces. Decomposed feces were hardly chosen, while oviposition on leaf litter varied seasonally. Very importantly, though, humidity was the third most chosen component (control, only water substrate), and relates to the high susceptibility of this immatures to drought. Early emerged immatures showed no preference for substrates and were highly vagile, walking an estimated 30 cm per day, but having the behaviour of gathering and then pupating more frequently on rotten carcasses. Early larval mobility might be a response to find moist microhabitats in the environment, as hatching and survival under 60-70% relative humidity was significantly lower than above 90% (eggs collapsed or immatures dried out and died after birth). The predominant choices for fresh feces and decomposing or fresh carcasses corroborate our hypothesis that *L. longipalpis* may have evolved in close association with wild canids. Previous data suggesting the relation *C. thous*-*L. longipalpis* (or also the fox *Lycalopex vetulus*) were circumstantial (Deane 1956), based on *L. infantum* infection. Our data is the first to support the whole life cycle of this sandfly could be associated to wild canids. Our experiments support that *L. longipalpis* might have evolved in association to organic matters related to predators, most likely, associated to canid dens or scattered sources within cave or in similarly mesic and sheltered conditions, depending on a combination of resources and hyper-humid microhabitats. These findings are in agreement with the natural habitat of this species, rocky habitats and, mostly, caves (Forattini 1973). Hence, we further explored the possibility of ancient humans in

association with these very same caves, and coexisting with foxes, could enhance both the amount and the predictability of organic matters. In this case, a high overlap of these species distribution around caves at a continental scale was expected to be found.

Casaril et al. (2019) showed a clear vicarious process of ongoing speciation within the complex of *L. longipalpis*, along a large geographical cline, in line with the Karst cave formations from North to South of Central South America. Such findings are in accordance with sympatric and clinal complex of *L. longipalpis* species, and incipient speciation process identified by Araki et al. (2009), using copulation song and pheromone analyses. The hypothesis of a cave-based system of sub-populations or ongoing speciation within the *L. longipalpis* species complex is compatible with a recent, Holocene, climatic change that may have isolated these subpopulations in the rocky and caves, after the surrounding vegetations became seasonal and air humidity much drier, since the Meghalayan chronozone, around 4,200 yrs BP (Utida et al. 2020). No authors explored the causes of the present distribution of this species complex, and a contraction of a previous larger and more continuous population, after overall climate drought or seesaw oscillation between drought-wet climate (Azevedo et al. 2021) during late Holocene could be an explanation.

Now-a-days, except in few caves, *L. longipalpis* is hardly found in natural habitats but in rural modified landscapes or, and more frequently, in degraded urban/suburban environments in modern cities, thus, among people. Parasitological debate on South American AVL ignored completely the pre-colonial large Guarani indigenous populations living in the same semi-arid, savanna, or rocky natural habitats of *L. longipalpis*. There is enough evidence that Guarani tribes domesticated foxes (Prates 2014; Perry et al. 2021), thus man-fox interaction in cave-like habitats could assure a more stable and predictable source of resources for both *L. longipalpis* immatures and adults.

This is a socio-ecological system which was likely to be invaded by *L. infantum*, in case domestic dogs from European colonizers were introduced into the indigenous communities. Worldwide, convergent man-canid-sandfly interaction around blood-rich organic matter could be a specific niche for the evolution of *L. infantum* or *L. donovani*, both related to canids and causing visceral leishmaniasis. There is a clear convergence between this interactive scenario in South America and the ecological conditions surrounding the Old-World pattern of distribution and prevalence of visceral leishmaniases (Lysenko 1971; Sterverding 2017). Hence, most likely *L. infantum* and *L. donovani* have evolved under a quite distinct environmental pressure than tegumentar, sylvatic leishmaniases, and could be consider a truly human habitat-related than a sylvatic born disease. The key ecological aspect in support of such

hypothesis lays upon the existence of a long-term adaptation of very few sandfly species to primitive human settlements, where canids co-occur.

### **3.2 Evolutionary Ecology of *Lutzomyia longipalpis*: from Human and Canid-Inhabited Caves to Primary Vector of *Leishmania infantum* in South America**

Sérvio Pontes Ribeiro<sup>1,2</sup>, Camila de Paula Dias<sup>1,2</sup>, Luccas Gabriel Ferreira Malta<sup>1</sup>, Alexandre Barbosa Reis<sup>2</sup>, Marcos Horácio Pereira<sup>1</sup>, Nelder Figueredo Gontijo<sup>1</sup>

<sup>1</sup> Laboratórios de Fisiologia de Insetos Hematófagos, Departamento de Parasitologia, ICB-UFMG

<sup>2</sup> Núcleo de Pesquisas em Ciências Biológicas, NUPEB-UFOP

#### *3.2.1 Abstract*

Literature has debated the likely sylvatic origin of South American visceral leishmaniasis (VL), caused by *Leishmania infantum*. The natural infection of crab-eating fox (*Cerdocyon thous*) was put as evidence. However, the lack of *L. infantum* genetic markers suggesting isolation between populations from the New and Old world provides supports to the hypothesis of a European (Portuguese) introduction of the disease, by infected domestic dogs. We tested the hypothesis that females of the VL vector, sandfly *Lutzomyia longipalpis*, can identify blood-rich organic matter related to canid burrows, and that newly hatched immatures would be able to choose between contrasting organic matter substrates. We tested: fresh mice corpses, 10 days decomposed mice corpses, fresh dog feces, 10 days decomposed dog feces, partially decomposed leaf litter and none of these substrates as control. Each substrate was macerated in 10 ml of distilled water; 1 ml was applied to filter papers placed on a humidified plaster surface in small open containers inside a 80x30x40 cm sealed terrarium. Four days after blood meal, females were released into this space in trials of 100, 200, 250, 300 and 500 females. Tests were carried out from wet (January – March) to dry (April – July) season of 2022. Further, 16 trials were carried out with newly hatched larvae (average 95 eggs per trail) for testing whether they would choose between these substrates and testing the effect of humidity conditions. Trials carried out in the dry season had 14 times less eggs per female than the trial with a similar number of females in the wet season. In the wet season, fresh feces and decomposed mice attracted more oviposition than the control, which received, though, more

oviposition than leaf litter and fresh mice. In the dry season, oviposition occurred more frequently in fresh mice followed by control and decomposed mice. The search for pure water added up to 23% of the total. Decomposed feces were hardly chosen, while oviposition on leaf litter varied seasonally. Early emerged immatures showed no preference for substrates and were highly vagile, walking an estimated 30 cm per day, but having the behaviour of gathering and then pupating more frequently on rotten corpses. Early larval mobility might be a response to find moist microhabitats in the environment, as hatching and survival under 60-70% relative humidity was significantly lower than above 90% (eggs collapsed or immatures dried out and died after birth). The predominant choices for fresh feces and decomposing or fresh carcasses corroborate our hypothesis that *L. longipalpis* may have evolved in close association with wild canids. Previous data suggesting the relation *C. thous*-*L. longipalpis* were circumstantial, based on *L. infantum* infection. Our data is the first to support the whole life cycle of this sandfly could be associated to wild canids. Still, we not necessarily support the hypotheses that VL is a sylvatic South American disease. This sandfly is hardly found in natural habitats but in rural modified landscapes or, and more frequently, in degraded environments in modern cities, thus among people. Parasitological debate on South American VL ignored completely the pre-colonial large Guarani indigenous populations living in the same semi-arid, savanna, or rocky natural habitats of *L. longipalpis*. The evidence that Guarani tribes domesticated foxes is also abundant, thus man-fox interaction in cave-like habitats could assure a more stable and predictable source of resources for both *L. longipalpis* immatures and adults. This is a socio-ecological system likely to be invaded by VL if domestic dogs from colonizers were added to the indigenous communities. Worldwide, convergent man-canid-sandfly interaction around blood-rich organic matter could be a specific niche for the evolution of *L. infantum*, most likely a human habitat-related than forest born disease.

Keywords – Visceral leishmaniasis, Disease Ecology, Insect Vectors, *Lutzomyia longipalpis*, canids

### 3.2.2 Introduction

The interaction between Leishmaniinae protozoans and Phlebotominae insects (sandflies) were formed from 300 to 200 million of years ago (Mya, hereafter), much before a heteroxenous life cycle in this subfamily of Trypanosomatid evolved, i.e., the capability of colonizing an invertebrate and a vertebrate host in a same life cycle (Akhoundi et al. 2011).

Considering the *Leishmania* genus, there is still intense debate about their origin and dispersal, been the most acceptable from the Old to the New world (Palaeartic – Lysenko 1971 – Neotropical – Lainson & Shaw 1987; Noyes 1998, Croan et al. 1997 – and Supercontinent origins – Momen & Cupolillo 2000). One widely accepted hypothesis is that they followed the radiation and dispersion of their main vertebrate hosts, the Muridae rodent species (Sterverding 2017). Muridae burrows produces a reasonable habitat-base for the sandfly species (Kerr 2000), and such association may have been followed by a co-radiation and distribution of the sandflies and these vertebrates, which ought to be followed by *Leishmania* species radiation (Sterverding 2017). Hence, *Leishmania*-Phlebotominae interactive pairs are supposed to have spread after Muridae rodent radiation and dispersion, especially from Asia to Americas 25 Mya, when Behringer bridge were there, and the climate was milder. Later (4-3 Mya), they dispersed from North to South America, after the Panama Isthmus creation (following specifically the Muridae's subfamily Sigmodontinae; Sterverding 2017).

Such diversification of sandflies species, along with the wide range of vertebrate hosts which are recorded infected by *Leishmania* (mostly tegumentary) provide support to the broadly accepted idea that Phlebotominae is genuinely a generalist hematophagous subfamily (xx). However, the much more restricted range of host of visceral leishmaniosis (VL, hereafter, or AVL for American Visceral Leishmaniasis) suggest that sandfly species which are infected and transmit this particular type of disease might be also adapted to a more restricted host range. Visceral leishmaniasis is caused by only a few *Leishmania* species: *L. infantum*, *L. donovani* (Ready 2014; Sterverding 2017) and, sporadically by *L. tropica* (Baneth et al. 2014). There are also quite few sandfly species capable to transmit them. In the New World: *Lutzomyia longipalpis*, secondarily *L. cruzi* (Lainson & Shaw 1987), and sporadically found in other species as *L. evansi*, *Nyssomyia whitmani* or species of *Evandromyia* (Bejarano et al. 2001; Saraiva et al. 2015; Sterverding 2017; Oliveira et al. 2018). In the Old World: *Phlebotomus perniciosus*, *P. major*, *P. chinensis*, *P. longicuspis* and few other sporadic species (Lysenko 1971; Filiciangeli 2004).

Although adults are capable to feed on various species of mammals, and also birds, these few VL vector species could have evolved in association with a group of mammals that are prompt to develop this type of leishmaniasis, the canids. For what is known in the Old World, Lysenko (1971) has proposed an evolutionary pathway for VL, from canids until is became a specialized human disease. His explanation did not mention at all the dog domestication history. However, no evolutionary mechanism driving this likely process was tested or proposed. Oddly,

the early human-canid domestication history was never taken into consideration while proposing an evolutionary adaptation of these parasites to humans and dogs.

For the New World, Lainson & Rangel (2005) and Rangel et al. (2018) re-visited and corroborate a similar hypothesis. Lainson et al. (1990) claimed that the eating-crab fox, *Cerdocyon thous*, was the sylvatic reservoir of the disease, which at some stage after European colonization infected dogs in small rural farms close to primary forests, and then, humans. This is well accepted so far, despite the still open dispute between AVL been caused by native *L. infantum* populations or only by introduced populations from Portuguese infected dogs (which has eventually happened, regardless the existence or not of a native strain, see Leblois et al. 2011). Deane (1956) and Lainson et al. (1990) tested several native species and besides *C. thous* and the fox *Lycalopex vetulus*, only opossum was infected. Nevertheless, neither the existence of pre-European complex societies, and densely distributed human populations, nor the indigenous domestication of foxes were taken into consideration to describe the natural history of this disease and its insect vector species in South America.

Many distinct canid species have experienced convergent domestication processes along the history of humanity, dating back 40 thousand years in North America, (Perri et al. 2021; Serpell 2021), but also in Egypt (7,000 BP), Iraq (8,000 BP), Cyprus (5,500 BP), Greece (6,000 BP) (Petter 1972; Nozais 2003), and also in South America (2,000-3,000 BP). Another aspect hardly discussed in VL ecology is that men-canid interactions, and not only canids, might have created richer and more predictable microhabitats, increasing recent conditions for specifically the immatures of *L. longipalpis* to further adapt to human settlements.

Although rodents' burrows are explicitly mentioned as a wet, suitable habitat for sandfly development (Deane 1956; Kerr 2000), a recent work has shown that dog feces are suitable substrate for a full development of *L. longipalpis* from eggs to adults (Carreira et al. 2018). However, canid dens and its prey blood-rich substrate, made of a combination of feces and prey corpses under distinct decaying stages, were never considered as an attractive and suitable habitat for sandfly oviposition.

Canids are found in all continents (Vilá et al. 2012) and may have originated in the same time that *Leishmania* did, around 60 Mya (Sterverding 2017). In South America, the 10 living species spread out along the whole continent, and are descendent of a sole ancestral species, which invaded the continent between 3.9 Mya and 3.5 Mya (Chavez et al. 2022), just before *Lutzomyia* genus is supposed to have arrived, all through the Panama Isthmus (Sterverding 2017; Chavez et al. 2022). Although South America canids are omnivorous, one

of the few studies on diet showed that the most abundant species, the crab-eating fox (*Cerdocyon thous*), had vertebrates contributing to 36.5 % of their diets (Rocha et al. 2004).

Forattini (1973) already described *L. longipalpis* as a species constrained to rocky-shelters, caves or deep creek valleys within the savanna or dry forest Biomes. Hence, after invading South America, nothing is known about how this species became restricted to east and northeast of continent, and absent from the wet Amazon Forest, for instance. Here we explore the possibility that cave ecosystems, especially karstic caves, could provide high humidity and rich resources when producing shelters for both foxes and humans. The paleovegetation seesaw due to climate large oscillations could ended up trapping the species to the high humidity of the caves and rocky-shelters (Utida et al. 2020; Azevedo et al. 2021).

Then, in the late Holocene, with a more predictable and milder weather, around 5000 years (ya), the spreading of Tupiguarani and Una cultures followed from central Brazilian Plateau towards Marajo Island (occupied around 3,000 ya, Schaan et al. 2010), in the borders of the Amazon Forest. Such demic expansion clearly happened along rocky cave-rich ecosystems, and also inside open savanna and dry forest domains, following large rivers (Souza et al. 2020). Hence, a common origin for those nations in present time occupying Marajo and the wetlands of Pantanal Matogrossense is possible (Souza et al. 2020). This would be the ancestor of the Guarani-Mbya, skilled water managers, capable to create large mounds, who may have occupied and transformed the landscape in regions not too far from complex cave systems previously occupied by the early Holocene populations (Goldberg et al. 2016; Bueno & Isnardis 2018; Moreno-Mayar et al. 2018).

The Marajo Island, in the mouth of the Amazon river, is predominantly a savanna-type floodplain, with few riparian forests (Schaan 2008). There, large urban populations gathered as many as 100,000 people each, in an intensely modified landscape, using techniques to manage water supplies and seasonal floodings, creating large mounds for litter, burial sites and even inhabitations (Schaan 2008; Schaan & Martins 2010). They formed a complex ceramist society from 400 BC to 1400 AC (Meggers 2001; Schaan et al. 2010), and their descendants held back the Portuguese for 20 years in war, until 1659, when they colonized the island. Nevertheless, Portuguese and their dogs were nearby in the opposite margin of the river since 1616, in the Belém city and surroundings, (Schaan & Martins 2010).

Marajo island happens to be the location where Lainson et al. (1990) incriminated eating-crab foxes as main sylvatic reservoir of AVL, living infected in primary forests. However, one hardly could consider Marajo as a place with any primary forest, as stated in this classical work. The island crab-eating fox population must have coexisted with native and

European people. The savanna type of vegetation along with a severe flooding season might have left few places with abundant resources than those densely populated, namely the human-made mounds, and the riparian coastal secondary forests. It is impossible to verify whether this early human plus foxes modified ecosystem was determinant of *L. longipalpis* distribution in the island. Even though, at the continental scale, the closely overlap between *L. longipalpis* and *C. thous* distribution with Holocene populations (especially in rocky hills and karst caves) is circumstantial evidence that this sandfly could have been well adjust to both foxes and native human populations after humans left the caves. At least, this presently urban insect, hardly sampled in a now-a-days forest insect surveys, could have been adapted to the simplified and enriched human pre-European settlements as much as the surroundings of a fox den, rather than to pristine, nutrient-poor forests.

The baseline assumption of this work is that the American Visceral Leishmaniasis is a canine-human evolved parasitism, depending on a sandfly vector species capable to coexist, in a predictable way, with the highly contaminated organic matter produced by these two predator hosts in a pre-historic scenario. Similar to the Visceral Leishmaniasis in the Old World, the disease may invade the niche created by the interaction of these host species (humans, canids and a sandfly species), which is most likely to be found in human modified environments than in sylvatic, resource-scattered and nutrient poorer habitats, as in a forest or open savanna. Hence, contrary to cutaneous and tegumentar leishmaniasis, caused by other *Leishmania* species, this would be an anthropomorphic rather than a sylvatic disease, challenging the perception about the AVL after Lainson et al. (1990) and Lainson & Rangel (2005). Nevertheless, as the existence of AVL previously to Portuguese colonization is still a debatable issue, this article focusses on the adaptation of *L. longipalpis* to canid-human organic matters, and patterns of distribution of this three-level interaction.

We tested the hypothesis that *L. longipalpis* immatures evolved to survive on carnivore organic matters, which may result in females been able to choose such substrates by scent. We predict that females prefer canid feces or remaining corpses at different decaying stages than other scents, and immatures would be able to fully develop choosing to eat on these substrates. Hence, we proposed a series of experiments intending to simulate such habitats, and so tested female choice for oviposition, and the insect immature phase responses to organic matter, simulating what could be found around a wild fox den, or in caves occupied by human hunters and domesticated foxes, in comparison to expected forest-type of substrates.

We then investigated the hypothesis that the organic matter resulted from corpses and feces of carnivores might constrain colonization by most sandfly species. Adaptation of *L.*



*longipalpis* and likely other species must demand some mechanism to deal with metal contaminants from decaying preys, especially iron from haemoglobin and other iron containing proteins. We predict that might be some ecophysiological barrier for species to colonize and survive on an organic matter composed with toxic concentrations of iron and other heavy metals, resulted from decaying corpses or found in the feces of a carnivore. If so, we expect to find some molecular evidence of adaptation to this resource in *L. longipalpis* and not in other hematophagous species with a distinct life cycle. For such, we analysed the ferritin protein structure and phylogeny among hematophagous Diptera. Ferritin is an essential protein for Iron transferring to the ovaria but is also a protein capable to be produced induced by contamination, and then be mobilized to eliminate excess of Iron from the cells (Geiser et al. 2019).

Finally, we explored the hypothesis that *L. longipalpis*' contemporaneous distribution may overlap with the caves occupied in the past by Holocene human populations, as a trace left from a pre-historic ecological association. Further, we also expect that the two fox species incriminated as reservoirs of AVL, *C. thous* and *L. vetulus*, should also overlap with Holocene human distribution at some extent. However, wild *L. longipalpis*-fox-human habitats no longer exist, due to the changes imposed on South America indigenous way of life after Portuguese colonization (including the widespread introduction of domestic dogs). Thus, this hypothesis is explored in a circumstantial way.

### 3.2.3 Methodology

In this chapter we explored a series of novel aspects of the Natural History of *L. longipalpis*, its likely interaction with wild canids in South America, and native humans, since the Holocene. In order to do so, we explored experimentally female oviposition behaviors, immature locomotion capability, environmental constraints to survive and complete a cycle in contrasting organic matters substrates (Figure 1). The experiments were designed to simulate conditions likely to be found in caves occupied with foxes or foxed and humans. Our cave model in the Lapinha cave, in Lagoa Santa Municipality, Minas Gerais State, in the region where the oldest Brazilian human skull was so far found.

Then, we investigated particularities in Ferritin evolution among different Diptera species (decomposers and hematophagous, from Brachycera and Nematocera) to understand its potential role in detoxication of environmental excess of iron. Finally, we used spatial statistical analysis to explore the patterns of distribution of *L. longipalpis*, ancient humans, and *C. thous*

and *L. vetulus* in South America, considering cave habitats distribution as a driver of co-occurrence.

The use of vertebrates in our experiments was approved by the UFMG's bioethical committee (CEUA 262/2021).



Figure 1 – Experimental scheme for testing substrate oviposition choices (a), immature locomotion and substrate choices (b), and oviposition in two phases/environments (c).

### 3.2.3.1 Experimental designs

#### 3.2.3.1.1 Female oviposition choices

Four days after blood feeding and copulation, females were sealed inside a glass container of 80x30 cm basis and 40 cm height. At equal distances, six smaller glass containers of 15x7 cm basis and 13 cm height were positioned inside this large container. Each small treatment container was covered with plaster on the bottom, and received a filter paper moist with 1 ml of the following substrates smells, extracted in water: 1) forest foliage and seeds partially decomposed, 2) fresh dog feces, 3) 10 days rotten dog feces, 4) macerated fresh

hairless mice (*Mus musculus*/Linage hairless HRS/J), 5) macerated 10 days rotten hairless mice, 6) only distilled water as control. For such, each substrate was taken in similar amounts (approximately 5 gr), macerated, and mixed in distilled water (10 ml), and left for 24 hours to impregnate the liquid with volatile compounds to produce their typical smells. For feces, the same stools were used for the two treatments levels (fresh and rotten), as well as a same mouse, sliced longitudinally, was used in order to reduce the effects of content variability. Five different stools were combined and two mice to produce for these smells. Mice are non-infected and previously sacrificed from other experiments, to diminish the number of animals sacrificed in the laboratory.

The experiment was carried out from wet to dry season of 2022. Each run last until all females died; As it is unlikely to set an exact number of females, they were counted after each run. Hence, groups of approximately 100 (07-15 Feb), 200 (21-26 Feb), 200 (25-30 March), 495 (31 March - 08 April), 300 (29 April – 06 May), 280 (15-22 June) and 250 (08-13 July) were used in the experiment. After all dead, the container was opened, and the treatments took to the stereo-microscope to count eggs. Other previous experiment with this sandfly colony showed that female avoid laying eggs on a glass surface, but the container was searched for eggs after each running. Results from 25 March, 29 April, and 15 June were not analysed for different reasons, from all females have died trying to escape the space without laying eggs, to failure in keeping high humidity in early dry season. Still, all running were used for recording behaviours, including the strange trend of forcing to escape the space without laying eggs, which we detailed below.

The size of the container aimed to simulate a micro-habitat compatible to what is expected to be found by natural populations in cave ecosystems, especially those form the karst, calcareous caves, which produced several small niches and holes where high humidity is guaranteed and organic matter (from primitive humans, canids or just animals felt by accident) could accumulated.

We chose to run the experiment in a semi-natural environment, in a mini shade greenhouse space, fully closed with a thin mesh, with temperature and humidity kept above 25oC and 70% (varying from around 80 to 60% from rainy to dry season), but exposed to natural light variation, in order to allow de description of daily changes in behaviour influenced by natural circadian rhythm. Also, due to the natural time taken for females from blood feeding, reproduction, transferring to the experiment until death, and the organization of the next experiment under the same conditions, we had to deal with seasonal variation. Despite an electric heater kept turned on along all time, and the container which was able to keep humidity

above 80% most of the time, the repetitions established into the dry season resulted in much less oviposition or other behaviours.

As we intended to reproduce the natural conditions in cave environments, we did measures of the gradient of humidity from six different locations within a cave, measuring lower and higher relative humidity for 30 minutes. We chose the Lapinha Cave, Minas Gerais State, (19°33'42"S, 43°58'98"W), a well-known cave with a long term established population of *L. longipalpis*. We measured at 09th May 2023 (early dry season) between 10 am and 13 pm, with an internal temperature of 20.5°C and 25.5 °C in the external environment. The capacity of a cave to retained humidity was even stronger than our experimental conditions, as the average within-cave humidity was 78% (varying from 60% to 92%) while externally, at the hottest hours of the day, was 41%, thus this cave maintained nearly the double humidity than the external environment.

As hen houses are known modern habitats for this species, we tested in separate chicken feces and dog feces attraction, to verify whether a modern population could be substantially better adapted to an urban, exotic food source. We found that out of 1,288 eggs, 55% was laid on chicken feces, suggesting no barrier for the habitat change from canid dens to hen houses, in the modern days.

### *3.2.3.1.2 Oviposition group behaviour: avoidance of fungi hyphae entanglement or collective choice of suitable sites?*

The rapid growth of fungi seems to kill immatures by trapping them, mainly the first instars. On the other hand, this species has fungivore behaviour, which was observed and suggested by the amount of trehalose (which helps in proteins and membrane protection) found in their guts (Vale et al. 2012). Thus, a greater number of first instar immatures could prevent trapping by hyphae entanglement due to fast fungi eating behaviour. Further, the oviposition choice could also benefit from a group behaviour of reinforcement up of an adequate site, as already described for this species (Dougherty et al. 1993) or *Aedes aegypti* (Abreu et al. 2015).

In order to test whether such grouping behaviour could produce a deterministic oviposition choice, based on detecting previous laid eggs, we set an experiment to simulate substrates with distinct egg densities. The hypothesis prediction is that there will be an optimum laying location choice based on a balanced amount of previously laid eggs, which could produce a greater number of immatures capable to control fungi growth or signaling a favourable oviposition choice, but also a threshold that could indicate excessive densities.

Dougherty & Hamilton (1997) had described dodecanoic acid as an oviposition pheromone for *L. longipalpis*. First, based on their experiment, we simulated an environment with a gradient of “egg concentration”. Then, we prepared different quantities of dodecanoic acid (SIGMA L4250-100G) dissolved in Hexane PA (SIGMA 270504-1L). In a plastic pot of 26 x 24 x 10 cm, 2kg of Paris plaster was used to fulfil 2 cm of depth, kept completely flat and regular. Along the laterals, in each corner and in the middle, holes of 2 cm diameter and 0.5 cm depth were made to accommodate filter circles soaked with Dodecanoic acid. In each circle, it was put 30 µl of Hexane containing the different quantities of dodecanoic acid: 300, 600, 1200, 2400 and 4800 ng, and only Hexane as control. These quantities are, according to Dougherty & Hamilton (1997), a variation from 750 to 12,000 eggs approximately. Considering in our experiments and also the above-mentioned authors, lab females lay an average of 50 eggs, thus we are simulating an oviposition from 15 to 240 females. We distributed the quantities in a way that the two lower concentrations and the control were closer together and the three higher concentrations likewise, in the opposite side.

From this preliminary result, we tested the existence of a threshold Dodecanoic acid concentration from which oviposition would be discouraged. Using the same pots in three replicates, now applying 14400 ng in one side and 28800 ng in the opposite side, and only Hexane as control in the middle. Considering 4800 ng was preferred than any lower quantity (see results) in the first essay, we tripled and again this quantity to saturate the environment. For this essay, we excavate three 20 x 0.5 cm crevices, as this species does prefer to lay eggs in hidden small spaces (Elnaiem & Ward 1992). As this is an area 3 times larger than the 3.14 cm<sup>2</sup> circles of the first essay, we spread 90 µl of acid dodecanoic dissolved in Hexane on filter paper strips posed on these crevices. Both experiments were made inside the colony room, at 80% relative humidity and 25°C, and with the plaster fully water-saturated, and with a nest roof to prevent excess water transpiration.

We also further tested whether insect density could affect the average number of eggs laid per female, thus, whether females could hold eggs and try to escape to a non-competitive environment. To do so, we left females in an environment until a certain number of eggs was laid, taking as reference the usual five days used for oviposition in the colony, and changed them to new clean pot for a longer period. With this, we aimed to verify likely density-dependent effect on the oviposition behaviour in artificial conditions that may affect our conclusions. Also, this experiment aimed to explain the fact that some of the previous replicates of the oviposition experiment ended with females dying with the abdomen full of eggs. We did 10 replicates of the usual 7.5 diameter x 5 cm depth reproductive pot used in the colony, and

tested the effect of density by means of a simple linear regression model, produced in MINITAB 21.3.

### *3.2.3.1.3 Larval survival analysis and substrate choices*

Experiments were built to test the capability of immatures to survive and develop into adults in the substrates offered in the oviposition experiment. Eight circular plastic pots of 17 cm diameter, and 6 cm depth, and covered with 2 cm of Paris plaster (average 484.7 gr per pot) were used. In each pot, six equidistant circular niches of 0.7 cm diameter and 0.5 cm depth were set along the border and on the plaster to accommodate the same substrates from the oviposition experiment. We produced two experiments, and in both we randomly sorted the sequence of substrates in the niches. Despite the controlled lab environment, each pot was rotated 180 degrees once a day, to avoid any uncontrolled conditions to favour accumulation of immatures in some particular position.

#### *A) 1<sup>st</sup> Experiment - Hatching and first instar choice of substrate and survival*

First, an average of 220 eggs were put in the centre of these pots, coming from 20 to 30 females' oviposition vessels from the UFMG colony. The amount of 1 ml of the smelly water (and a residual amount of organic matter) taken from the five tested substrates, and distilled water as control, were posed on each niche.

This experiment started with a pilot trial from 9th to 19th May of 2022, when necessary, adjustments were evaluated. For instance, because of fast growth of fungi on the niches half of the pots (four pots ~ 880 eggs) were left open to verify choices in a drier environment, which resulted in the definition of a humidity threshold of 70% relative humidity for survival. We found that around and below 70% eggs collapsed and did not hatch. Eggs re-watered, even after 14 days, were able to hatch, but immatures of first instar were also too sensitive and died resected below and around 70% relative humidity. We also realized that first instar individuals moved around quite more than expected, not staying in a selected niche.

As most immatures walked along the pot wall, we took a subset of approximately 2,000 eggs from the colony and set a complementary experiment, in a rectangular plastic box (37 cm x 26 cm) covered with 2 cm of plaster. In two corners of the recipient, the typical colony food was put at 32 cm from the eggs, put in the opposite side. When hatched, immatures were left to walk along, being the usual behaviour to walk close to the borders. We observed the capability

to walk at least up to one metre per day, but due to limited capacity to set a systematic observation, an exact longest distance was not established.

Then, after implementing adjustments based on the pilot experiments, two repetitions of the full experiment were set: from 15th June to 11th July. On 25th June, due low hatching, a re-entrance of eggs was made; then from 14th July to 17th September 2022. The immatures were observed and counted in each niche or walking freely between the niches, and the experiment stopped after second instars were detected. Regardless the residual amount of organic matter placed in this experiment, due to the fungi growing on these, the immatures were capable to survive and exchange to a new instar, but in low numbers. The results were analysed in a contingency table and using Qui-Square test.

### *B) 2<sup>nd</sup> Experiment - Last instars survival and pupae in contrasting substrates*

Finally, using the same pots after cleaned and disinfected, we set an experiment to investigate whether third and fourth instars could be able to finish development and become adults on the tested substrates. After setting the substrate's distribution using the same criteria of the previous experiment, we put approximately 1 g of each, in this case, not macerated but intact pieces (mouse leg, a decaying leaf, piece of feces stool). From 02nd to 14th September 2022 the number of individuals per substrate and walking in the pot were counted, as well as the number of pupae. At this later date, more than half individuals had pupated and the first adults appeared, preventing a safe counting. The pots were frozen for a final counting on immatures, pupae and adults. The results were analysed in a contingency table and using Chi-Square test.

#### *3.2.3.2 Ferritin phylogeny and differentiation among Diptera species*

We predicted that organic matter produced by predators' dens should be rich in heavy metals released from prey bodies in decomposition and digested tissues in feces, especially iron (Fe) salt in their free form or attached to Heme groups. Therefore, we predicted that the capacity of immatures to deal with excessively contaminated resources might request some distinguished molecular response. Ferritin is a well know protein involved in transporting of Fe from the ingested blood to the ovarium in hematophagous insects, and thus is a key protein for the production of eggs after blood feeding (Geiser et al. 2019). As it is also induced by exposition to the Fe and are described expelling out the cells attached to excess of metal (Geiser et al.

2019), it is a likely protein involved in processing excess of Fe in the immature's digestion of metal-rich organic matter substrates. We produced a phylogenetic tree to verify whether *L. longipalpis* could have distinct ferritin protein from other hematophagous Diptera taxonomies, as well as whether *L. longipalpis* ferritin could somehow differentiate further, as an adaptative response to the immature niche associated to predator's organic matter.

In other to do so, we survey BCM and VectorBase data for all hematophagous Diptera with genes for ferritin available (and *Drosophila melanogaster*). However, species with an excessive number of internal ORFs, suggesting a weak notation, as *Aedes* and *Hermetia* species, were removed. As this is a composed protein, with a heavy and light chain submitted to distinct natural selection histories, we built a phylogenetic tree for each chain and for both combined. We also search for ferritin orthologues and syntenies between *Phlebotomus papatasi* and *L. longipalpis* (using *D. melanogaster* as outer group), in order to explore conservative genes between these genera within Phlebotominae.

The evolutionary history was inferred using the Minimum Evolution method. This method assumes that the tree with the smallest sum of branch length estimates is the most realistic one. The bootstrap consensus tree inferred from 2000 replicates (Felsenstein 1985) is taken to represent the evolutionary history of the taxa analyzed (Felsenstein 1985). Branches corresponding to partitions reproduced in less than 50% bootstrap replicates are collapsed. The percentage of replicate trees in which the associated taxa clustered together in the bootstrap test (2000 replicates) are shown next to the branches (Felsenstein 1985). The evolutionary distances were computed using the number of differences method (Nei & Kumar 2000). and are in the units of the number of amino acid differences per sequence. This is an unbiased estimate of evolutionary distance, thus appropriated for this analysis (Rzhetsky & Nei 1992). The ME tree was searched using the Close-Neighbor-Interchange (CNI) algorithm (Nei & Kumar 2000) at a search level of 1. The Neighbor-joining algorithm (Saitou & Nei; 1987) was used to generate the initial tree. The ME tree was searched using the Close-Neighbor-Interchange (CNI) algorithm (Nei & Kumar 2000) at a search level of 1. The Neighbor-joining algorithm (Saitou & Nei; 1987) was used to generate the initial tree. This analysis involved 15 amino acid sequences. All positions containing gaps and missing data were eliminated (complete deletion option). There was a total of 85 positions in the final dataset.

Finally, to verify whether the *L. longipalpis* ferritin was derived or have evolved differently from other sandfly species non-transmitting Visceral Leishmaniasis, we compared *L. longipalpis* with *P. papatasi*, using *D. melanogaster* as an outer group. The same previous Minimum Evolution method was used, but in this case, the analysis involved seven amino acid



sequences. The coding data was translated assuming a Standard genetic code table. All positions containing gaps and missing data were eliminated (complete deletion option). There was a total of 120 positions in the final dataset. Evolutionary analyses were conducted in MEGA11 (Rzhetsky & Nei 1992). Further, we then adjusted a Timetree analysis using the RelTime method.

A timetree inferred by applying the RelTime method (Rzhetsky & Nei 1992; Felsenstein 1985) to the user-supplied phylogenetic tree whose branch lengths were calculated using the Maximum Likelihood (ML) method and the Tamura-Nei substitution model (Nei & Kumar 2000). The timetree was computed using 4 calibration constraints. The Tao et al. method (Saitou & Nei; 1987). was used to set minimum and maximum time boundaries on nodes for which calibration densities were provided. Confidence intervals were computed using the Tao et al. method (Saitou & Nei; 1987). Times were not estimated for outgroup nodes because the RelTime method uses evolutionary rates from the ingroup to calculate divergence times and does not assume that evolutionary rates in the ingroup clade apply to the outgroup. The estimated log likelihood value of the tree is -739.77. This analysis involved 7 nucleotide sequences. All positions containing gaps and missing data were eliminated (complete deletion option). There was a total of 117 positions in the final dataset. Evolutionary analyses were conducted in MEGA11 (Tamura et al. 2021). Evolutionary time and time interval between the appearance of each species were taken from Timetree.org Initiative (<http://timetree.org/>).

Complementarily, we produced a NBCI's global alignment (<https://blast.ncbi.nlm.nih.gov/Blast.cgi>) between *L. longipalpis* and *P. papatasi* ferritin genes, and then between the two *L. longipalpis*' ferritin genes. Based on the time of separation between these genus (<http://timetree.org/>; Sterverding 2017), we estimated a time interval when most likely the ferritin gene duplicated in *L. longipalpis*.

### 3.2.3.3 Biogeographic overlap between Holocene humans, *L. longipalpis*, foxes and cave-rich ecosystems

South America has a diverse and abundant number of caves (Jansen et al. 2012). According to governmental survey, Brazil has documented caves in 995 municipalities (<https://www.gov.br/icmbio/pt-br/assuntos/centros-de-pesquisa/cecav/>), which correspond to 18% nationwide number of municipalities. Rocha et al. (2019) pointed out a total of 16,089 known caves, 68% of them are limestone caves (Brazilian Karst), and 49.7% found in the savanna (Brazilian cerrado) vegetation, where *L. longipalpis* predominates, along with the two

fox species (*Cerdocyon thous* and *Lycalopex vetulus*) which are incriminated as reservoirs for VL. Also, according to Goldberg et al. (2016)'s kernel density distribution of humans during the Holocene in South America (13,000 to 4,000 BP), their occurrence overlap quite substantially with biogeographic regions with abundance of caves.

Considering the Forattini (1973) original description of *L. longipalpis* distribution in rocky soils, caves and shaded creek valleys, and the results of our study on the immature susceptibility to low humidity, we expect that caves, due to their high air humidity, must be a key habitat for this species within xeric biomes as the savanna and dry forest. Considering the organic matter in caves now-a-days, from dead small animals trapped in holes to feces of carnivore dens in various small cave entrances, we predicted this sandfly species still have some connection with such natural habitats. Although in modern times most of *L. longipalpis* samples are found in urban areas (Pasquali et al. 2019), we expect them to happen in locations with similar ecological conditions of den-like habitats, i.e., neighbourhoods experiencing poverty with spots of soil and water contaminated with rich organic matter, from dog feces to open air sewage, and more exclusively in wet, and protected dwelling spaces. Moreover, we predicted that most vulnerable cities to VL should be in the vicinities of cave-rich ecosystems.

To test this hypothesis, we first verified whether *L. longipalpis* distribution might be restricted to those biogeographic regions rich in caves, testing presence or absence of the sandfly in function of cave abundance. We used the coordinates of all recorded samples of *L. longipalpis* in the Fiocruz data base (<https://specieslink.net/search/> samples from 1956 to 2015) and the known cave location from ICMBio/CECAV database (<https://www.gov.br/icmbio/pt-br/assuntos/centros-de-pesquisa/cecav/>). Cities with confirmed occurrence of the species and no record in Fiocruz's database were also added (taking the core coordinate of the city) to decrease sampling bias. We used municipality as territory unit as this is the most reliable scale, but also corrected by neighbour caves. For each occurrence of *L. longipalpis* we associated the number of caves in its municipality, and then checked by actual cave proximity matching each sampling location with the cave occurrence within a radius of 100 Km. Caves found in neighbour municipalities within this radius were summed up for that sandfly occurrence. All remaining Brazilian municipalities with no sampling or confirmed records of *L. longipalpis* were added as a "zero" occurrence, and the species distribution tested with a logistic regression, in MINITAB 21.3.

Finally, we tested the overlap in the distribution of *L. longipalpis*, *C. thous* and *L. vetulus* with the Holocene humans. For such we built a nonmetric multidimensional scaling (NMDS) analysis for all four species together and also for *L. longipalpis* and humans in separate, using

PAST 4.13. As a simple dissimilarity matrix-based and non-metric method, it is adequate to take coordinates as environmental variables and so scale up species by similarity in their positioning (Somerfield et al. 2021; Hammer 2023). We tested the models with an Permutational Multivariate Analysis of Variance (PERMANOVA), which compare groups of species and test whether their distribution centroids or spreading in space are different (Somerfield et al. 2021; Hammer 2023). As such, it is ideal test when dealing with different distribution of abundances, as *L. longipalpis*, which tends to binomial negative distribution, along with foxes and humans, that might follow Poisson or Poisson with overdispersion distributions. In addition, Kernel density maps were produced for each species base on the distribution in the database mentioned above and on the Goldberg et al. (2016)'s published database. All distributions were overlap with Jansen et al. (2012) projections of high potential for the occurrence of caves in Brazil. Maps were produced in Arcmap 10.3 using default search radius for sandfly and foxes, and a search radius of 660 Km for Holocene humans.

### 3.2.4 Results

#### 3.2.4.1 Experimental designs

##### 3.2.4.1.1 Female oviposition choices

A total of 5,704 eggs were laid along the experiment, with a large variation between experimental runs, but not significantly correlated to number of females per run ( $F_{1,3} = 0,007$ ,  $p > 0.05$ ). Experimental runs which were carried out in the dry season had 14 times less eggs per female than those with a similar number of females in the wet season. In the overall experiment, average number of eggs per female (mean = 5.14, varying from 0.87 to 18.9) was much lower than usually obtained in the current colony procedures. Testing female density in smaller pots as used in the colony, we found that eggs per female decreased significantly with female density (ANOVA,  $F_{1,7} = 13.5$ ,  $p < 0.005$ , on LN egg/female transformation), but still, the numbers were much higher than found in our, much larger, experimental container (mean = 25.9 eggs/female).

Furthermore, in an essay with 635 females split in six replicates, we found that an average of 43% of eggs may be retained and laid latter when surviving females (26% of females died in the first environment) were transferred to new, clean environment, against 55.6% laid in the first five days in the original environment (died leaving 1.2% of eggs left inside dead

females). Hence, both the average total eggs and eggs laid per female were not significantly different from early and late environment (Total, t test = 0.78,  $p > 0.05$ ; d.f = 10 – eggs per female, t-test = 0.12,  $p > 0.05$ , d.f. = 10). Considering, though, that more females survived until the transferring to the second environment than died early after a sole oviposition (t-test = 4.4,  $p < 0.001$ , d.f. = 10), it is clear that this species has the strategy to search for new oviposition locations and so spread-out progenies the maximum they can. Consequently, the first oviposition site might never accumulate but less than half eggs a cohort can spread in nature.

As our oviposition choice experiment showed clear substrate preferences (see below), we expect that after the best locations are overtaken by previous laid eggs, females tried to go to a more distant location and died in the process. As our container allowed a wide flight and more natural behaviour, females might have responded to an imprint impulse to lay a certain proportion of eggs and fly to other places. The colony's small oviposition pots impose, on the contrary, a stressed condition that could induce an atypical, urgency to lay most of eggs before dying in an overcrowded space.

Oviposition was significantly different between substrates, regardless date (Chi-square = 613.3;  $p < 0.0001$ ; d.f. = 5). In the wet season, fresh feces and decomposed mice attracted more oviposition than control, which received, though, more oviposition than leaf litter and fresh mice. In the dry season, oviposition occurred more frequently in fresh mice followed by pure water and decomposed mice. The search for pure water added up to 23% of the total. Decomposed feces were hardly chosen, while oviposition on leaf litter varied seasonally (Figure 2).

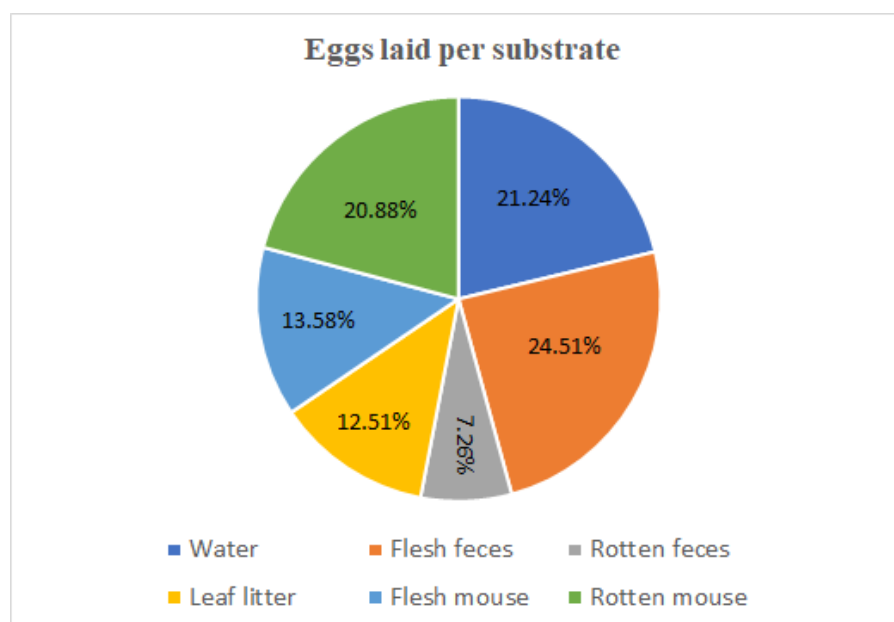


Figure 2 – Distribution of *L. longipalpis* oviposition choice per organic matter substrates, across the whole experiment run, from February to July 2023, across seven essays.

### *3.2.4.1.2 Oviposition group behaviour: avoidance of excessive fungi growth VS collective choice of better sites*

For the first experiment, a total of 1236 eggs were laid, 1081 fittingly inside the experimental slots. The egg distribution was disproportionately greater in the three higher concentrations than in the two lower and the control, with 73.6% of eggs in the slots simulating greater previous oviposition (Chi -Square = 344.4,  $p < 0.0001$ , d.f. = 12), being 30% of total eggs laid in 4800 ng, and 35% in 2400 ng, and 8.6% in 1200 ng. Still, as in the experiment of oviposition choices on substrates, the control (only water slot), showed 9.5% preference, suggesting that after preferred places are taken, the best oviposition place is a moist place. This result corroborates our hypothesis that a very aggregated oviposition pattern might take place in nature, based on a greater advantage of aggregated immature behaviour, eventually controlling fungi growth, or some other adaptative advantage.

Further, we aimed to explain why in our experiments a large number of females preferred to die trying to escape from the experimental container than to lay eggs. Our second assay with dodecanoic acid doubled from the best-chosen concentration for oviposition found in the first assay, thus placing 14400 ng in one side (best choice in the first assay) and 28800 ng in the opposite one. In the three replicates, an irrelevant number of eggs was laid, a total of only 316 eggs. Although 60.75% of these eggs were found in the 320 ng/ml side, the most relevant result was the substantially less eggs than expected from the total of females put in the experiment. While in the first assay only 34% of the females died with the abdomen full of eggs, in this one 95.2% of females died packed of eggs, thus suggesting an urge to escape to another oviposition site.

This result corroborates that even though aggregate oviposition behaviour is a selected trait, it has a clear threshold, likely based on competitive costs of excessive eggs in only one location. Indeed, our assay on eggs laid per female in function of female density showed that the number of eggs laid per female decreased significantly with the number of females in a same pot ( $y = -0,0028x + 3,5966$ ;  $r^2 = 0.67$ ;  $F_{1,8} = 13.53$ ;  $p < 0.01$ ; Figure 3). The experiment of oviposition in two environments showed that the number of females fully laying eggs and dying in the first seven days was smaller than those surviving with eggs inside for longer (Student T test,  $t = 4.37$ ,  $p < 0.001$ ). Although the number of laid eggs per females was greater in the first habitat (Student T test,  $t = 3.2$ ,  $p < 0.05$ ), the larger number of females moving to a new location and then laying eggs, resulted in a statistically equivalent number of eggs laid in

the first and second habitat (8,195 vs 6,358 eggs, respectively; Student T test,  $t = 0.78$ ,  $p > 0.05$ ), corroborating the hypothesis of a threshold for aggregated oviposition, which forces dispersion and a subdivided oviposition.

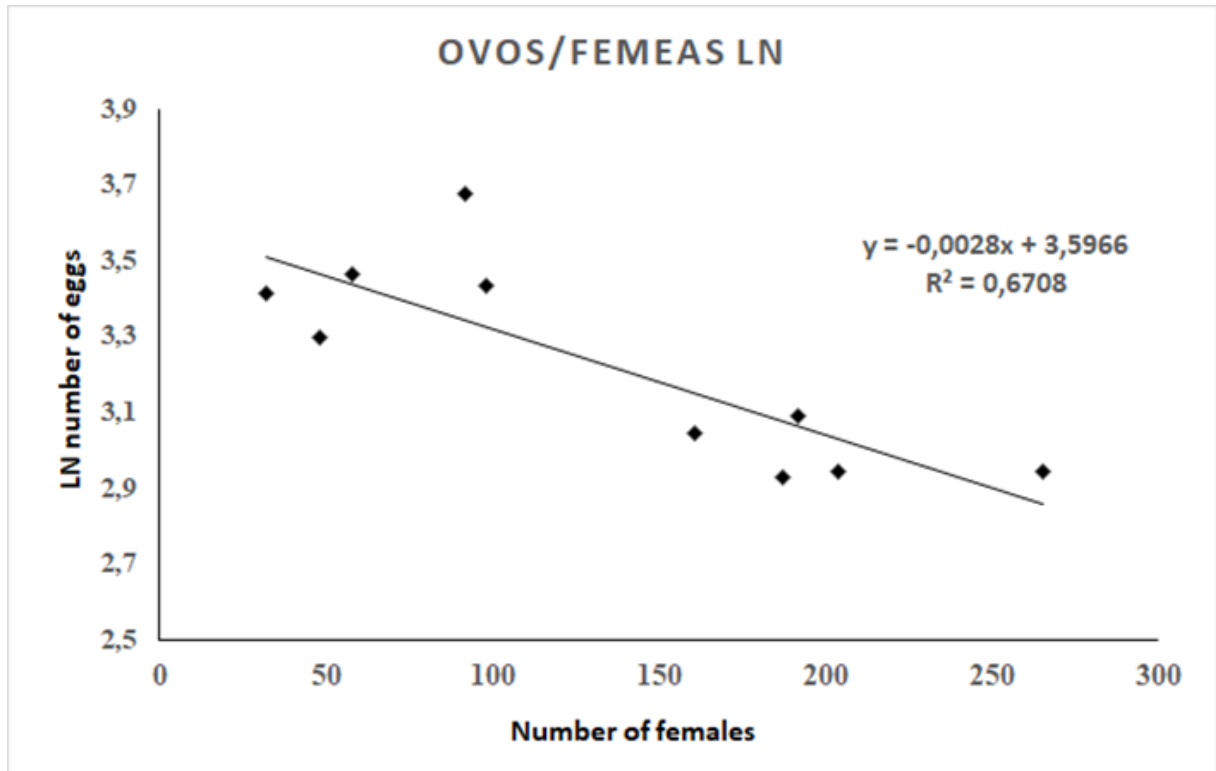


Figure 3 – Number of *L. longipalpis* eggs laid per female (natural logarithm transformed) in an experiment with contrasting densities of females in a same volumetric space.

#### 3.2.4.1.3 Larval survival analysis and substrate choices

##### A) 1<sup>st</sup> Experiment - Hatching and first instar choice of substrate and survival

The experiment last from 02 July to 17th August 2002. The distribution of the first instar immatures varied significantly between substrates at each date (Chi -square = 66.78,  $p < 0.001$ ; d.f. = 5), but did not show a consistently preferred substrate until 25th July. Early emerged immatures were highly vagile, walking an estimated 30 cm per day and then shifting from one substrate to the next. Nevertheless, from 27th July they stayed on rotten mouse corpses where most died.

### B) 2<sup>nd</sup> Experiment - Last instars survival and pupae in contrasting substrates

Running from 03rd to 14th September 2022, the substrate choice by last instar varied along the experiment. After five days, most immatures were found on fresh or rotten feces and leaf litter (Chi-square = 16.2;  $p < 0.001$ ; d.f. = 5), but such initial choice was not consistent until the end of the experiment, when those that did not die pupated on any substrate, where emerged as adult (Chi-square = 7.8;  $p > 0.05$  d.f. = 5). Interestingly, though, this experiment showed that these immatures can develop and emerge as adult on dead corpses or feces, both rotten and fresh, evidencing the capability to cope with the chemical composition of these substrates (Figure 4). Along the experiment, immatures were observed eating directly on feces or mouse flash, as well as on fungi. Our observations reinforce the well-known behaviour of fungivory, but also proved this is part of a range of generalist feeding behaviour.



Figure 4 – Fourth instar, pupae and emerged adult found in the remaining of the rotten mouse carcass. They were seen feeding directly from the flesh, and finished their life cycle in this spot. Only bones and hairs were left over.

#### 3.2.4.2 Ferritin phylogeny and differentiation among Diptera species

The phylogeny showed ferritin as a very conservative protein, potentially kept across species radiation by significant purifying selection. Similar conclusions are valid for light and

heavy chains, which evolved as clearly separated branches, and with distinct similarities among taxonomies (Figure 5). For the heavy chain, our tree showed a greater similarity between the sandfly species and the Brachycera species than to Culicidae species. Psychodidae/Phlebotominae belongs to suborder Nematocera along with Culicidae, but is a much older Family than the latter, as well as it is the whole Brachycera suborder (Grimaldi & Engel 2006). Conversely, genome tree for the light chain, Brachycera and Nematocera were fully separated, and those from the two Phlebotominae species were closer to those from Culicidae species (Figure 5).



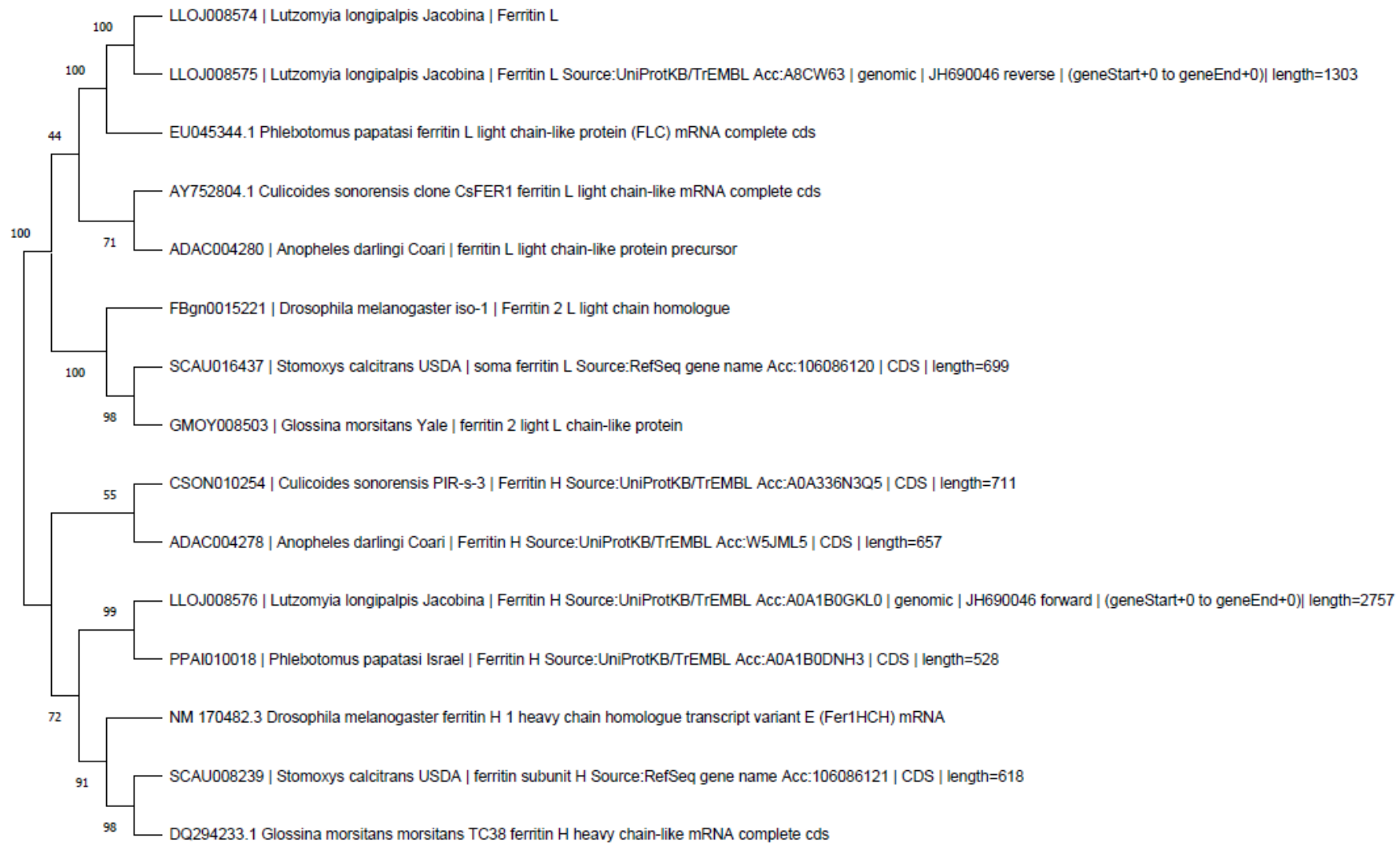


Figure 5 – Rooted tree inferred using the Minimum Evolution method for both Ferritin Heavy and Light chain of hematophagous Diptera species.

Further, we found two copies of the light chain gene in *L. longipalpis*, not found in other species. The overall tree showed with high confidence the separation of the two light chains from *L. longipalpis* to that one in *P. papatasi*. Also, the *L. longipalpis* two independent light chain genes showed no synteny with ferritin chains from other species, neither with *P. papatasi*, differently to the heavy chain (Figure 6). Then, we tried to estimate the time of duplication. From the TreeTime produced with RelTime method we could not estimate time from each branch separation, as divergence between proteins were too low for a robust calculation (Figure 7). Thus, we used the estimate times from the origin of *Phlebotomus* and *Lutzomyia* genera (<http://timetree.org/>; Sterverding 2017), and the NCBIs Global Blast to compare the dissimilarities between these species' ferritin and the two *L. longipalpis* ferritin genes, and so be able to approximate a date of duplication. *Phlebotomus* appeared between 23 to 34 Mya before *Lutzomyia* and summed up 131 substitutions in the ferritin gene comparing to each other (81% identity), while the two ferritin in *L. longipalpis* has only 7 substitutions, suggesting a very recent duplication or a strong purifying selection (indeed, the proteins produced are identical). Hence, we assumed that only substitutions in the third, neutral, nucleotide in a codon may have survived, by extrapolation and using weighted average (to ponder all possible substitutions and combinations in the three codon positions) to calculate a time for the duplication. We found that this duplication appeared between 3 Mya to 3.6 Mya, around the time the genus invaded South America through the Panama Isthmus

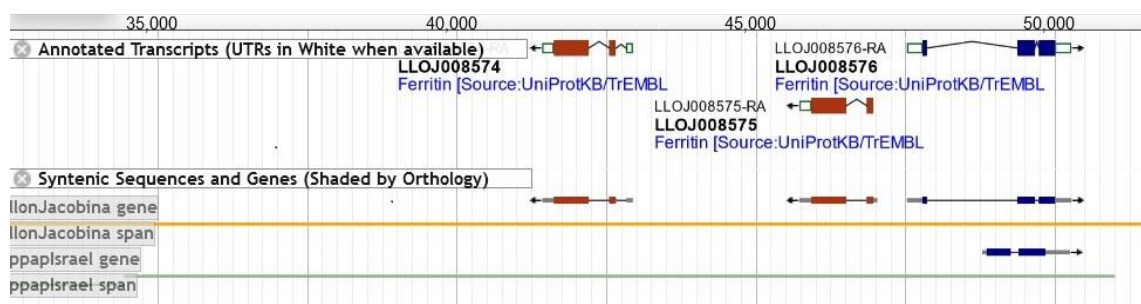


Figure 6 – Annotated transcripts and syntenic sequences for genes of Ferritin from *Lutzomyia longipalpis*. Light chains in red (LLOJ008574 and LLOJ008575) and Heavy chains in blue (LLOJ008576).

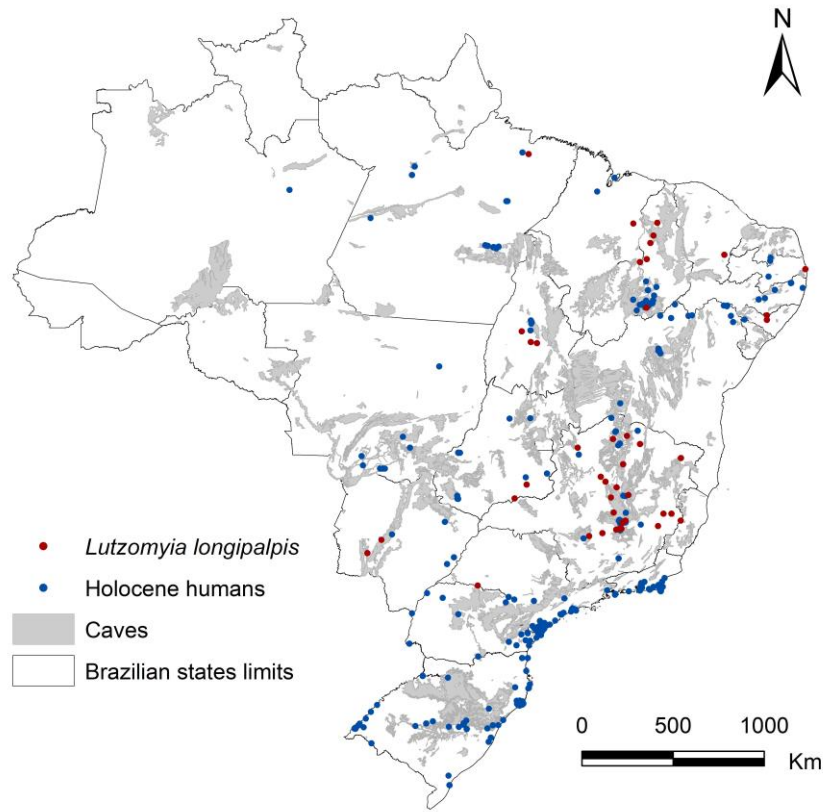


Figure 7 – TreeTime produced with RelTime method, taking *L. longipalpis* and *P. papatasi* against the Brachycera genera *Stomoxys* and *Glossina*, and *Drosophila melanogaster* as an outer group (non-hematophagous Diptera).

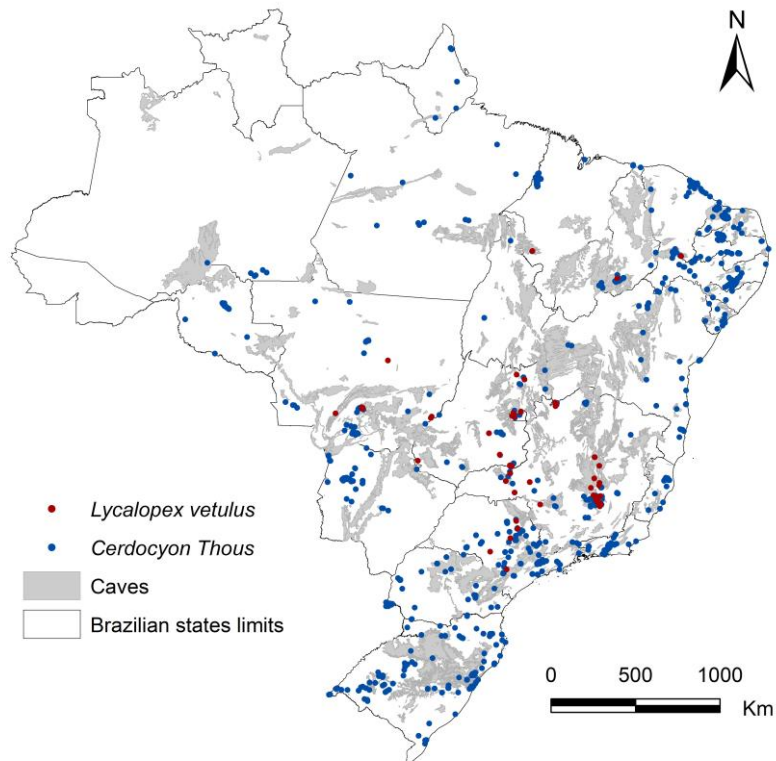
### 3.2.4.3 Biogeographic overlap of Holocene humans, *Lutzomyia longipalpis* and foxes distribution to cave-rich ecosystems

*Lutzomyia longipalpis* were significantly more frequent in municipalities with caves or at least 100 Km nearby a cave in a neighbour municipality (logistic regression:  $y = -4.67 + 0.00436 \cdot \text{number of caves}$ ; Chi-Square = 15.33,  $p < 0.0001$ , d.f. = 1). Also, this sandfly species showed a significant overlap distribution with Holocene humans and the two foxes species incriminated as reservoirs of *L. infantum* (Figure 8). The human distribution in the Holocene, as presented in Goldberg et al. (2016), was clearly broader than around the caves, namely spreading in coastal areas and inner wetlands, such as the Pantanal Matogrossense in Centre-West, or the Marajo Island, in the amazon river mouth. Nevertheless, these regions were colonized in a second moment after the Holocene cave period (estimated to have finished around 4,000 BP), when a more predictable, though drier, climate was widely established. These lowlands and wetlands were then occupied by new migrating populations, namely the Tupi-Guarani linages, but were not actually too far from the complex cave system of the Central Brazilian plateau, especially the karst caves, as large fluvial and wetland systems are entangled around the large biogeographic regions covered by caves.

These regions also overlap with the present-days distribution of the two foxes species which are pointed as reservoirs of VL, *C. thous* and *L. vetulus* (Figure 8). However, both foxes' distribution were significantly different than *L. longipalpis* or Holocene humans, as they occupy a much larger territory than the pair *L. longipalpis*-Holocene humans (PERMANOVA  $F = 3.34$ ,  $p < 0.007$ , Figure 9). Then, the exclusion of the foxes from the NMDS analyses showed no significant difference in the distributions of present days *L. longipalpis* and Holocene humans and caves (PERMANOVA 0.51,  $p > 0.5$ , Figure 10). The expected distribution of all four species strongly suggest that coexistence must have existed among them in many locations in the central Brazil, and for quite some time (Figure 11).



Datum: SIRGAS 2000  
Projection: Geografic Coordinate System (South America)



Datum: SIRGAS 2000  
Projection: Geografic Coordinate System (South America)

Figure 8 – Distribution of Holocene humans, *L. longipalpis* (A), *C. thous* and *L. vetulus* (B) overlap with the expected distribution of caves in Brazil.

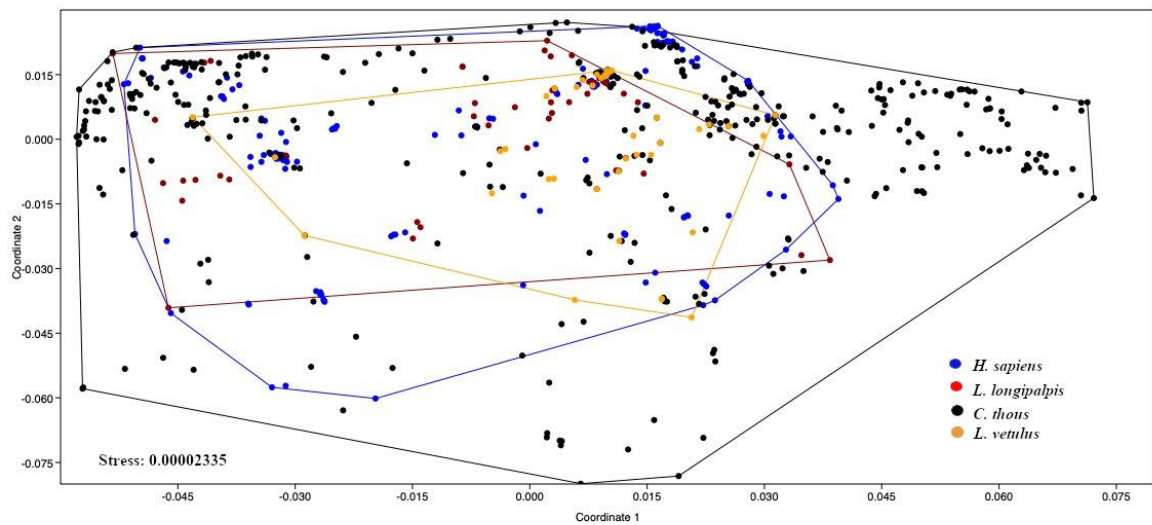


Figure 9 – NMDS from coordinates of occurrence of Holocene humans, *L. longipalpis*, *C. thous* and *L. vetulus*. The coordinate axes are the collapsed information from original multivariate factors, in this case, the geographical actual coordinates for each location where species were recorded. These combined coordinates created by rank orders allow statistical comparison of co-occurrences.

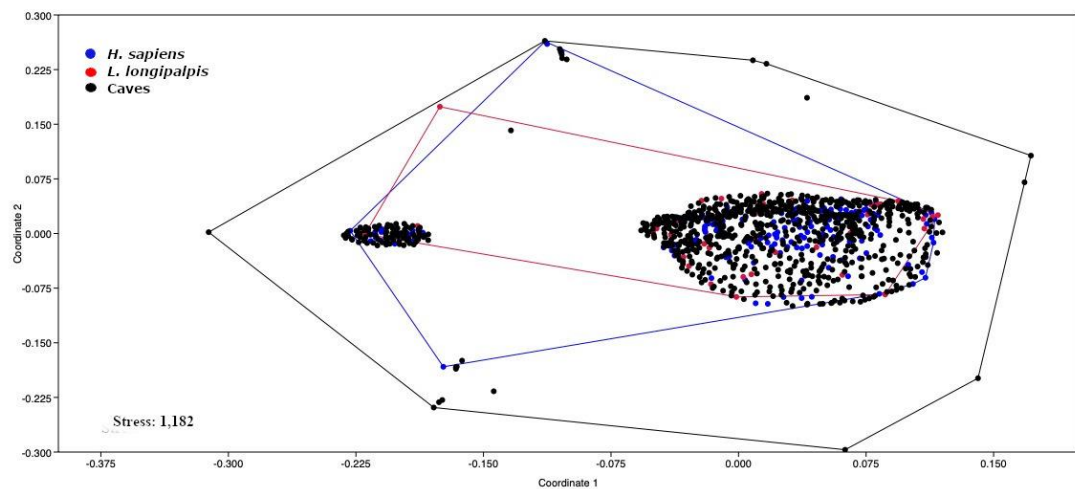


Figure 10 – NMDS from coordinates of occurrence of Holocene humans, *L. longipalpis* and caves. The coordinate axes are the collapsed information from original multivariate factors, in this case, the geographical actual coordinates for each location where species were recorded. These combined coordinates created by rank orders allow statistical comparison of co-occurrences.

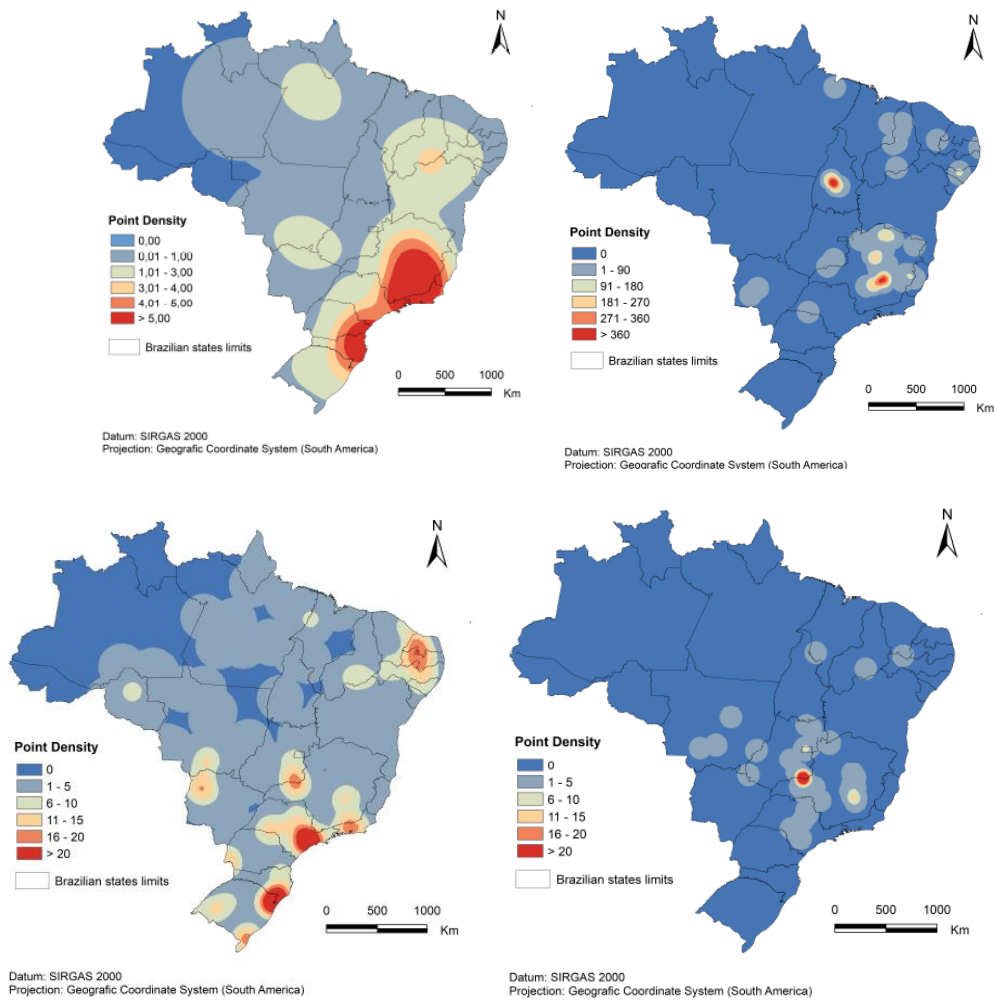


Figure 11 – Kernel maps for the Holocene humans, *L. longipalpis*, *C. thous* and *L. vetulus* overlap with the expected distribution of caves in Brazil. Point densities show the regions with the highest to the lowest occurrence of each studied event.

### 3.2.5 Discussion

Regardless the difficulty to produce verifiable evidence of a pre-historic association between *L. longipalpis* and humans in caves, we found enough ecological and historical requisites for its existence, so that this work raised acceptable inference from tangible evidence (*sensu* Wallach 2019). From oviposition behaviour, immature development on carnivore originated, metal-rich, organic matter, both carcasses and dog feces, to its very restrict distribution in the vicinities of cave abundant ecosystems, there are evidence that, at least, this might be a species fully associated to canids, and those are likely to have been associated to human vicinities since the Holocene (Perri et al. 2021; Serpell 2021).

The event of ferritin gene duplication in this species could have been an evolutionary driver for immatures to associate to a much richer and iron-contaminated organic matter than

what is found in rodent burrows. As such duplication might have happened around the time *L. longipalpis* and canids invaded South America, one may expect foxes- *L. longipalpis* to be an evolutionarily well-established interaction. Ferritin is a protein with translation induced by excessive ingestion of iron and helps to decontaminate cells by been expelled out in faeces after attached to this metal (Geiser et al. 2019). This protein is key for the hematophagous diet in insects but may have an extra function for immature development in *L. longipalpis*.

The data on *L. longipalpis* and foxes' distribution showed a clear association of these species with cave habitats where, in the past, human had a consistent occupation. For instance, the oldest South America skeleton, Luzia, a 10,000 years old women, was found in a cave few kilometres from the cave where is found the well-studied FIOCRUZ *L. longipalpis*, the Lapinha population. This macro-region is also a hotspot for visceral leishmaniosis in Minas Gerais State, including the State capital, Belo Horizonte city (in a municipality with 29 natural caves). Fox dens are found in the crevices and holes around and in the entrances of this particular cave system. In one particular fox den in Lapinha cave, we sampled *L. longipalpis* females around feces in the early morning, when they are harder to find dropped inside the cave (Figure 12a).

Likewise, these caves are abundant in natural pitfalls for small mammals, and a reasonable number of rodent skeletons are normally found (Figure 12b). These could be the necessary source of organic matter inside the cave for this sandfly species now-a-days, and in a much lesser competitive environment, as few insect species tend to be found within caves, even in the tropics (Culver & Pipan 2018). An unknown ecological aspect is how these small sandfly immatures deal with corpses/feces natural succession, which involves much bigger and abundant fly species in open areas (Silva et al. 2014). In fact, other *Lutzomya* and related Phlebotominae species are known to be cave-specialists and are just not studied enough (Almeida et al. 2019; Teodoro et al. 2021; Dutra-Rego et al. 2022). Caves are likely to provide ecological niche for several species of this genus, as far as a considerable source of organic matter is found closer to the entrances. Concerning *L. longipalpis*, our findings on oviposition choices, group behaviour, along with the behaviour of splitting oviposition into subgroups laid separately in space, are quite compatible with an adaptation to this habitat and scattered resource distribution.



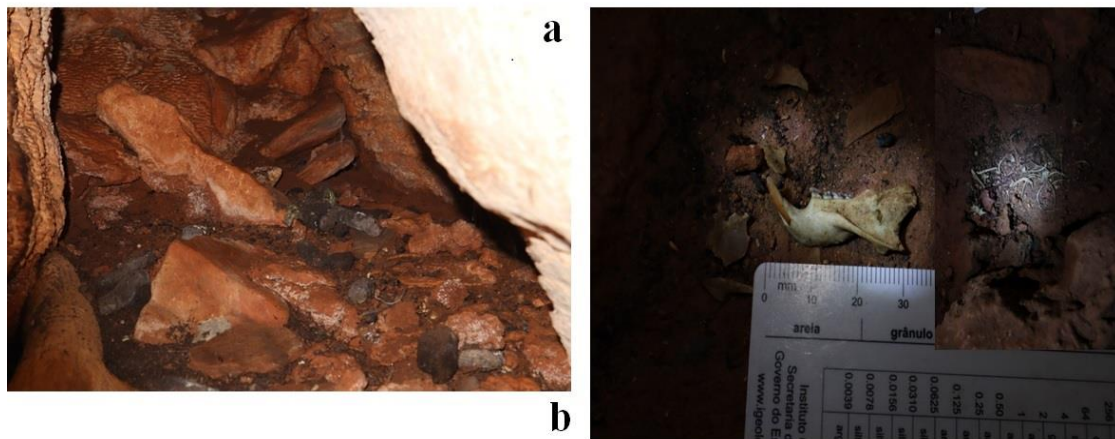


Figure 12 – Surrounds of Lapinha Limestone cave, showing several fox dens or latrines, which are open to outside (a), and rodent carcasses felt into natural pitfalls (b), nearby some entrances.

The likely association with Holocene humans was certainly after a pre-established association of the *L. longipalpis* with ancestor of the two fox species here mentioned. Here, we assumed the possibility that this sandfly species invaded South America following an interaction with an ancestor canid (likely a direct ancestor to the *Lycalopex* genus or a *Cerdocyon* species), as both events are dated to the same period (Sterverding 2017; Chavez et al. 2022). The accepted scenario is that canids spread thru the continent following xeric habitats, as savanna predominated (and thus ecological filter) by that time in the Panamanian corridor (Chavez et al. 2022). A savanna route could have been decisive for the widespread and radiation of most South American foxes around 1.0 Mya, when dry Pleistocene periods made savannas predominant in the whole continent (Webb 2006; Chavez et al. 2022). The hypothesis of *L. longipalpis* spreading towards its present days' distribution already in association with fox species is quite compatible with the “savanna route” hypothesis, assuming the existence of some level of mesic microhabitats around dens, eventually within gallery forests (Forattini 1973; Costa et al. 2013), for the immature development. After, this interactive pair of species may have occupied the rock-shelters and cave habitats along the Brazilian central plateau, from south to north, where they are found today. Much later humans arrived, and likely due to climate unpredictability during the Younger Dryas (from 12,999 to 11,700 BP) started to occupy sheltered habitats as caves (Feathers et al. 2010; Bueno & Isnardis 2018). Peopling around caves were intensified in early Holocene, from 10,000 to 9,000 BP (Bueno & Isnardis 2018). Thus, our hypothesis is that humans stepped into this fox-sandfly habitat, transformed it into a much more eutrophic, and full of predictable organic matter spots, to which *L. longipalpis* may quickly adapted.

Considering that *L. longipalpis*, *C. thous* and *L. vetulus* were there much earlier than the first humans, we must have just added a layer into this interactive system, and easily became an additional host and habitat source for *L. longipalpis*. If so, later human new wave of Tupi-Guarani migrations towards wetlands (Souza et al. 2020) must have created the ecological conditions for this species to have followed humans up to new, tribe-transformed habitat. *Lutzomyia longipalpis* could have adjusted to human settlements and wastes accumulated in mound-like constructions, and later moved to European rural colonies. This is a plausible narrative for the pattern of occurrence of this species along with *C. thous* in the Marajo Island in the modern days.

### *3.2.5.1 Wetlands with late Holocene indigenous' mounds as new habitat for foxes- L. longipalpis: revisiting the classical Lainson 's hypothesis on AVL evolution from foxes to dogs*

Lainson & Rangel (2005), after Lainson et al. (1990), supported the hypothesis that *C. thous* was the sylvatic reservoir of the AVL, which infected dogs in small rural farms close to primary forests, and then, humans. This well accepted hypothesis was built from a sample in the Marajo Island, in Salvaterra village, in a location nearby a so-called Primary Forest. However, being the Island previously highly occupied, the possibility of a pristine forest is remote, and even so, it could be a remaining of a largely human-modified environment, and one which is predominantly composed by savanna and wetlands, and not forests (Meggers 1954). Here we offered an alternative interpretation to their pioneering and important findings.

The Meghalayan chronozone climate transition, 4,200 BP, affected human population distribution, as pointed out by Bueno & Isnardis (2018) and Utida et al. (2020). These populations' contraction were, thousands of years later, substituted by the migration and arrival of the ancestral of Jê and Tupi-guarani groups (Goldberg et al. 2016; Souza et al. 2020; Utida et al. 2020). Especially the latter were able to deal with agriculture in the semi-arid, seasonal environments, and occupied wetlands from the Pantanal Matogrossense to, likely, Marajo Island (Souza et al. 2020). This people built mounds of large sizes to deal with their waists and debris, as well as to manage water flow (Schaan 2008). These human-modified, and organic matter-rich habitats could then have become the substitute for the original human-foxes cave habitats for *L. longipalpis*. Therefore, the case of Marajo, taken by parasitology literature as an example of a wide source of VL to humans, could not be sustained. Even the foxes as reservoirs might also be closely associated with human populations.

The Marajo Island was probably colonized around 3,100 BP. At the Marajoara phase the island could have reached up to 1 million people (Meggers 2001), with the summing up of villages and cities at the denser regions capable to accommodate up to 100,000 people (Meggers 1954). The Marajoara phase was a complex society of mound constructors and pottery makers, with intense landscape management and urban structures of up to 3,000 inhabitants each, lasted from 400 to 1350 AD (Schaan 2008). Such mounds seemed to have a common origin among several Guarani people (Gaspar 2000), although there are rooms for doubt about the ethnic group who occupied Marajo Island (Meggers 1954; Schaan 2008; Batista & Nogueira 2016;). The Guarani Mbya ethnic are well adapted to open vegetations and wetlands, been abundant in the Pantanal, Cerrado and some coastal regions (Souza et al. 2020). Therefore, quite overlapping with the distribution of both *L. longipalpis* and the *C. thous*.

In the case of Marajo Island, since 1620 the whole region was still heavily populated by native communities, but also taken by a combination of Portuguese, Dutch and English invaders, based on both official forts and settlements as well as pirates (Pacheco 2010). Mostly important, the Marajoara society (Nheengaíba nation) survived and resisted for 20 years of a war promoted by Portuguese (Bettendorff 1990; Pacheco 2010). Such war finished only when Jesuit missionaries were allowed in the island, promoting partially pacific annexation, in 1659 (Bettendorff 1990). Our main point here is whether the *L. Infantum* evolved in South America from the Gondwana or was introduced by the Portuguese infected dogs (mostly plausible hypothesis so far), it may have found a suitable interactive system to invade, based on *L. longipalpis* proximity to native, densely populated, human communities, opportunistic approximation of *C. thous* individuals to these anthropomorphic habitats, and then followed by the constant presence of European dogs.

Schaan (2008) also described an elitist society at the last Marajoara phase, which means the mounds were also rich in wasted food, probably most of their aquatic food, which could create both a rich substrate for *L. longipalpis* development as well as an attraction for the *C. thous*. In addition, there are reports on different Nations of Guarani ethnical groups who used to bury domesticated foxes of different species, highlighting the human-canid relationship (Prates 2014; Perri et al. 2021). Although *C. thous* has not been found with indigenous cemeteries, this species is among the most abundant ones in the savanna, or wetlands of Brazil, and might have been at least tolerated close to the Marajoaras and other Guarani Nations and communities. Even if domestication per se was never registered for this species, it was for several others, and may imply that foxes were, at best, tolerated around. The open question this

work leaves is that density of *C. thous*, as well as *L. vetulus*, could have been affected positively by the native human settlements.

Therefore, a recent adaptation to peri-urban and suburb habitats may never have happened from *L. longipalpis* populations coming from the wild, but from a direct spillover from primitive but still human-modified habitats, previously found in the same regions the species has been spreading now-a-days.

### 3.2.5.2 *The adaptation of L. longipalpis to a long extinct fox-human habitat in caves as a pre-condition to invade modern suburbs and habitats exposed to swage and dog waste*

Our experiments support that *L. longipalpis* might have evolved in association to organic matters related to predators, most likely, associated to canid dens or scattered sources within cave or in similarly mesic and sheltered conditions, depending on a combination of resources and hyper-humid microhabitats. Casaril et al. (2019) showed a clear vicarious process of ongoing speciation along a large geographical cline, in line with the Karst cave lines from North to South of Central South America. Such findings are in accordance with sympatric and clinal complex of *L. longipalpis* species, and incipient speciation process identified by Araki et al. (2009), using copulation song and pheromone analyses. Although Casaril et al. (2019) proposed a much older than Holocene date for the formation of this clinal geographic series, the later study suggest likely recent introgression between incipient species in peri-urban habitats. This is more likely an event possibly related to recent isolation, or possibility recently intensified isolation between populations.

The hypothesis of a cave-based system of sub-populations or ongoing speciation within the *L. longipalpis* species complex is compatible with a recent, Holocene, climatic change that may have isolated these subpopulations in the rocky and caves, after the surrounding vegetations became seasonal and air humidity much drier, since the Meghalayan chronozone, around 4,200 yrs BP (Utida et al. 2020). No authors explored the causes of the present distribution of this species complex, and a contraction of a previous larger and more continuous population, after overall climate drought or seesaw oscillation between drought-wet climate (Azevedo et al. 2021) during late Holocene could be an explanation.

The much older reproductive isolation markers detected along the wide biogeographic distribution of these sandflies, on the other hand, suggest that specialized cave/rocky dwelling immature habits could have constrained dispersion, especially if female relied on predictable organic matter-rich sites closer to human-foxes' territories. Important to notice, the cave-

related, lithic techno-complex civilization ended a densely populated and continuous phase around 8,000 yrs BP (Goldberg et al. 2016), when this so-called Itaparica Tradition became smaller and fragmented. If *L. longipalpis* became dependent on this human-made habitat, that may have contributed to the sandfly population retractions as well, before its adjustment to the newcomers human populations, as already described.

However, one most relevant fact to be discussed is that the parasitological literature ignored completely the existence of dense human populations in the South America pre-colonial times. The historical reports on Adolph Lutz's experiments, ideas, and field work, found in Benchimol & Jogas Jr (2020) leave few doubts on the origins of such European-centred view on the Tropical Medicine and interpretation of the landscape. In many cases, indigenous when taken into consideration, were just another poor rural gathering of people. Hardly the antiquity of the landscape occupation or the before-colonization much larger native populations were taken into consideration. These societies transformed dramatically the landscape, creating vast anthropomorphic environments (Carson et al. 2013), likely to sustain and favour both insect hematophagous as well as associated diseases. Such hypothesis may be a hard one to follow, due to the lack of robust data, or biological material for confirmation of these species co-existence in time and space. Still, there are methodological tools for such, and to understand the evolutionary origin of *L. longipalpis* could be vital for its control and should be seek.

All classic studies on Phlebotominae suggest that adult insect is obligately associated to vertebrate shelters (Sherlock 1996; Tatcher & Hertig 1966; Forattini 1973), or to stable, mild, humid, nitrogen-rich immature microhabitat, sheltered from sun and rain (Bettini 1989). However, the most ancient species of sandflies seemed to be better adapted to savanna and semiarid habitats (Akhoundi et al. 2011), as well as *L. longipalpis* in the South America (Forattini 1973). Hence, for these species the dependency of immature phases to a hyper-humid microhabitat must result in a whole life cycle of these species in nature obliged to vertebrate burrows as described for *Hyrax* in the Palestine (Salah et al. 2020) or canid dens, as we proposed here for *L. longipalpis*. Among these species associated to semiarid and savanna habitats, one will find all vectors of VL, for both *L. infantum* and *L. donovani*.

The well-known association of different VL sandfly vectors to hen houses, in both Old and New Worlds (Alexander et al. 2002; Svobodová et al. 2003), might have obliterated the interest in searching for a more natural habitat of these insects. Also, the present days association of these specific vector species in both Old and New World to urban habitats, may have undermined the interest in finding the wild origins of the species, which should be

associated to canid species, and eventually to the several convergent histories of canid domestication.

### 3.2.5.3 Was human-foxes-*L. longipalpis* interaction system a vacant niche for a European introduced *Leishmania infantum*?

Lysenko (1971) proposed the VL in the Old World is in the process of evolving from an enzootic natural jackal's disease to stages of semi-synanthropic, synanthropic and, finally, anthroponosis. The Indian Kala azar, transmitted only from people to the sandfly would be this last stage in the specialization of this disease to humans. The semi-synanthropic stage happened in Middle Asia (jackal-sandfly-dog-sandfly-man) and "Transcaucasia Europe" (fox-sandfly-dog-sandfly-man). Momen & Cupolillo (2000) argued that visceralizing *Leishmania* species as *L. tropica*, *L. infantum* and *L. donovani* complex had evolved in Africa as an anthroponotic parasite, hence, evolved in human populations.

While most tegumentar-cutaneous leishmaniosis seemed to have evolved and radiated from infecting wild rodents hosts in natural forests in the tropics, the systems VL-canines-humans may have evolved separately and in the north Africa and Mediterranean Europe. Nevertheless, for this host-parasite system to thrive, habitat-specific insect vector species also should have to adapt to the habitats created by humans, as well as by canine packs. In both cases, heavily eutrophic dens, caves, and primitive human-made litter and ceremonial mounds, rich in feces and carcasses may have shaped the environments around these vertebrate species (and also, may have been a main driver of canid domestication, see Serpell 2021), imposing specific selection on insects associated to such extreme conditions.

### 3.2.6 Conclusions

From our experiments and the literatures data on natural distribution of this sandfly species, it is reasonable to suppose that human settlements in caves, protected humidity sites, as deep valleys with creeks and rocks, typically found within the Cerrado ecosystem, could produce the expected hyper-humid microclimate for the immature development. Where these locations were associated to food waste, especially from hunting, all the conditions for the whole insect development could be in place. Contrary to previous works, we propose that this sandfly species could have existed close to humans much earlier European colonization, due to the opportunistic proximity of foxes to them, and the production of hyper-wet and nutrient rich

microhabitats around caves or primitive constructions. Usually, Tropical Medicine and parasitological literature concern much more to present time scenarios and epidemiological patterns, and unfortunately have neglected pre-Colombian civilizations and its role in perpetuation of modern human diseases, eventually evolved in the environments we transformed long ago.

*Lutzomyia longipalpis* has not been explicitly associated to such specific conditions before, and to realize its capability to survive and develop on very wet conditions rich in feces and carcasses, open new perspectives to understand the origin of urban outbreaks. Eventually, public health services could take advantage of seeking methodically for *L. longipalpis* in swage entrances, rat burrows, hidden places for dead animals, especially in the poorest neighbourhoods. Also, policy makers should consider linking cities vulnerabilities to AVL to their proximity to natural cave-rich biogeographic regions.

### 3.2.7 References

Abreu, F., Morais, M., Costa, L., Ribeiro, S.P.; Eiras, A. 2015. Influence of breeding site's availability on the oviposition behavior of *Aedes aegypti*. Mem Inst Oswaldo Cruz 110: 669 - 676.

Akhoundi, M., Kuhls, K., Cannet, A., Votýpka, J., Marty, P., Delaunay, P., et al. 2016. A Historical Overview of the Classification, Evolution, and Dispersion of *Leishmania* parasites and sandflies. PLoS Negl Trop Dis 10: e0004349. doi:10.1371/journal.pntd.0004349.

Alexander, B., Carvalho, R.L., McCallum, H., Pereira, M.H. 2002. Role of the domestic Chicken (*Gallus gallus*) in the epidemiology of urban visceral leishmaniasis in Brazil. Emerg Infect Dis 8: 1480-1485.

Almeida, P.S., Paula, M.B., Brilhante, A.F., Medeiros-Sousa, A.R., Neitzke-Abreu, H.C., Carrijo, G.J.S. Filho, P.C.C., Galati, E.A.B. 2019. Phlebotomine (Diptera: Psychodidae) fauna in a cavern containing cave paintings and its surrounding environment, Central-West Brazil. Acta Tropica 199: 105151.

Araki, A.S., Vigoder, F.M., Bauzer, L.G.S.R., Ferreira, G.E.M., Souza, N.A., et al. 2009. Molecular and Behavioral Differentiation among Brazilian Populations of *Lutzomyia longipalpis* (Diptera: Psychodidae: Phlebotominae). PLoS Negl Trop Dis 3: e365. doi:10.1371/journal.pntd.0000365.

Azevedo, V., Strikis, N.M., Novello, V.F., Roland, C.L., Cruz, F.W., Santos, V., Vuille, M., Utida, G., Andrade, F.R.D., Cheng, H., Edwards, R.L. 2021. Paleovegetation seesaw in Brazil since the late Pleistocene: a multiproxy study of two biomes. Earth Planet Sc Lett 563: 116880. <https://doi.org/10.1016/j.epsl.2021.116880>.

Baneth, G., Nasereddin, A., Abdeen, Z., Jaffe, C.L. et al. 2014. *Leishmania tropica* infection in wild and domestic canines. Parasite Vector 7:O27. doi:10.1186/1756-3305-7-S1-O27.

Batista, K.N., Nogueira, A.F.S. 2016. Povos indígenas do Marajó: os Anajás. ANAIS do III Colóquio de Letras da FALE/CUMB, Universidade Federal do Pará, Breves, 18, 10 e 20 fevereiro 2016. ISSN 2358-1131.

Bejarano, E.E., Uribe, S., Rojas, W., Vélez, I.D. 2001. Presence of *Lutzomyia evansi*, a vector of American visceral leishmaniasis, in an urban area of the Colombian Caribbean coast. Trans R Soc Trop Med Hyg 95:27-8. doi: 10.1016/s0035-9203(01)90320-7. PMID: 11280058.

Benchimol, J.L., Junior, D.G.J. 2020. Uma história das leishmanioses no Novo Mundo: fins do Sec. XIX aos anos 1960. FinoTraço Ed & Ed. Fiocruz, Rio de Janeiro, 790 p.

Bettendorff, J.F. 1990. Crônica dos padres da Companhia de Jesus no Estado do Maranhão. FCPTN-SECULT, Belém.

Bettini, S. 1989. Sandfly Breeding Sites. In: Hart, D.T. (eds) Leishmaniasis. NATO ASI Series, vol 171. Springer, Boston, MA. [https://doi.org/10.1007/978-1-4613-1575-9\\_24](https://doi.org/10.1007/978-1-4613-1575-9_24)

Bueno, L., Isnardis, A. 2018. Peopling Central Brazilian Plateau at the onset of the Holocene: building territorial histories, Q Intern 473: 144-160. <https://doi.org/10.1016/j.quaint.2018.01.006>.



Campos, A.M., Santos, C.L.C., Stumpp, R., Silva, L.H.D., Maia, R.A., Paglia, A.P., Andrade-Filho, J.D. 2017. Photoperiod differences in sand fly (Diptera: Psychodidae) species richness and abundance in caves in Minas Gerais State, Brazil. *J Med Entomol* 54: 100–105. doi: 10.1093/jme/tjw135.

Carreira, J.C.A., Brazil, R.P., dos Santos, C.B., Silva, A.V.M. 2018. *Lutzomyia longipalpis* Breeding—A Probable Breeding Substrate for *Lutzomyia longipalpis* in Nature. *Open J An Sc* 8: 370-380. <https://doi.org/10.4236/ojas.2018.84028>.

Carson, J.F., Whitney, B.S., Mayle, F.E., Iriarte, J., Prumers, H., Soto, J.D., Watling, J. 2013. Environmental impact of geometric earthwork construction in pre-Columbian Amazonia. *PNAS* 111: 10497-10502. [pnas.org/cgi/doi/10.1073/pnas.1321770111](https://doi.org/10.1073/pnas.1321770111).

Casaril, A.E., Alonso, D.P., Franco, K.G., Alvarez, M.V.N., Barrios, S.P.G., Fernandes W.S., et al. 2019. Macrogeographic genetic structure of *Lutzomyia longipalpis* complex populations using Next Generation Sequencing. *PLoS ONE* 14: e0223277. <https://doi.org/10.1371/journal.pone.0223277>.

Chavez, D.E., Gronau, I., Hains, T., Dikow, R.B., Frandsen, P.B., Figueiró, H.V., Garcez, F.S., Tchaicka, L., de Paula, R.C., Rodrigues, F.H.G., Jorge, R.S.P., Lima, E.S., Songsasen, N., Johnson, W.E., Eizirik, E., Koepfli, K.P., Wayne, R.K. 2022. Comparative genomics uncovers the evolutionary history, demography, and molecular adaptations of South American canids. *PNAS* 119: e2205986119.

Costa, P.L., Dantas-Torres, F., Silva, F.J., Guimarães, V.C.F.V, Gaudêncio, K., Brandão-Filho S.P. 2013. Ecology of *Lutzomyia longipalpis* in an area of visceral leishmaniasis transmission in north-eastern Brazil. *Acta Tropica* 126: 99– 102

Croan, D.G., Morrison, D.A., Ellis, J.T. 1997. Evolution of the genus *Leishmania* revealed by comparison of DNA and RNA polymerase gene sequences. *Mol Biochem Parasitol* 89:149–59.

Culver, D.C., Pipan, T. 2018. Insects in caves. In Footttit, R.G., Adler, P.H. (eds). *Insect Biodiversity: Science and Society*. Wiley & Sons, ISBN 9781118945575, DOI:10.1002/9781118945582.

Deane, L.M. 1956. Leishmaniose visceral no Brasil. Estudos sobre reservatórios e transmissores realizados no Estado do Ceará. Serviço Nacional de Educação Sanitária, Rio de Janeiro, Brasil, 162 pp.

Dougherty, M., Hamilton, G. 1997. Dodecanoic acid is the oviposition pheromone of *Lutzomyia longipalpis*. J Chem Ecol 23:2657-2671.

Dougherty, M., Hamilton, J.G.C., Ward, R.D. 1993. Semiochemical mediation of oviposition by the phlebotomie sandfly *Lutzomyia longipalpis*. Med Vet Entomol 7:219-224.

Dutra-Rego, F., Freire, M.L., Carvalho, G.M.L., Andrade-Filho, J.D. 2022. Revisiting the cave-dwelling sand flies (Diptera, Psychodidae, Phlebotominae) from Brazil: Diversity and potential role in the transmission of *Leishmania Ross, 1903* (Kinetoplastida: Trypanosomatidae). Med Vet Entomol 36: 408-423. DOI: 10.1111/mve.12578

Elnaiem, D.A., Ward, R.D. 1992. The thigmotropic oviposition response of the sandfly *Lutzomyia longipalpis* (Diptera: Psychodidae) to crevices, AnnTrop Med Parasitol 86:4, 425-430, DOI: 10.1080/00034983.1992.11812688.

Feathers, J., Kipnis, R., Piló, P., Arroyo, M., Coblenz, D. 2010. "How old is Luzia? Luminescence dating and stratigraphic integrity at Lapa Vermelha, Lagoa Santa, Brazil"; Geoarchaeology 25: 395–436.

Feliciangeli, M.D. 2004. Natural breeding places of Phlebotominae sandflies. Med Vet Entomol 18: 71-80.

Felsenstein, J. 1985. Confidence limits on phylogenies: An approach using the bootstrap. Evolution 39:783-791.

Forattini, O.P. 1973. Entomologia médica: 4º volume: Psychodidae. Phlebotominae. Leishmanioses. Bartonelose. São Paulo; Edgard Blucher; 1973. 658 p. Ministério da Saúde | ID: mis-13213.

Gaspar, M. 2000. Sambaqui: arqueologia do litoral brasileiro. Jorge Zahar Editor, Rio de Janeiro. ISBN 85-7110-530-8.

Geiser, D.L., Thai, T.N., Love, M.B., Winzerling, J.J. 2019. Iron and Ferritin Deposition in the Ovarian Tissues of the Yellow Fever Mosquito (Diptera: Culicidae). *J Ins Sci* 19: 11; 1–9. doi: 10.1093/jisesa/iez089.

Goldberg, A., Mychajliw, A.M., Hadly, E.A. 2016. Post-invasion demography of prehistoric humans in South America. *Nature* 532: 232-235. doi:10.1038/nature17176.

Grimald, D, Engel, M.S. 2006. *Evolution of the Insects* (Cambridge Evolution Series). Cambridge University Press, Cambridge. New York, ISBN 978-0-521-82149-0.

Hammer, O. 2023. PAST, Paleontological Statistics Reference Manual, V4.13, Natural History Museum, University of Oslo.

ICMBio, 2023. Sistema de Avaliação do Risco de Extinção da Biodiversidade – SALVE. Disponível em: <https://salve.icmbio.gov.br/>. Acesso em: 07 de May. de 2023.

Jansen, D.C; Cavalcanti, L.F. Lamblém, H.S. 2012. Mapa de Potencialidade de Ocorrência de Cavernas no Brasil, na escala 1:2.500.000. *Rev Brasil Espeleol* 2: n.1.

Kerr, S.F. 2000. Palaeartic origin of *Leishmania*. *Mem Inst Oswaldo Cruz* 95: 75–80.

Lainson, R., Shaw, J.J. 1987. Evolution, classification and geographical distribution. In: Peters, W., Killick-Kendrick, R., eds. *The Leishmaniasis in Biology and Medicine*, Vol. 1. Biology and Epidemiology. London: Academic; 1987. p. 1–120.

Lainson, R., Dye, C., Shaw, J.J., MacDonald, D.W., Courtenay, O., Souza, A.A.A., Silveira, F.T. 1990. Amazonian visceral leishmaniasis – Distribution of the vector *Lutzomyia longipalpis* (Lutz & Neiva) in relation to the fox *Cerdocyon thous* (Linn) and the efficiency of this reservoir host as a source of infection. *Mem Inst Oswaldo Cruz* 85: 135-137.

Lainson, R., Rangel, E.F. 2005. *Lutzomyia longipalpis* and the eco-epidemiology of American visceral leishmaniasis, with particular reference to Brazil - A Review. Mem Inst Oswaldo Cruz, 100: 811-827.

Leblois, R., Kuhls, K., François, O., Schonian, G., Wirth, T. 2011. Guns, germs and dogs: On the origin of *Leishmania chagasi*. Infect Genet Evol 11: 1091–1095.

Lysenko, A.J. 1971. Distribution of leishmaniasis in the Old World. Bull World Health Organ 44:515–20.

Meggers, B.J. 1954. Environmental Limitation on the Development of Culture. Am Anthropol 56: 801-824.

Meggers, B.J. 2001. The mystery of the Marajoara: an ecological solution. Amazoniana XVI: 421-440.

Momen, H., Cupolillo, E. 2000. Speculations on the origin and evolution of the genus *Leishmania*. Mem Inst Oswaldo Cruz 95:583–8.

Moreno-Mayar, J.V., Vinner, L., Damgaard, P.B., Fuente, C., Chan, J., Spence, J.P. et al. 2018. Early human dispersal within the Americas. Science 362: eaav2621. DOI: 10.1126/science.aav2621.

Nei, M., Kumar S. 2000. Molecular Evolution and Phylogenetics. Oxford University Press, New York.

Noyes, H. 1998. Implication of a Neotropical origin of the genus *Leishmania*. Mem Inst Oswaldo Cruz 93:657–61.

Nozais, J.P. 2003. The origin and dispersion of human parasitic diseases in the Old World (Africa, Europe and Madagascar). Mem Inst Oswaldo Cruz 98:13–9.

Oliveira, F.E., Galati, E.A.B., Oliveira, A.G.D., Rangel, E.F., Carvalho, B.M.D. 2018. Ecological niche modelling and predicted geographic distribution of *Lutzomyia cruzi*, vector of

*Leishmania infantum* in South America. PLoS Negl Trop Dis 12: 0006684. <https://doi.org/10.1371/journal.pntd.0006684>.

Pacheco, A.S. 2010. A conquista do ocidente Marajoara: índios, portugueses e religiosos em reinvenções históricas. In Schaan, D.P., Martins, C.P. (eds). Muito Além dos campos: arqueologia e história na Amazônia Marajoara. Gknoronha, Belém. Pp.11-30

Pasquali, A.K.S., Baggio, R.A., Boeger, W.A., Gonzalez-Britez, N., Guedes, D.C., Chaves, E.C. et al. 2019. Dispersion of *Leishmania (Leishmania) infantum* in central-southern Brazil: Evidence from an integrative approach. PLoS Negl Trop Dis 13: e0007639. <https://doi.org/10.1371/journal.pntd.0007639>.

Perri, A.R., Feuerborn, T.R., Frantz, L.A.F., Larson, G., Malhi, R.S., Meltzer, D.J., Witt, K.E. 2021. Dog domestication and the dual dispersal of people and dogs into the Americas. PNAS 118: 6 e2010083118.

Petter, F. 1972. L'origine des mammifères domestiques. In La Vie des Mammifères, Bordas, Paris.

Prates, L. 2014. Crossing the boundary between humans and animals: the extinct fox *Dusicyon avus* from a hunter-gatherer mortuary context in Patagonia (Argentina). Antiquity 88: 1201–1212.

Rangel, E.F., Lainson R., Afonso, M.M.S., Shaw, J.J. 2018. Eco-epidemiology of American Visceral Leishmaniasis with particular reference to Brazil. In Rangel EF, Shaw JJ (eds). Brazilian Sand Flies. Biology, Taxonomy, Medical Importance and Control. Fiocruz-Springer, Brasília. DOI.org/10.1007/978-3-319-75544-1.

Ready, P. 2014. Epidemiology of visceral leishmaniasis. Clinical Epidemiology, 147. doi:10.2147/clep.s44267 10.2147/CLEP.S4426.

Rocha, V.J., Rels, N.R., Seklama, M.L. 2004. Dieta e dispersão de sementes por *Cerdocyon thous* (Linnaeus) (Carnívora, Canidae), em um fragmento florestal no Paraná, Brasil. Rev Bras Zool 21: 871–876.

- Rocha, M.C., Costa, L.A.F., James, M.J. 2019. A gis-based spatial analysis of the distribution of caves in Brazil. *Brazil Geogr J: Geosc Hum Res Medium* 9: 149-162.
- Rzhetsky, A., Nei, M. 1992. A simple method for estimating and testing minimum evolution trees. *Mol Biol Evol* 9:945-967.
- Saitou, N., Nei, M. 1987. The neighbor-joining method: A new method for reconstructing phylogenetic trees. *Mol Biol Evol* 4:406-425.
- Salah, I., Abbasi, I., Warburg, A., Davidovitch, K.B. 2020. Ecology of Leishmaniasis in an urbanized landscape: Relationship of sand fly densities, and *Leishmania tropica* infection rates with reservoir host colonies. *Acta Tropica* 204: 105332.
- Saraiva, L., Silva, R.A., Rugani, J.M.N., Pereira, A.A.P., Rêgo, F.D., Lima, A.C.V.M.R., et al. 2015. Survey of Sand Flies (Diptera: Psychodidae) in an Environmentally Protected Area in Brazil. *PLoS ONE* 10: e0134845. doi:10.1371/journal.pone.0134845.
- Schaan, D.P. 2008. The nonagricultural chiefdoms of Marajó Island. In Silverman, H., Isbell, W.H., Springer, New York. Pp 339-357.
- Schaan, D.P., Martins, C.P. 2010. Muito Além dos campos: arqueologia e história na Amazônia Marajoara. Gknoronha, Belém.
- Schaan, D.P., Martins, C.P., Portal, V.L.M. 2010. Patrimônio arqueológico do Marajó dos campos. In Schaan, D.P., Martins, C.P. (eds). *Muito Além dos campos: arqueologia e história na Amazônia Marajoara*. Gknoronha, Belém.
- Serpell, J.A. 2021. Commensalism or Cross-Species Adoption? A Critical Review of Theories of Wolf Domestication. *Front. Vet. Sci* 8:662370. doi:10.3389/fvets.2021.662370.
- Sherlock, I.A. 1996. Ecological Interactions of Visceral Leishmaniasis in the State of Bahia, Brazil. *Mem Inst Oswaldo Cruz* 91: 671-683.

Silva, A.Z., Hoffmeister, C.H., Anjos, V.A., Ribeiro, P.B., Kruger, R.F. 2014. Necrophagous Diptera associated with wild animal carcasses in southern Brazil. *Rev Brasil Entomol* 58: 337–342.

Somerfield, P.J., Clarke, K.R., Gorley, R.N. 2021. Analysis of similarities (ANOSIM) for 2-way layouts using a generalised ANOSIM statistic, with comparative notes on Permutational Multivariate Analysis of Variance (PERMANOVA). *Austral Ecol* 46: 911-926. DOI:10.1111/aec.13059

Souza J.G., Mateos J.A., Madella M. 2020. Archaeological expansions in tropical South America during the late Holocene: Assessing the role of demic diffusion. *PLoS ONE* 15: e0232367. <https://doi.org/10.1371/journal.pone.0232367>.

Sterverding, D. 2017. The History of Leishmaniasis. *Parasite Vector* 10:82 DOI 10.1186/s13071-017-2028-5.

Svobodová, M., Sádlová, J., Chang, K.P., Volf, P. 2003. Short report: distribution and feeding preference of the sand flies *Phlebotomus sergenti* and *P. papatasi* in a cutaneous leishmaniasis focus in Sanliurfa, Turkey. *Am. J. Trop. Med. Hyg.* 68: 6–9.

Tamura, K., Stecher, G., Kumar, S. 2021. MEGA 11: Molecular Evolutionary Genetics Analysis Version 11. *Molecular Biology and Evolution* <https://doi.org/10.1093/molbev/msab120>.

Teodoro, L.M., Carvalho, G.M.L., Campos, A.M., Cerqueira, R.F.V., Souza-Silva, M., Ferreira, R.L., Barata, R.A. 2021. Phlebotomine sand flies (Diptera, Psychodidae) from iron ore caves in the State of Pará, Brazil. *Subt Biol* 37: 27-42.

Thatcher, V.E.; Hertig, M. 1966. Field studies on the feeding habits on diurnal shelters of some *Phlebotomus* sand flies (Diptera: Psychodidae) in Panama. *Ann. Ent. Soc. Amer.*, v. 59, p. 46-52.

Utida, G., Cruz, F.W., Santos, R.V., Sawakuchi, A.O., Wang, H., Pessenda, L.C.R., Novello, V.F., Vuille, M., Strauss, A.M., Borella, A.C., Stríkis, N.M., Guedes, C.C.F., Andrade, F.R.D.,

Vale, V.F., Moreira, B.H., Moraes, C.S., Pereira, M.H., Genta, F.A., Gontijo, N.F. 2012. Carbohydrate digestion in *Lutzomyia longipalpis* larvae (Diptera - Psychodidae). *J Insect Physiol* 58:1314-24. doi: 10.1016/j.jinsphys.2012.07.005. Epub 2012 Jul 25. PMID: 22841889.

Vilà, C., Savolainen, P., Maldonado, J.E., Amorim, I.R., Rice, J.E., Honeycutt, R.L., Crandall, K.A., Lundeberg, J., Wayne, R.K. 1997. Multiple and ancient origins of the domestic dog. *Science* 276: 1687-1689.

Wallach, E. 2019. Inference from absence: the case of archeology. *Nature Palgrave Communications* 5:94. [i.org/10.1057/s41599-019-0307-9](https://doi.org/10.1057/s41599-019-0307-9).

Webb, S.D. 2006. The great American biotic interchange: Patterns and processes. *Ann. Mo. Bot. Gard.* 93: 245–257.

Zhang, H., Cheng, H., Edwards, R.L. 2020. Climate changes in Northeastern Brazil from deglacial to Meghalayan periods and related environmental impacts. *Q Sci Rev* 250: 106655- .



## **4 PART 3 - THE SARS-COV-2 PANDEMIC: MOST FAVOURABLE ENVIRONMENT FOR ORTHOCORONAVIRINAE SPILLOVERS AND ECOLOGICAL MECHANISMS BEHIND DISSEMINATION**

### **4.1 Preface**

In this series of articles on eco-epidemiology of the pandemic, we first investigated what were the ecological conditions in places where all Orthocoronavirinae species deposited in the GenBank were found (Ribeiro et al. 2022; pg 86). Concerning the pandemic dynamic, we explored the virus dissemination worldwide (Ribeiro et al. 2020a; pg 97) and inside Brazil (Ribeiro et al. 2020b; pg 113) based on neutral ecological theory and algebraic (SIR – Susceptible-Infected-Recovered + metapopulation models) and statistical models. Finally, we explored the community transmission, with a special focus on Manaus city (Ribeiro et al. 2021; pg 123; Silva et al. 2022; pg 137). For such, and for the first time in this type of populational modelling, we combined a Lattice model (spatially explicit individuals moving between different buildings, and having an explicit location) approach with algebraic modelling (SIR model), testing the virus spreading and prevalence in urban environments with and without vaccination.

Ribeiro et al. (2022) used the coordinates of all reliable deposited coronavirus in GenBank to seek a common pattern for the locations where Orthocoronavirinae species have been found. We compared various socio-environmental parameters, using global database on deforestation and arboreal cover, population density, CO<sub>2</sub> emission, and indexes reflecting human consumerism. We found that a likely landscape to produce a new coronavirus spillover is an intensely human modified, urban regions with disturbed remaining of natural vegetation, with high levels of CO<sub>2</sub> emissions, and a population under high Human Developing Index, HDI, which reflected good life conditions, but also high consumerism. The Chinese and North American East coasts, transformed and densely populated for very large and continuous extension, are then quite risky regions for this virus subfamily to be encounter. Based on these patterns, we incriminated animal trafficking as a likely hidden mechanism for appearance of these virus among humans. A further aspect was climate, as this is a type of virus strongly dependent of high air humidity, unlikely to be found in desertic regions.

Ribeiro et al. (2020 a,b) showed that after SARS-CoV-2 pandemic started, a sole mechanism explained the dissemination trend. The quantity of flight passengers alone

explained which were the most vulnerable Countries, and within Brazil, the order and intensity of Brazilian capitals been reached by the virus.

For pandemic situations, the classical algebraic ecological models of species population growth, from Verhulst, and species interaction models from Lotka-Volterra, are theoretical frameworks capable to describe the phenomenon and to propose actions to stop it. In many aspects, social distancing is a way to severely reduce carrying capacity, i.e., the resources available for the virus dissemination. This was the best action for within-city pandemic spreading of this new coronavirus, since the main form of transmission is direct contact between people.

On the other hand, the dynamics of disease spreading among cities are entirely distinct. In order to understand subpopulation flow between demes – which are cities – connected by roads or air flight networks, several complex details may be raised in the process of modelling. For instance, probabilistic motivated effective distance, which is the actual proximity caused by business, culture, and investments between two cities, is much more important than real geography, especially for airlines network. Nevertheless, for such theoretical approach to infection disease dissemination, an ecological concept is key: metapopulation. The ecological approach may focus on the most biological aspect of these dynamics, which is simply virus dissemination inside an infected person. As typically designed in Ecology, the first attempt will be based on the most neutral model, i.e., the directions taken through the most frequent and intensively used links.

Sadly, our predictions were confirmed by the facts. We produced a Pre-print material and a briefing for governmental agents, and distributed these material two weeks before the first case reached Brazil. The total lack of reaction from the Federal government followed and, thus, the avoidable scale of the tragedy lived in our Country.

Finally, Ribeiro et al. (2021) and Silva et al. (2022) explored the drivers of case waves, using Manaus as a model. First, using H1N1 parameters and historical data from the Spanish Flu, we repeated the dramatically mortal outbreaks of the Flu disease in that city, from 1918 to 1919. Similarly to Covid-19, Spanish Flu was substantially more lethal in Manaus than in the rest of the Country. Based on that initial model, we simulated a Manaus with no lockdown or masks. After, in Silva et al. (2022) we added the layer of vaccination in these analyses. We predicted that without any action for lockdowns, masks or vaccination, that city would have suffered waves of high number of cases and deaths for at least 5.4 years. Along this period, the accumulation of recovered and then immune people and the elimination of those more

vulnerable, would weaken up the waves until the disease became little virulent. Of course, the price to pay would be the dramatic deaths to up to 20% of the population.

## RESEARCH PAPER

# Long-term unsustainable patterns of development rather than recent deforestation caused the emergence of Orthocoronavirinae species

Sérvio P. Ribeiro<sup>1</sup>  | Debmalya Barh<sup>2,3</sup> | Bruno Silva Andrade<sup>4</sup> |  
 Raner José Santana Silva<sup>5,6</sup>  | Diogo Henrique Costa-Rezende<sup>7</sup> |  
 Paula Luize Camargos Fonseca<sup>8</sup> | Sandeep Tiwari<sup>3</sup> | Marta Giovanetti<sup>9,10</sup> |  
 Luiz Carlos Junior Alcantara<sup>9,10</sup> | Vasco Ariston Azevedo<sup>3</sup> | Preetam Ghosh<sup>11</sup> |  
 José Alexandre F. Diniz-Filho<sup>12</sup> | Rafael Loyola<sup>12,13</sup> |  
 Maria Fernanda Brito de Almeida<sup>1,14</sup> | Aristóteles Góes-Neto<sup>15</sup>

<sup>1</sup>Laboratório de Ecologia do Adoecimento & Florestas NUPEB/ICEB, Universidade Federal de Ouro Preto, Ouro Preto, Minas Gerais, Brazil

<sup>2</sup>Centre for Genomics and Applied Gene Technology, Institute of Integrative Omics and Applied Biotechnology (IIOAB), Purba Medinipur, West Bengal, India

<sup>3</sup>Departamento de Genética, Ecologia e Evolução, Instituto de Ciências Biológicas, Universidade Federal de Minas Gerais, Belo Horizonte, Minas Gerais, Brazil

<sup>4</sup>Laboratório de Bioinformática e Química Computacional, Departamento de Ciências Biológicas, Universidade Estadual do Sudoeste da Bahia (UESB), Jequié, Bahia, Brazil

<sup>5</sup>Departamento de Ciências Biológicas (DCB), Universidade Estadual de Santa Cruz (UESC), Ilhéus, Bahia, Brazil

<sup>6</sup>Programa de Pós-Graduação em Genética e Biologia Molecular (PPGGBM), Universidade Estadual de Santa Cruz (UESC), Ilhéus, Bahia, Brazil

<sup>7</sup>Programa de Pós-Graduação em Botânica (PPGBot), Departamento de Ciências Biológicas, Universidade Estadual de Feira de Santana (UEFS), Feira de Santana, Bahia, Brazil

<sup>8</sup>Departamento de Microbiologia, Instituto de Ciências Biológicas, Universidade Federal de Minas Gerais, Belo Horizonte, Minas Gerais, Brazil

<sup>9</sup>Laboratório de Genética Celular e Molecular, Universidade Federal de Minas Gerais, Belo Horizonte, Minas Gerais, Brazil

<sup>10</sup>Laboratório de Flavivírus, Instituto Oswaldo Cruz Fiocruz, Rio de Janeiro, Rio de Janeiro, Brazil

## Abstract

We investigated whether a set of phylogeographical tracked emergent events of Orthocoronavirinae were related to developed, urban and polluted environments worldwide. We explored coronavirus records in response to climate (rainfall parameters), population density, CO<sub>2</sub> emission, Human Developmental Index (HDI) and deforestation. We contrasted environmental characteristics from regions with spillovers or encounters of wild Orthocoronavirinae against adjacent areas having best-preserved conditions. We used all complete sequenced CoVs genomes deposited in NCBI and GISAID databases until January 2021. Except for Deltacoronavirus, concentrated in Hong Kong and in birds, the other three genera were scattered all over the planet, beyond the original distribution of the subfamily, and found in humans, mammals, fishes and birds, wild or domestic. Spillovers and presence in wild animals were only reported in developed/densely populated places. We found significantly more occurrences reported in places with higher HDI, CO<sub>2</sub> emission, or population density, along with more rainfall and more accentuated seasonality. Orthocoronavirinae occurred in areas with significantly higher human populations, CO<sub>2</sub> emissions and deforestation rates than in adjacent locations. Intermediately disturbed ecosystems seemed more vulnerable for Orthocoronavirinae emergence than forested regions in frontiers of deforestation. Sadly, people experiencing poverty in an intensely consumerist society are the most vulnerable.

<sup>11</sup>Virginia Commonwealth University,  
Richmond, Virginia, USA

<sup>12</sup>Departamento de Ecologia, Universidade  
Federal de Goiás, Goiânia, Goiás, Brazil

<sup>13</sup>Fundação Brasileira para o  
Desenvolvimento Sustentável, Rio de Janeiro,  
Rio de Janeiro, Brazil

<sup>14</sup>Programa de Pós-Graduação em Ecologia,  
Universidade Federal de Viçosa, Viçosa,  
Minas Gerais, Brazil

<sup>15</sup>Laboratório de Biologia Molecular e  
Computacional de Fungos, Instituto de  
Ciências Biológicas, Universidade Federal de  
Minas Gerais, Belo Horizonte, Minas Gerais,  
Brazil

#### Correspondence

Sérvio P. Ribeiro, Laboratório de Ecologia do  
Adoecimento & Florestas NUPEB/ICEB,  
Universidade Federal de Ouro Preto, Campus  
Morro do Cruzeiro, Ouro Preto, Minas Gerais,  
Brazil.

Email: [serviopr@gmail.com](mailto:serviopr@gmail.com)

#### Funding information

INCT - Instituto Nacional de Ciências e  
Tecnologia - UFG, Grant/Award Number:  
465610/2014-5; Conselho Nacional de  
Desenvolvimento Científico e Tecnológico/  
CNPq, Brazil, Grant/Award Numbers:  
310764/2016-5, 306694/2018-2,  
301799/2016-4, 312045/2020-4,  
306572-2019-2; Graduate Program of  
Biological Science (UFOP); Graduate Program  
in Parasitology (UFMG); Graduate Program in  
Microbiology (UFMG); Graduate Program in  
Bioinformatics (UFMG)

## INTRODUCTION

The increasing emergence of zoonotic diseases in the XXI century raised concerns about the drivers of epidemic and pandemic events of zoonotic origin (Buck & Weinstein, 2020; Ellwanger et al., 2020; Johnson et al., 2015). A country's sum of bird and mammal diversity is highly correlated to the richness of human pathogens (Dunn et al., 2010). However, the abundance of some animal populations is a key driver of spillover events, mainly when host/reservoir abundance responds positively to environmental disturbance (Karesh et al., 2012). Earlier studies in the ecology of diseases had already emphasized the role of habitat disturbance on the balance of host–parasite interactions (McCallum & Dobson, 1995). Namely, rapid changes in the host population size under stressful conditions may alter the effects of parasites on the infected hosts, shifting from being a population regulator to become an unpredictable outbreak force, likely to result in spillover to domestic animals and human populations (Karesh et al., 2012; McCallum & Dobson, 1995). Modern emerging diseases are more likely to be influenced by ecological factors affected by climate, land-use change, and agricultural practices than by

evolutionary changes in the pathogen–host interactions (Schrag & Wiener, 1995).

A human-modified ecosystem, such as a city, if managed to be kept healthy, may also be kept highly biodiverse (Alvey, 2006). Hypothetically, a highly biodiverse city (or, more realistically, a conventional city entangled with large and well-preserved green areas) tends to have smaller and scattered populations of various animal species, regulated by ecological interactions such as competition and predation. Considering parasites and infections, a diverse animal community could cause the so-called dilution effect (Ostfeld & Keesing, 2000), which buffers possibilities of disease spillover to humans or domestic animals. On the other hand, as most cities nowadays are environmentally constrained, they are dominated by few tolerant animal species with fast life histories and, thus, with large populations (Keesing & Ostfeld, 2021). Large populations come along with densely distributed individuals, which facilitate the dissemination of diseases. Furthermore, infections spread better in fast-growing and highly reproductive species (Keesing & Ostfeld, 2021; Pattanayak et al., 2017; Plourde et al., 2017).

Data about environmental drivers of zoonotic spillover are rare and circumstantial (Allen et al., 2017;

Jones et al., 2008; Keesing & Ostfeld, 2021), as well as proper interpretations and predictions of emerging infectious diseases (EIDs) are still similarly fragile and preliminary (Daszak et al., 2000; Singh et al., 2021). Even contradictory predictions for some parts of the world are published by distinct authors using similar models (Allen et al., 2017; Singh et al., 2021). Comparing regions surveyed very differently also makes some models questionable, which is the case of models that predict that highly biodiverse tropical regions have high risks of EIDs, with no real cases in the ground (Allen et al., 2017; Jones et al., 2008). Most likely, human coexistence with high diversity may be less dangerous than with low diversity and dominant and abundant resilient species (Keesing & Ostfeld, 2021; Pattanayak et al., 2017; Tallavaara et al., 2018), especially with groups that are hotspots of parasite diversity, such as rodents and bats (Dáttilo et al., 2020; Latinne et al., 2020).

The Orthocoronavirinae subfamily is a good candidate for a more specific investigation on spillover scenarios, considering not only SARS-CoV-2's recent impact on human societies but also several other species which have spilled over during recent decades. The subfamily phylogeny is sufficiently understood (Machado et al., 2021). Likewise, the species diversity and association with bats, and the primary mechanisms for host switching, especially for *Betacoronavirus* and *Alphacoronavirus* genera, are intensively studied (Latinne et al., 2020; Shi & Hu, 2008). The most likely origin of *Alphacoronavirus* and *Betacoronavirus* genera is the Southwestern region of China, in Yunnan, and the neighbouring countries such as Myanmar, Laos, or Vietnam, but SARs and MERs may have appeared in the Southern regions of Guangdong and Fujian (an area also with substantial diversity of avian *Deltacoronavirus*) (Machado et al., 2021). Perhaps the most relevant aspect of this viral subfamily evolution is the extreme facility to jump between species, resulting in a complex host network, a pattern made even more complicated due to human–animal domestication along with the consumption of wild species (Daszak et al., 2000; Woo et al., 2012).

For SARS-CoV-2, genomic studies of human isolates indicated a likely mammal origin. It appears to share 96% of genomic similarity with the (SARS)-like RaTG13 virus, found in *Rhinolophus affinis* bat (Benvenuto et al., 2020; Rothan & Byrareddy, 2020; Zhang & Holmes, 2020). From the most comprehensive phylogeny of Orthocoronavirinae so far generated, Machado et al. (2021) recently corroborate Benvenuto et al. (2020) and Liu et al. (2020a) hypotheses that a direct infection from a bat to human occurred with no intermediate host, but after mutation conferring the ability to spillover successfully. The free-living horseshoe bats *Rhinolophus* spp. are reported reservoirs of many

SARS-like Orthocoronavirinae (Field, 2009). The recent discovery of four *Rhinolophus*-related sarbecoviruses closely related to SARS-CoV-2 and three to SARS-CoV, with at least one able to bind to human ACE2, reinforces the natural origin of SARS-CoV-2 from the assembly of viruses associated with this bat genus (Zhou et al., 2021).

Interestingly, these species are among the most consumed wild animals as food in China and many other countries (Mildenstein & Tanshi, 2015), besides also being used as medicine (for instance, *R. affinis* faeces are used in traditional Chinese medicine) (Machado et al., 2021). Nevertheless, the ideal setting for the spillover needs an enhanced probability of human infection. This may be reached by multiple transmission events between various animals sold together in poor health conditions, preferentially in a densely populated place. Hence, urban wet markets may produce larger chances of the emergence of SARS-related diseases than the hunting place (Maxmen, 2021; Shi & Hu, 2008). Taylor et al. (2001) have shown that 75% of emerging pathogens are zoonotic; Jones et al. (2008) showed that 71.8% of zoonosis originates in wildlife. These data, along with strong evidence that loss of biodiversity, human population density, and land change related to development are causes of EIDs (Keesing & Ostfeld, 2021; Singh et al., 2021) set human-driven habitat disturbance as a main determinant of finding new virus in nature, or in human and domestic animals.

Considering the impossibility to trace back the precise origin of most EIDs related to Orthocoronavirinae, it may be more profitable to chase the general habitat conditions where these viruses have been found. In this article, we tested the hypothesis that the discovery of Orthocoronavirinae events is related to various human changes in the ecosystems and landscape in general. To do so, we investigated a set of phylogeographically tracked emergent events of Orthocoronavirinae, whether cases appeared in human, domestic or wild animals all over the world. We predict that direct impact on natural and well-preserved regions may not result in detectable spillovers or discovery of natural coronavirus events. Conversely, the consumerism of hunted animals living under distressful conditions and traded to big cities, mixed with domestic species in poorly managed landscapes or markets, is the most likely scenario to produce detectable viral occurrences. Therefore, we hypothesize that densely populated and developed regions, under poor environmental management are the most dangerous places for new EIDs, particularly those related to Orthocoronavirinae. We further explored coronavirus distribution in response to rainfall patterns, as transmission and environmental contamination by respiratory diseases seemed more likely in wet climates (Omonijo et al., 2011).

## EXPERIMENTAL PROCEDURES

### Orthocoronavirinae viral species

To establish a sampling event criterion considering the phylogenetic relationships within Orthocoronavirinae, we used 85 CoVs genomes deposited in NCBI and GISAID databases to perform the analyses. All fully sequenced CoVs genomes with high coverage, and deposited until January 2021, were taken to maintain the fidelity in our analyses. Furthermore, the representatives of the known viral species of all the genera from the Orthocoronavirinae subfamily were used to guarantee non-biased analyses. All the predicted proteins and corresponding genes in the selected CoV genomes were identified using the ORF-finder tool (Sayers et al., 2010), considering the standard codon usage and minimal ORF length of 600 bases. Supplementary Table 1 displays the studied viral species.

### Phylogenetic analyses

Amino acid and RNA sequences from genes ‘ORF1 a-b’ and ‘S’ of the 85 Orthocoronavirinae sequences were used in the phylogenetic analysis. Initially, the following four datasets were constructed: (i) RNA ‘ORF1 a-b’, (ii) amino acid ‘ORF1 a-b’, (iii) RNA ‘S’ and (iv) amino acid ‘S’. The amino acid datasets were aligned using MAFFT 7 (Kato et al., 2019) using the G-INS-I alignment method. The RNA datasets were aligned by codon using MUSCLE (Edgar, 2004) with default settings. We used PartitionFinder v.2 (Lanfear et al., 2017) to estimate the best-fit partitioning strategy and the best-fit model of nucleotide evolution for each of the RNA datasets using three data blocks (first, second and third codon positions) with the following settings: branch lengths = linked, models = all, model\_selection = AICc and search = greedy. The best-fit model of nucleotide evolution for each amino acid dataset was estimated in Model Test-NG (Darriba et al., 2019). Details in Supplementary Methods and Results.

### Environmental traits

We described and compared several environmental conditions from where our series of phylogenetically linked events of Orthocoronavirinae happened. We identified that these places were in their majority densely populated and human-modified landscapes. We compared these locations with the most relevant and better-preserved adjacent regions at a comparable scale. For instance, Yunnan’s description paired with the neighbouring North Myanmar region; Guangxi with Vietnam; the Uganda ecopark Bwindi was paired with

the wild and continuous forests of the Democratic Republic of Congo. Inside China, a neighbour province or a neighbour country was picked as a pair, depending on each case.

In the case of Hong Kong, a hotspot of *Deltacoronavirus*, the surrounding province of Guangdong was the adjacent region, as the political status of Hong Kong and suburbs provided us with outstanding local data on CO<sub>2</sub>, HDI, population, and so on. Hence, for some regions, the adjacent area was as developed as the core one. However, the densely and somehow differently managed Territory of Hong Kong needed to be highlighted.

We put together all the cases from Dinghai District (an entirely urbanized ocean island) with the next province of Zhejiang, as the Orthocoronavirinae cases in this province were all found on the heavily urbanized coast, and then we paired them with the more rural Fujian Province. For the United States, ecoregions dominated by cities were, likewise, considered as a special case. That was the case for New Jersey, assumed as a densely urbanized ecosystem including New York and Philadelphia (although, politically, the latter belongs to the Pennsylvania State), and contrasted against rural Pennsylvania State. Besides, we chose to compare locations within a similar scale for cases out of megacities, such as Province with Province or State with State, in the largest countries, or regions of similar sizes and belonging to the same ecoregion (Global Forest Watch, 2021).

We investigated the following environmental characteristics at the studied sites: total precipitation, precipitation of the driest month, 2010 regional forest (primary and other arboreal formation) size, 2002–2019 deforestation, population size (at logarithm scale) and density, Human Development Index (hereafter HDI) measured for 2018, CO<sub>2</sub> emissions (in a million metric tons and per capita). We also tested the local 2002–2019 contribution to the nationwide deforestation (in percentage squared-rooted and arcsine transformed), reflecting political trends towards the environment. The studied regions are listed in Supplementary Table 2 and the data sources are in the Supplementary Table 3. All forestry data were taken from the Global Forest Watch database (Global Forest Watch, 2021).

The explanatory variables were verified for collinearity and correlation, *a priori* designing the models. The number of Orthocoronavirinae detected (in wild animals or by spillovers altogether) was tested as ln-transformed values or raw data using Poisson distribution. Several modelling strategies were used to try to understand the role of environmental variables on known Orthocoronavirinae events. Initially, we tested the response of ln number of occurrences of Orthocoronavirinae to environmental variables by fully contrasting the locality of the event and the paired adjacent location. This analysis produced the difference of each

value between the location-adjacent region pairs, thus testing the size of environmental contrast as a cause of events. In other words, we verified the relative effect of wild places close to the developed ones on the number of events at a regional scale. Subsequently, a complete comparison of absolute values for those locations with coronavirus occurrence was produced by an ordinary least square (OLS), using model selection by AIC, with Poisson distribution on coronavirus occurrences. Complementarily, two stepwise regression models were built to verify the effect of these variables while looking exclusively at the places with coronavirus occurrence (using again ln of occurrence checking for a normal distribution of model residuals), considering: (i) only testing the environmental variables; (ii) adding the Orthocoronavirinae genera as a categorical variable. Finally, a principal component analysis (PCA) was constructed to assemble countries according to their similarities for the following parameters: total precipitation, precipitation in the driest month, forest size, local deforestation rates, % of nationwide deforestation at the local scale, population density, HDI and CO<sub>2</sub> emission.

Country deforestation rates were correlated to HDI and were removed, and CO<sub>2</sub> per capita was correlated with total CO<sub>2</sub> emissions. Analyses were performed in RStudio (R Team Core 2016).

## RESULTS

### The geophylogeny of Coronaviridae

Phylogenetic analyses and divergence time estimation resulted in a tree coherent with other recent works and are presented in the supplementary materials (Figures S.1 to S.3). The representation of the phylogeny of Orthocoronavirinae (ML—‘ORF1ab’ RNA) on a geographic map showed a distinct distribution pattern for the four genera. The studied samples of *Deltacoronavirus* and *Gammacoronavirus* had a more restricted distribution, occurring in Hong Kong (*Deltacoronavirus*) and the United States and Canada (*Gammacoronavirus*) (Figure 1). Subgenera with only one representant in the phylogeny, with missing data or

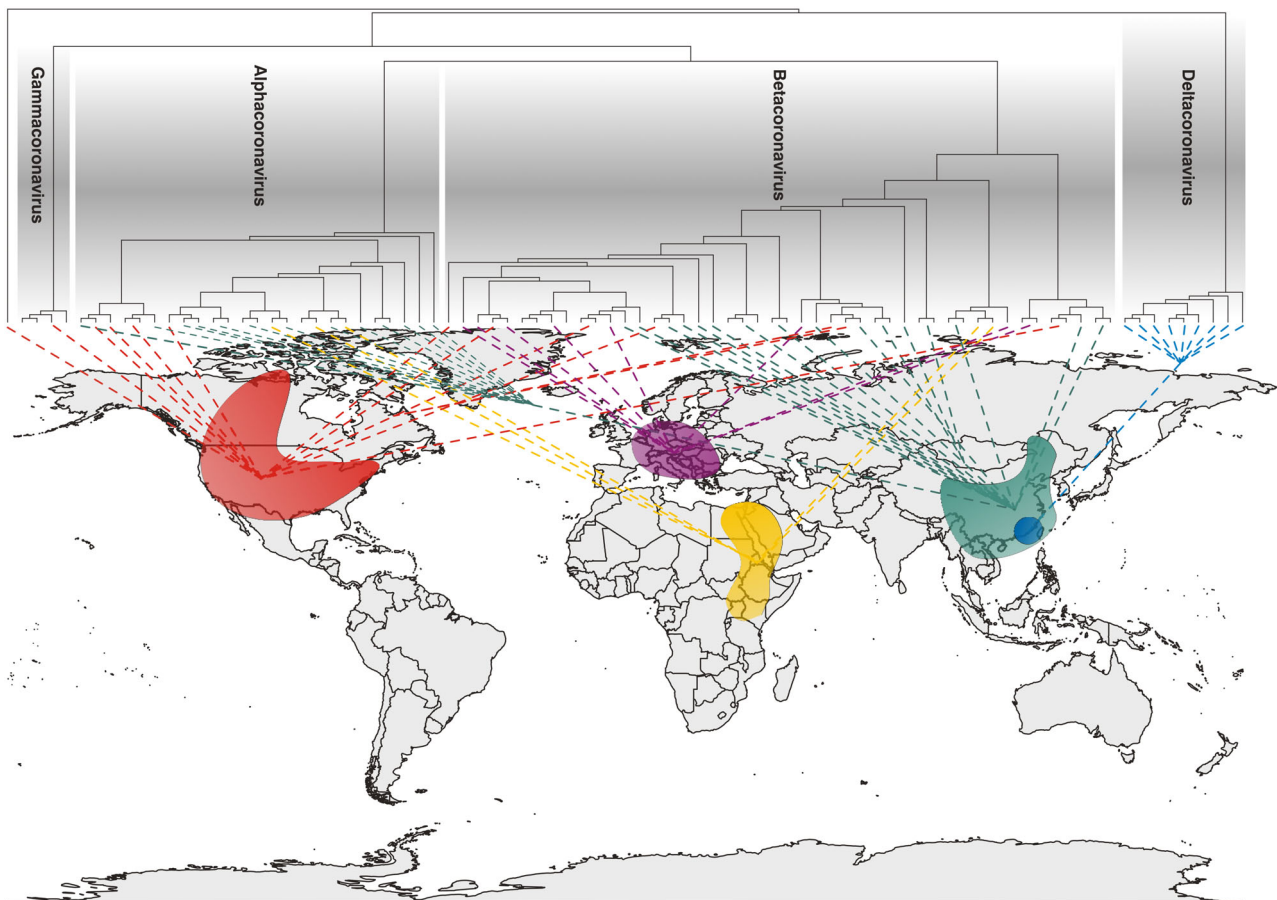


**FIGURE 1** Distribution of occurrences of Orthocoronavirinae worldwide, arranged according to the phylogenetic tree. The colour shapes represent approximated areas from where the events were detected. All Deltacoronavirus are from Hong Kong, thus resulting in a sub-region within China for clarity. For the sake of simplicity, the lines depart from the core position within each biogeographic region and not the exact location (see coordinates of events in Table 2)



recovered as polyphyletic (*Merbecovirus*), are not displayed.

Both *Alphacoronavirus* and *Betacoronavirus* exhibited a broad distribution, with samples from Asia, Europe and North America. Subgenera within *Alphacoronavirus* showed a heterogeneous distribution pattern. Some subgenera presented a restricted distribution, such as *Decacovirus* and *Rhinacovirus* (China) and *Minunacovirus* (Hong Kong). Conversely, others occurred in two continents, including *Minacovirus* and *Tegacovirus* (Europe and North America) and *Nyctacovirus* (Europe and Asia). Subgenera within *Betacoronavirus* also appeared to be a heterogeneous distribution pattern. *Embecovirus* samples occur both in the United States and China, and *Sarbecovirus* across Asia, Europe and North America, while *Nobecovirus* had a restricted distribution, occurring only in China.

Regarding the general phylogenetic affinities (e.g. between genera, subgenera, or specific clades), no clear relation between the topology and geographic distribution can be speculated by a qualitative pattern analysis based on world distribution. However, the lack

of a clear correlation between phylogeny and geographic distance suggests a worldwide scattered distribution compatible with the hypothesis of humans moving hosts around by trading.

## Environmental characteristics

The analysis of the differences between environmental conditions where the Orthocoronavirinae occurred and the adjacent regions showed that virotic events happened in places with significantly greater populations, CO<sub>2</sub> emissions and higher deforestation rates within a particular area. There were significant differences in the variables between the local of Orthocoronavirinae occurrences and the adjacent best-preserved region, and all tested variables significantly affected the probabilities of finding an Orthocoronavirinae (Table 1). The same for pluviosity, although total rainfall had a slight influence on the equation compared to the amount of rain in the driest month, suggesting that seasonality plays a more relevant role than total pluviosity in the occurrence and distribution of Orthocoronavirinae.

**TABLE 1** Stepwise regression tests the contrasting environmental scenarios between pairs of regions with and without Orthocoronavirinae occurrences

Regression equation ( $R^2 = 92.04\%$ )					
$\text{Invirus} = 0.7474 - 0.000650 \text{ (A)} + 0.01563 \text{ (B)} + 0.000001 \text{ (C)} + 0.000618 \text{ (D)} + 0.001310 \text{ (E)}$					
Term	d.f.	SS (adj)	MS (adj)	F value	p-value
Regression	5	5.74	1.15	23.13	0.0001
total precipitation	1	0.57	0.57	11.52	0.007
precipitation of the driest month	1	0.39	0.39	7.96	0.018
2002–2019 deforestation	1	1.99	1.99	40.09	0.0001
Population density km <sup>2</sup>	1	4.90	4.90	98.66	0.0001
CO <sub>2</sub> emission	1	0.52	0.52	10.48	0.009
Error	10	0.49	0.05		
Total	15	6.24			

(A) Total precipitation, (B) precipitation of the driest month, (C) 2002–2019 deforestation, (D) population density km<sup>2</sup>, (E) CO<sub>2</sub> emission in a million metric tons.

**TABLE 2** Stepwise regression for testing the environmental determinants of Orthocoronavirinae events around the world

Regression equation ( $R^2 = 53.75\%$ )					
$\text{Invirus} = -1.004 + 0.000771 \text{ (A)} - 0.01005 \text{ (B)} + 1.731 \text{ (C)} + 0.000580 \text{ (D)}$					
Term	d.f.	SS (adj)	MS (adj)	F value	p-value
Regression	4	4.22	1.05	10.75	0.0001
total precipitation	1	3.63	3.63	37.03	0.0001
precipitation of the driest month	1	1.05	1.05	10.7	0.002
HDI 2018	1	0.95	0.95	9.68	0.004
CO <sub>2</sub> emission	1	0.30	0.30	3.01	0.091
Error	37	3.63	0.098		
Total	41	7.85			

(A) Total precipitation, (B) precipitation of the driest month, (C) HDI—2018, (D) CO<sub>2</sub> emission in a million metric tons.

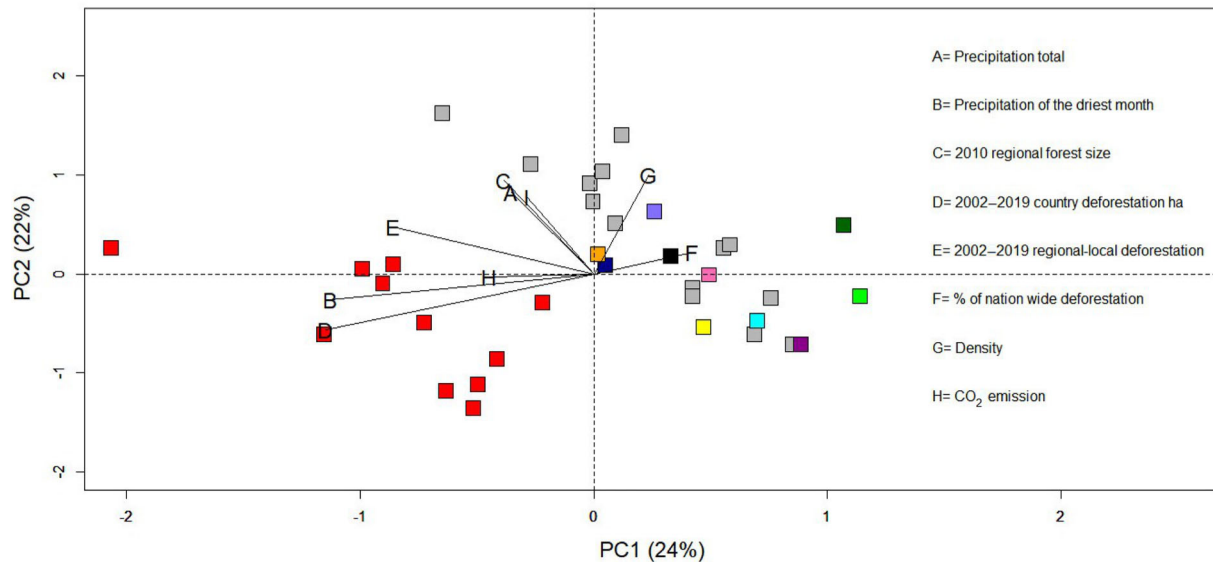


**FIGURE 2** PCA first two axes, sampling sites per country, and vector directions of the variable influences. Legend for countries

Places with a stormy wet season or with a less seasonal but more constantly wet along the year might favour the occurrence of these viral species (Table 1).

We found that the Orthocoronavirinae viruses responded positively to seasonality (more viruses with more annual rainfall but with fewer rains in the driest months) and higher HDI (OLS; Precipitation:  $t_{d.f. = 10} = 5.03$ , std. coef. = 0.76,  $p < 0.001$ ; Precipitation in the driest month:  $t_{d.f. = 10} = 2.8$ , std. coef. =  $-0.47$ ,  $p < 0.001$ ; HDI:  $t_{d.f. = 10} = 2.84$ , std. coef. = 0.46,  $p < 0.01$ ). These variables were significant in another model, comparing only the places with Orthocoronavirinae occurrences among themselves. In this last model, CO<sub>2</sub> emission was also significant and positively related to the amount of Orthocoronavirinae occurrence (Table 2). While adding the distribution of viral genera in the latter model, it had a considerable role (strongly influenced by the biased distribution of *Deltacoronavirus* in Hong Kong, along with annual rainfall and HDI) (ANOVA  $F_{5,34} = 20.97$ ,  $p < 0.0001$ ).

Finally, by looking at the complete characterization of the studied territories, we found that those most developed and urbanized provinces of China were grouped by precipitation, forest size and deforestation patterns, as well as CO<sub>2</sub>, whereas the United States, Germany, Netherlands and Hong Kong were grouped by precipitation in the driest month, HDI and population density. In addition, these two groups were different from all the African countries, North Korea, Myanmar and the poorest provinces of China; all of these were partially influenced by their contribution to nationwide deforestation, forest size and precipitation (besides having contrastingly lower values for the variables defining the two previous groups; Figure 2). Regardless

of a clear separation of regions in groups, the variance explained by this analysis was not high (Figure 2).

## DISCUSSION

Our results suggest that ongoing destruction of highly diverse habitats seemed not to be an immediate or direct source of Orthocoronavirinae disease emergence or, at least, not the most likely places for them to be discovered. Conversely, environmental variables that indicate long-term landscape modification and consumerist societies were considered significantly associated with occurrences of these viruses. HDI, CO<sub>2</sub> emission, and population density were the main drivers of the Orthocoronavirinae distribution worldwide (see also Maxmen, 2021). Our more conservative model showed significant HDI and total precipitation as positive drivers of the emergence of Orthocoronavirinae, whereas precipitation in the driest month was negatively related to the occurrence of Orthocoronavirinae species (Table 2). These results support the hypothesis that these viruses are environmentally constrained by climate and more likely to appear in mesic biogeographic regions. The amount of deforestation in the last 20 years per country or per region where Orthocoronavirinae occurred, or in the provinces or states in the vicinities where the virus subfamily occurred, had no significant relation with these events. Hence, our analyses support that might have a causal link between a particular type of disturbance, namely, long-term human-made habitat disturbances (related to high population densities, CO<sub>2</sub> emissions and poorly managed land use and changes) and detection of

Orthocoronavirinae, consequently, of emergence of infectious diseases related to these viruses.

## The role of climate

When exploring more restricted viral taxonomic groups, an abiotic driver as rainfall might be among the most relevant natural factors affecting the risk of spillover, at least for respiratory diseases (Omonijo et al., 2011). We showed a combination of significant effects of total annual rainfall and rainfall in the driest month, but the relationship between these parameters is not linear. Total precipitation and the precipitation in the driest month are highly correlated among them only for places below 10 mm in the driest month and below 500 mm annually. Sites between 1000 and 2000 mm had a relatively constant amount of rain in the driest months compared to arid locations, regardless of total precipitation. Therefore, year-round relatively dry, and less seasonal biogeographic regions appeared to be the least likely places for Orthocoronavirinae to spill over to domestic animals or people. The mechanism behind this pattern could be a simple fact that respiratory aerosols will dry out faster, inactivating the virus, a phenomenon found below 24% relative humidity (Zhang et al., 2020).

## High HDI and risks of EIDs: a case for Orthocoronavirinae or an overlooked general pattern involving inequality?

HDI is an index that combines measures of healthy life (life expectancy), access to education (mean number of years of schooling) and gross national income per capita, taken together as a measure of a decent standard of living (Roser, 2019). Nevertheless, these correlate with industrialized societies and high consumption of goods in general. Hence, the consumerism of wildlife animals or animal-derived products in markets in highly developed cities could be the primary driver of spillover of Orthocoronavirinae diseases. Thus, well-kept, and sustainable cities at a landscape scale still may hide paths to future contamination in the complex food trading network and, highly probable, in the illegal market of wild animals (which may have been neglected as a likely primary source of EID, Bernstein et al., 2022).

An essential aspect in discussing HDI as a driver of emergent diseases is that most of the index's components, such as people's long-life expectancy, decrease in the number of children, good sanitation conditions and long schooling periods, are undoubtedly positive values related to reduced health risks. The problem is that HDI is an average value per geopolitical region, and the disparity between the richest and the poorest is not shown. Hence, the poorest will be more exposed than expected for the average wealth of the place.

Singh et al. (2021) have recently shown a relationship between high HDI and population density with zoonotic pathogen diversity, emergent pathogen diversity and human pathogen diversity. On the other hand, Allen et al. (2017) argued that high risks of EID in urban landscapes in unweighted models ought to be related to sampling bias, that is, the more you survey, the greater the chances of finding something. Particularly for the Americas, studies of bat coronavirus are few and mostly happened in response to 2003's SARS-CoV emergence (Dominguez et al., 2007; Góes et al., 2016). Olival et al. (2017) showed that most of the potentially unstudied zoonotic viruses in the world might be related to the New World bats, especially from the Amazon region and Central and North America. Most importantly, there is insufficient data to fully understand the confounding between animals traded as food, medicine or pets, and city-wildlife natural interactions.

## Animal traffic as a seriously neglected spillover source

Wildlife hunting and trade have imposed huge pressure on animal populations, with recorded extinctions in places where we describe high coronavirus spillover risks, such as Southeast Asia (Bernstein et al., 2022). Moreover, zoonotic disease risks related to animal traffic have been neglected, even by the most influential international conventions on endangered species trade (Bernstein et al., 2022). Different worldwide reports on wildlife illegal traffic have shown that destination hotspots of hunted animals match some of our locations with Orthocoronavirinae events. Below we discuss wildlife consumerism in China and the United States, as key cases happened where animal traffic destinations and urban centres are usually the same.

## The China-Central Africa case

China is the leading wildlife consumer on Earth, but given the population decline of national species and the recent prohibition for hunting and trade after COVID-19, Africa has become a growing source of animals for China. Increasing trade of pangolin scale, for example has been noticed from the DEM Republic of Congo, Congo and Uganda since 2013 (UNODC, 2020). The *Betacoronavirus* in our survey found in Uganda came from a bat sampled inside the large, forested biome crossing these three countries, where poaching has been intensified in recent years.

This large, forested biome was also the origin of HIV, namely, in Congo. For that pandemic spillover, however, science still knows very little about its exact origin and in which environmental scenario. From

seminal papers to recent reviews, there are little data on how this virus, first detected in humans in 1959, became pandemic in 1980 decade (Zhu et al., 1998; Keele et al., 2006). Interestingly, the first human HIV recorded case was not in the bushes, but in the capital, Brazzaville, showing a close relationship between human population density, hunting and spillover (Zhu et al., 1998). When HIV became a pandemic virus, Congo had nearly zero systemic deforestation (Megevand et al., 2013) but was immersed in a decade of severe violence and poverty (DFID, 2008); thus, likely to have intense hunting and alive animals traded under stressed conditions in the cities.

Currently, the African hunted pangolins go primarily to China and Vietnam, and places where Orthocoronavirinae are commonly found, such as Guangzhou (UNODC, 2020). The Pangolin is one important coronavirus host and a bioindicator of a culture devoted to wildlife consumption in that part of the world.

## The United States case

The United States is the fourth largest open market of wild animals globally and the third consumer of wildlife online (TRAFFIC, 2021). Furthermore, 29% of its population consider buying wildlife products, and 12% are likely or very likely to do so, against 9% of the world population (TRAFFIC, 2021). American law does not consider most wildlife trading as illegal, which includes wild cats as pets. Hence, the United States has the largest number of facilities for tigers in the world (355), with 2729 individuals, just behind China in the number of animals (UNODC, 2020). This same report showed that the United States share of tiger traffic is 3.5% of known destination, but 87.3% of illegally hunted tigers go to unknown places, and the United States are likely to share some of these lots. We found 16 cases of Orthocoronavirinae in the United States from 10 different mammals, and 25% of these were cats, domestic and wild. There are plenty of room for unmonitored disease emergences in the United States wild animal trading scenario.

## Risks of Orthocoronavirinae EIDs in human-modified ecosystems under long-term intermediate disturbance

Models describing risks of overall EIDs from wild tropical areas are speculative and influenced by weighted data to fix the absence of uniform information worldwide (Allen et al., 2017). Nonetheless, there is substantial uncertainty in most of these models, suggesting risks of EIDs from places where deforestation is ongoing. At least for Orthocoronavirinae, it seems more reasonable to consider a different global scenario:

emergence might be related to intermediate disturbances caused by long-term exploitation of some areas rather than a result of newly expanding deforestation.

Forest fragments are constantly under threat and subject to hunting and selective logging, which exposes humans to forests under a certain degree of disturbance. Such conditions may be more suitable to accommodate and keep wild animals closer to humans and, thus, under some mild-to-intense stress. The scenarios our present model suggests as the most dangerous places for EID correspond to some of the proposed hotspots for surveillance used by the USAID-Predict Programme, based on the importance of increasing urbanization as a driver of increased risk zoonotic viruses spillover (Olival et al., 2017).

Disturbed forests in densely populated and relatively developed regions, but with chronic poverty, seemed more likely to raise spillover risks than far wild places. Eventually, after human settlements start to grow in a frontier of deforestation, it may become a similarly riskier scenario, and this is an increasingly frequent situation in the three largest tropical forests in the world: Amazon basin, Congo basin and Indonesia (Taylor et al., 2001; Volpato et al., 2020). Our analyses tested total deforestation and arboreal cover, which did not consider secondary and continuously impacted forests as deforested but as part of the arboreal cover. None were significant, as in developed places, the major deforestation may have happened before the 20 years of records we used, and remaining forests are, for several reasons, too variable in size. Urban and industrialized regions in developing countries are increasingly coexisting with forest remains, but if the protection of these relics is not adequate, it could cause as much damage as benefits. Nature conservation within intensely modified landscapes is desired and demands investments, monitoring and management, and, thus, social and political engagement.

Our study; however, was unable to separate the effect of people's exposure to disturbed nature inside a wealthy region/city from the impact of animal consumption in these places, regardless of the origin of the animal. Most importantly, any too general EID risk models may never untangle the differences between heavy deforestation and mild disturbance (Allen et al., 2017; Jones et al., 2008; Karesh et al., 2012; Singh et al., 2021).

## Concluding remarks: the case of SARS-CoV-2 and bat viruses

The SARS-CoV-2 pandemic exacerbated the urgency to increase investments for a global programme of viral surveillance. Nevertheless, there are still many caveats to produce a predictive programme to avoid a severe future spillover. Most of these caveats relate to the unbalanced research on the virus and mammal–bird

hosts, and an unexplained high viral richness variance (Olival et al., 2017), as well as the discontinuity and flaws in large funding programmes (Schmidt, 2020). There is also the urgency to deepen a thorough dialogue between virology, ecology and conservation science.

The way of life in most developed parts of the planet, both East and West, imposes extreme pressure on natural resources, which is a direct, not indirect, cause of the current pandemic crisis. Consumerism in general, causing excessive and unnecessary exploitation of wild places, along with wildlife traffic and bad environmental management in developed regions and cities, might have been the origin of many emergent infectious diseases and spillovers from Orthocoronavirinae species along the history. Sadly, people experiencing poverty in an intensely consumerist society are the most likely to get contaminated.

## ACKNOWLEDGEMENTS

This work was supported by the Graduate Program in Bioinformatics (UFMG), Graduate Program in Microbiology (UFMG), Graduate Program in Parasitology (UFMG) and Graduate Program of Biological Science (UFOP). S.P.R. (306572-2019-2), V.A.A. (312045/2020-4), J.A.F.D.-F. (301799/2016-4), R.L. (306694/2018-2) and A.G.-N. (310764/2016-5) are researchers granted by Conselho Nacional de Desenvolvimento Científico e Tecnológico/CNPq, Brazil. J.A.F.D.-F. is INCT granted (465610/2014-5). D.B. is Visitor Professor at UFMG.

## DATA AVAILABILITY STATEMENT

The data that support the finding of this study are available in the Supporting Information of this article. It includes one excel file with raw data detailing each species detail and GenBank accession, three complementary figures and one word file with bioinformatic analytical methodology in details.

## CONFLICT OF INTEREST

The authors declare that they have no competing interests.

## ORCID

Sérvio P. Ribeiro  <https://orcid.org/0000-0002-0191-8759>

Raner José Santana Silva  <https://orcid.org/0000-0002-0805-2003>

## REFERENCES

- Allen, T., Murray, K.A., Zambrana-Torrel, C., Morse, S.S., Rondinini, C., Di Marco, M. et al. (2017) Global hotspots and correlates of emerging zoonotic diseases. *Nature Communications*, 8, 1124. doi:10.1038/s41467-017-00923-8
- Alvey, A.A. (2006) Promoting and preserving biodiversity in the urban forest. *Urban Forestry & Urban Greening*, 5, 195–201. <https://doi.org/10.1016/j.ufug.2006.09.003>
- Benvenuto, D., Giovanetti, M., Ciccozzi, A., Spoto, S., Angeletti, S. & Ciccozzi, M. (2020) The 2019-new coronavirus epidemic: evidence for virus evolution. *Journal of Medical Virology*, 92, 455–459. <https://doi.org/10.1002/jmv.25688>
- Bernstein, A.S., Ando, A.W., Lock-Temzelides, T., Vale, M.M., Li, B. V., Li, H. et al. (2022) The costs and benefits of primary prevention of zoonotic pandemics. *Science Advances*, 8, eabl4183.
- Buck, J.C. & Weinstein, S.B. (2020) The ecological consequences of a pandemic. *Biology Letters*, 16, 20200641. <https://doi.org/10.1098/rsbl.2020.0641>
- Darriba, D., Posada, D., Kozlov, A.M., Stamatakis, A., Morel, B. & Tomas, F. (2019) Model test-NG: a new and scalable tool for the selection of DNA and protein evolutionary models. *Molecular Biology and Evolution*, 37, 291–294. doi:10.1093/molbev/msz189
- Daszak, P., Cunningham, A.A. & Hyatt, A.D. (2000) Emerging infectious diseases of wildlife—threats to biodiversity and human health. *Science*, 287(5452), 443–449. <https://doi.org/10.1126/science.287.5452.443> (Erratum in: *Science* 10: 287(5459),1756).
- Dáttilo, W., Barrozo-Chávez, N., Lira-Noriega, A., Guevara, R., Villalobos, F., Santiago-Alarcon, D. et al. (2020) Species-level drivers of mammalian ectoparasite faunas. *The Journal of Animal Ecology*, 89, 1754–1765. doi:10.1111/1365-2656.13216
- DFID (2008) Democratic Republic of Congo (DRC). Available from: [https://assets.publishing.service.gov.uk/government/uploads/system/uploads/attachment\\_data/file/913352/Democratic-Republic-Congo-Profile.pdf](https://assets.publishing.service.gov.uk/government/uploads/system/uploads/attachment_data/file/913352/Democratic-Republic-Congo-Profile.pdf) [Accessed 20th August 2021]
- Dominguez, S.R., O'Shea, T.J., Oko, L.M. & Holmes, K.V. (2007) Detection of group 1 coronaviruses in bats in North America. *Emerging Infectious Diseases*, 13, 1295–1300.
- Dunn, R.R., Davies, T.J., Harris, N.C. & Gavin, M.C. (2010) Global drivers of human pathogen richness and prevalence. *Proceedings of the Royal Society B*, 277, 2587–2595. doi:10.1098/rspb.2010.0340
- Edgar, R.C. (2004) MUSCLE: a multiple sequence alignment method with reduced time and space complexity. *BMC Bioinformatics*, 5, 113. doi:10.1186/1471-2105-5-113
- Ellwanger, J.H., Kulmann-Leal, B., Kaminski, V.L., Valverde-Villegas, V.L., Veiga, A.B.G., Spilki, F.R. et al. (2020) Beyond diversity loss and climate change: impacts of Amazon deforestation on infectious diseases and public health. *Anais da Academia Brasileira de Ciências*, 92, e20191375. <https://doi.org/10.1590/0001-3765202020191375>
- Field, H.E. (2009) Bats and emerging zoonoses: Henipaviruses and SARS. *Zoonoses and Public Health*, 56, 278–284. doi:10.1111/j.1863-2378.2008.01218.x
- Global Forest Watch. (2021) *Forest monitoring designed for action*. Available from: <https://www.globalforestwatch.org/> [Accessed 25th July 2021].
- Góes, L.G.B., Campos, A.C.A., Carvalho, C., Ambar, G., Queiroz, L. H., Cruz-Neto, A.P. et al. (2016) Genetic diversity of bats coronaviruses in the Atlantic forest hotspot biomes, Brazil. *Infection, Genetics and Evolution*, 44, 510–513.
- Johnson, P.T.J., Roode, J.C. & Fenton, A. (2015) Why infectious disease research needs community ecology. *Science*, 349, 1259504. <https://doi.org/10.1126/science.1259504>
- Jones, K.E., Patel, N.G., Levy, M.A., Storeygard, A., Balk, D., Gittleman, J.L. et al. (2008) Global trends in emerging infectious diseases. *Nature*, 451, 990–993. doi:10.1038/nature06536
- Karesh, W.B., Dobson, A., Lloyd-Smith, J.O., Lubroth, J., Dixon, M. A., Bennett, M. et al. (2012) Ecology of zoonoses: natural and unnatural histories. *Lancet*, 380, 1936–1945. [https://doi.org/10.1016/S0140-6736\(12\)61678-X](https://doi.org/10.1016/S0140-6736(12)61678-X)
- Katoh, K., Rozewicki, J. & Yamada, K.D. (2019) MAFFT online service: multiple sequence alignment, interactive sequence choice and visualization. *Briefings in Bioinformatics*, 20, 1160–1166. doi:10.1093/bib/bbx108
- Keele, B.F., Heuvelink, F.V., Li, Y., Bailes, E., Takehisa, J., Santiago, M.L. et al. (2006) Chimpanzee reservoirs of pandemic and nonpandemic HIV-1. *Science*, 28, 523–526.
- Keesing, F. & Ostfeld, R.S. (2021) Impacts of biodiversity and biodiversity loss on zoonotic diseases. *Proceedings. National*

- Academy of Sciences United States of America, 118, e2023540118. <https://doi.org/10.1073/pnas.2023540118>
- Lanfeard, R., Frandsen, P.B., Wright, A.M., Senfeld, T. & Calcott, B. (2017) Partition finder 2: new methods for selecting partitioned models of evolution for molecular and morphological phylogenetic analyses. *Molecular Biology and Evolution*, 34, 772–773. doi:10.1093/molbev/msw260
- Latinne, A., Hu, B., Olival, K.J., Zhu, G., Zhang, L., Hongying, L. et al. (2020) Origin and cross-species transmission of bat coronaviruses in China. *Nature Communications*, 11, 4235. doi:10.1038/s41467-020-17687-3
- Liu, Z., Xiao, X., Wei, X., Li, J., Yang, J., Tan, H. et al. (2020a) Composition and divergence of coronavirus spike proteins and host ACE2 receptors predict potential intermediate hosts of SARS-CoV-2. *Journal of Medical Virology*, 92, 595–601. <https://doi.org/10.1002/jmv.25726>
- Machado, J.D., Scott, R., Guirales, S. & Janies, D.A. (2021) Fundamental evolution of all Orthocoronavirinae including three deadly lineages descendent from Chiroptera-hosted coronaviruses: SARS-CoV, MERS-CoV and SARS-CoV-2. *Cladistics*, 37, 461–488. doi:10.1111/cla.12454
- Megevand, C. (2013) Deforestation trends in the Congo basin: reconciling economic growth and forest protection. Washington DC, US: World Bank.
- Maxmen, A. (2021) Who report into COVID origins zeroes in on animal markets. *Nature*, 592, 173–174.
- McCallum, H. & Dobson, A. (1995) Detecting disease and parasite threats to endangered species and ecosystems. *Trees*, 10, 190–194.
- Mildenstein, T. & Tanshi, I.R.P.A. (2015) Exploitation of bats for bushmeat and medicine. In: *Bats in the anthropocene: conservation of bats in a changing world*. Cham: Springer.
- Olival, K.J., Hosseini, P.R., Zambrana-Torrel, C., Ross, N., Bogich, T.L. & Daszak, P. (2017) Host and viral traits predict zoonotic spillover from mammals. *Nature*, 546, 646–650.
- Omonijo, A.G., Oguntoke, O., Matzarakis, A. & Adeofun, C.O. (2011) A study of weather related respiratory diseases in eco-climatic zones. *African Review of Physics*, 5, 41–56.
- Ostfeld, R.S. & Keesing, F. (2000) Biodiversity series: the function of biodiversity in the ecology of vector-borne zoonotic diseases. *Canadian Journal of Zoology*, 78, 2061–2078. doi:10.1139/z00-172
- Pattanayak, S.K., Kramer, R.A. & Vincent, J.R. (2017) Ecosystem change and human health: implementation economics and policy. *Philosophical Transactions of the Royal Society of London. Series B, Biological Sciences*, 372, 20160130. doi:10.1098/rstb.2016.0130
- Plourde, B.T., Burgess, T.L., Eskew, E.A., Roth, T.M., Stephenson, N. & Foley, J.E. (2017) Are disease reservoirs special? Taxonomic and life history characteristics. *PLoS One*, 12, e0180716. doi:10.1371/journal.pone.0180716
- R Core Team. (2016) *A language and environment for statistical computing*. Vienna, Austria: R Foundation for Statistical Computing. <https://doi.org/10.1016/j.jaut.2020.102433>
- Roser, M. (2019) *Human development index (HDI)*. Available from: [www.ourworldindata.org](http://www.ourworldindata.org) [Accessed 16th April 2021].
- Rothan, H.A. & Byrareddy, S.N. (2020) The epidemiology and pathogenesis of coronavirus disease (COVID-19) outbreak. *Journal of Autoimmunity*, 109, e102433.
- Sayers, E.W., Barret, T., Church, D.M., DuCuccio, M., Federhen, S., Feolo, M. et al. (2010) Database resources of the national center for biotechnology information. *Nucleic Acids Research*, 39, 38–51.
- Schmidt, C. (2020) *Why the coronavirus slipped past disease detectives?* Available from: <https://www.scientificamerican.com/article/why-the-coronavirus-slipped-past-disease-detectives/> [Accessed 27th July 2021].
- Schrag, S.J. & Wiener, P. (1995) Emerging infectious disease: what are the relative roles of ecology and evolution. *Trees*, 10, 319–324.
- Shi, Z. & Hu, Z. (2008) A review of studies on animal reservoirs of the SARS coronavirus. *Virus Research*, 133, 74–87. <https://doi.org/10.1016/j.virusres.2007.03.012>
- Singh, B.B., Ward, M.P. & Dhand, N.K. (2021) Geodemography, environment and societal characteristics drive the global diversity of emerging, zoonotic and human pathogens. *Transboundary and Emerging Diseases*, 69, 1131–1143. <https://doi.org/10.1111/tbed.14072>
- Tallavaara, M., Eronen, J.T. & Luoto, M. (2018) Productivity, biodiversity, and pathogens influence the global hunter-gatherer population density. *Proceedings of the National Academy of Sciences of the United States of America*, 115, 1232–1237. doi:10.1073/pnas.1715638115
- Taylor, L.H., Latham, S.M. & Woolhouse, M.E.J. (2001) Risk factors for human disease emergence. *Philosophical Transactions of the Royal Society B*, 356, 983–989. doi:10.1098/rstb.2001.0888
- TRAFFIC. (2021) 2021 END Wildlife Trafficking Report. Available from: <https://www.state.gov/2021-end-wildlife-trafficking-report/> [Accessed 20th August 2021]
- UNODC. (2020) World Wildlife Crime Report 2020: trafficking in protected species. New York, US: United Nations.
- Volpato, G., Fontefrancesco, M.F., Gruppiso, P., Zocchi, D.M. & Pieroni, A. (2020) Baby pangolins on my plate: possible lessons to learn from the COVID-19 pandemic. *Journal of Ethnobiology and Ethnomedicine*, 16, 19. doi:10.1186/s13002-020-00366-4
- Woo, P.C., Lau, S.K.P., Lam, C.S.F., Lau, C.C.Y., Tsang, A.K.L., Lau, J.H.N. et al. (2012) Discovery of seven novel mammalian and avian coronaviruses in the genus deltacoronavirus supports bat coronaviruses as the gene source of alphacoronavirus and betacoronavirus and avian coronaviruses as the gene source of gammacoronavirus and deltacoronavirus. *Journal of Virology*, 86, 3995–4008. <https://doi.org/10.1128/JVI.06540-11>
- Zhang, Y.Z. & Holmes, E.C. (2020) A genomic perspective on the origin and emergence of SARS-CoV-2. *Cell*, 181, 223–227. <https://doi.org/10.1016/j.cell.2020.03.035>
- Zhang, Z., Li, Y., Zhang, A.L., Wuang, Y. & Molina, M.J. (2020) Identifying airborne transmission as the dominant route for the spread of COVID-19. *Proceedings of the National Academy of Sciences of the United States of America*, 117, 14857–14863. doi:10.1073/pnas.2009637117
- Zhou, H., Ji, J., Chen, X., Bi, Y., Li, J., Wang, Q. et al. (2021) Identification of novel bat coronaviruses sheds light on the evolutionary origins of SARS-CoV-2 and related viruses. *Cell*, 184, 1–12. <https://doi.org/10.1016/j.cell.2021.06.008>
- Zhu, T., Korber, B.T., Nahmias, A.J., Hooper, E., Sharp, P.M. & Ho, D. D. (1998) An African HIV-1 sequence from 1959 and implications for the origin of the epidemic. *Nature*, 391, 594–597.

## SUPPORTING INFORMATION

Additional supporting information can be found online in the Supporting Information section at the end of this article.

**How to cite this article:** Ribeiro, S.P., Barh, D., Andrade, B.S., José Santana Silva, R., Costa-Rezende, D.H., Fonseca, P.L.C. et al. (2022) Long-term unsustainable patterns of development rather than recent deforestation caused the emergence of Orthocoronavirinae species. *Environmental Microbiology*, 1–11. Available from: <https://doi.org/10.1111/1462-2920.16121>

# Severe airport sanitarian control could slow down the spreading of COVID-19 pandemics in Brazil

Sérvio Pontes Ribeiro<sup>1,2,3,\*</sup>, Alcides Castro e Silva<sup>4,\*</sup>, Wesley Dáttilo<sup>5</sup>, Alexandre Barbosa Reis<sup>1,6</sup>, Aristóteles Góes-Neto<sup>7</sup>, Luiz Carlos Junior Alcantara<sup>8,9</sup>, Marta Giovanetti<sup>8</sup>, Wendel Coura-Vital<sup>1,10</sup>, Geraldo Wilson Fernandes<sup>11</sup> and Vasco Ariston C. Azevedo<sup>9</sup>

<sup>1</sup> Núcleo de Pesquisas em Ciências Biológicas, Universidade Federal de Ouro Preto, Ouro Preto, Minas Gerais, Brazil

<sup>2</sup> Laboratório de Ecohealth, Ecologia de Insetos de Dossel e Sucessão Natural-ICEB, Universidade Federal de Ouro Preto, Ouro Preto, MG, Brazil

<sup>3</sup> Laboratório de Fisiologia de Insetos Hematófagos-DEPAR, Universidade Federal de Minas Gerais, Belo Horizonte, MG, Brazil

<sup>4</sup> Laboratório da Ciência da Complexidade-Departamento de Física, Universidade Federal de Ouro Preto, Ouro Preto, Minas Gerais, Brazil

<sup>5</sup> Red de Ecoetología, Instituto de Ecología AC, Xalapa, Veracruz, Mexico

<sup>6</sup> Laboratório de Imunopatologia-Departamento de Análises Clínicas-Escola de Farmácia, Universidade Federal de Ouro Preto, Ouro Preto, Minas Gerais, Brazil

<sup>7</sup> Laboratório de Biologia Molecular e Computacional de Fungos-Departamento de Microbiologia-ICB, Universidade Federal de Minas Gerais, Belo Horizonte, Minas Gerais, Brazil

<sup>8</sup> Laboratório de Flavivírus, Instituto Oswaldo Cruz, Fundação Oswaldo Cruz, Rio de Janeiro, Rio de Janeiro, Brazil

<sup>9</sup> Laboratório de Genética Celular e Molecular-Departamento de Genética, Ecologia & Evolução-ICB, Universidade Federal de Minas Gerais, Belo Horizonte, MG, Brazil

<sup>10</sup> Laboratório de Epidemiologia e Citologia-Departamento de Análises Clínicas-Escola de Farmácia, Universidade Federal de Ouro Preto, Ouro Preto, MG, Brazil

<sup>11</sup> Departamento de Genética, Ecologia & Evolução/ICB, Universidade Federal de Minas Gerais, Belo Horizonte, Minas Gerais, Brazil

\* These authors contributed equally to this work.

Submitted 23 March 2020

Accepted 8 June 2020

Published 25 June 2020

Corresponding authors

Sérvio Pontes Ribeiro,

spribeiro@ufop.edu.br

Wesley Dáttilo,

wesley.dattilo@inecol.mx

Academic editor

Morenike Folayan

Additional Information and  
Declarations can be found on  
page 13

DOI 10.7717/peerj.9446

© Copyright

2020 Ribeiro et al.

Distributed under

Creative Commons CC-BY 4.0

## ABSTRACT

**Background:** We investigated a likely scenario of COVID-19 spreading in Brazil through the complex airport network of the country, for the 90 days after the first national occurrence of the disease. After the confirmation of the first imported cases, the lack of a proper airport entrance control resulted in the infection spreading in a manner directly proportional to the amount of flights reaching each city, following the first occurrence of the virus coming from abroad.

**Methodology:** We developed a Susceptible-Infected-Recovered model divided in a metapopulation structure, where cities with airports were demes connected by the number of flights. Subsequently, we further explored the role of the Manaus airport for a rapid entrance of the pandemic into indigenous territories situated in remote places of the Amazon region.

**Results:** The expansion of the SARS-CoV-2 virus between cities was fast, directly proportional to the city closeness centrality within the Brazilian air transportation network. There was a clear pattern in the expansion of the pandemic, with a stiff

## OPEN ACCESS

exponential expansion of cases for all the cities. The more a city showed closeness centrality, the greater was its vulnerability to SARS-CoV-2.

**Conclusions:** We discussed the weak pandemic control performance of Brazil in comparison with other tropical, developing countries, namely India and Nigeria. Finally, we proposed measures for containing virus spreading taking into consideration the scenario of high poverty.

**Subjects** Computational Biology, Ecology, Mathematical Biology, Virology, Statistics

**Keywords** SIR model, Metapopulation dynamics, Amazonia, Indigenous people, One-Ecohealth, SARS-CoV-2 pandemic

## INTRODUCTION

The new disease COVID-19 has been spreading rapidly around the world since early January. It started in China at the end of 2019, been declared a “Public Health Emergency of International Concern” in 30 January and a pandemic in 11 March (*World Health Organization (WHO), 2020a; Zhu et al., 2020*). Its form of transmission is mainly through respiratory droplets of infected patients and contact with surfaces infected by aerosols (*Fathlzadeh et al., 2020*). However, the transmission dynamics has changed quickly in few months, with  $R_0$  varying from 0.3 to 2.0 in some countries and close to 3.0 in others (*Lai et al., 2020a; World Health Organization (WHO), 2020a*). Large continental countries are likely to be very vulnerable to the occurrence of pandemics (*Morse et al., 2012; Dáttilo et al., 2020*). While the dissemination dynamics have varied between regions, country sanitary policies play a key role. For instance, two very large developing countries, India and Brazil, have a very different epidemical pattern. On March 18th, India had 137 cases and Brazil 621, as recorded in the Brazilian Ministry of Health (<https://covid.saude.gov.br/>, 2020) and John Hopkins (<https://gisanddata.maps.arcgis.com/>, 2020) monitoring sites dedicated to SARS-CoV-2 and COVID-19. From 17th to 18th March, Brazil had an increase of 31% in 1 day, with only four capitals exhibiting community transmission, which was the same in India. Nonetheless, a very distinct pattern in the ascending starting point for the reported disease exponential curve was observed in each country.

By enlarging the comparison to another developing tropical country in the Southern Hemisphere (thus, in the same season), we selected Nigeria since it was the first country to detect a COVID-19 case in sub-Saharan Africa (*World Health Organization (WHO), 2020d*). Nigeria reported eight confirmed cases during the same period of time (*Nigeria Centre for Disease Control, 2020*). Furthermore, Nigeria has a population similar to that of Brazil (201 million and 211.1 million, respectively, according to *United Nations, 2019*).

Both India (*Airports Authority of India, 2020*) and Nigeria (*Federal Airports Authority of Nigeria, 2020*) ensured severe entrance control, and close follow up of each confirmed case, as well as their living and working area, and people in contact with them, differently from Brazil. In Brazil, the Ministry of Health has developed a good monitoring network and a comprehensive preparation of the health system for the worst-case scenario. Nonetheless, apparently, the decisions from the Ministry of Health did not cover airport control, and only on March 19th, eventually too late, the government



decided to limit the number of flights coming from Europe or Asia. Hence, the entrance of potentially exposed passengers to SARS-CoV-2 in Brazil has been occurring with no control, at least until the aforementioned date. Moreover, after confirming that a person is infected with SARS-CoV-2, his/her monitoring is initiated but there is no monitoring of potential contacts.

For pandemic situations, the classical algebraic ecological models of species population growth from Verhulst, and species interaction models from Lotka-Volterra, are theoretical frameworks capable to describe the phenomenon and to propose actions to stop it (*Pianka, 2000*). In many aspects, social distancing is a way to severely reduce carrying capacity, that is, the resources available for the virus dissemination. This is the best action for within-city pandemic spreading of this new coronavirus (*Hellewell et al., 2020*), since the main form of transmission is direct contact between people or by contact with fomite, mainly in closed environments, such as classrooms, offices, etc. (*Rothe et al., 2020; Bedford et al., 2020*). Regardless of virulence, for a highly contagious virus such as SARS-CoV-2, the occurrence of the first case in a nation will result in a strongly and nearly uncontrollable exponential growth curve, depending only on the number of encounters between infected and susceptible people, and fueled by a high  $R_0$ , which is ranging from 0.8 to 3.6 for COVID-19, depending on region and period analyzed (*Lai et al., 2020a, 2020b*).

On the other hand, the dynamics of disease spreading among cities are entirely distinct. This is a growing scientific area, an obliged interdisciplinary field, where neural network driven epidemiological phenomena is central (*Brockmann & Helbing, 2013*); however, it must be defined by metapopulation and closeness, as well as by an individual gene flow driven phenomenon (*Colizza & Vespignani, 2007*). In order to understand subpopulation flow between demes—which are cities—connected by roads or air flight networks, several complex details may be raised in the process of modelling such as reality (*Balcan et al., 2010*). For instance, probabilistic motivated effective distance, which is the actual proximity caused by business, culture, and investments between two cities, is much more important than real geography, especially for airlines network (*Brockmann & Helbing, 2013*). Nevertheless, for such theoretical approach to infection disease dissemination, an ecological concept is key: metapopulation (*Hanski, 1998*). However, ecologists are those who are least devoted to explore human–pathogen interaction at a global or continental scale. The ecological approach may focus on the most biological aspect of these dynamics, which is simply virus dissemination inside an infected person. As typically designed in Ecology, the first attempt will be based on the most neutral model (sensu *Hubbell, 2001*), that is, the directions taken through the most frequent and intensively used links.

In this work, we present an epidemiological model describing the free entrance of people coming from two highly infected countries with close links to Brazil: Italy and Spain. We show how SARS-CoV-2 had spread into the Brazilian cities by the international airports, and then to other, less internationally connected cities, through the Brazilian airport network. For exploring the dynamics of a continent size, nationwide spreading of

SARS-CoV-2, as it is the case of Brazil, we assumed cities connected by airports (simply cities hereafter) formed a metapopulation structure.

Each person in a city was taken as a component of a superorganism, that is, an interdependent entity where living individuals are not biologically independent between them in various subtle ways. By doing so, we dealt with cities as the sampling units, not the people, and, therefore, our model is slightly different from classic bolsonic models (Colizza & Vespignani, 2007; Nicolaidis et al., 2012). Flights coming from foreign countries with COVID-19 (namely Spain and Italy for this article) represent the probability of an external introduction of infection in each city. Additionally, we also further explored the vulnerability of the Amazon region, especially of those remote towns where indigenous and traditional communities predominate.

## MATERIALS AND METHODS

In order to describe the pattern of air transportation and its role in the spreading of the disease, we built a Susceptible-Infected-Recovered (SIR) model (Hethcote, 1989; Anderson, 1991) split amongst the cities that are interconnected by flights. In this model, the population size inside each city is irrelevant. Moreover, the number of flights is highly correlated with city population ( $R^2 = 0.76$ ;  $p < 0.0001$ ) and, thus, a good proxy of city size. Similarly, to our purpose the time when the collective infection stage was reached inside each city was irrelevant. Thus, we assumed that the city was fully infected and became infectious to the whole system, and, therefore, became a source and not a sink of infection events, after a certain amount of arriving contaminated people sums up. Hence, the SIR model started having cities with only susceptible events and change of these to the infected stage was counted as proportion of the population. Infected events only appeared by migration, that is, travelers only from Italy and Spain, for sake of simplicity and proximity to the early facts.

After the first occurrence having been recorded in the country, infected people started to spread through the national airlines, and this spreading is proportional to the amount of infected people accumulating in a city (see the model explanation below). Because of that, the model causes a transient timing, when the amount of infected people arriving is greater than the community transmission. Afterwards, the city started to disseminate to other places by probability rules. As the transmission is quite likely to happen by the simple proximity person-to-person, due to the resistance of the virus in air droplets and surfaces, as hands or metals, we assumed that a simple encounter will cause infection. However, this became an inner trait of each city that after having local transmission, starts to transmit to other cities as explained above. In addition, the model assumes that there is no public control in people circulation after arriving of an infected person. Ethical approval was not necessary as human participants were not involved in the study.

We used a modified version of the SIR model, which took into account the topology of how the cities-demes were linked by domestic flights. In the SIR original model, the infection of susceptible cities occurs by probability  $\beta$  of a healthy being (S) encounters an

infected one ( $I$ ). Conversely, the model has a probability of an infected one get recovered ( $R$ ) given by a parameter  $\gamma$ . Analytically:

$$S_{t+1} = S_t - \frac{\beta}{N} S_t I_t$$

$$I_{t+1} = I_t + \frac{\beta}{N} S_t I_t - \gamma I_t$$

$$R_{t+1} = R_t + \gamma I_t$$

where the indexes  $t$  and  $t + 1$  represent the present time and the next time, respectively, and  $N = S + I + R$  is the total constant population. In this work, we proposed two modifications of the SIR model. The first one is related to the fact that we considered all the Brazilian cities that have an airport as subpopulations, meaning that each city has its own SIR variables set. Thus, we had  $S^i$ ,  $I^i$ , and  $R^i$  where  $i$  was a given city. In our case study,  $1 \leq i \leq 154$ . The second important modification was related to the connections among the cities, which we used as a network of disease dissemination. This city network is given by the domestic flights among all the airports in Brazil, taking into account the number and the direction of flights. Therefore, we have a weighted network, where the weighted closeness centrality of each city was measured. Thus, the flights provided a dependent mechanism by which the between-cities connections caused a coupling of SIR equations based on the network flight structure. This coupling is provided by the last equation and is mediated by the new introduced parameter alpha. Using [Agência Nacional de Aviação Civil \(ANAC\) \(2020\)](#) data, it was possible to track all the domestic flights in Brazil ([Fig. 1](#)).

The modified version of SIR model is then described as follows:

$$S_{t+1}^i = S_t^i - \frac{\beta}{N} S_t^i (I_t^i + \bar{I}_t^i)$$

$$I_{t+1}^i = I_t^i + \frac{\beta}{N} S_t^i (I_t^i + \bar{I}_t^i) - \gamma (I_t^i + \bar{I}_t^i)$$

$$R_{t+1}^i = R_t^i + \gamma (I_t^i + \bar{I}_t^i)$$

where the upper index  $i$  indicates the city, and  $t$  the time. The term  $\bar{I}_t^i$  represents the infection added to the  $i$ th city due to traveling diseases, and it is calculated as follow:

$$\bar{I}_t^i = \alpha \sum_{j=0}^{154} k_{j,i} I_j$$

where  $k_{j,i}$  is the number of flights departing at city  $j$  and arriving at city  $i$ , and  $\alpha$  is a newly introduced parameter, which represents the fraction of traveling infected population.

For the time, considering the geographic of Brazil and the time-lag for the dissemination

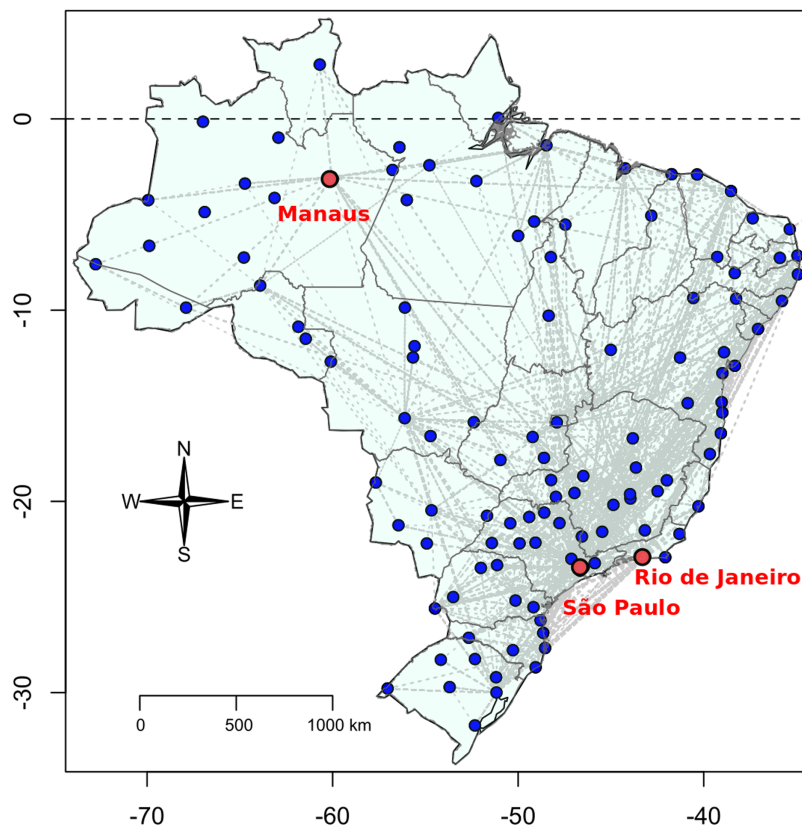


**Figure 1** Brazilian flight network, taken from ANAC database.

Full-size  DOI: 10.7717/peerj.9446/fig-1

towards the most remote cities, we estimated 90 days of disease expansion and assumed  $\gamma$  as 0, in other words, no recovery. Despite the artificiality of this assumption, we considered that the amount of people still to be infected is larger than those recovered and, thus, becoming resistant. For instance, by 19th May the recovery rates in Brazil reached 85%, but this corresponded to only 100.5 thousand people around the country ([www.worldometers.info/coronavirus/country/brazil/](http://www.worldometers.info/coronavirus/country/brazil/), 2020). Divided between each infected city, this makes mathematically small numbers, and thus resistance becomes demographically irrelevant to our output of early disease dissemination. Furthermore, by dealing with only the infected portion of the population (proportion of infected), we avoided the uncertainties related to the little known COVID-19 resistance development (*Li et al., 2020*).

The model was developed in C and is available as [Supplemental Material 1](#) (and the database as [Supplemental Material 2](#)). In addition, we also used a linear model to test whether those cities with higher city closeness centrality (i.e., important cities for connecting different cities within the Brazilian air transportation network) were more vulnerable to SARS-CoV-2 dissemination. The Beta parameter was defined by calibrating the model with real time series from Johns Hopkins Coronavirus Research Center (<https://coronavirus.jhu.edu/map.html>), which leads to  $\beta = 0.3035$  ([Supplemental Material 1](#)). We used the value  $\alpha = 0.0001$  based on the amount of flights

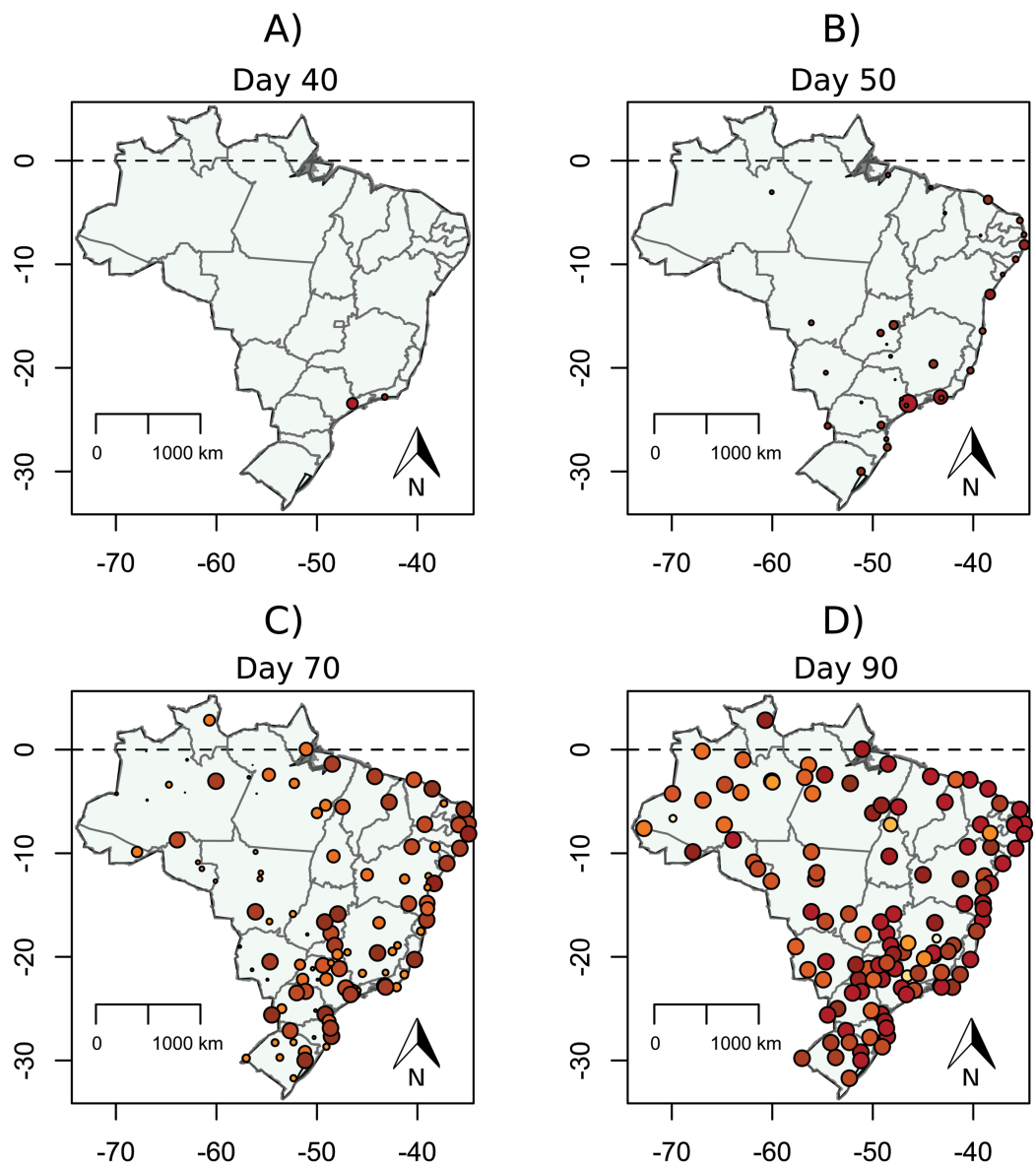


**Figure 2** Proportion of infected population of each Brazilian city in 40 (A), 50 (B), 70 (C), and 90 (D) days. Circle colour temperature represents a gradient in percentage of the infected population. Circle size also reflects the size of the pandemics locally in the logarithm scale.

Full-size [DOI: 10.7717/peerj.9446/fig-2](https://doi.org/10.7717/peerj.9446/fig-2)

needed from the peak of the disease in Italy until an infected person was recorded from that country in Brazil.

## RESULTS

The expansion of the SARS-CoV-2 virus between cities was fast, directly proportional to the city closeness centrality within the Brazilian air transportation network. The disease spread from São Paulo and Rio de Janeiro to the next node-city by the flight network, and, in 90 days, virtually all the cities with airport(s) were reached; however, it occurred with a distinct intensity (Fig. 2; Supplemental Material 3). There was a clear pattern in the

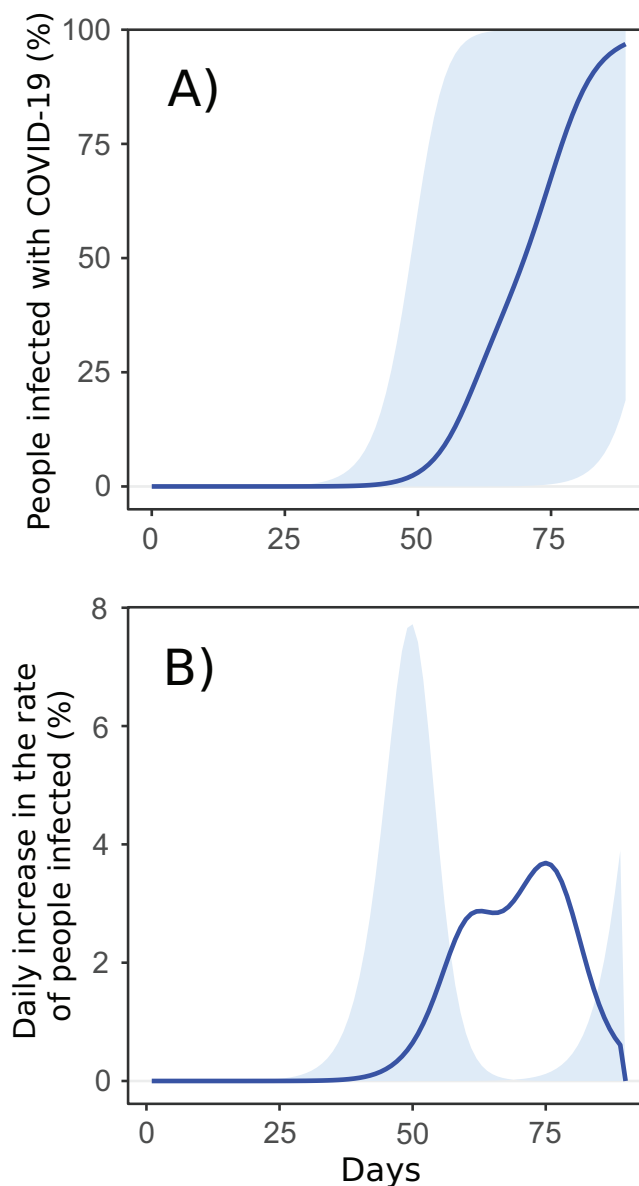


**Figure 3** Proportion of infected people per cities until 90 days. (A) Cumulative increment rate. The blue line is the national average, and the shadow area is the summing up of minimum and maximum values of all the cities per time interval; (B) daily increment rate. The blue line is the average, showing the overall high rate of infection occurring from 50 to 80 days. Shadow shows the first and the highest peak in the hub cities, around 50 days, and, subsequently, a peripheric peak after 75 days.

Full-size  DOI: [10.7717/peerj.9446/fig-3](https://doi.org/10.7717/peerj.9446/fig-3)

expansion of the pandemic, with a stiff exponential expansion of cases (measured as the cumulative percentage of infected people per city) for all the cities. On average, the model showed an ascendant curve starting at day 50 (around 15 April), with the most connected cities starting their ascendant curve just after 25 days, and the most isolated ones from day 75 (10th May; Fig. 3A). Looking at the daily increment rates, it is clear a fast and high peak of infections in the hub cities, happening around 50 days and, starting from 75 days, a new peripheric peak (Fig. 3B).

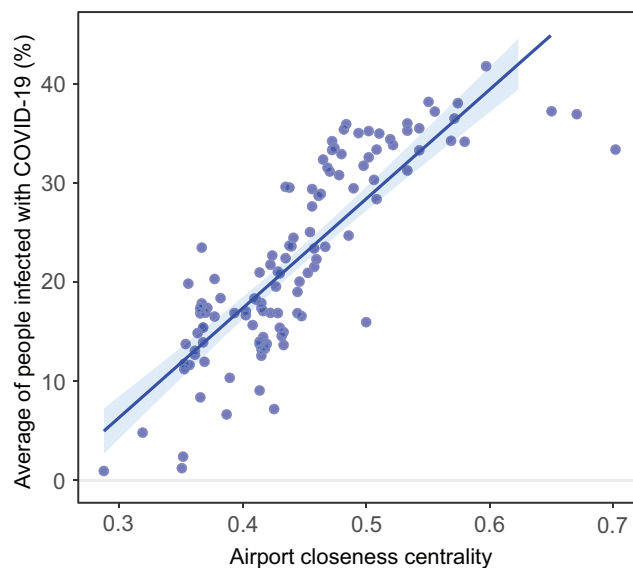


**Figure 4** Airport closeness centrality within the Brazilian air transportation network, and its effect on the vulnerability of each city. Correlation between airport closeness centrality within the Brazilian air transportation network, and its effect on the vulnerability of each city (represented by the average of the percentage of cases per city for the whole 90 days running:  $r^2 = 0.71$   $p < 0.00001$ ).

Full-size  DOI: 10.7717/peerj.9446/fig-4

The first ten cities to ascend infection rates (São Paulo, Rio de Janeiro, Salvador, Recife, Brasília, Fortaleza, Belo Horizonte, Porto Alegre, Curitiba, and Florianópolis) will actually reach this point about the same time, which is a concerning pattern for the saturation of the public health services. Moreover, this peak in those cities will saturate all the best hospitals in the country simultaneously.

Therefore, we defined the average proportion of infected people for the 90 days as a measure of the vulnerability to COVID-19 dissemination. Henceforth, we found the more a city shows closeness centrality within the air transportation network, the greater was its vulnerability to disease transmission (Fig. 4). This scenario confirmed the importance of a city connecting different cities within the Brazilian air transportation network and, thus, acting as the main driver for the pandemic spreading across the country.

### Consequences for the Amazonian cities and indigenous people

Herein, we showed that an uncontrolled complex airport system made a whole country vulnerable in few weeks, allowing the virus to reach the most distant and remote places, in the most pessimistic scenario. According to our model, any connected city will be infected after 3 months. As the number of flights arriving in a city is the driver for the proportion of infected people, Manaus, which is a relevant regional clustering, was infected sooner. Indeed, on the 17th of March, Manaus was the first Amazonian city with confirmed cases (without community transmission yet, according to the Ministry of Health: <https://covid.saude.gov.br/>, 2020), and it is a node that is one or two steps to all the Amazonian cities. Thus, according to our model, Manaus may reach 1% of the infected

population by the 44th day, while, for instance, the far west Amazonian Tabatinga will take 61 days to reach the same 1% of the population infected. By day 60, Manaus may have an average of 50% of its population infected if nothing is done to prevent it. Tabatinga may also reach the aforementioned value by day 78, if nothing is done to avoid it. To sum up, within 46 days, all the Amazonian cities will have 1% of their population infected and a mean of 50% by day 70.

## DISCUSSION

Our model suggests that Brazil must be prepared for an exponential rise in COVID-19 cases within 3 months from end of February, starting synchronously by the wealthiest cities. Such increase is expected based only on the dissemination among cities by the commercial airports and may get worse without the measures of social distancing proposed by the WHO (Coelho *et al.*, 2020). The Country has failed to contain COVID-19 in airports and to closely monitor those infected people coming from abroad, as well as their living network. According to the Brazilian Airport Authority (Agência Nacional de Aviação Civil (ANAC), 2020), Brazil has the second-largest flight network in the world (just after the USA), with a total of 154 airports registered to commercial flights of which 31 are considered international. In comparison, airport control may be much easier to set up in Nigeria (31 airports of which only five are international: Federal Airport Authority of Nigeria, 2020). Nonetheless, with a population 6.4 times higher than Brazil (United Nations 1919), India, in turn, has a similar sized airport network to Brazil, harboring a total of 123 airports of which 34 are considered international (Airports Authority of India, 2020).

Nevertheless, the situation of COVID-19 in India is currently much milder than in Brazil, and it is hard to blame the complexity of the airport networks for the contrasting exponential curve of these two countries. In 20 days, from the first infection in Brazil (February 26th) against 47 days after the first Indian case (January 30th), Brazil has already had 5.4 more confirmed cases than India (<https://covid.saude.gov.br/>, 2020; <https://gisanddata.maps.arcgis.com/>, 2020). Clearly, one country is doing much better in preventing the entrance of cases and the spreading of the disease by controlling infected citizens. Indeed, according to the WHO, the Ministry of Health and Family Welfare (MoHFW) of India has taken an early action, and “aggressively stepped up the response measures—find, isolate, test, treat and trace” (World Health Organization (WHO), 2020b).

Nigeria, a country poorer (27th world GDP position with \$446,543 billions nominal) than Brazil (9th world GDP position with \$1.85 trillion nominal) but with a similar population (United Nations, 2019), had imposed a very successful control so far, with guidelines and laws for within all the cities embracing social distancing and obliging wearing of face masks, starting from 31st March, 2 weeks before than Brazil (Nigeria Centre for Disease Control, 2020). As in most of the African countries, screening at the points of entries have been conducted in Nigeria’s airports (World Health Organization (WHO), 2020c). The Federal Airports Authority of Nigeria (2020) had established precautionary measures to be observed by inbound passengers, the opposite that Brazilian authorities did (Agência Nacional de Aviação Civil (ANAC), 2020).



In order to find and isolate is, from an ecological perspective, the most efficient way to reduce the carrying capacity of a new disease, and thus, restrict its wide spreading, and this must start at the airports. As Brazil is just struggling to impose social distancing, a State-to-State decision with little support from the Federal Government, the scenario is evolving more severely. Regardless of flaws in the comparisons of confirmed cases between the countries, by 16th April, India still had 12,380 cases and 414 deaths while Brazil had 25,262 cases and 1,532 deaths (*World Health Organization (WHO), 2020c*). Nigeria has 373 cases and 11 deaths (*World Health Organization (WHO), 2020c*). Despite the clearly more severe airport sanitarian control in Nigeria than in Brazil, one needs to be aware of the unexpectedly low number of cases in the continent, which may be related to a very young population or to other situations not well understood yet (*Vaughan, 2020*). For Brazil, on the contrary, enhanced case detection would make the scenario even worse. Considering the high probability of a synchronizing SARS-CoV-2 spreading in various capitals, the country may face a quick health service collapse.

Besides the within-city pattern of virus spreading, one must take into account the pattern of dispersion between cities after the virus has invaded. Additionally, for the Brazilian case, one cannot ignore that, eventually, the occurrence of the first case may have occurred nearly 1 month before official records, during the carnival period. This is the largest popular street party on the planet, with 6.4 million people in Rio de Janeiro, and 16.3 million in Salvador, and the *Brazilian Ministry of Tourism (2020)* revealed that 86,000 foreigners from France, Germany, Spain, Italy, UK, and the US had visited Brazil in this period. As airport control might have been even more lax in small airports, it might unavoidably result in strengthening of the capability of an infected city to infect the next new one, if no public policy is adopted.

Without a social distancing policy, virus propagation may result in chaotic dynamics, sensu *May (1976)*. The lack of control for these situations may result in a dramatic rate of host infection, and an eventual collapse of the host-parasite interaction in a given population, depending on the amount of susceptible, infected, and recovered events. Nonetheless, if the population is split into deme-cities, in a metapopulation structure, the collapse takes longer, and a much greater amount of people in different locations may eventually be infected, as found in our model. It is worthwhile to mention that this model, already pessimistic, did not consider the Brazilian road network, one of the largest on the planet. Most importantly, the best road-connected cities are exactly those mostly connected by airport, and that will be vulnerable earlier, and thus, probably spreading the disease faster than our model can predict, unless roads are soon blocked for people. Another weakness of the model is that it cannot account for a great number of small airports not registered for commercial flights, very common in the Amazonian and Western regions. Taking this into a global scale, for a highly interconnected human population, the consequences may be catastrophic, as it was for the influenza pandemic (Spanish flu) in 1918 (*Ferguson, Alison & Bush, 2003*). Furthermore, one aspect that must not be neglected is the way an increasing number of infected people in a city drives the pandemic towards the next city or country. In this context, the complex and large flight network of Brazil, which is also key for the whole Latin America, if not properly

monitored and controlled, may cause a window of opportunity for the virus to spread over the entire continent.

The consequences of this uncontrolled SARS-CoV-2 spreading is particularly serious if one takes into consideration the chances of a mutant virulent strain appearing and spreading into poorer and little monitored places of the world. Specifically, for the Amazon region, the lack of any control will make the city of Manaus a very sensitive cluster for public health, due to predominantly poor and indigenous-dominated cities in the region, which are connected to Manaus and will be rapidly infected. Reaching isolated regions means reaching indigenous or traditional communities, whose individuals are classically more susceptible to new pathogens than western-influenced or mixed urban populations. Therefore, a way to prevent such spreading, if still there is time, would be to deal with airports as entrances that need severe infection barriers.

## CONCLUSIONS

The Brazilian media and the Ministry of Health have announced that 50 days from the introduction of SARS-CoV-2 in the country, it has spread across the regions and cities quite like we had predicted, even slightly faster. For instance, the time taken for Manaus to be compromised by the disease was as short as we predicted. A combination of being an important regional clustering in the airport network, and relatively limited hospital capability, resulted in a fast saturation of intensive care units, in cities as Manaus, Recife, and São Luis. As Manaus will disseminate the disease across the region, quickly reaching far remote indigenous communities, it should be on lockdown right now, to cause an invasion threshold, sensu *Colizza & Vespignani (2007)*. The first indigenous person, a teenager girl, has been already killed by COVID-19.

An eventual lesson to take for the whole country is that inflexible, severe, and easy to repeat protocols must be applied to all the cities with airports. Likewise, the follow-up monitoring of suspicious individuals and their living network should be reinforced as a national strategy to prevent a large territory to be taken over by a pandemic in a short period of time. In other words, internationally accepted procedures must be taken and even be reviewed to adjust to complex national flight networks of any country. Such procedures must be considered as a priority for national remote airports too, in order to keep poorer and worse equipped cities away from a rapid spread of a pandemic disease.

It is clear, at this point, that a fast spread of the SARS-CoV-2 is a reality in Brazil, and across most of the country. We proposed this model in order to emphasize the fragility of Brazilian surveillance in the airport network, in an attempt to cause some policy change in time to preserve at least the most remote regions, which are also the most vulnerable, with a weaker health service. Moreover, most of the Eastern part of the country must stay in social distancing in order to prevent a health public collapse by mid-May, as the Brazilian Ministry of Health predicted. So far, this has been a State-to-State decision, similarly to the United States, and those States that have been stronger in isolation measures, are indeed delaying the peak. Moreover, even if it is too late for the first

wave of infection in many cities, one must be prepared for a second likely wave, mainly considering the lack of a central government policy for social distancing.

In addition, we also could consider the generalized poverty of Brazil as a further problem that our model did not deal with. The chances to produce home-to-home isolation, even legally imposed, is impossible for these poor communities. Nonetheless, considering the few main entrances of most of the Brazilian shanty towns and communities, a similar to airport entrance severe control must be considered to protect a larger but closely connected set of people, eventually following the protocols used for the control of Ebola during the last epidemic in Africa (*Lau et al., 2017*).

## ACKNOWLEDGEMENTS

We thank Christina Vinson and Thomas C.A. Williams for the English revision. We thank Muhammed Afolabi and two anonymous referees that contributed enormously to the improvement of this article.

## ADDITIONAL INFORMATION AND DECLARATIONS

### Funding

The CNPq agency guaranteed research grant scholarships for Sérgio Pontes Ribeiro, Alexandre Barbosa Reis, Aristóteles Góes-Neto, Luiz Carlos Junior Alcantara, Geraldo Wilson Fernandes and Vasco Ariston C Azevedo. The funders had no role in study design, data collection and analysis, decision to publish, or preparation of the manuscript.

### Grant Disclosures

The following grant information was disclosed by the authors:  
CNPq Agency.

### Competing Interests

Aristóteles Góes-Neto and Vasco Ariston C Azevedo are Academic Editors for PeerJ.

### Author Contributions

- Sérgio Pontes Ribeiro conceived and designed the experiments, performed the experiments, analyzed the data, prepared figures and/or tables, authored or reviewed drafts of the paper, and approved the final draft.
- Alcides Castro e Silva conceived and designed the experiments, performed the experiments, analyzed the data, prepared figures and/or tables, authored or reviewed drafts of the paper, and approved the final draft.
- Wesley Dáttilo conceived and designed the experiments, performed the experiments, analyzed the data, prepared figures and/or tables, authored or reviewed drafts of the paper, and approved the final draft.
- Alexandre Barbosa Reis conceived and designed the experiments, authored or reviewed drafts of the paper, and approved the final draft.
- Aristóteles Góes-Neto analyzed the data, authored or reviewed drafts of the paper, and approved the final draft.

- Luiz Carlos Junior Alcantara analyzed the data, authored or reviewed drafts of the paper, and approved the final draft.
- Marta Giovanetti analyzed the data, authored or reviewed drafts of the paper, and approved the final draft.
- Wendel Coura-Vital conceived and designed the experiments, analyzed the data, authored or reviewed drafts of the paper, and approved the final draft.
- Geraldo Wilson Fernandes conceived and designed the experiments, authored or reviewed drafts of the paper, and approved the final draft.
- Vasco Ariston C Azevedo analyzed the data, authored or reviewed drafts of the paper, and approved the final draft.

### Data Availability

The following information was supplied regarding data availability:

Raw data and code are available in the [Supplemental Files](#).

### Supplemental Information

Supplemental information for this article can be found online at <http://dx.doi.org/10.7717/peerj.9446#supplemental-information>.

## REFERENCES

- Airports Authority of India. 2020.** Airports Authority of India Flight Schedule. Available at <https://www.aai.aero/en/airports/flights-schedule/allAirports/hadapsar.jsp> (accessed 13 April 2020).
- Agência Nacional de Aviação Civil (ANAC). 2020.** Histórico De Voos. Available at <https://www.anac.gov.br/assuntos/dados-e-estatisticas/historico-de-voos> (accessed 13 April 2020).
- Anderson RM. 1991.** Discussion: the Kermack–McKendrick epidemic threshold theorem. *Bulletin of Mathematical Biology* 53(1–2):1–32 DOI 10.1007/BF02464422.
- Balcan D, Gonçalves B, Hu H, Ramasco JJ, Colizza V, Vespignani A. 2010.** Modelling the spatial spread of infectious diseases: the Global Epidemic and Mobility computational model. *Journal of Computing Science* 1(3):132–145 DOI 10.1016/j.jocs.2010.07.002.
- Bedford J, Enria D, Giesecke J, Heymann DL, Ihekweazu C, Kobinger G, Lane HC, Memish Z, Oh M, Sall AA, Schuchat A, Ungchusak K, Wielwer LH. 2020.** COVID-19: towards controlling of a pandemic. *Lancet* 395(10229):1011–1088.
- Brazilian Ministry of Tourism. 2020.** Ministério Do Turismo: Página Inicial. Available at <http://www.turismo.gov.br/> (accessed 13 April 2020).
- Brockmann D, Helbing D. 2013.** The hidden geometry of complex, network-driven contagion phenomena. *Science* 342(6164):1337–1342 DOI 10.1126/science.1245200.
- Coelho FC, Lana RM, Cruz OG, Villela D, Bastos LS, Piontti AP, Davis JT, Vespignani A, Codeço CT, Gomes MFC. 2020.** Assessing the potential impact of COVID-19 in Brazil: mobility, morbidity, and the burden on the health care system. *medRxiv preprint* DOI 10.1101/2020.03.19.20039131.
- Colizza V, Vespignani A. 2007.** Invasion threshold in heterogeneous metapopulation networks. *Physical Review Letters* 99(14):148701 DOI 10.1103/PhysRevLett.99.148701.

- Dáttilo W, Silva AC, Guevara R, MacGregor-Fors I, Ribeiro SP. 2020. COVID-19 most vulnerable Mexican cities lack the public health infrastructure to face the pandemic: a new temporally-explicit model. *medRxiv* DOI 10.1101/2020.04.10.20061192.
- Fathlzadeh H, Maroufi P, Momen-Heravi M, Dao S, Köse S, Ganbarov K, Pagliano P, Espolto S, Kafli HS. 2020. Protection and disinfection policies against SARS-CoV-2 (COVID-19). *Le Infezioni in Medicina* 2:185–191.
- Federal Airports Authority of Nigeria. 2020. Federal Airports Authority Of Nigeria. Available at <https://www.faan.gov.ng/> (accessed 13 April 2020).
- Ferguson NM, Alizon P, Bush RM. 2003. Ecological and immunological determinants of influenza evolution. *Nature* 422(6930):428–433 DOI 10.1038/nature01509.
- Hanski I. 1998. Metapopulation dynamics. *Nature* 396(6706):41–49 DOI 10.1038/23876.
- Hellewell J, Abbott S, Gimma A, Bosse NI, Jarvis CI, Russell TW, Munday JD, Kucharski AJ, Edmunds WJ, Funk S, Eggo RM, Centre for the Mathematical Modelling of Infectious Diseases COVID-19 Working Group. 2020. Feasibility of controlling COVID-19 outbreaks by isolation of cases and contacts. *Lancet* 8(4):e488–e496 DOI 10.1016/S2214-109X(20)30074-7.
- Hethcote HW. 1989. Three basic epidemiological models. *Applied Mathematical Ecology* 18:119–144.
- Hubbell SP. 2001. *The unified neutral theory of biodiversity and biogeography*. Princeton: Princeton University Press.
- Lai A, Bergna A, Acciarri C, Galli M, Zehender G. 2020a. Early phylogenetic estimates of the effective reproduction number of SARS-CoV-2. *Journal of Medical Virology* 92(6):675–679 DOI 10.1002/jmv.25723.
- Lai C, Ship T, Ko W, Tang H, Hsueh P. 2020b. Severe acute respiratory syndrome coronavirus 2 (SARS-CoV-2) and coronavirus disease-2019 (COVID-19): the epidemic and the challenges. *International Journal of Antimicrobial Agents* 55(3):105924 DOI 10.1016/j.ijantimicag.2020.105924.
- Lau MSY, Dalziel BD, Funk S, McClelland A, Tiffany A, Riley S, Jessica C, Metcalf E, Grenfell BT. 2017. Spatial and temporal dynamics of superspreading events in the 2014–2015 West Africa Ebola epidemic. *Proceedings of the National Academy of Sciences of the United States of America* 114(9):2337–2342 DOI 10.1073/pnas.1614595114.
- Li G, Fan Y, Lai Y, Han T, Li Z, Zhou P, Pan P, Wang W, Hu D, Liu X, Zhang Q, Wu J. 2020. Coronavirus infections and immune responses. *Journal of Medical Virology* 92(4):424–432 DOI 10.1002/jmv.25685.
- May RM. 1976. Simple mathematical models with very complicated dynamics. *Nature* 261(5560):459–467 DOI 10.1038/261459a0.
- Morse SS, Mazet JAK, Woolhouse M, Parrish CR, Carroll D, Karesh WD, Zambrana-Torrel C, Lipkin WL, Daszak P. 2012. Prediction and prevention of the next pandemic zoonosis. *The Lancet* 380(9857):1956–1965 DOI 10.1016/S0140-6736(12)61684-5.
- Nicolaides C, Cueto-Felgueroso L, Gonzales MC, Juanes R. 2012. A metric of influential spreading during contagion dynamics through the air transportation network. *PLOS ONE* 7(7):e40961 DOI 10.1371/journal.pone.0040961.
- Nigeria Centre for Disease Control. 2020. NCDC coronavirus (COVID-19) information minisite. Available at <https://covid19.ncdc.gov.ng/> (accessed 14 April 2020).
- Pianka ER. 2000. *Evolutionary ecology*. Sixth Edition. San Francisco: Addison Wesley Longman.
- Rothe C, Schunk M, Sothmann P, Bretzel G, Froeschl G, Wallrauch C, Zimmer T, Thiel V, Janke C, Guggemos W, Seilmaier M, Drosten C, Vollmar P, Zwirgmaier K, Zange S,

- Wölfel R, Hoelscher M. 2020.** Transmission of 2019-nCoV infection from an asymptomatic contact in Germany. *New England Journal of Medicine* **382(10)**:970–971  
DOI 10.1056/NEJMc2001468.
- United Nations. 2019.** World population: prospects 2019, Volume II: demographic profiles (ST/ESA/SER.A/427). Available at <https://population.un.org/wpp/DataQuery/> (accessed 17 April 2020).
- Vaughan A. 2020.** We don't know why so few Covid-19 cases have been reported in Africa: new scientist. Available at <https://www.newscientist.com/article/2236760-we-dont-know-why-so-few-covid-19-cases-have-been-reported-in-africa/> (accessed 17 April 2020).
- World Health Organization (WHO). 2020a.** Novel coronavirus (2019-nCoV). Available at [https://www.who.int/docs/default-source/coronaviruse/situation-reports/20200121-sitrep-1-2019-ncov.pdf?sfvrsn=20a99c10\\_4](https://www.who.int/docs/default-source/coronaviruse/situation-reports/20200121-sitrep-1-2019-ncov.pdf?sfvrsn=20a99c10_4) (accessed 14 April 2020).
- World Health Organization (WHO). 2020b.** Coronavirus disease (COVID-19). Available at <https://www.who.int/india/emergencies/novel-coronavirus-2019> (accessed 16 April 2020).
- World Health Organization (WHO). 2020c.** Coronavirus disease 2019 (COVID-19). Available at [https://www.who.int/docs/default-source/coronaviruse/situation-reports/20200416-sitrep-87-covid-19.pdf?sfvrsn=9523115a\\_2](https://www.who.int/docs/default-source/coronaviruse/situation-reports/20200416-sitrep-87-covid-19.pdf?sfvrsn=9523115a_2) (accessed 16 April 2020).
- World Health Organization (WHO). 2020d.** COVID-19: Situation update for the WHO African Region. Available at [https://apps.who.int/iris/bitstream/handle/10665/331330/SITREP\\_COVID-19\\_WHOAFRO\\_20200304-eng.pdf](https://apps.who.int/iris/bitstream/handle/10665/331330/SITREP_COVID-19_WHOAFRO_20200304-eng.pdf) (accessed 14 April 2020).
- Zhu N, Zhang D, Wang W, Li X, Yang B, Song J, Zhao X, Huang B, Shi W, Lu R, Niu P, Zhan F, Ma X, Wang D, Xu W, Wu G, Gao GF, Tan W. 2020.** A novel coronavirus from patients with pneumonia in China, 2019. *New England Journal of Medicine* **382(8)**:727–733  
DOI 10.1056/NEJMoa2001017.



## BIOLOGICAL SCIENCES

# Worldwide COVID-19 spreading explained: traveling numbers as a primary driver for the pandemic

SÉRVIO P. RIBEIRO, WESLEY DÁTILLO, DAVID S. BARBOSA, WENDEL COURA-VITAL, IGOR A.S. DAS CHAGAS, CAMILA P. DIAS, ALCIDES V.C. DE CASTRO E SILVA, MARIA HELENA F. MORAIS, ARISTÓTELES GÓES-NETO, VASCO A.C. AZEVEDO, GERALDO WILSON FERNANDES & ALEXANDRE B. REIS

**Abstract:** The spread of SARS-CoV-2 and the distribution of cases worldwide followed no clear biogeographic, climatic, or cultural trend. Conversely, the internationally busiest cities in all countries tended to be the hardest hit, suggesting a basic, mathematically neutral pattern of the new coronavirus early dissemination. We tested whether the number of flight passengers per time and the number of international frontiers could explain the number of cases of COVID-19 worldwide by a stepwise regression. Analysis were taken by 22 May 2020, a period when one would claim that early patterns of the pandemic establishment were still detectable, despite of community transmission in various places. The number of passengers arriving in a country and the number of international borders explained significantly 49% of the variance in the distribution of the number of cases of COVID-19, and number of passengers explained significantly 14.2% of data variance for cases per million inhabitants. Ecological neutral theory may explain a considerable part of the early distribution of SARS-CoV-2 and should be taken into consideration to define preventive international actions before a next pandemic.

**Key words:** SARS-CoV-2, virus dissemination, emergent diseases, air transportation.

## INTRODUCTION

SARS-CoV-2 pandemic has spread around the world, but the patterns of dissemination, number of cases and deaths per country, as well as demographic trends, are challenging to be understood. The intensity of the outbreak among countries and continents cannot be fully explained by the management of the disease locally, neither by demographic traits alone (Ferguson et al. 2020). Some studies have suggested Asian and black communities are more vulnerable, as well as males, despite comorbidities, but such vulnerabilities have not defined any ethnogeographic pattern

so far (Laurencin & McClinton 2020) or even genetic patterns. Neither has the culture, as the countries considered among those with more rigid hygienic habits (based on many times washing hand per day) are evenly distributed from the hardest to the lightest hit countries, such as Brazil and Germany among the top infected, and Australia and Japan mildly infected (UNICEF & WHO 2018). According to UNICEF & WHO (2018), the countries in which people wash their hands less are China and Malaysia, and the latter had as many cases as Australia in the early months of the pandemic (UNICEF & WHO 2018). Along with the habit of washing hands, oriental

countries used to previous virus outbreaks have already developed a proper and correct practice of mask usage, eventually affecting the patterns of local transmission in comparison to western countries. Finally, there would also be climatic issues, such as effects of temperature or humidity (Coelho et al. 2020, Pequeno et al. 2020, Sajadi et al. 2020), and pollution, which changes how successfully the virus spread (Ogen 2020). Nevertheless, such environmental conditions are usually similar to broad regions, and, thus, it is hard to explain based solely on them why side by side countries with similar climates and biomes are so distinctly affected, as, for instance, Iraq and Iran, or nearby cities such as New York (U.S.A.) and Toronto (Canada).

There are many hypotheses on the global pattern of distribution of COVID-19, ranging from population age, environment, and governmental reactions; however, none of them are entirely conclusive (Fathizadeh et al. 2020, Ferguson et al. 2020). Besides, even for modelling in “war times” (sensu Vespignani et al. 2020) implies in uncertainties and constant reviewing. We are experiencing an epidemiologically complex event, where several of the aforementioned hypotheses need to be evaluated together. Despite the experience of other previous pandemic and large epidemic events, SARS-Cov-2 is unique in many aspects of its natural history, about which we are getting to know in the course of the pandemic. The unpredictability of the starting conditions of outbreaks at a local scale, and the role of stochastic situations typical of an early host invasion, such as super spreading events, increase the uncertainties within each affected human population and its epidemiologic dynamics (Vespignani et al. 2020). However, at the larger scale of disease dissemination across the globe, the typical pattern of having the wealthiest and busiest cities hit harder and first, may provide the clue

for an emergent property of the disease, which may have the most straightforward explanation: it hits harder where it hits more! Two recent models based on the air transportation network of two large countries, Brazil (Ribeiro et al. 2020) and Mexico (Dattilo et al. 2020), have clearly shown that centrality in the network makes a city more vulnerable than another spatially close, but less central in the network (Coelho et al. 2020). This prediction was confirmed with the outbreak in Fortaleza, Rio de Janeiro, and, most hardly, São Paulo, in Brazil, as well as Mexico City and Tijuana, in Mexico.

Furthermore, for Brazil, the aforementioned authors predicted and alerted the government about an unexpected case, the city of Manaus, one of the hubs of the Amazonian region, due to the lousy hospital and health care conditions (Ribeiro et al. 2020). In the early stage of the pandemic, Manaus was listed among the worst Brazilian cities in terms of incidence and mortality per 100 thousand inhabitants, along with other Amazonian cities (G1 2020). Manaus is an essential regional clustering for passengers in the Amazon region, receiving and distributing most people coming from the South and South-eastern regions of the country. Big cities and capitals that are only intermediate hubs or peripherals in the Brazilian air transportation network, such as Belo Horizonte and Curitiba, were spare from an accentuated number of cases or fast starting infection rate. Such slow outbreak start may, eventually, have helped local authorities who applied sufficiently severe quarantine impositions.

Other examples of distinct international scenarios, inside a similar biogeographic region and between countries of similar ethnic and cultural basis, are the significant number of cases in Iran (10<sup>th</sup> worst number of cases) and very few in Iraq (position 67 in COVID-19 cases), or, similarly, for Dominican Republic (position 42 in



cases) versus Haiti (position 116 in cases; ranking of cases collected from wordometers.info/coronavirus/on May 22, 2020). These contrasting situations of biogeographically similar countries also can be explained by exposition to migrants/visitors. The conflictive Iraq, which had 7,382,934 arriving flight passengers in 2018, had 2.6 times fewer visitors than Iran, with 19,403,070. Likewise, the poor and earthquake severely injured Haiti is the 7<sup>th</sup> least visited country in the world, receiving nearly eight times fewer flight passengers than the neighbouring touristic Dominican Republic (IATA 2019).

The transmission of SARS-CoV-2 is mainly caused by human contact, regardless of the presence of symptoms (Fathizadeh et al. 2020). Thus, the more people arriving from anywhere previously infect, the higher is the chance of reaching the point of community transmission (Ribeiro et al. 2020, Dattilo et al. 2020). Hence, despite various national contrasting authority acts against the pandemics, demographic trends, culture, or ethnobeaviours that affect how safe the citizens are inside a city, the mere rates of migration from contaminated regions could explain *per se* the number of cases after a few months from the first case. Hence, the hypothesis is that international travelling may be a main driver for the pandemic early distribution, with the prediction that countries which receive more visitors from abroad in a same interval of time, will suffer more severely the impacts of pandemic transmission.

## MATERIALS AND METHODS

In order to investigate this hypothesis, we tested the total number of cases against the explanatory factor “number of passengers” per country, summed up with the number of national passengers (as passengers per

1 million; and, thus, correcting for the largest countries). The moment chosen for ranking the number of cases per country was May 22<sup>nd</sup>, when most of the countries had had the first COVID-19 case for more than one month. Furthermore, the total cases and deaths were highly correlated, for absolute values or for cases per 1 million (Pearson value 0.85 and 0.70, respectively). Regardless of the lower precision of the total number of cases compared to death cases, we chose to analyse the former attribute to cover a broad range of countries, since many of them still had a negligible amount of deaths by the time we chose to study. Finally, as the error related to total cases will be mainly due to subnotification (and as there may be similar levels of underreporting expected for most of the countries worldwide), we assumed that by using the logarithm scale, we reduced the error variance sufficiently to compare records between countries and, thus, made the official cases values a proxy to the actual pattern of cases distribution.

As the simple preliminary regressions (Figures 1 and 2) showed that most cases below the regression curve were islands or countries with few international borders, such as Portugal, we included, in a stepwise regression, the factor “number of international borders” to add a proxy for the immigration by land. Subsequently, we repeated the analysis using the number of cases per 1 million people and compared the regression residuals to detect the relevance of population size in affecting the disease distribution. As the number of cases correlates with population size ( $r=0.57$ ), hardly the latter could be tested directly as an explanatory factor. However, the role of the number of people *per se* can be subtracted from the analysis by comparing the coefficient of determination and residuals between regressions with the absolute and relative number of cases. Data were taken

from the worldmeters site (Worldometer 2020; Supplementary Material - Table SI). Regardless of the fact that cases are strongly amplified due to local community transmission, we chose a date when the pandemic might have already consolidated worldwide. Even with local transmission varying between places, it seems that dissemination by travelling is indeed highly correlated with and sensitive to the early phase of exponential growth of the disease (Ribeiro et al. 2020, Coelho et al. 2020, Dattilo et al. 2020).

For the number of passengers arriving in a country, we used the IATA's WATS: World Air Transportation Statistics 2019 report (IATA 2019), which provides as the latest figures the number of flights worldwide in 2018 and, thus, a period of time that reflects well the flight frequencies between countries before the declaration of the pandemic (Table SI). Conversely to Coelho et al. (2020), we were not interested in the air transportation network or modular connectivity effects, but in the effect of the number of

travellers reaching each country per period, and therefore, a proxy of viral load pressure on the population. Because SARS-CoV-2 may have started spreading much before countries decided to slow or close down airports (Ribeiro et al. 2020, Wu et al. 2020), we assumed the number of passengers before the crisis as the best estimate of exposition to traveling load.

## RESULTS

As expected, countries receiving more flights were those most densely populated, regardless of GDP (such as China, India, United States, Indonesia), most developed ones (Japan, top European Countries, Canada, Australia, and United States) or among the 20<sup>th</sup> largest economies (previous list plus Brazil, South Korea, Mexico). We found that, both the number of passengers arriving in a country and the number of international borders, explained significantly

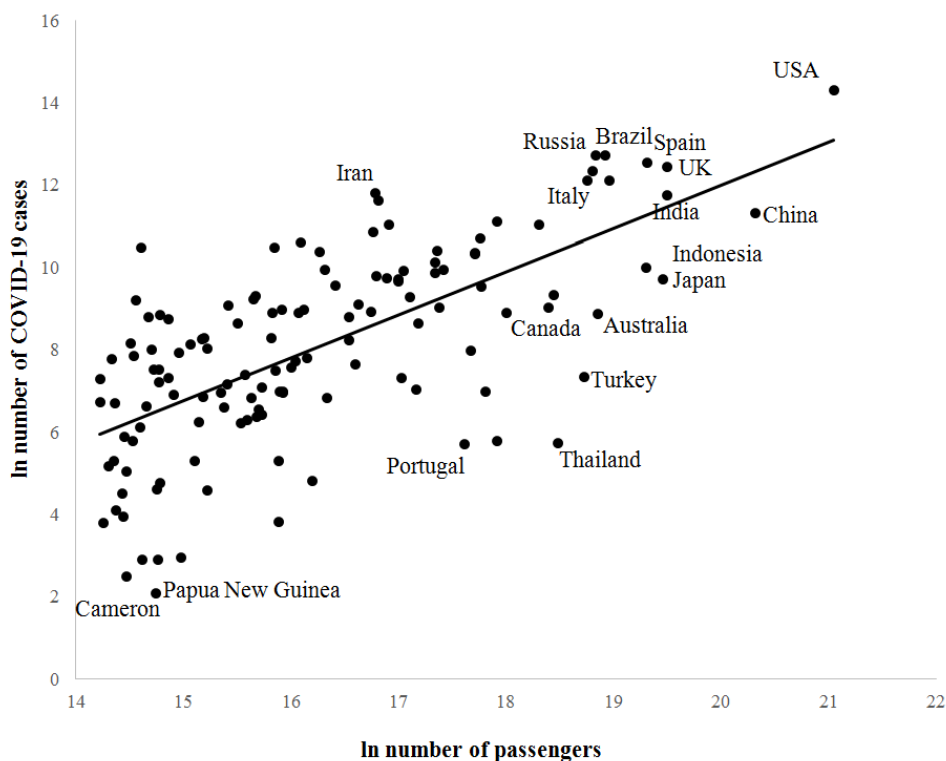


**Figure 1.** Number absolute of COVID-19 cases per country on May 22<sup>nd</sup>, 2020, by the number of passengers in 2018.

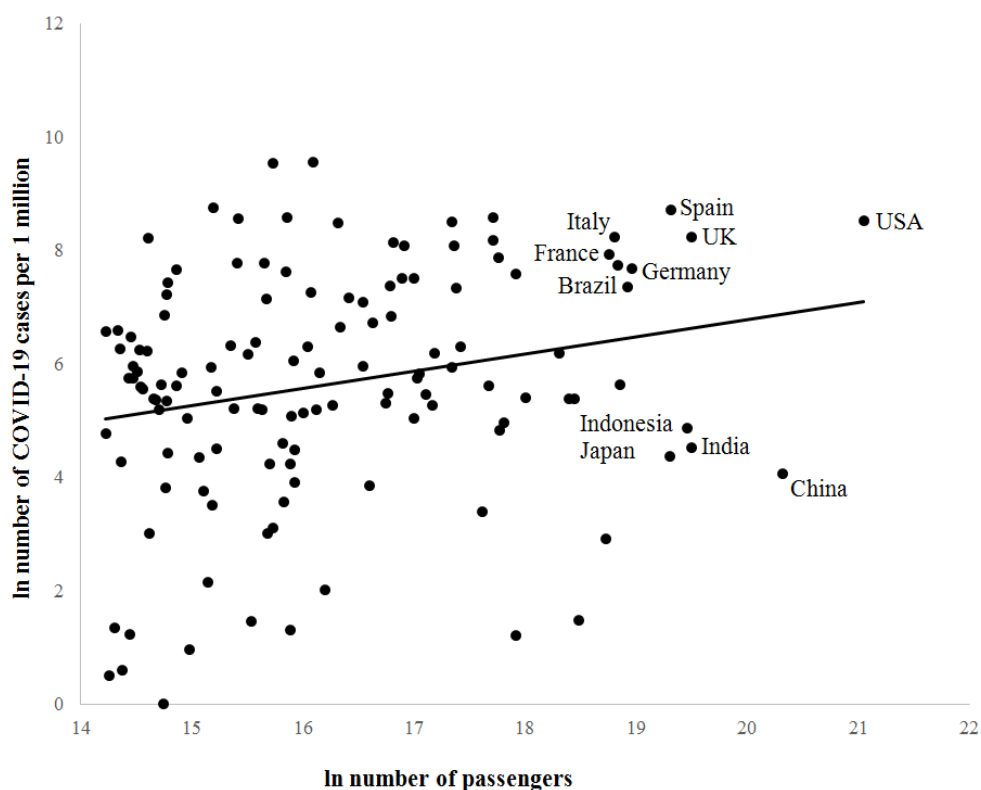


**Figure 2.** Number of deaths by COVID-19 per 1 million inhabitants per country on May 22, 2020, by the number of passengers in 2018.

the number of cases of COVID-19 on May 22, 2020. These combined variables had irrelevant collinearity (tested by VIF, taken  $VIF < 2.5$ ), thus were complementary explanations, covering 49.9% of the data variance (Fig. 1; Table I).

The response of the number of cases corrected by country population size was also significant but explained a lower percentage of the data variance. In addition, at this scale, the number of terrestrial borders were not significant in the model (Fig. 2; Table II). On the other hand, the residual analysis showed a more uniform structure for the relative number than for the absolute number of cases (only four atypical cases against 12 for the first model), which corroborates the hypothesis that population size absorbed a substantial part of the data variance, given that the number of confirmed infected cases is still a tiny proportion of the total population of any country. The adjustment herein produced separated the countries

highly connected by traveling in a densely populated group (China, India, Japan, and Indonesia) below the model line, and a western (geographically speaking) and developed group, above the model line. The pattern in evidence, by comparing these two models, is that highly connected countries contributed similarly to the early spreading of COVID-19, but with contrasting impact on each country demography and structure. Additionally, European and American profoundly affected countries (the USA in evidence) were proportionally more affected than oriental countries (Fig. 2).

## DISCUSSION

Our results demonstrated how the international traffic of people may have influenced the transmission of SARS-CoV-2 between countries and contributed to the establishment of the

**Table I. Stepwise regression summary for total COVID-19 cases by passengers and international frontiers.**

<b>Regression equation</b>					
<b>Ln cases = -8.36 + 0.969 Ln passengers + 0.1920 number of terrestrial frontiers</b>					
<b>Coefficients</b>					
Term	Coef	SE Coef	T value	p value	VIF
Constant	-8.36	1.60	-5.23	0.000	
Ln passageiros	0.969	0.100	9.70	0.000	1.05
Number of terrestrial frontiers	0.1920	0.0559	3.43	0.001	1.05
<b>Model Summary</b>					
S	R2	R2(aj)	R2(pred)		
1.71734	49.92%	49.14%	47.50%		
<b>Analysis of Variance</b>					
Source	DF	SQ (Adj.)	QM (Adj.)	F	p value
Regression	2	376.37	188.187	63.81	0.000
Ln passageiros	1	277.39	277.390	94.05	0.000
Number of terrestrial frontiers	1	34.78	34.782	11.79	0.001
Error	128	377.51	2.949		
Total	130	753.88			

pandemic. These results are important to reinforce the containment measures proposed in the RSI2005, considering the world panorama with the current pandemic. Far from denying the functional effects of quarantine or lockdowns, our results showed that a more strict entrance control, if internationally coordinated early in the current year, could have greatly reduced the level and speed of SAR-COV-2 dissemination, by decelerating the rates of transmission through the borders and ports. As this did not happen, it is evident that those countries or States, where local government acted faster and ahead before the moment when uncontrolled community transmission was in place, managed to prevent a too stiff case curve (Wu et al. 2020).

Moreover, the disproportionately high amount of cases of COVID-19 in European and American large and highly connected countries

are directly associated with the fact that their cities receive more flights, and, therefore, are central hubs in the international flight network (Coelho et al. 2020). These highly connected cities were those that needed to block airports first. As they did not, cities such as Milan, Madrid, New York, London, Paris, São Paulo, and Rio de Janeiro were hit harder. Considering the further flight network leaving from these central hub-cities nationally, it would be essential to have them detected early to prevent each infected city from becoming an internal source of the disease, as was the case for Brazil. By locking down only those most important airports in the flight transportation network, a government could manage a more efficient and less economically damaging airport sanitarian control (Ribeiro et al. 2020).

**Table II. Stepwise regression summary for COVID-19 cases per 1 million inhabitants by passengers and international frontiers.**

Regression equation					
<b>Ln cases = 1.44 + 0.281 Ln passengers</b>					
Coefficients					
Term	Coef	SE Coef	T value	p value	VIF
Constant	1.44	1.90	0.76	0.451	
Ln passengers	0.281	0.114	2.46	0.015	1.02
Number of terrestrial frontiers	-0.1047	0.064	-1.64	0.103	1.02
Model Summary					
S	R2	R2(aj)	R2(pred)		
1.99470	7.21%	5.76%	2.4%		
Analysis of Variance					
Source	DF	SQ (Adj.)	QM (Adj.)	F	p value
Regression	2	39.57	19.784	4.97	0.008
Ln passengers	1	24.16	24.159	6.07	0.015
Number of terrestrial frontiers	1	10.73	10.734	2.70	0.103
Error	128	509.29	3.979		
Number of terrestrial frontiers total	130	548.86			

## CONCLUSIONS

In conclusion, we found that one of the likely most straightforward explanations for country vulnerability is how well connected it is internationally in the early stages of a pandemic, and prior a severe local community transmission to be in place, both due to the number of flight passengers and to the number of international borders. Closing the borders took time to be accepted worldwide, as well as the COVID-19 pandemic traveling consequences have been neglected in the literature. It seems like most of the studies appearing in preprint repositories or already published, at the epidemiologic level, are concerned with the management of community transmission in already established outbreaks.

Herein, we considered one aspect of the virus basic ecology, i.e., the mechanism of dissemination, which is fundamental aspect both to understand its early spreading as well its zoonotic origin and spillover, and that might request more in-depth studies, as shown by Zhao et al. (2020). Despite human cultural and civilization complexity, for the virus, we are just an abundant host, and the intensity and how we connect populations by travelling/migration is a basic biologic component of the viral species dissemination worldwide (Allen et al. 2017, Johnson et al. 2019). Ecological theory has shown that species dispersion follows basic, neutral mathematical rules (sensu Hubbell 2001). Considering a country as a habitat to be invaded, the larger the border, or the closer the habitat is to the source, the more virus load it

will receive (Macarthur & Wilson 1967). Based on this simple principle, and on WHO's RSI2005 guidelines (that should have been severely observed), countries could have produced customized protocols for early warning of airports along a gradient of risk. By applying neutral theory principles to virus dissemination, one can understand in an uncomplicated way the beginning of a new disease outbreak, which may be a key aspect in stopping future pandemic events, mostly because essential details on the infectious disease biology are still unknown when a pathogen spillover towards human kind (Andersen et al. 2020; Vespignani et al. 2020). In conclusion, the pandemic was strongly sensitive to the initial conditions of the virus dissemination, prior complex social, political, and anthropologic components of community transmission take place.

Sadly enough, essential details for proper predictive mapping of infectious diseases, such as human distribution and vulnerability, or disease-relevant environmental covariates, are still not sufficiently studied (Hay et al. 2013). Assuming there will be a future zoonotic virus pandemic threat, the world could coordinately create a strategy for fast and efficient blocking of any traveling infectious disease. Therefore, it would require humans to develop robust governance, monitoring, and knowledge sharing at the international level.

### Acknowledgments

This research did not receive any specific grant from funding agencies in the public, commercial, or not-for-profit sectors. The authors declare that there are no conflicts of interest.

### REFERENCES

ALLEN T, MURRAY KA, ZAMBRANA-TORRELIO C, MORSE SS, RONDININI C, DI MARCO M, BREIT N, OLIVAL KJ & DASZAK P. 2017.

Global Hotspots and Correlates of Emerging Zoonotic Diseases. *Nat Commun* 8(1): 1124.

ANDERSEN KG, RAMBAUT A, LIPKIN WI, HOLMES EC & GARRY RF. 2020. The Proximal Origin of SARS-CoV-2. *Nat Med* 26(4): 450-452.

COELHO MTP, RODRIGUES JFM, MEDINA AM, SCALCO P, TERRIBILE LC, VILELA B, DINIZ-FILHO JAF & DOBROVOLSKI R. 2020. Global Expansion of COVID-19 Pandemic Is Driven by Population Size and Airport Connections. *PeerJ* 8(August): e9708.

DATTILO W, CASTRO E SILVA A, GUEVARA R, MACGREGOR-FORS I & RIBEIRO SP. 2020. COVID-19 Most Vulnerable Mexican Cities Lack the Public Health Infrastructure to Face the Pandemic: A New Temporally-Explicit Model. *MedRxiv*, no. April: 2020.04.10.20061192.

FATHIZADEH H, MAROUFI P, MOMEN-HERAVI M, DAO S, KÖSE Ş, GANBAROV K, PAGLIANO P, ESPOSITO S & KAFIL HS. 2020. Protection and Disinfection Policies against SARS-CoV-2 (COVID-19). *Infez Med* 28(2): 185-191.

FERGUSON NM ET AL. 2020. Impact of Non-Pharmaceutical Interventions (NPIs) to Reduce COVID-19 Mortality and Healthcare Demand. *Imperial Ac Uk*, no. March: 3-20.

G1. 2020. Casos de coronavírus e número de mortes no Brasil em 26 de maio, <https://g1.globo.com/bemestar/coronavirus/noticia/2020/05/26/casos-de-coronavirus-e-numero-de-mortes-no-brasil-em-26-de-maio.ghtml>; 2020 [accessed 26 May 2020].

HAY SI ET AL. 2013. Global Mapping of Infectious Disease. *Philos Trans R Soc B* 368(1614): 20120250.

HUBBELL SP. 2001. *The Unified Neutral Theory of Biodiversity and Biogeography* (MPB-32), New Jersey: Princeton University Press, 375 p.

IATA. 2019. *World Air Transport Statistics 2019* 2019: 7.

JOHNSON EE, ESCOBAR LE & ZAMBRANA-TORRELIO C. 2019. An Ecological Framework for Modeling the Geography of Disease Transmission. *Trends Ecol Evol* 34(7): 655-668.

LAURENCIN CT & MCCLINTON A. 2020. The COVID-19 Pandemic: A Call to Action to Identify and Address Racial and Ethnic Disparities. *J Racial Ethn Health Disparities* 7(3): 398-402.

MACARTHUR RH & WILSON EO. 1967. *The Theory of Island Biogeography*. New Jersey: Princeton University Press, 203 p.

OGEN Y. 2020. Assessing Nitrogen Dioxide (NO<sub>2</sub>) Levels as a Contributing Factor to Coronavirus (COVID-19) Fatality. *Sci Total Environ* 726(July): 138605.

PEQUENO P, MENDEL B, ROSA C, BOSHOLN M, SOUZA JL, BACCARO F, BARBOSA R & MAGNUSSON W. 2020. Air Transportation,

Population Density and Temperature Predict the Spread of COVID-19 in Brazil. *PeerJ* 8 (June): e9322.

RIBEIRO SP, CASTRO E SILVA A, DÁTILLO W, REIS AB, GÓES-NETO A, ALCANTARA LCJ, GIOVANETTI M, COURA-VITAL W, FERNANDES GW & AZEVEDO VAC. 2020. Severe Airport Sanitarian Control Could Slow down the Spreading of COVID-19 Pandemics in Brazil. *PeerJ* 8(June): e9446.

SAJADI MM, HABIBZADEH P, VINTZILEOS A, SHOKOUHI S, MIRALLES-WILHELM F & AMOROSO A. 2020. Temperature, Humidity, and Latitude Analysis to Estimate Potential Spread and Seasonality of Coronavirus Disease 2019 (COVID-19). *JAMA Network Open* 3(6): e2011834.

UNICEF - UNITED NATIONS CHILDREN'S FUND & WHO - WORLD HEALTH ORGANIZATION. 2018. Drinking Water, Sanitation and Hygiene in Schools: Global Baseline Report 2018. Unicef. [https://washdata.org/sites/default/files/documents/reports/2018-11/JMP\\_WASH\\_in\\_Schools\\_WEB\\_final.pdf](https://washdata.org/sites/default/files/documents/reports/2018-11/JMP_WASH_in_Schools_WEB_final.pdf).

VESPIGNANI A ET AL. 2020. Modelling COVID-19. *Nat Rev Phys* 2(6): 279-281.

WORLDOMETER. 2020. COVID-19 CORONAVIRUS PANDEMIC, <https://www.worldometers.info/coronavirus/>; 2020 [accessed 22 May 2020].

WU JT, K LEUNG & LEUNG GM. 2020. Nowcasting and Forecasting the Potential Domestic and International Spread of the 2019-NCoV Outbreak Originating in Wuhan, China: A Modelling Study. *The Lancet* 395 (10225): 689-697.

ZHAO S, ZHUANG Z, RAN J, LIN J, YANG G, YANG L & HE D. 2020. The Association between Domestic Train Transportation and Novel Coronavirus (2019-NCoV) Outbreak in China from 2019 to 2020: A Data-Driven Correlational Report. *Travel Med Infect Dis* 33 (January): 101568.

## SUPPLEMENTARY MATERIAL

### Table S1. Raw data.

#### How to cite

RIBEIRO SP, DÁTILLO W, BARBOSA DS, COURA-VITAL W, CHAGAS IAS, DIAS CP, CASTRO E SILVA AVC, MORAIS MFH, GÓES-NETO A, AZEVEDO VAC, FERNANDES GW & REIS AB. 2020. Worldwide COVID-19 spreading explained: traveling numbers as a primary driver for the pandemic. *An Acad Bras Cienc* 92: e20201139. DOI 10.1590/0001-3765202020201139.

*Manuscript received on August 7, 2020;*  
*accepted for publication on August 9, 2020*

**SÉRVIO P. RIBEIRO**<sup>1,2,3</sup>

<https://orcid.org/0000-0002-0191-8759>

**WESLEY DÁTILLO**<sup>4</sup>

<https://orcid.org/0000-0002-4758-4379>

**DAVID S. BARBOSA**<sup>5</sup>

<https://orcid.org/0000-0002-5241-5940>

**WENDEL COURA-VITAL**<sup>1,6</sup>

<https://orcid.org/0000-0002-1434-7676>

**IGOR A.S. DAS CHAGAS**<sup>1,2</sup>

<https://orcid.org/0000-0002-7409-5669>

**CAMILA P. DIAS**<sup>1,2</sup>

<https://orcid.org/0000-0002-4852-6488>

**ALCIDES V.C. DE CASTRO E SILVA**<sup>7</sup>

<https://orcid.org/0000-0003-2863-8076>

**MARIA HELENA F. MORAIS**<sup>8</sup>

<https://orcid.org/0000-0002-6025-2774>

**ARISTÓTELES GÓES-NETO**<sup>9</sup>

<https://orcid.org/0000-0002-7692-6243>

**VASCO A.C. AZEVEDO**<sup>10</sup>

<https://orcid.org/0000-0002-4775-2280>

**GERALDO WILSON FERNANDES**<sup>11</sup>

<https://orcid.org/0000-0003-1559-6049>

**ALEXANDRE B. REIS**<sup>1,12</sup>

<https://orcid.org/0000-0001-8123-4164>

<sup>1</sup>Universidade Federal de Ouro Preto, Núcleo de Pesquisas em Ciências Biológicas/NUPEB, St. Três, 408-462, Bauxita, 35400-000 Ouro Preto, MG, Brazil

<sup>2</sup>Universidade Federal de Ouro Preto, Laboratory of Ecology of Diseases and Forests, Departamento de Biodiversidade, Evolução e Meio Ambiente, St. Quatro, 786, Bauxita, 35400-000 Ouro Preto, MG, Brazil

<sup>3</sup>Universidade Federal de Minas Gerais, Laboratory of Physiology of Hematophagous Insects, Departamento de Parasitologia, Ave. Pres. Antônio Carlos, 6627, Pampulha, 31270-901 Belo Horizonte, MG, Brazil

<sup>4</sup>Instituto de Ecología AC, Red de Ecoetología, Carretera Antigua a Coatepec, 351, El Haya, Xalapa, 91070, Veracruz, Mexico

<sup>5</sup>Universidade Federal de Minas Gerais, Departamento de Parasitologia, Ave. Pres. Antônio Carlos, 6627, Pampulha, 31270-901 Belo Horizonte, MG, Brazil

<sup>6</sup>Universidade Federal de Ouro Preto, Laboratory of Epidemiology and Cytology, Departamento de Análises Clínicas, St. Nove, 27, Bauxita, 35400-000 Ouro Preto, MG, Brazil

<sup>7</sup>Universidade Federal de Ouro Preto, Laboratory of Complexity Science, Departamento de Física, St. Quatro, 786, Bauxita, 35400-000 Ouro Preto, MG, Brazil

<sup>8</sup>Secretaries of Public Health of Minas Gerais State and Belo Horizonte Municipality, Ave. Afonso Pena, 1212, Centro, 30130-003 Belo Horizonte, MG, Brazil

<sup>9</sup>Universidade Federal de Minas Gerais, Laboratory of Molecular and Computational Biology of Fungi, Departamento de Microbiologia, Ave. Pres. Antônio Carlos, 6627, Pampulha, 31270-901 Belo Horizonte, MG, Brazil

<sup>10</sup>Universidade Federal de Minas Gerais, Laboratory of Cell and Molecular Genetics, Departamento de Genética, Ecologia e Evolução, Ave. Pres. Antônio Carlos, 6627, Pampulha, 31270-901 Belo Horizonte, MG, Brazil

<sup>11</sup>Universidade Federal de Minas Gerais, Laboratory of Evolutionary Ecology and Biodiversity, Departamento de Genética, Ecologia e Evolução, Ave. Pres. Antônio Carlos, 6627, Pampulha, 31270-901 Belo Horizonte, MG, Brazil

<sup>12</sup>Universidade Federal de Ouro Preto, Laboratory of Immunopathology, Departamento de Análises Clínicas, St. Três, 408-462, Bauxita, 35400-000 Ouro Preto, MG, Brazil

Correspondence to: **Sérvio Pontes Ribeiro**

E-mail: [serviopr@gmail.com](mailto:serviopr@gmail.com)

## Author contributions

SPR - Conceptualization; Data curation; Formal analysis; Investigation; Methodology; Project administration; Writing-original draft; Writing-review & editing. WD - Formal analysis; Investigation; Methodology; Validation; Writing-review & editing. DSB - Formal analysis; Investigation; Writing-review & editing. WCV - Formal analysis; Investigation; Writing-review & editing. IASC - Data curation; Investigation; Methodology; Writing-review & editing. CPD - Investigation; Writing-review & editing. AVCCS - Formal analysis; Investigation; Writing-review & editing. MHFM - Investigation; Writing-review & editing. AGN - Investigation; Writing-review & editing. VACA - Funding acquisition; Supervision; Writing-review & editing. GWAF - Project administration; Supervision; Validation; Writing-review & editing. ABR - Funding acquisition; Project administration; Supervision; Writing-review & editing.







## HEALTH SCIENCES

# From Spanish Flu to Syndemic COVID-19: long-standing sanitarian vulnerability of Manaus, warnings from the Brazilian rainforest gateway

SÉRVIO P. RIBEIRO, ALEXANDRE B. REIS, WESLEY DÁTILLO, ALCIDES V.C. DE CASTRO E SILVA, EDUARDO AUGUSTO G. BARBOSA, WENDEL COURAVITAL, ARISTÓTELES GÓES-NETO, VASCO A.C. AZEVEDO & GERALDO WILSON FERNANDES

**Abstract:** A second deadlier wave of COVID-19 and the causes of the recent public health collapse of Manaus are compared with the Spanish flu events in that city, and Brazil. Historic sanitarian problems, and its hub position in the Brazilian airway network are combined drivers of deadly events related to COVID-19. These drivers were amplified by misleading governance, highly transmissible variants, and relaxation of social distancing. Several of these same factors may also have contributed to the dramatically severe outbreak of H1N1 in 1918, which caused the death of 10% of the population in seven months. We modelled Manaus parameters for the present pandemic and confirmed that lack of a proper social distancing might select the most transmissible variants. We succeeded to reproduce a first severe wave followed by a second stronger wave. The model also predicted that outbreaks may last for up to five and half years, slowing down gradually before the disease disappear. We validated the model by adjusting it to the Spanish Flu data for the city, and confirmed the pattern experienced by that time, of a first stronger wave in October-November 1918, followed by a second less intense wave in February-March 1919.

**Key words:** SARS-CoV-2, Tropical urban health, Ecohealth, Native communities, modelling disease dissemination, Manaus.

## INTRODUCTION

Historical investigations and mathematical predictive models are methods to search out solutions for upcoming problems. A complex network model simulating Brazilian flight-interconnected cities as a metapopulation structure was published by Ribeiro et al. (2020a). That study explored the number of flights as a driver for SARS-CoV-2 dissemination, based on a SIR-adjusted model. The study correctly predicted which were the crucial international and national hub airports in Brazil, as well as the sequence of cities to be hit by the pandemic

in the subsequent weeks, anticipating each actual city infection date by seven to 14 days. The persistence of the disease in São Paulo, Rio de Janeiro, and Manaus were also explained by this ecologically neutral model (Ribeiro et al. 2020a).

For several reasons, the world failed to refrain the spreading of SARS-CoV-2, and, in Brazil it followed the most expected neutral pattern (i.e., it followed the most used routes and spread with no contention towards the whole country, Ribeiro et al. 2020b). Antiscientific discourse and misleading actions prevented any control of the disease arrival and its subsequent spreading

in Brazil, as well as delayed and undermined control after community transmission was in place (Fraser 2020). Nevertheless, cultural aspects, poverty, and inadequately planned and overcrowded tropical cities, such as Manaus, might most likely ended up having the pandemic arrival turned into a syndemic problem, eventually longer and more severe than it needed to be.

Herein we explored the dynamics related to the urban spreading of the COVID-19 and evaluated the intricate history of urban behaviours and politics affecting public health guidance during a pandemic. For such, we used Manaus as a model, and explored how the social, political-driven environment, and undermining of scientific facts left the city fully vulnerable to the exposition of more transmissible variants and a longer recurrent pandemic. Manaus was selected because its first COVID-19 outbreak was sufficiently vast to raise the hypothesis that the city could have reached the herd immunity (Buss et al. 2021), which had to be completely revisited when a second and deadlier wave returned early in 2021 (Sabino et al. 2021). Furthermore, Manaus was hit harder than previously expected, having the double of mortality rate than the rest of the country (FVS/MSa 2020), even considering it to be a very interconnected travelling route. Moreover, the same pattern had happened before, during the Spanish Flu, which caused the death of 10% of Manaus inhabitants, a much higher rate than the 0.12% national rate (Gama 2020, ATLAS FVG 2021).

In this review, we first described the facts related to the two first waves of COVID-19 in Manaus and compared with the historical facts related to the Spanish Flu in this city, in order to discuss both past and present social and urban scenarios and fragilities. Secondly, based on the assumption that lack of political guidance would lead to an uncontrolled epidemiologic dynamic,

including favouring the spread of new more transmissible viral mutants, we mathematically simulated Manaus exposed to both COVID-19 and Spanish Flu. Finally, we used the same algorithm to simulate a competitive scenario with all the combinations of more transmissible and more lethal variants. The ecology of emergent viral diseases, from the dissemination to the natural selection towards higher transmissibility, and scenarios for the natural ending of the pandemic, at the scale of one city, were verified by our mathematical modelling and discussed in this context of a misleading guidance of the disease progression.

## **MANAUS COVID-19 SECOND WAVE AND PUBLIC HEALTH COLLAPSE**

Manaus showed the first public health collapse in Brazil by April 2020 (precisely, the peak of deaths happened in the epidemiological week 17, 19-25 April – FVS/AMB 2021), as predicted by the model built by Ribeiro et al. (2020a). Warnings from science were especially bold about the vulnerability of Native communities in the Amazon, and the urgency to restrict flights and impose a severe control to the Manaus airport since the city is also the main hub for fluvial transport (Ribeiro et al. 2020a, OBSERVATÓRIO COVID-19 2021). Months after the first collapse, by early January 2021, Manaus had entire hospital blocks with patients dying due to lack of oxygen, dozens of COVID-19 patients being sent to other Brazilian States by the army, and 60 premature babies under the risk of death by the competition for oxygen used to COVID-19 patients. One week after, a shortage of oxygen was reported in other cities in the Amazon region (OBSERVATÓRIO COVID-19 2021). After one month, the lack of oxygen and public health collapse continued, and, by early March, simultaneously,

nine out of the 27 Brazilian States displayed more than 90% of occupation of intensive care units, and 18 States exhibited occupation above 80%, according to the Fundação Instituto Oswaldo Cruz FIOCRUZ report (OBSERVATÓRIO COVID-19 2021). FIOCRUZ also reported to the press by that same date, that about half of the tested cases in the nine aforementioned states belonged to highly transmissible variants, those with the E484K mutation. Either the Gamma P.1, the Alpha B.1.1.7 or the Beta B.1.351 were frequently found. This outcome might confidently be associated to the total lack of airport effective surveillance in the country, political undermining of social distancing, masks, and lockdown (OBSERVATÓRIO COVID-19 2021).

The second week of March came with more than 2,000 deaths per day and with a forecast of 3,000 deaths per day until April. Nevertheless, unfortunately, the federal government still maintained a position against lockdown and port controls. Additionally, questionable policies in another area, environment, raised deep health concerns among scientists. By weakening environmental law enforcement, which has been pointed out as the main cause of deforestation in the Amazon (Barbosa et al. 2020), the federal government may bring the region close to the risk of overlapping COVID-19 with future emergent zoonoses, which could occur as a result of environmental disruption (Jones et al. 2008, Karesh et al. 2012). Currently, many cases of COVID-19 among Native communities were spread from clandestine miners and land invaders, acting confidently on a lack of punishment (COVID-19.SOCIOAMBIENTAL 2021).

Ribeiro et al. (2020a, b) models predicted that hub airport cities are unlikely to succeed in controlling the number of cases unless they control passenger arrivals. This is valid for cities as New York and London, or Rio de Janeiro and São Paulo, but also valid for the smaller cities,

such as Manaus, with 2 million inhabitants. Furthermore, the constant adding of new infected individuals from the Manaus airport found a quite particular city for community spread. Eventually, a similar political behaviour might have produced a terrifying scenario during the Spanish flu in Manaus.

### **A TROPICAL BELLE ÉPOQUE CITY AND ITS RESILIENT SANITARIAN VULNERABILITIES UNTIL PRESENT DAYS**

Manaus reflects many of the country's political problems, along with a very particular way of life. It is a complex city for public health, largely due to its expansion along the banks of the Negro River, intrinsically linked to the harbour activity, and entangled with poverty. In November to December the river floods and can even reach downtown streets. The river seasonal dynamics adds to a hygienically compromised environment in the harbour. By having densely populated margins, and mostly lacking sewage treatment, flooding events could spread contaminated water even farther (and created habitats for insect vectors), increasing overall health vulnerabilities in a seasonal way. The context of having many people exposed to other diseases may have contributed to both Spanish Flu and COVID-19 outbreak severities, which occurred in the same months of rains and flooding, despite being separated by 102 years. In spite of few reported studies, Caldas & Pozzetti (2017) described that there are no monitoring protocols to assess the quality of water applied to the harbour, nor a cleaning and disinfection daily program.

The poor urban sanitary policy is historical and led the city to a previous epidemiological collapse during the Spanish flu pandemic in 1918, when 10% of the total population died

within seven months. Gama (2020) described trucks transporting putrefied bodies left on the streets, as there was no space in cemeteries (curiously, the author described that newspapers reported an anti-malarian quinine-based drug proposed as a cure, which disappeared from the pharmacies' shelves by that time). A deadly combination of idiosyncrasies in the Manaus urbanization and social vulnerability made it highly vulnerable to the Spanish flu (Fig. 1). It is already well understood that socioeconomic problems, slums, and spatial distribution of poverty in a city are highly influential determinant of the incidence and distribution of COVID-19 (Buckley 2020, Maroko et al. 2020, Mishra et al. 2020, Mena et al. 2021), along with undermining non-pharmaceutical interventions (Ferrante et al. 2021). The same may have intensified Spanish Flu back in 1918 (Schwarcz & Starling 2020).

These sanitarian temerities overpass the harbour and repeat in the markets and downtown public areas. Also, a large number of persons live in their boats, usually anchored in bays with stagnant water, where their wastes are dumped with absolutely no treatment, and from where most of them collect water for their consumption, cooking, bathing, etc. Such behaviours towards the river waters, likely born in remote regions, are common among Amazonian river towns. Hence, not only SARS-CoV-2 but also secondary infections may spread quickly, which is a serious concern considering overload cemeteries due to excess of bodies along the pandemic. From the Manaus port, the "gaiolas", bird-cage boats, normally leave towards many cities, literally "packed with passengers". Regardless of being open boats, dozens sleep in hammocks side by side, in the same space where they eat. From Manaus to Belém (the largest and most populated cities of Brazilian Amazon region), for instance, the trip usually takes six days, which is a very

simple explanation for how both Spanish Flu and COVID-19 fastly spread along the river cities after Manaus had previously started community transmission (Gama 2020, TRANSPARÊNCIA COVID-19 2021).

Hence, without strong sanitarian rules and governmental guidance, it is hard to enforce changes in behaviours based on strong and ancient cultural background, and traditions of close physical contacts. In many of these aspects, Manaus is no different from the rest of Brazil, the city just got hit earlier and stronger, and its unfortunate example should be used as a bold warn for the rest of the country.

### **THE SIMULATION OF COVID-19 AND SPANISH FLU DYNAMICS IN MANAUS AND NATURAL SELECTION DRIVING THE PANDEMIC INTENSITY AND DURATION**

Mathematical predictions on host-parasite interactions (May & Anderson 1983) may help to disentangle the causes and consequences of human behaviour versus virion evolutionary determinism in the output of cases and deaths. We explored the combined effects of a soft social isolation, which is currently applied to some Brazilian cities, and the appearance of new more transmissible variants, using Manaus parameters. We applied the same model for the Spanish Flu in order to validate it, using available historical data. Finally, it was simulated the natural evolution of the disease with competing variants in one city that takes no precautions, but still has a certain amount of self-isolated individuals. The program algorithm is described as a Supplementary Table, available at [https://github.com/leaflaboratory/COVID-19-selection-Model/blob/main/Manaus\\_def.cpp](https://github.com/leaflaboratory/COVID-19-selection-Model/blob/main/Manaus_def.cpp).

We simulated Manaus 2020-21 as an intensely interconnected medium size city, of



**Figure 1.** Large picture shows a channel reaching Negro river in Manaus, and some features of the urbanization around the harbour region. Detailed picture focused on a packed and convoluted under poverty neighbourhood, with floating houses in a small channel with stagnated water. An unlikely urbanization for effective social distancing and public areas cleaning. Obtained from Google Earth.

2,000,000 inhabitants and a daily turnover of 0.7% of its population (which is a proxy of its airport daily movement plus fluvial and road travellers). From these constantly arriving of people, we randomly defined 3% infected with the original virus strain (i.e.: already circulating in the city), or with a variant 2.6 times more transmissible than the former, simulating the Gamma P1 variant as described in Coutinho et al. (2021). Thus, we simulated a sudden appearance of Gamma, whatever its real origin. The city was designed as a lattice model, with explicit public places of different sizes (thus, with distinct carrying capacity), and one private size for houses, capable to accommodate 3.3 persons (sorted following Poisson distribution). People were randomly sorted to stay home (conservatively at 60%) and the remaining to

move around, visiting several public areas by random, and staying out for 8 hours. We then run an adapted SIR model with contrasting  $\beta$ -infection rates for each variant (reflecting the greater variance of Gamma, as previously described, S.1).  $\beta$ -infection rate is the infection constant that represents the proportion of encounters between an infected and a susceptible person, which result in the infection of the latter. Infection occurs when a susceptible person shares a public space with an infected one, with a chance proportional to the  $\beta$  of each variant, and to the density of infected and susceptible people in the same place. After five days of incubation, the person became a source of virus and infected others for the following 14 days, unless she/he died, which happened for 1% of the infected ones (considering recent

estimates of asymptomatic persons – Loannidis 2020, and their transmissibility – Johansson et al. 2021). After recovery, a person maintained his/her immunity for 180 days and after returned to the susceptible stage, except for 4% whom maintained immunity for 360 days, and 5% that stayed immune forever. Thus, we attempted to reproduce the variance in immunity observed between those with light and heavy symptoms (Stephenson et al. 2021).

Based on historical records taken from both Gama (2020) and Schwarcz & Starling (2020), we used the same model to simulate a 1918-19 Manaus under the H1N1 outbreak: 60,000 inhabitants, three days of incubation after infected, and six days transmitting the virus. Based on the epidemiological descriptions of the Influenza's mortality and  $R_t$  (Taubenberger & Morens 2006, Andreasen et al. 2008), we calculated  $\beta$  and run the model with the parameters:  $R_t = 5.4$  ( $R_t$  as the number of persons infected by one infected person) and  $\beta = 0.92$ . Based on the reports from these authors, hardly any social distancing was observed except for closing down schools, public services, and theatres. Hence, we have assumed a conservative social distancing of 20%. We also assumed in the SIR model that immunity was retained by three months, to simulate the fact that this influenza virus mutated much faster than coronavirus (Day et al. 2020), and that the city may have been hit by various new variants from Europe since the onset of Spanish flu pandemic (Schwarcz & Starling 2020). According to Schwarcz & Starling (2020), the dissemination of the Flu towards and at Manaus was as such: in 09 October the city of Belém, Para State, the first Amazonian harbour near the ocean, had 3,000 infected people, from where the ship "Ceará" left to Manaus with infected passengers; 28 October the vessel Valparaiso reached Manaus with individuals suffering of a more severe version of the disease; 02 November hospitals had no

bed for flu patients anymore and one week after the officials reported 1,000 infected people; by 14 November the funerary services reported 33 deaths in one day, above the average of five per day, a number that stabilized above 40; the first newspapers articles describing corpses left in the streets arrived by this same day, and the municipality started a service of collecting the dead in a truck, heading to a collective graveyard; by December officials reported 1,500 deaths in November, but Gama (2020) pointed out that this was from official cemeteries, and that unofficial burials in the backyards, and several corpses just thrown in the Negro river would summed up from 6,000 to 8,000 (Schwarcz & Starling 2020); in February and March 1919 new cases and deaths increased again but with much less strength in the city; reports of disappearance of whole ethnic groups, as the Avá-canoeiro, occurred in early 1919, along with reports of cases in riverside cities, such as Tefé, Maués, Parintins.

The artificialities of the model, for sake of simplicity, are as follow: there is no overlapping infections, immunity and susceptibility are equal to both variants (for COVID-19), and travelling time within the city was taken as irrelevant. Furthermore, there is no age structure, and all have equal chances to get infected. Hence, this model emphasizes the transmissibility by pre-symptomatic and asymptomatic, as no constraint in the movement of an infected person is imposed but when someone dies.

### COVID-19 simulation

Our model for COVID-19 described a several years long-lasting epidemic, with an unavoidable second wave stronger than the first, and continuous new waves, in spite of being gradually weaker along time (Fig. 2). Nonetheless, the second wave and following outbreaks were virus variant-dependent, since

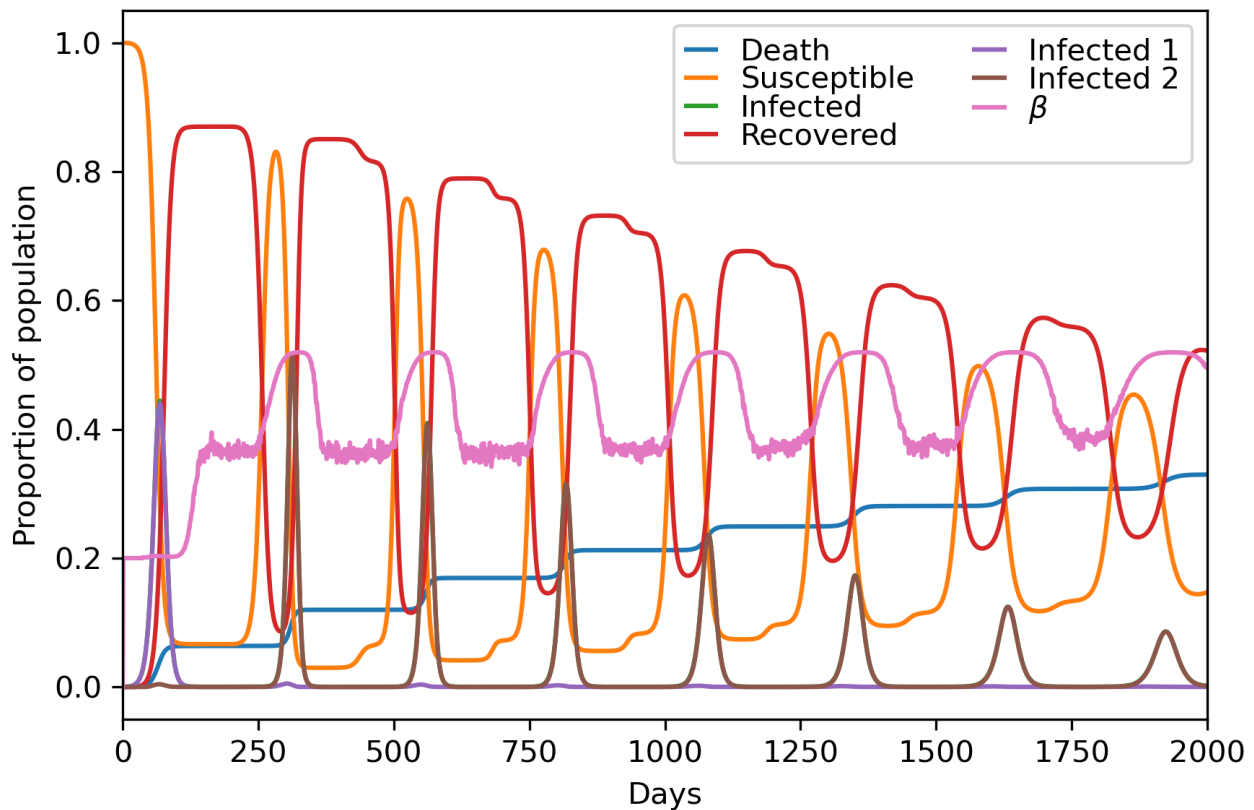


**Figure 2.** SIR adjusted dynamic of COVID-19 evolution along 2,000 days, adjusted for the Manaus population, migration rates, and original (Infected 1, blue line) and Gamma P1 (Infected 2, orange line) variants.  $\beta$  (green line) = combined  $\beta$ -infection rate for both variants ( $\Sigma\beta_i/\Sigma$  infected). Oscillation are due to the variation of number of infected people.

the accumulation of new infections ended up producing a prolonged large proportion of immunized subpopulation, along with the death of those vulnerable individuals. Hence, with little isolation, neither travelling restrictions, nor vaccination, the disease could prevail as long as 2000 days (five and half years) before it becomes unable to produce new relevant outbreak waves. By leaving the disease to die out with time, this city could accumulate a mortality close to 40% of its population, before death cumulative rates decreases to an irrelevant value.

### Spanish Flu simulation

The model adjusted for the existing conditions in 1918-19, when Spanish Flu hit Manaus and killed 10% of its population, was able to

reproduce the two waves in the exact months they happened (September to November 1918 and February to March 1919), with the first stronger than the second, as it was the case (Fig. 3). Our model predicted 60% of deaths in the city, but considering the intense flux of people through Manaus, this high value could explain the spreading of the disease in the interior by 1919.

### Competition between variant traits simulation

We also further tested different variants with distinct transmissibility or lethality. The variants with less transmissibility than the original strain were not able to invade the city while the more transmissible variants substituted the original one after 200 days and following a second

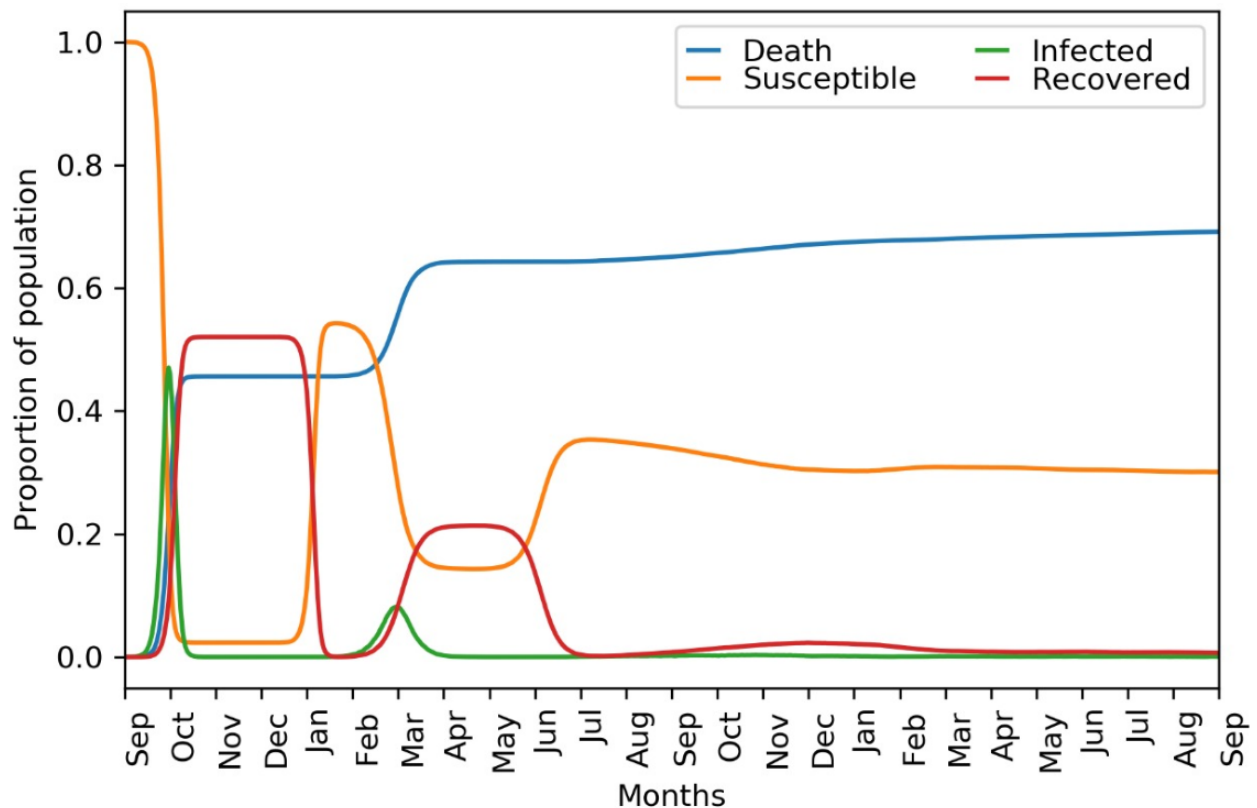


**Figure 3.** SIR adjusted dynamic of Spanish Flu evolution along the period recorded for its occurrence in Manaus. We assumed only one variant of H1N1 and showed the variables responses to the simulation of the population size and published parameters of mortality and transmissibility for the Influenza 1918-19 (see the text for details).

wave. Interestingly, the lesser lethal variant overcame the more lethal one in all the waves, which is expected for a long-term evolution of an emergent disease if the lack of host illness favours transmission, i.e., loss of virulence (Fig. 4). Due to the full shifting of the original strain by new variants, the  $\beta$ -infection rate was permanently higher after the second wave than it was in the beginning of the pandemics.

## DISCUSSION

A mathematical model does not aim to reproduce the reality, but to emphasise parameter-driven patterns that could help us understanding the date, intensity, and duration of host-pathogen dynamics. Our simulations reproduced some important dynamics that happened in both

Spanish flu and COVID-19 pandemics in Manaus. A limitation of our model for both pandemic events was that it produced an excessive number of deaths as our simulation reflects movement and isolation from individual to individual but did not consider populational heterogeneity, which may cause transient collective immunity and, thus, retain a larger amount of the population untouched by the virus and, consequently, susceptible (as in Tkachenko et al. 2021). Still, our large number of deaths, for both scenarios, may somehow reflects one particular possibility: the city may become a source of infected travellers in a close regional space, which may keep a certain number of imperceptible cases for much longer than the end of the collapse of the public health, especially in contained outbreaks in poor and forgotten suburbs or in



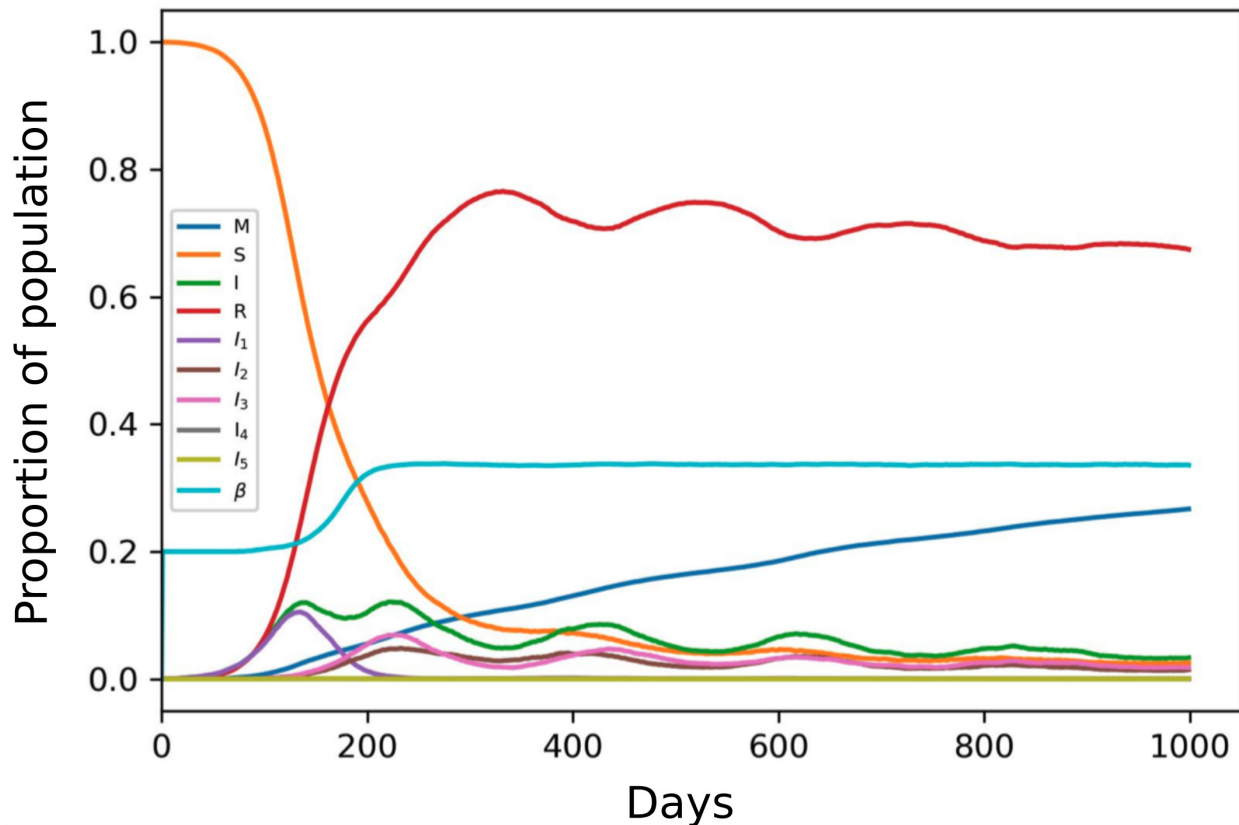


**Figure 4.** SIR adjusted dynamic of COVID-19 evolution along 1,000 days in a 100,000 simulated town, with 1% of population turnover with outsider source of persons. M = mortality; S = susceptible; I = infected; R = recovered;  $I_1$  = portion of infected population carrying the indigenous strain. In comparison with the indigenous strain:  $I_2$  = portion of infected population carrying the variant more transmissible and more lethal;  $I_3$  = portion of infected population carrying the variant more transmissible and less lethal;  $I_4$  = portion of infected population carrying the variant less transmissible and more lethal;  $I_5$  = portion of infected population carrying the variant less transmissible and less lethal;  $\beta$  = combined  $\beta$ -infection rate for all existing variants in a time  $t$ . Any less transmissible variants than the indigenous were not able to establish and that most transmissible eliminated the indigenous strain after established. Also, important to note that along the time, the more transmissible and more lethal variant cannot overpass the frequency of the more transmissible but less lethal, pointing toward the evolution of lower virulence along time.

small villages. Indeed, long after Spanish Flu was considered ended in Manaus, March of 1919, several reports of villages with excessive deaths and even indigenous ethnies that have just vanished from civilized contact, were brought about from explorers of the interior (Schwarcz & Starling 2020).

### **Causes of a second deadlier wave of distinct pandemics: Spanish flu and COVID-19 in Manaus and Brazil**

If something should be learned from history, the 1918 flu pandemic had a second and more lethal wave worldwide (matching the first wave in Manaus) surged in the middle of lack of information (hidden by war propaganda) and political denials (Taubenberger & Morens 2006). Many unanswered questions are still in place about the actual driver of a second much more

severe wave in different pandemics. Unstable and temporary highly pathogenic strains may emerge if a huge number of susceptible hosts are constantly made available during an emerging disease, as predicted by Lenski and May (1994). Hence, neglecting social distancing in the middle of a pandemic might be a driving force for increasing death rates, by favouring both more lethal or more transmissible strains before high transmissibility with low lethality takes a definitive place in the evolution of the disease, and mortality declines for good, if it follows the prediction of May & Anderson (1983) or Berngruber et al. (2013).

Presently, a similar pattern has repeated worldwide, with families and youngsters not willing to hold in isolation since the 2020 Christmas and 2021 New Year celebrations. In Manaus, the hardest public health collapse happened exactly two weeks after the New Year celebrations. This also coincided with the appearance of a new virulent strain of SARS-CoV-2 found in the Amazon, the Gamma P.1. Since then, the daily number of cases is above the average for the whole pandemic period, and an increasing number of hospitalized cases under 60 years old has been reported, even before the vaccination. This was a bold evidence of a more resilient and concerning moment of the pandemic in the region, which is also consistently more lethal among Amazonian Natives (TRANSPARÊNCIA COVID-19 2021).

Most respiratory viral pandemics in history are reported to return in waves, and commonly, the second waves are stronger with several likely explanations for this pattern (Berngruber et al. 2013, Gagnon et al. 2013). After a few waves of outbreaks, the disease eventually disappeared, which was the case since the Russian flu (1890), the Spanish flu (1918-19), Asian flu (1957), and the Hong Kong flu (1968). Recent coronavirus outbreaks were caused by viruses with a very

high pathogenic capacity and, thus, less likely to produce a pandemic, such as the SARS-CoV and the MERS, which killed above 10% of infected people. Concerning dissemination, the present SARS-CoV-2 seems to behave more closely to Influenza type A virus, which suggests that transmissibility might be a more important ecological driver of a second wave than virus taxonomical identity, specific infection mechanisms or host immune response.

A recurrent aspect about emergent disease pandemics is that they may disappear with time, as the pathogen adjusts evolutionarily to the new host, by losing lethality or declining to unperceivable levels, as host immunity humps up and more vulnerable host genotypes are eliminated (May & Anderson 1983, Taubenberger et al. 2000, Reid et al. 2004, Taubenberger & Morens 2006). Even considering that virulent mutants may be transiently favourable in the early stages of a disease emergence, their tendency is of losing competitiveness with highly transmissible variants, which could result in prevalence and low lethality, a hypothesis supported mathematically (May & Anderson 1983), experimentally (Berngruber et al. 2013), and genetic-and-historically, in the studies of 1918 lineages of H1N1 in humans (Taubenberger et al. 2000, Reid et al. 2004, Taubenberger & Morens 2006). Furthermore, there might have situations when lethality may prevail for longer than expected after a disease invades a new host. A special case is arbovirus diseases, which can sustain virulent strains for decades, as observed for dengue. The insect vector-host is a key aspect for that, namely when vertical transmission in the insect population may be frequent (Ferreira-de-Lima & Lima-Camara 2018).

Additionally, a large uncertainty raises from the fact that COVID-19 is a disease with a larger proportion of transmission happening

from pre-symptomatic or fully asymptomatic individuals (Johansson et al. 2021), leading to several possible evolutionary outputs, including the absence of selection against virulence (Day et al. 2020). The possibility of virulence remaining despite selection of more transmissible variants, as indeed was confirmed to the Alpha B.1.1.7 variant (Davies et al. 2021), is a likely scenario for SARS-CoV-2. Nevertheless, if the time span between infection and death is a key period of transmission, it may result in the mechanism for virulence loss. Among the possible outputs from the models of SARS-CoV-2 evolution in Day et al. (2020), there is substantial theoretical support for selection in favour of a mutant with greater transmissibility without increased lethality. Eventually, even with decreasing the intensity of symptom onset. A mutant prevails if its selection coefficient is positive, and one likely way for such is that it “remains infectious for longer” (Day et al. 2020). Therefore, it is not the neutrality of lethality (i.e., lethality has little evolutionary cost as most transmissions are before symptom), but the advantage of prolonging transmission in a continuously healthy host, the possible driver of increasing transmissibility with decreasing virulence.

A humanitarian problem with leaving a pandemic to run its course is the unbearable life cost, as observed in 1918 influenza pandemic, with certainly more than 50 million people dead out of a world population of 2 billion people. The least lethal a virus is, the more it might kill by silent transmission (Li et al. 2020). Hence, the present model tries to predict for how long and which proportion of a population may be taken if a society leaves a pandemic to run to exhaustion.

## CONCLUSIONS

### **The Brazilian public health and funerary collapses of 2021: predictions and responsibilities**

In a few months of great mortality, the Spanish flu caused a major socio-economic disruption in Brazil from 1918 to 1919. Although much more lethal globally than COVID-19, that pandemic killed a much lower proportion of the population in the, by that time, marginal Brazil (0.12%), compared with central economies in Europe, Asia, and North America. It killed at least 35,000 out of the 28,900,000 Brazilian population (ATLAS FVG 2021). It was, thus, much more severe in Manaus than in other cities. By June 2021, COVID-19 had already killed more than 500,000 Brazilians, and, thus, over 0.24% of the 210,000,000 population, which makes Brazil an unfortunate international outlier. On 12 March, Brazil overpassed India in number of cases, a country with 5.6 more individuals. In these same days, scientists, cemetery managers, and hospital directors were alerting for the worse, in the verge of a collapse in the coming weeks of March and April 2021, which was confirmed. With no clear central government guidance, individuals, institutions, state and city managers were using social and conventional media, trying to overwhelm the federal negligence and contradictory messages. The natural ending of a pandemic is certain, but hardly recorded scientifically (Taubenberger & Morens 2006), which makes difficult to review on the subject, unless one mix medical literature with historical descriptions, mostly taken from the media, as we did in this study. However, the few articles enlightening the intensity and duration of the Spanish Flu in US, for instance, clearly demonstrated that social distancing and nonpharmaceutical interventions were the best and fastest solutions, both economically as humanitarily (Hatchett et al. 2007).

Cities in tropical developing countries are hard to be maintained healthy safe. The unacceptable humanitarian catastrophe of Manaus, twice, and its worry interconnection with Native communities still are our main concerns. A severe restriction to flights and river boats, especially from Manaus to the interior of Amazon and Pará states, is essential to stop the spreading of new variants. Months after the first collapse of 2020, it was proposed that the population in Manaus was above herd immunity (Buss et al. 2021) but that did not prevent them to face a second and stronger wave, nearly one year ahead.

Eventually, this might be the moment to send back the term “herd immunity” to where it belongs: the vaccinology. It is hard to assume in a natural infection process how many persons out of those with moderate or no disease would actually be protected by having produced immunologic memory or, alternatively, be simply resistant (would not get infected at all after exposed). Despite a well-designed serologic study might help to sort out asymptomatic from susceptible individuals, it does not explain why some will be in contact and not infected (a population component absorbs and simulated by the  $\beta$ -infection rates in SIR models). Indeed, TCI (transient collective immunity - Tkacenko et al. 2021) would emerge during early, high-paced stages of the pandemic and, therefore, leading to the decrease of each epidemic wave individually. Hence, TCI might be a better explanation for the consecutive waves in Manaus, and potentially an evolutionary scenario of greater chances of a mutant to survive stochastic extinction (as explained in Day et al. 2020). Hence, a substantial number of persons might still be susceptible after a first contact with the virus, and even more to a mutant variant, and especially in a city with the characteristics of Manaus.

## Acknowledgments

S P. Ribeiro, Alexandre B. Reis, Aristóteles G. Neto, Vasco A.C. Azevedo and Geraldo W. Fernandes are researchers granted by CNPq. We thanks Hildeberto de Caldas Sousa for double checking on facts about life in Manaus. This study has no financial support.

## REFERENCES

- ANDREASEN V, VIBOUD C & SIMONSEN L. 2008. Epidemiologic characterization of the 1918 Influenza pandemic summer wave in Copenhagen: implications for pandemic control strategies. *J Infect Dis* 197: 270-278.
- ATLAS FGV. 2021. GRIPE ESPANHOLA. Available at: <https://atlas.fgv.br/verbetes/gripe-espanhola>. accessed 10 March, 2021.
- BARBOSA LG, ALVES M & GRELE CEV. 2020. Actions against sustainability: dismantling of the environmental policies in Brazil. *Land Use Pol* 104: 105384.
- BERNGRUBER TW, FROISSART R, CHOISY M & GANDON S. 2013. Evolution of virulence in emerging epidemics. *PLOS Pathog* 9(1-8): e1003209.
- BUSS LF ET AL. 2021. Three-quarters attack rate of SARS-CoV-2 in the Brazilian Amazon during a largely unmitigated epidemic. *Science* 371: 288-292.
- BUCKLEY RM. 2020. Targeting the world’s slums as fat tails in the distribution of COVID-19 Cases. *J Urban Health* 97: 358-364.
- BUTLER JC ET AL. 2001. Emerging infectious diseases among indigenous peoples. *Emerg Infec Dis* 7: 554-555.
- CALDAS JN & POZZETTI VC. 2017. Hygienic and sanitarian conditions of Manaus ports, AM (Condições higiênic-sanitárias dos portos de Manaus-AM), 2007-2010. *Soc Ci Tecn* 5: 53-59.
- COUTINHO RM ET AL. 2021. Model-based estimation of transmissibility and reinfection of SARS-CoV-2 P1 variant. medRxiv <https://doi.org/10.1101/2021.03.03.21252706>.
- COVID-19.SOCIOAMBIENTAL 2021. Plataforma de monitoramento da situação indígena na pandemia do novo coronavírus (COVID-19) no Brasil. Disponível em <https://covid19.socioambiental.org/>. Accessed 28 Feb, 2021.
- DAVIES NG ET AL. 2021. Estimated transmissibility and impact of SARS-CoV-2 lineage B.1.1.7 in England. *Science* 372: eabg3055. <https://doi.org/10.1126/science.abg3055>.

- DAY T, GANDON S, LION S & OTTO SP. 2020. On the evolutionary epidemiology of SARS-CoV-2. *Curr Biol* 30: R849-R57.
- FERRANTE L ET AL. 2021. Brazil's policies condemn Amazonia to a second wave of COVID-19. *Nat Medic* 26: 1315.
- FERREIRA-DE-LIMA VH & LIMA-CAMARA TN. 2018. Natural vertical transmission of dengue virus in *Aedes aegypti* and *Aedes albopictus*: a systematic review. *Parasit Vectors* 11: 77 <https://doi.org/10.1186/s13071-018-2643-9>.
- FRASER B. 2020. How anti-science attitudes have impacted the coronavirus pandemic in Brazil. *Sci Am* May 22.
- FVS/AM - FUNDAÇÃO DE VIGILÂNCIA EM SAÚDE DO AMAZONAS. 2020. Coronavírus: situação epidemiológica da COVID-19 no Estado do Amazonas, 2020. *Bol Epidem* 15: 1-2. Disponível em [https://www.fvs.am.gov.br/media/publicacao/Boletim\\_15\\_f84a1qO.pdf](https://www.fvs.am.gov.br/media/publicacao/Boletim_15_f84a1qO.pdf).
- FVS/AM - FUNDAÇÃO DE VIGILÂNCIA EM SAÚDE DO AMAZONAS. 2021. Painel Covid-19 AMAZONAS. 2021. <http://saude.am.gov.br/painel/corona/>. accessed 2021 April 30.
- GAGNON A, MILLER MS, HALLMAN SA, BOURBEAU R, HERRING DA, EARN DJD & MADRENAS J. 2013. Age-specific mortality during the 1918 Influenza pandemic: unravelling the mystery of high young adult mortality. *PLOS One* 8: e69586. <https://doi.org/10.1371/journal.pone.0069586>.
- GAMA RM. 2020. Mephistophelic days: the Spanish flu in Manaus by the newspapers of 1918-1919. *Dias mefistofêlicos: a gripe espanhola em Manaus através dos jornais de 1918 - 1919*. Editora dialética, Belo Horizonte (Brazil), 205 p.
- HATCHETT RJ, MECHER CE & LIPSICH M. 2007. Public health interventions and epidemic intensity during the 1918 influenza pandemic. *PNAS* 18: 7582-7587.
- JOHANSSON MA, QUANDELACY TM, KADA S, PRASAD PV, STEELE M, BROOKS JT, SLAYTON RB, BIGGERSTAFF M & BUTLER JC. 2021. SARS-CoV-2 transmission from people without COVID-19 symptoms. *JAMA Net Open* 4: e2035057.
- JONES KE ET AL. 2008. Global trends in emerging infectious diseases. *Nature* 451: 990-994.
- KARESH WB ET AL. 2012. Ecology of zoonoses: natural and unnatural histories. *Lancet* 380: 1936-1945.
- LENSKI RE & MAY RM. 1994. The evolution of virulence in parasites and pathogens: reconciliation between two competing hypotheses. *J Theor Biol* 169: 253-265.
- LI R, PEI S, CHEN B, SONG Y, ZHANG T, YANG W & SHAMAN J. 2020. Substantial undocumented infection facilitates the rapid dissemination of novel coronavirus (SARS-CoV-2). *Science* 368: 489-493.
- LOANNIDIS JPA. 2020. Infection fatality rate of COVID-19 inferred from seroprevalence data. *Bull. WHO Org.* 99: 19-33F. <https://doi.org/10.2471/BLT.20.265892>.
- MAY RM & ANDERSON RM. 1983. Epidemiologic and genetics in the coevolution of parasites and hosts. *Proc R Soc Lond B* 219: 281-313.
- MAROKO AR, NASH D & PAVILONIS BT. 2020. COVID-19 and Inequity: a Comparative Spatial Analysis of New York City and Chicago Hot Spots. *J Urban Health* 97: 461-470.
- MENA GE, MARTINEZ PP, MAHMUD AS, MARQUET PA, BUCKEE CO & SANTILLANA M. 2021. Socioeconomic status determines COVID-19 incidence and related mortality in Santiago, Chile. *Science*: eabg5298. <https://doi.org/10.1126/science.abg5298>.
- MISHRA SV, GAYEN A & HAQUE SM. 2020. COVID-19 and urban vulnerability in India. *Habitat Int* 03: 102230.
- OBSERVATÓRIO COVID-19. 2021. Informação para ação. Available at: <https://portal.fiocruz.br/observatorio-covid-19>. Accessed 03 March 2021.
- REID AH, TAUBENBERGER JK & FANNING TG. 2004 Evidence of an absence: the genetic origins of the 1918 pandemic influenza virus. *Nat Rev Microbiol* 2: 909-914.
- RIBEIRO SP ET AL. 2020a. Severe Airport Sanitarian Control Could Slow down the Spreading of COVID-19 Pandemics in Brazil. *PeerJ* 8: e9446.
- RIBEIRO SP ET AL. 2020b. Worldwide COVID-19 spreading explained: traveling numbers as a primary driver for the pandemic. *An Acad Bras Cienc* 92: e20201139. <https://doi.org/10.1590/0001-3765202020201139>.
- SABINO EC ET AL. 2021. Resurgence of COVID-19 in Manaus, Brazil, despite high seroprevalence. *Lancet* 397(10273): 452-455.
- SCHWARCZ M & STARLING HM. 2020. A Bailarina da morte: a gripe espanhola no Brasil. *Companhia das Letras, São Paulo*.
- STEPHENSON E ET AL. 2021. Single-cell multi-omics analysis of the immune response in COVID-19. *Nature Med* 27: 904-916.
- TAUBENBERGER JK & MORENS DM. 2006. 1918 Influenza: the mother of all pandemics. *Emerg Infect Dis* 12: 15-22.
- TAUBENBERGER JK, REID AH & FANNING TG. 2000. The 1918 influenza virus: a killer comes into view. *Virology* 274: 241-245.
- TKACHENKO AV, MOSLOV S, ELBANNA A, WONG GN, WEINER ZJ & GOLDENFELD N. 2021. Time-dependent heterogeneity

leads to transient suppression of the COVID-19 epidemic, not herd immunity. PNAS 118: e2015972118.

TRANSPARÊNCIA COVID-19. 2021. Séries Temporais COVID-19 no Amazonas. [http://www.fvs.am.gov.br/indicadorSalaSituacao\\_view/69/2](http://www.fvs.am.gov.br/indicadorSalaSituacao_view/69/2). Accessed 28 Feb, 2021.

#### How to cite

RIBEIRO SP, REIS AB, DÁTILLO W, CASTRO E SILVA AVC, BARBOSA EAG, COURA-VITAL W, GÓES NETO A, AZEVEDO VAC & FERNANDES GW. 2021. From Spanish Flu to Syndemic COVID-19: long-standing sanitarian vulnerability of Manaus, warnings from the Brazilian rainforest gateway. *An Acad Bras Cienc* 93: e20210431. DOI 10.1590/0001-3765202120210431.

*Manuscript received on March 22, 2021,  
accepted for publication on June 19, 2021*

#### SÉRVIO P. RIBEIRO<sup>1,2,3</sup>

<https://orcid.org/0000-0002-0191-8759>

#### ALEXANDRE B. REIS<sup>1,4</sup>

<https://orcid.org/0000-0001-8123-4164>

#### WESLEY DÁTILLO<sup>5</sup>

<https://orcid.org/0000-0002-4758-4379>

#### ALCIDES V.C. DE CASTRO E SILVA<sup>6</sup>

<https://orcid.org/0000-0003-2863-8076>

#### EDUARDO AUGUSTO G. BARBOSA<sup>7</sup>

<https://orcid.org/0000-0001-5652-7344>

#### WENDEL COURA-VITAL<sup>1,8</sup>

<https://orcid.org/0000-0002-1434-7676>

#### ARISTÓTELES GÓES-NETO<sup>9</sup>

<https://orcid.org/0000-0002-7692-6243>

#### VASCO A.C. AZEVEDO<sup>10</sup>

<https://orcid.org/0000-0002-4775-2280>

#### GERALDO WILSON FERNANDES<sup>11</sup>

<https://orcid.org/0000-0003-1559-6049>

<sup>1</sup>Universidade Federal de Ouro Preto, Núcleo de Pesquisas em Ciências Biológicas – NUPEB, St. Três, 408-462, Bauxita, 35400-000 Ouro Preto, MG, Brazil

<sup>2</sup>Universidade Federal de Ouro Preto, Laboratory of Ecology of Diseases and Forests, Departamento de Biodiversidade, Evolução e Meio Ambiente, St. Quatro, 786, Bauxita, 35400-000 Ouro Preto, MG, Brazil

<sup>3</sup>Universidade Federal de Minas Gerais, Laboratory of Physiology of Hematophagous Insects, Departamento de Parasitologia, Ave. Pres. Antônio Carlos, 6627, Pampulha, 31270-901 Belo Horizonte, MG, Brazil

<sup>4</sup>Universidade Federal de Ouro Preto, Laboratory of Immunopathology, Departamento de Análises Clínicas, St. Três, 408-462, Bauxita, 35400-000 Ouro Preto, MG, Brazil

<sup>5</sup>Instituto de Ecología AC, Red de Ecoetología, Carretera Antigua a Coatepec, 351, El Haya, Xalapa, Veracruz, 91070 Mexico

<sup>6</sup>Universidade Federal de Ouro Preto, Laboratory of Complexity Science, Departamento de Física, St. Quatro, 786, Bauxita, 35400-000 Ouro Preto, MG, Brazil

<sup>7</sup>Centro Federal de Educação Tecnológica de Minas Gerais, Programa de Pós-Graduação em Modelagem Matemática e Computacional, 30510-000 Belo Horizonte, MG, Brazil

<sup>8</sup>Universidade Federal de Ouro Preto, Laboratory of Epidemiology and Cytology, Departamento de Análises Clínicas, St. Nove, 27, Bauxita, 35400-000 Ouro Preto, MG, Brazil

<sup>9</sup>Universidade Federal de Minas Gerais, Laboratory of Molecular and Computational Biology of Fungi, Departamento de Microbiologia, Ave. Pres. Antônio Carlos, 6627, Pampulha, 31270-901 Belo Horizonte, MG, Brazil

<sup>10</sup>Universidade Federal de Minas Gerais, Laboratory of Cell and Molecular Genetics, Departamento de Genética, Ecologia e Evolução, Ave. Pres. Antônio Carlos, 6627, Pampulha, 31270-901 Belo Horizonte, MG, Brazil

<sup>11</sup>Universidade Federal de Minas Gerais, Laboratory of Evolutionary Ecology and Biodiversity, Departamento de Genética, Ecologia e Evolução, Ave. Pres. Antônio Carlos, 6627, Pampulha, 31270-901 Belo Horizonte, MG, Brazil

Correspondence to: **Sérvio Pontes Ribeiro**

E-mail: [serviopr@gmail.com](mailto:serviopr@gmail.com)





#### Author contributions

SPR - Conceptualization; Data curation; Formal analysis; Investigation; Methodology; Project administration; Writing-original draft; Writing-review & editing. WD - Formal analysis; Investigation; Validation; Writing-review & editing. AVCCS - Formal analysis; Investigation; Writing-review & editing. EAGB - Formal analysis. WCV - Formal analysis; Investigation; AGN - Investigation; Writing-review & editing. VACA - Supervision; Writing-review & editing. ABR - Project administration; Supervision; Writing-review & editing. GWF - Project administration; Supervision; Validation; Writing-review & editing.



## Article

# Successive Pandemic Waves with Different Virulent Strains and the Effects of Vaccination for SARS-CoV-2

Alcides Castro e Silva <sup>1,\*</sup>, Américo Tristão Bernardes <sup>1</sup>, Eduardo Augusto Gonçalves Barbosa <sup>2</sup>,  
Igor Aparecido Santana das Chagas <sup>3</sup>, Wesley Dáttilo <sup>4</sup>, Alexandre Barbosa Reis <sup>5,6</sup> and Sérgio Pontes Ribeiro <sup>7</sup>

<sup>1</sup> Laboratory of Complexity Science, Department of Physics, Universidade Federal de Ouro Preto, ICEB, St. Quatro, 786, Bauxita, Ouro Preto 35400-000, MG, Brazil; atb@ufop.edu.br

<sup>2</sup> Centro Federal de Educação Tecnológica de Minas Gerais, Graduate Program in Mathematical and Computational Modeling, Ave. Amazonas, 7675, Nova Gameleira, Belo Horizonte 30510-000, MG, Brazil; eduardo.agbarbosa@pbh.gov.br

<sup>3</sup> Graduate Program in Biological Sciences, NUPEB, Universidade Federal de Ouro Preto, St. Três, 408-462, Bauxita, Ouro Preto 35400-000, MG, Brazil; igor.chagas@aluno.ufop.edu.br

<sup>4</sup> Instituto de Ecología AC, Red de Ecoetología, Carretera Antigua a Coatepec, 351, El Haya, Xalapa 91070, Veracruz, Mexico; wesley.dattilo@inecol.mx

<sup>5</sup> Laboratory of Immunopathology, Department of Clinical Analysis, Universidade Federal de Ouro Preto, NUPEB, St. Três, 408-462, Bauxita, Ouro Preto 35400-000, MG, Brazil; alexreis@ufop.edu.br

<sup>6</sup> Instituto Nacional de Ciência e Tecnologia em Doenças Tropicais (INCT-DT), Salvador 40000-000, BA, Brazil

<sup>7</sup> Laboratory of Ecology of Diseases and Forests, Department of Biodiversity, Evolution and Environment, Universidade Federal de Ouro Preto, ICEB, St. Quatro, 786, Bauxita, Ouro Preto 35400-000, MG, Brazil; spribeiro@ufop.edu.br

\* Correspondence: alcides@ufop.edu.br; Tel.: +55-31-3559-1667



**Citation:** Castro e Silva, A.; Bernardes, A.T.; Barbosa, E.A.G.; Chagas, I.A.S.d.; Dáttilo, W.; Reis, A.B.; Ribeiro, S.P. Successive Pandemic Waves with Different Virulent Strains and the Effects of Vaccination for SARS-CoV-2. *Vaccines* **2022**, *10*, 343. <https://doi.org/10.3390/vaccines10030343>

Academic Editor: Joseph Tak-fai Lau

Received: 10 December 2021

Accepted: 7 February 2022

Published: 22 February 2022

**Publisher's Note:** MDPI stays neutral with regard to jurisdictional claims in published maps and institutional affiliations.



**Copyright:** © 2022 by the authors. Licensee MDPI, Basel, Switzerland. This article is an open access article distributed under the terms and conditions of the Creative Commons Attribution (CC BY) license (<https://creativecommons.org/licenses/by/4.0/>).

**Abstract:** One hundred years after the flu pandemic of 1918, the world faces an outbreak of a new severe acute respiratory syndrome, caused by a novel coronavirus. With a high transmissibility, the pandemic has spread worldwide, creating a scenario of devastation in many countries. By the middle of 2021, about 3% of the world population had been infected and more than 4 million people had died. Different from the H1N1 pandemic, which had a deadly wave and ceased, the new disease is maintained by successive waves, mainly produced by new virus variants and the small number of vaccinated people. In the present work, we create a version of the SIR model using the spatial localization of persons, their movements, and considering social isolation probabilities. We discuss the effects of virus variants, and the role of vaccination rate in the pandemic dynamics. We show that, unless a global vaccination is implemented, we will have continuous waves of infections.

**Keywords:** COVID-19; pandemic; vaccination; ABM-SIR model

## 1. Introduction

At the end of 2019, the world received news about a novel disease that started in Wuhan, China. This illness, called COVID-19, is caused by a SARS class virus named SARS-CoV-2. Due to its high transmission capability, the disease rapidly reached all countries around the globe, mainly through airports networks [1–3], and, on 11 March 2020, the World Health Organization (WHO) declared it a pandemic. As of September 2021, the Johns Hopkins COVID-19 dashboard [4] showed more than 200 million cases and more than 4 million deaths globally. Such a number shows how fast the SARS-CoV-2 can spread through an entire population if no coordinated actions to prevent and reduce infections are in place.

Any responsible sanitary policy adopted to slow down the progress of COVID-19 pandemic should make use of the following three strategies:

1. Social distancing: the obvious way to reduce susceptible-infected interaction and subsequent contagion;

2. Mask wearing and hygiene: this was implemented once it became known that transmission is mainly through respiratory droplets of infected patients and contact with surfaces infected by aerosol;
3. Vaccines: a correct vaccination program can decrease overall transmission and the intensity of the disease symptoms among those infected and vaccinated, reducing the public health collapse risk and the mortality rates, as susceptible but vaccinated people become asymptomatic. Still, the virus will circulate, and the lack of a proper vaccination will create outbreaks due to contact between an increasing number of “asymptomatic” people with susceptible people. As [5] demonstrated, the existence of transient collective immunity may prolong an epidemic, and a bad vaccine scheme may exacerbate this pattern.

For the specific case of COVID-19 vaccination, one of the subjects of the present work is that there are many factors that must be considered for a suitable immunization policy. Among all of them, this work focuses mainly on two aspects: how the virus is evolving into new variants of concern and reinfection.

Every time SARS-CoV-2 infects a susceptible person, it starts to make copies of itself replicating its RNA [6,7]. As this process is not 100% error proof, some changes can be introduced, and different copies can be created. These changes or mutations in RNA can lead to different scenarios: it can be an evolutionary dead end and kill the virus, it can be an irrelevant and not noticeable change, or it can bring some advantages, for example, better response to the immune system or a better enhanced ability to invade the cells [8]. Even more rarely, whole clusters of mutations can be acquired by the virus during a single infection. When a virus with a single or clusters of mutations is capable of an epidemiologically significant spread through populations, they are named “Variants of Concern” or VOC. According to US Center of Disease Control and Prevention (CDC) [9], a variant becomes a VOC *when there is evidence of an increase in transmissibility, or in lethality and severity of the disease, significant reduction in neutralization by antibodies generated during previous infection or vaccination, reduced effectiveness of treatments or vaccines, or diagnostic detection failures.*

Although there are thousands of different genetic lineages of SARS-CoV-2, there are few Variants of Concern [10]. Both the variant  $\beta$  (former B.1.351), which was first detected in South Africa, and variant  $\gamma$  (former P.1), which was first seen in Brazil and Japan, contain mutations that appear to weaken the ability of antibodies to neutralize the virus by binding to it, which would normally prevent it from infecting cells [11]. Variant  $\alpha$  (former B.1.1.7), detected in the UK and reported in 93 other countries, and variant  $\delta$  (former B.1.617.2), from India, show less of an ability to escape from antibodies, but they have gained mutations that allows them to reproduce faster, rapidly increasing the viral load in an infected person, with consequences for the transmissibility than the original version of the virus [12,13]. The latest Omicron variant has an extremely high transmissibility, even higher than  $\delta$ , but it is less likely to infect the lungs [14,15].

Apart from VOCs, there are still the “Variants of Interest” or VOIs (variants  $\epsilon$ ,  $\eta$ ,  $\iota$ ,  $\kappa$ , and  $\zeta$ ) and “Variants of High Consequence” (there are no SARS-CoV-2 variants that rise to the level of high consequence until now) [16]. The CDC definition of a VOI is a variant with specific genetic markers that have been associated with changes to receptor binding, reduced neutralization by antibodies generated against previous infection or vaccination, reduced efficacy of treatments, potential diagnostic impact, or predicted increase in transmissibility or disease severity. On the other hand, a variant has high consequences when there is clear evidence that prevention measures or medical countermeasures (MCMs) have significantly reduced effectiveness relative to previously circulating variants.

The second factor that can impact an immunization policy is the reinfection caused by the loss of immunity. Some works have shown that immunity with greater memory is acquired by infected people who developed severe symptoms, recovered, and were vaccinated with at least one dose. However, even in these cases, immunity is not permanent, requiring a new dose of vaccine [17,18]. The reinfection was assumed as rare just before



the spreading of the new variants of concern in early 2021 [19]. However, risks may rise if the pandemic is not controlled and the virus is left to evolve freely [20–22]. Reduced neutralization of the Delta variant in comparison to the ancestral Wuhan-related strain was already observed [23], and a complex relation between different variants is also possible. For instance, it was found that people infected with Beta variant are more susceptible to reinfection by Delta variant [23]. Hence, there is room for the evolution of new variants that could escape vaccination more aggressively, especially if the vaccination scheme continues to follow a heterogeneous pattern, leaving the most vulnerable populations exposed for longer [24].

In this work, we developed an epidemiological model where events such as the appearance of new variants and reinfection are taken into account. Our results point to an optimal vaccine frequency that should be conducted in a given epidemiological setting.

Mathematical models for the evolution of epidemics have been proposed in the last century; one with the concept of compartmental models was introduced by Ross (1916), followed by the most known and referenced model, proposed by Kermack and McKendrick (1927) [25]: the SIR or “susceptible-infected-removed” model (nowadays, the term recovered is also used). Many incremental evolutions of the original models have been studied, by considering many other “compartments”, such as non-asymptomatic, hospitalized, and other situations.

While in the ordinary versions of SIR and its descendants, the population is simulated by densities, which assumes an infinite population and does not capture effects of finite or even small communities, in the present work, an Agent-Based Model [26] version of the SIR model is introduced. The population is represented by individuals which can interact, but the health conditions are defined by a few states. This allows us to better understand the pandemic dynamics.

## 2. Materials and Methods

### *The Model*

In the present paper, we simulate a version of the SIR model [25] in a city with a population  $N(t)$  that may vary over time. Many variants of SIR model were used to simulate different scenarios of the SARS-CoV-2 pandemic [27–29]. However, to have a better understanding of how cities’ structures and citizen dynamics affect the spreading of a transmissible disease such as SARS-CoV-2, we chose to develop an ABM-SIR (Agent-Based Model) [30–33] of a “city” in which citizens start to become infected.

The city represents a geographically limited region in which only the arrival and departure of visitors and the deaths of its inhabitants can change its population. As in the previous versions of the SIR model, a  $S_i$  variable defines the health state of each individual: susceptible ( $S_i = 0$ ), infected ( $S_i = 1$ ), and recovered or immunized ( $S_i = 2$ ). In this work, we have included a fourth state: dead ( $S_i = 3$ ). Factors such as age, sex, or race are not considered.

In the simulated city, the residents live in houses, and they can move to public establishments (e.g., such as malls, stadiums, stores, restaurants, etc.). In some simulations, people can move to other people’s houses. The day starts with all the residents in their homes, to which they will be linked throughout the simulation. That is, if they leave for another home or any establishment, at the end of the day, they will return to their own home. Each person has a probability of movement  $P_{mov}$ , and this probability defines the social isolation mobility.

There is no natural movement, and to go from one location to the next takes zero time. The agents disappear from a place and reappear in another. We considered that the time of permanence in public or private places is longer than the travel time. On the other hand, for big cities, one can suppose that the time they stay in a mode of public transport, if prolonged, may also be considered as staying in a small public place with the same infection conditions.

Every public area has a carrying capacity of  $K$ , so that  $\sum K_i = N_0$ , that is, the city allows all of its residents to leave at the same time. There are several public areas with different  $K_i = \{10, 000, 1, 000, 100, 50\}$ , so that the sum of the capacity of each area of the same type is equal to  $0.25 N_0$ . The number of places of a specific kind  $i$  is the total number of individuals they can support divided by its  $K_i$ . Thus, the number of sites that support fewer people is higher than those which support more people: in other words, there are more smaller stores than big stadiums. When individuals can move to other people's houses, we define a carrying capacity of 12 individuals.

The time scale of our simulations is one day. For each day, individuals are chosen at random, among the number of alive people on that day. A resident can either not be drawn or could be drawn more than once. After this, we test if they will move, with the probability given by  $P_{\text{mov}}$ . Each individual may visit other places a maximum of three times during the day. If a person is going to move, the places to which they will go are chosen at random: houses, small shops, or large stores. Its maximum capacity gives the likelihood of going to a location: they are more likely to go to a large store than to someone else's home. If a selected place reaches its capacity, a new site is drawn until the person moves, ensuring that whoever was chosen to move will make a move. COVID-19 has a high transmissibility during the pre-illness period, and the model assumed seven days of transmission before causing any disease, which was estimated by the pandemic for previous variants and the Delta variant. The mobility defined in the model emphasizes the transmissibility by pre-symptomatic and asymptomatic individuals, as no constraint on the movement of an infected person is imposed until someone dies [34–36].

The person arriving at a new location may be in one of three states: susceptible, infected, or immunized. If the person is vulnerable, it is verified if there is someone infected at that location. If not, the person stays there until they move again or until they return home at the end of the day. However, if there is an infected person(s) at that location, first, we calculate the probability of contact with the infected person, given by:

$$P_{\text{contact}} = \frac{N_{\text{infected}}}{N_{\text{max}}} \quad (1)$$

where  $N_{\text{infected}}$  is the total number of infected persons at that place (house or mall) and  $N_{\text{max}}$  is the maximum capacity of that place.

Two steps define the infection of a susceptible person: first, we calculate if they come into contact with a contaminated person. If so, we test if they will contract the virus, as contact does not imply infection. The probability of infection is  $\beta$ . In the case of COVID-19,  $\beta$  is estimated between [0.2, 0.3]. In the cases simulated in this work, we use a value of  $\beta = 0.2$  for a "normal" variant and we assume  $\beta > 0.2$  for more transmissible variants [37].

The probability of becoming infected with one of the variants present in that location is proportional to how often that variant is in that location, weighted by the transmissibility of the strain. The higher the  $n_i \times \beta_i$ , the higher the probability of being infected, where  $n_i$  is the total number of individuals infected by the strain  $\beta_i$  at that location. The infected individual then becomes a potential transmitter of the disease.

If an individual who arrives at a place is infected or immunized ( $S_i = 1$  or  $2$ ), nothing happens to those who are already at that place. The arrival of an infected person will create the conditions for those who arrive later to be infected. Hence, there is an asymmetry in the model. If an infected person arrives at a place, we do not test if they will infect the susceptible ones already there. This kind of procedure corresponds to a sequential order in the contact/contagion process. It is understood that for huge populations and many days of simulation, the results will not be different from those here reported.

At the end of the day, after performing some movements, all individuals return to their homes. Of course, if they have not moved, nothing is tested. However, for those who return to their home, the same set of procedures to check for infection is adopted: If the person returning home is susceptible, and someone infected is in the house, the same steps described above are carried out for contact and contagion.

The dynamics can be summarized as follows: To each individual  $i$  is assigned a variable  $S_i$  that can be in four states: susceptible (0); infected (1); recovered or immunized (2); and dead (3). The entire population starts the simulation as susceptible:  $S_i = 0$ . A single person among the residents is infected at  $t = 0$  with the less lethal variant  $\beta = 0.2$ . The dynamics is given by the process shown in Figure 1.

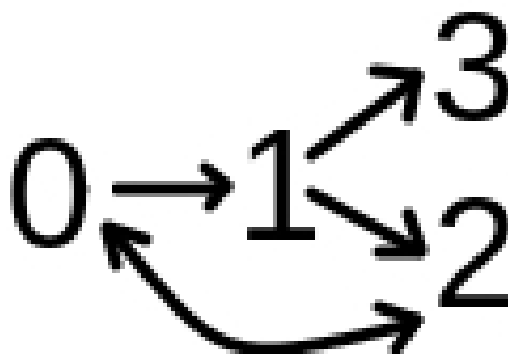


**Figure 1.** Schematic representation of transitions between states in our model. Probabilities are discussed in the text.

The figure represents the possible changes of state. A susceptible individual  $S_i = 0$  can become infected  $S_i = 1$  with the probability given by  $P_{\text{contact}} \times \beta_i$ .  $\beta_i$  is the transmission rate of an individual which contaminates a susceptible individual, as described above. An infected individual  $S_i = 1$  can die  $S_i = 3$  if their time of infection is greater than 7 days and with probability of death given by  $P_{\text{death}}$ . In case of contamination with the most lethal variant  $\beta + \delta\beta$ , the value of  $P_{\text{death}}$  is increased by  $\delta_{\text{death}}$ . This antagonism creates a tension between the strain's lethality and the individual's probability of death. That is, hosts with a more lethal variant are more likely to die.

The state of infection in an individual remains for a maximum of  $1/\gamma = 14$  days. It is assumed that the potential for infecting another person does not change during this period. It depends only on the  $\beta$  value, which does not change for a contaminated individual.

We have also simulated the case of incubation. In this case, the susceptible individuals become infected after five days of incubation.

After  $1/\gamma$  days, the infected individual,  $S_i = 1$ , either recovers or is immunized,  $S_i = 2$ . After  $T$  days, the immunized individual,  $S_i = 2$ , returns to the susceptible condition,  $S_i = 0$ . In the case of a vaccination program in that community, a susceptible or infected individual, either  $S_i = 0$  or  $S_i = 1$ , can be immunized with probability  $P_{\text{vac}}$ . This probability is related to the vaccination rate, which is the percentage of the total population that is vaccinated every day after the campaign started. The status of a vaccinated individual becomes  $S_i = 2$ . Similar to the recovered one, the immunization protects an individual for  $T$  days. During this period, they cannot be infected with any variant of the new coronavirus [38,39].

In our simulations, vaccination starts from the 300th day. This date roughly corresponds to the beginning of vaccination campaigns in several countries: between December/2020 and January/2021, considering the detection of the pandemic as time zero (around February or March 2020). There is no need to use two doses or intervals between doses of the vaccine to gain immunity. In this simplified version of the model, immunity is acquired at the time of vaccination. Although it is possible that vaccinated individuals can infect and transmit the virus, it happens more rarely or with lower intensity than with infected non-vaccinated individuals; thus, for sake of simplicity, in our model, vaccinated individuals did not get infected [40]. Due to its structure and complexity, we used the Brazilian vaccination numbers as reference. We performed simulations with two vaccination rates. Some simulations used a vaccination probability of  $P_{\text{vac}} = 1/200$ , representing the typical value of vaccination campaigns in Brazil, when close to 1 million people are vaccinated per day. Brazil has a public health system formed by about 40 thousand health

centers, belonging to three levels of administration, but forming a cooperative network. This system has vast experience on vaccination campaigns and can easily reach a rate of 1 million vaccinations per day, roughly 1/200. The second value we have tested is a rate of 1/1000, which represents the values that we have observed for the vaccination against COVID-19 in the first two months of vaccination, close to 200 to 300 thousand people per day. From 23 January 2021 to 29 March 2021, 14 million people received the first dose of one of the two available vaccines. In Brazil, the vaccines that were used were those that required two doses. The vaccination rate increased in April but then oscillated, since Brazil had no plan of vaccine acquisition. In the USA, the vaccination rate reached 0.006 of the whole population in March. By the beginning of March, Israel had already vaccinated practically its entire population of around 9 million people.

Our model assumes that visitors arrive and leave the city every day. The number of visitors coming and leaving each day is around 1/1000 of the total residents. These visitors have a probability of movement equal to 1. This means that a visitor will go to three places (houses, small shops, or large stores). The likelihood of a visitor being infected is 0.1%. In principle, if infected, they will have the virus variant  $\beta = 0.2$ , but some can have a more transmissible variant. We have implemented a version in which visitors are 1% of the population. Of the visitors, 3% may have the new, more transmissible type of virus.

If that visitor is susceptible, they may become infected during the day and transmit the infection. However, as they only spend one day in the city, they will not be subject to death, nor will they be able to recover. They will also not be vaccinated.

In this model, there are no births. There is no increase in the number of inhabitants, except the increase caused by visitors, which represents a zero change in the population, as visitors only arrive and leave. The only factor that can change the resident population is death caused by disease. We study the effects of a new variant of the virus, which enters via visitors, studying the competition dynamics between different strains. Moreover, we also want to study the effects of vaccination, not considering other variables. A local variant is not supposed to mutate.

We show the results with two versions of the model: in the first one, we simulate a city with houses and small and big stores, where the visitors may carry just one virus variant with higher transmissibility. Residents can move to other residents' houses. In the second version, the towns have homes and just one type of store, and the visitors carry many virus variants (described below).

We studied the effects of vaccination only in the first version of the model. The central aspect of the first version is to look at the spread of a higher transmissibility strain with vaccination. In addition, we used real COVID-19 cases and vaccination strategies from two populations in similar countries, i.e., Portugal and Israel, to validate our mathematically based conclusions. The second version aims to study the competition between different strains, and thus, the natural evolution of the pandemic without vaccination. In both cases, we consider that variants with different transmissibility also have different lethality.

In this work, as usual in computer simulations, we assumed some simplifications and assumptions in order to optimize the model, and to capture the most significant possibilities according to some objectives. One of these simplifications is the absence of traffic and commuting, i.e., the time required for displacement. The introduction of a transportation network could improve the model, and is likely to bring new features to the study. Another limitation of our work is the population structure. In our "city" model, the population does not have any age or gender structure. For COVID-19, it is known that the response to infection can vary depending on the infected age; thus, the use of an age-structure AMB-SIR model also could bring more realism to the simulation. Finally, our work assumes that all variants are affected equally by vaccinations, which does not reflect the real-life situation. Thus, adding different responses to the vaccine-variant interaction could strongly improve the model. Similar to other models, as we have discussed, we tried to shed some light on the main effects of the dynamics. On the other hand, the assumptions we made in order to allow a feasible but simplified model to run expectations of the effects caused by

an effective vaccination program allowed us to test the difference between having or not having an effective vaccination program in an open-to-migration city during an evolving pandemic. Thus, our model considered a successional dynamic of variants with distinct life traits. Even the simplifications we assumed did not undermine the effectiveness of vaccines, considering we built up a more vulnerable society (where everybody was equally susceptible) combined with realistic combinations of lethal-transmissible variants.

### 3. Results

#### 3.1. Model with Two Strains

The first set of results were obtained in simulations of cities with two populations:  $N \sim 875$  thousand residents and  $N \sim 8.75$  million residents. In the first case, they live in 250 thousand households. When allocating people, it was decided that a house had 3 or 4 residents; thus, there were 3.5 residents on average per household [41]. These residents can move to 20,000 stores with a maximum capacity of 50 people or 2000 establishments which support 500 people. The houses, small shops and big shops can accommodate all citizens, which means that there is enough space for all people to move to any location.

In the simulations described below, values of  $P_{\text{mov}} = 0.6, 0.5,$  or  $0.3$  were adopted, meaning an average isolation of 40%, 50%, and 70%. In the case of Brazil, the average isolation, measured while individuals stay in their homes for a day, has fluctuated between 30% to 40%, and on weekends, it can reach 50%. It increased a little in February and March 2021 due to the imposition of new measures of restriction and operation of the establishments. At the beginning of the pandemic, in March 2020, there were higher values in Brazil, in the range of 60%.

For each day, individuals are chosen at random, as described above. It was verified if they were going to leave the house. If so, we drew the total number of moves they would make: 1 up to 3. Then, we randomly chose the places for visitation: other houses or small or large stores. Then, they left the house and went to each establishment. Each person executed their movements, and after completing them, stayed at the last site until they returned home at the end of the day.

In all the simulations discussed below, 10% of the population had a probability of movement of  $P_{\text{mov}} = 0.1$ , representing the people who were most often at home. As described above, visitors would come and go. We assumed a proportion of visitors of 0.1% of the total initial population per day. The people who arrived and left remained in the city for only one day. A ratio of 1/1000 may be contaminated. The contamination strain had  $\beta = 0.2$ . In total, 1/90 of the contaminated individuals had a more lethal variant, with  $\beta = 0.25$ . Visitors had a probability of movement equal to 1.0 and always visited three locations (drawn at random, as described above).

In the results shown below,  $P_{\text{contact}}$  is given by Equation (1),  $\beta = 0.2$ ,  $\delta\beta = 0.05$ ,  $P_{\text{death}} = 0.01$ ,  $\delta_{\text{death}} = 0.004$ ,  $1/\gamma = 14$ , and  $T = 120$  days.

On the simulation's 300th day, a vaccination campaign could start. Figure 2 represents the evolution of a population with 40% of social isolation,  $P_{\text{mov}} = 0.6$ , without vaccination. The values represent the densities relative to the initial number of residents, in this case, 874,975 people. There is an oscillating evolution of the numbers caused by the ongoing entry of infected individuals: the visitors. The curve called  $\beta_{\text{av}}$  represents the average value of  $\beta$  taken among all individuals with  $S = 1$ . It is observed that in the peaks of infection, the most lethal variant tends to dominate. The decrease in the infected population is typical of the SIR model, but the permanence of the most lethal variant is an important characteristic. The number of individuals who died is in the order of 10% of the original population. Certainly, this is a very high number when compared to real data. This model and the simulations do not intend to project expected values, but they represent the dynamics of disseminating the most lethal variant qualitatively.

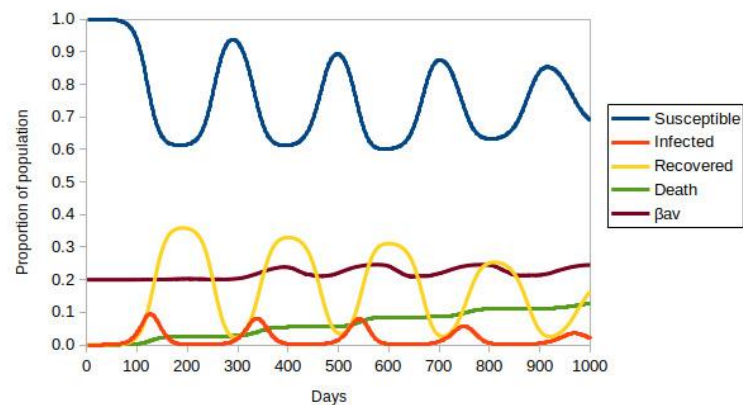
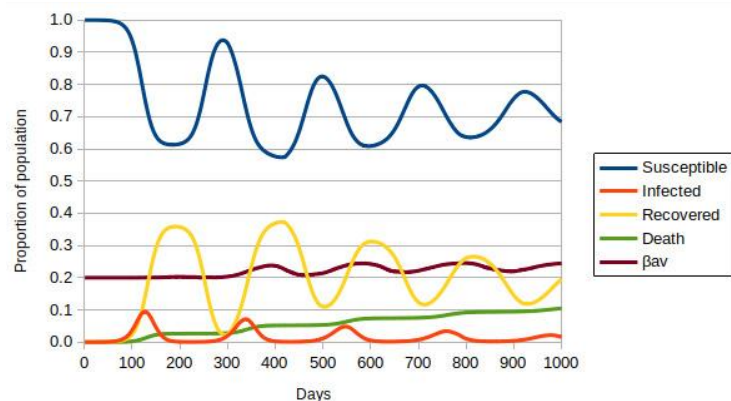


**Figure 2.** ABM-SIR dynamic of COVID-19 (i.e., Susceptible-Infected-Recovered Agent-Based model) evolution over 1000 days with a social isolation of 40%, adjusted for the initial population of  $\sim 8.75 \times 10^5$  individuals. There is no vaccination. Each color represents a population group, defined in the legend. The value of  $\beta_{av}$  is the average for all infected people.

Figure S1 shows the percentage of people dying each day (blue line) and the percentage of people who died due to the most lethal variant (red line). The results were obtained from the simulation described above. One can observe that the number of people who die each day increases in the periods of infection. However, the quantity of those who die from the new variant rises more rapidly, becoming  $\sim 50\%$  at the end of the simulation.

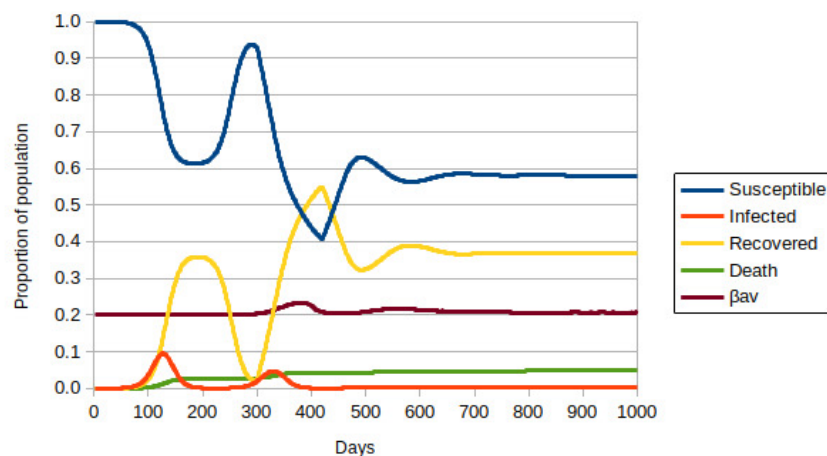
Change in this kind of dramatic evolution is only achieved when social isolation is about 70%, without vaccination. Figure S2 shows a simulation obtained with the previous parameters, but now with  $P_{mov} = 0.3$ . In this case, the susceptible population remains basically between 0.95 and 1, the density to the original number of residents. Infected people cannot contaminate significant fractions of the population, and the infection stops.

Figure 3 shows the result obtained with vaccination at a rate of 1/1000, with a probability of movement of 60% corresponding to a social isolation of 40%, the peak value currently in Brazil. The numbers of infected and the progression of the pandemic do not stop. The numbers of deaths and the spread of the most lethal variant follow the patterns observed previously. This happens because the rate of vaccination, that is, the transition from susceptible and infected to immunized, is low compared to the rate of change from vaccinated to susceptible. Note that the time for this transition is  $T = 120$  days, meaning four months on our time scale.



**Figure 3.** ABM-SIR dynamic of COVID-19 (i.e., Susceptible-Infected-Recovered Agent-Based model) evolution over 1000 days for social isolation of 40%, adjusted for the initial population of  $\sim 8.75 \times 10^5$  individuals. Each color represents a population group, defined in the legend. The value of  $\beta_{av}$  is the average for all infected people. The vaccination rate is 1/1000 of susceptible or recovered individuals per day.

When the immunization rate assumes a value of  $1/200$ , the picture changes radically, as shown in Figure 4. Vaccination started on day 300 of the simulation. One can observe a second wave of infections because the virus is widespread in the population. However, the number of immunized people increases rapidly, which is a blocking factor for the spread of the pandemic. One can also observe that the most lethal variant is contained, as the value of  $\beta_{av}$  is closer to 0.2. It is important to remember that the rate of contaminated visitors is the same in the three cases discussed so far. The number of deaths also stabilizes with the blockade caused by vaccination.



**Figure 4.** ABM-SIR dynamic of COVID-19 (i.e., Susceptible-Infected-Recovered Agent-Based model) evolution over 1000 days for social isolation of 40%, adjusted for the initial population of  $\sim 8.75 \times 10^5$  individuals. Each color represents a population group, defined in the legend. The value of  $\beta_{av}$  is the average for all infected people. The vaccination rate is  $1/200$  of susceptible or recovered individuals per day.

Figure S3 reproduces the relationship between daily deaths and the presence of the most lethal variant. This variant is still present in the second wave but with a smaller percentage than in Figure S1. Later, this variant becomes marginal. It is necessary to remember that this most lethal variant enters the population from the visitors, and therefore, in this model, this variant will always be present.

In summary, we show that there is a dynamic relating the number of infected people to isolation and vaccination rates. Without vaccination, we observe that only with an isolation rate of 70% the pandemic is stopped. On the other hand, when the vaccination rate is  $1/1000$ , a small value, it is observed that there is no significant impact on infection dynamics. Only with a higher vaccination rate, as in the cases of Chile or Portugal, can the pandemic be stopped, even with lower isolation rates.

To better understand the influence of the city size, the number of individuals, as well as the period of immunization after vaccination, we performed simulations with  $N = 8.75$  million individuals and  $T = 180$  days, meaning that a recovered or immunized stays in the  $S = 2$  state for six months.

All the parameters are the same as those used in the simulations described above:  $P_{mov} = 0.6$ ;  $\beta = 0.2$  for residents; number of visitors,  $1/1000$ ; contaminated visitors,  $1/1000$ ; contaminated visitors with the highest transmissibility rate,  $1/90$ . Vaccination, when it occurs, starts on the 300th day.

Qualitatively, the behavior observed in the curves is the same as discussed above for populations that are ten times smaller. Notice that the change in the immunization period  $T$  does not change the evolution of successive waves for the cases without vaccination or with a low vaccination rate.

Figure 5 shows the evolution of cases and vaccination of two countries with approximately the same population, Israel and Portugal [42]. It is clear how the difference in the vaccination policy adopted in those two countries has shaped the cases curve. Both

countries started their vaccination around the same period (12/2020). However, the rate of vaccination was completely different. Israel started at a high rate, but it faded around three months later, while Portugal kept an increasing rate. The impact in the cases can be seen in the last peak caused by the Delta variant in the last months of 2021, which was much stronger in Israel than Portugal. The huge increase of cases on the right of both plots (early 2022) are due to the spread of Omicron, which is not affected by vaccination.

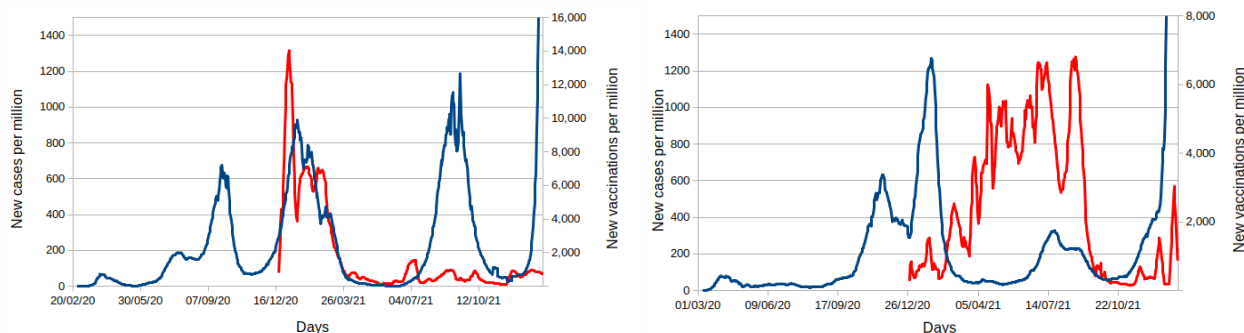


**Figure 5.** Real data for new cases (blue line) and new vaccinations (red line) for Israel (left plot) and Portugal (right plot). All curves are standardized per million and are not cumulative.

### 3.2. Model with Many Strains

We have implemented a second version of the model where residents can move only to public places. We have considered a more significant number of visitors who can bring different variants of the virus. In this version, for each instant of time (day), residents leave their houses with a probability that defines social isolation. They stay at home or move to public areas, making one or two movements per day. We simulated the initial isolation of 45% as default. In this second model, the flux of visitors is 1% of the total population, but infected visitors are 3% of the total number of visitors. All the other parameters are the same as the original model.

The objective of the second version of our model is to simulate how different strains compete among themselves in an epidemic scenario. This is achieved in the following way: the simulation starts with just one type of variant (called variant 1); after 5% of the population gets infected, four other variants (2, 3, 4, and 5) are introduced via infected visitors. These variants have different contagion and mortality probabilities, as can be seen in Table 1. It shows that, compared with the original strain, we have a combination of 70% and 50% more and less contagious and lethal variants, respectively.

**Table 1.** Contagion ( $\beta$ ) and lethality of the original and variant strains used in the second model.

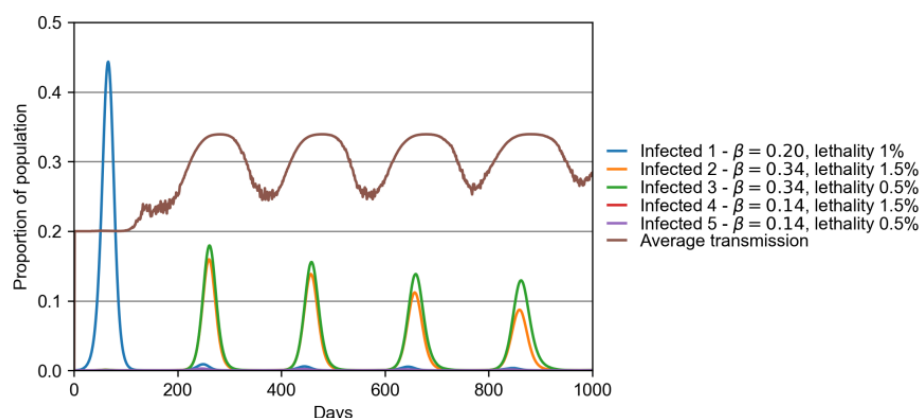
Variant	$\beta$	Lethality (%)
1 (original)	0.2	1.0
2	$1.7 \times 0.2$	1.5
3	$1.7 \times 0.2$	0.5
4	$0.7 \times 0.2$	1.5
5	$0.7 \times 0.2$	0.5

Figure S4 shows the evolution in a simulated city with a population of 1 million, with 45% of social distancing, and a more contagious variant introduced via visitors. The result shows the waves of infection caused mostly by loss of immunity after 120 days in a similar way to the results of the first model without vaccination.

The competition among different variants can be better viewed in Figure 6. This plot shows, for the same parameters of the previous plot, how the different strains are present in the population over time. It can be seen how the original strain causes a peak of  $\sim 45\%$  of people infected in a first wave around day 80. However, once the four new variants are introduced in the system, the following waves show that the original variant is rapidly



replaced by the two most transmissible ones (variants 2 and 3 of Table 1). Since the second wave (starting between days 200 and 300), the simulation shows a dominance of variant 3 (more transmissible, less lethal), followed by variant 2 (more transmissible, more lethal), until finally, the original variant is barely present. This plot shows two important results: (A) the new variants with less transmissibility than the original strain (variants 4 and 5) are not able to invade the city, while the more transmissible variants substituted the original one from the second wave on; (B) interestingly, the lesser lethal variant overcame the more lethal one in all the waves, which is expected for a long-term evolution of an emergent disease if the lack of host illness favors transmission, and thus, loss of virulence [43,44]. Due to the full shifting of the original strain by new variants, the  $\beta$ -infection rate was permanently higher after the second wave than it was at the beginning of the pandemics, as shown by the average transmission in Figure 6.



**Figure 6.** Presence of virus in population, same scenario of Figure S4. This plot show how rapidly infection caused by variants 2 and 3 overcome the original one from the second wave.

#### 4. Discussion

The majority of papers modeling vaccination strategies are likely to fit in three categories: (1) extrapolation or estimation using real epidemiological data, for example [45], (2) compartmental models (SIR, SEIR, etc.), based on differential equations and epidemiological quantities defined as density of states (susceptible, infected, recovered, etc.), as in [46–48], and (3) Agent-Based Models (ABM) [32,49], which can be defined as an epidemic dynamic that takes place in a discrete way, with host/people as individualized entities of action, called “agents”. Models in family (2) have variables defined in a continuum and, thus, there is no “person” or “agent”, while in (3), ABM models are more versatile to describe a population where a set of characteristics must be considered, for example, age structure, topological distribution, and all kinds of spatial and temporal data.

Models based on estimates taken from real data can be useful if high-quality data are available, with good extrapolations as a response to a very specific scenario. However, such models fail in exploring multiple parameters and “what if” questions. Compartmental models compose the majority of the publications and are very powerful tools. Although SIR models can deliver similar results as ABM, they are not as versatile as ABM models. As the ABM dynamic does not rely in differential equations, any change in the model can be done in a punctual way, only changing the agent parameters. Generally speaking, compartmental models are used in more generalist problems, while ABM appear to model real places.

Our model is a hybrid ABM-SIR, meaning it has a base structure of agents while the infection logic follows the SIR model. Using agents, our model was capable to sustain a population that moves in an independent way, while this same population could have citizens in different epidemiological states, stages, and places. This construct made it possible, with few modifications, to find out the optimum vaccination rate, as seen in Figure 4, and the competition among many variants in Figure 6. Our group proposed this

novel hybrid model to compare the Spanish Flu with COVID-19 dynamics in the Brazilian city of Manaus [20].

After some waves of infections of COVID-19, the world is facing a new challenge. By the end of January 2022, 61% of the world population received at least one dose of the COVID-19 vaccine out of a total of 10.06 billion doses administered globally [50]. However, only 10% of people from low-income countries were vaccinated with one dose at that date. Even in largely vaccinated countries with severe inequalities, such as Brazil, there were areas with low vaccine coverage [51]. Additionally, vaccine hesitance and rejection spread in the developed world due to misinformation. Consequently, countries with a larger availability of vaccines and an early vaccinal program, such as the US and Germany, had a smaller proportion of overall vaccinated people by end of January 2022 than Brazil and Argentina, for instance, where anti-vax movements are irrelevant. Brazil and France vaccinated proportionally the same at this date, but France presented a more significant resistance against it, as in contrast to Brazil, the absolute availability of vaccines in France was higher for both adults and children [50]. Although it is a global problem, vaccine refusal has been properly studied mostly in the US [52–55]. Both vaccine inequality and hesitancy are likely to cause the spread of new variants [56]. Vaccination slowed down and this may cause the present situation [57,58]. In Israel, a new wave has been observed. However, since they have a high vaccination rate, the number of deaths is smaller than in the previous wave [59]. Brazil presents a different situation. The country started vaccination at a low rate, due to the delay to acquire vaccines from the federal government [60,61]. However, there was a strong engagement of the population and, after public pressure and the action of political sectors, the rates of vaccination increased in the second semester of 2021. The number of contaminated and dead people plateaued during the first months of 2021, but declined due to the increase in the vaccination rate. Different scenarios can be observed in different countries. However, they are a product of the spread of new variants and the vaccination of the population.

In this paper, we simulated the competition between virus strains, the role of the vaccination rate, and social isolation, which are believed as one of the main aspects to detain the virus's circulation. In many countries, such as Brazil, it is very complicated to maintain social isolation for long periods. For instance, we observed, in parts of the population, stress among children out of schools, increase in domestic violence, and difficulties for individuals to obtain a basic income to sustain their families [62–64]. Poverty increased in many countries. In the case of Brazil, social isolation never reached adequate or recommended levels, which was responsible for the long plateau of infections and deaths.

Thus, we show that the only way to stop the circulation of the virus, or at least to diminish the contamination rates, is to increase the vaccination rates despite the current vaccination hesitancy and challenges to mass vaccination. Low vaccination rates allow the circulation of the many variants, and we observed a cyclic problem. The situation gains a much more dramatic feature with the existence of new variants with a higher transmissibility.

The many different variants will compete and those with higher transmissibility will win this competition, even in cases of combined higher lethality. This picture was observed anywhere the  $\delta$  variant appeared. This variant rapidly infected people, even those already vaccinated, and caused a higher increase in contamination [65]. Thus, it brought humanity back to the beginning of the pandemic, struggling to flatten the infection curve, as even non-lethal new variants can overload health systems.

In a world where “vaccine nationalism” (i.e., governments supply the population of their countries with vaccines ahead of them becoming available to other countries) prevailed once more, the pandemic might find its way towards a natural evolution in those less vaccinated corners [66]. Our mathematical model was built considering a continuous immunization, with a single dose, and with a regular immunization rate in a scenario with no vaccine shortage. In addition, our mathematical model considered that vaccination was able to generate a four-month temporary immunity with only one dose, so immunization

and booster doses every six months were not included for the calculations that we propose in this work. However, it is important to consider that the emergence of the Delta and now Omicron variant further reinforces the importance of access to COVID-19 vaccines, globally and equitably, for the health of all [67]. Constrained vaccine supply has driven opportunities for SARS-CoV-2 to mutate and be more infectious.

The emergence of Omicron has emphasized that further delay in widely delivering at least the first two doses is fraught with peril for all [68]. On the other hand, our model reinforces the need to plan more strategic and specific vaccination schedules, to review current vaccines, and to design vaccines with the ability to prevent infection. The current vaccines have been overtaken by variants of concern and strains that can escape the protection given by the vaccine, despite maintaining protection against hospitalization and deaths. Nonetheless, we agree with the recommendation that in countries with a high prevalence of previous infections and a low proportion of over-60-year-old people, prioritizing delivering the first dose will have the greatest effect on preventing severe COVID-19 cases due to high vulnerability [69,70]. Conversely, in countries with a low prevalence of previous infections and a high proportion of old people, protection against severe disease in adults requires at least two doses, as well as booster doses in people who are severely immunocompromised or older than 60 years. Evidence suggests that although booster doses for all adults might prevent severe diseases, it could also compromise timely global availability of first doses [36].

Vaccination, more than natural infection, in addition to inducing the production of neutralizing antibodies, establishes a cellular immune response by activating memory T cells, which leads to a favorable clinical outcome and considerably reduces the number of deaths [71,72]. The most recent data have clearly shown that 70% of ICU admissions in European countries, the USA, and even in Latin America (Brazil) are people who have either not been vaccinated or who have not had two or three complete vaccine doses [73]. Finally, vaccination changes the dynamics, as it reduces the time of infection in vaccinated individuals and, consequently, interferes with the dynamics of the virus in the human body, preventing serious, long-term infections and, consequently, reducing the risks of new variants [74]. The existence of countries with low vaccination coverage is worrying, as in some European countries and several others African countries [75]. Particularly for some African countries, there is still a concern about the number of HIV+ and, thus, immune suppressed people without access to treatment, which may become sources for the emergence of new variants [76,77].

The Omicron strain, detected by the end of 2021, in South Africa, might fit the most consistent theoretical prediction: evolution of virulence loss [78]. This strain is amazingly contagious, spreading in a substantially faster rate than even the Delta strain, but which, as first evidence suggest, causes mainly mild symptoms, and may open the path for wide non-lethal dissemination [79]. Such a variant, if it indeed appears with these specific traits, might, and already has, overcome numerically any other, as Delta did before. However, the theoretical prediction of an emergent disease may not help lower the human and social costs. For instance, what level of hospitalization will be required with a too fast spreading strain, even if it is not lethal? Moreover, what sort of sequelae will it leave, increasing the public health cost of so-called long COVID syndrome?

## 5. Conclusions

The sudden disappearance of historic viral pandemic events might all have followed the path of natural selection favoring transmissibility against lethality, but there is a catch with SARS-CoV-2. Because transmissibility is high before symptoms, the positive selection based on losing lethality is weaker than it was, for instance, for Spanish Flu [20]. Even though natural loss of lethality may happen to a strain rapidly spreading worldwide, other strains may also appear in many places with non-fully vaccinated individuals and in places which are less internationally connected. There is, likewise, no impediment for new mutants which transmit fast and are still lethal. Hence, outbreaks of more virulent strains

may keep surging for decades, according to our previous and present models [2,20]. The most relevant fact is that a planet of nearly eight billion people should not allow the luxury of leaving a pandemic to evolve widely.

The main purpose of this paper is to shed some light on the main aspects of the actual dynamics of the pandemic. A global governance is needed to deal with the immunization process, as the pandemic dynamics exhibits successive peaks with a distance of about 4 months between them. Without global control, new variants will continue to appear and when the infection is partially controlled in one country or region, but increases in other parts, a dramatic cyclic wheel of death may prevail.

**Supplementary Materials:** The following are available online at <https://www.mdpi.com/article/10.3390/vaccines10030343/s1>, Figure S1: ABM-SIR dynamic of COVID-19 evolution over 1000 days, adjusted for the initial population of  $\sim 8.75 \times 10^5$  individuals. Only the proportion of new dead individuals is shown, represented by the blue line. The proportion of those who died by the most lethal variant is represented by the red line; Figure S2: ABM-SIR dynamic of COVID-19 evolution over 1000 days with 70% of social isolation, adjusted for the initial population of  $\sim 8.75 \times 10^5$  individuals, without vaccination. Each color represents a population group, defined in the legend. The value of  $\beta_{av}$  is the average for all infected people; Figure S3: ABM-SIR dynamic of COVID-19 evolution over 1000 days with 40% of social isolation, adjusted for the initial population of  $\sim 8.75 \times 10^5$  individuals. Only the proportion of new dead individuals is shown, represented by the blue line. The proportion of those who died by the most lethal variant is represented by the red line. The vaccination rate is 1/200 of susceptible or recovered individuals per day; Figure S4: ABM-SIR dynamic of COVID-19 evolution over 1000 days, adjusted for the initial population of 1 M, with variants entering via visitors. The social distancing is 45%. The values of  $\beta$  and mortality for infected individuals can be seen in Table S1. In this scenario, all recovered individuals lost their immunity after 120 days; Code 1: Code-C++; Code 2: Code-Fortran95.

**Author Contributions:** Conceptualization, A.C.eS., A.T.B., W.D., and S.P.R.; Formal analysis, A.C.eS., A.T.B., W.D., A.B.R., and S.P.R.; Funding acquisition, S.P.R.; Investigation, A.C.eS., A.T.B., W.D., and S.P.R.; Methodology, A.C.eS., A.T.B., and S.P.R.; Software, A.C.eS., A.T.B., and E.A.G.B.; Supervision, A.C.eS., A.T.B., W.D., and S.P.R.; Writing—original draft, A.C.eS. and A.T.B.; Writing—review and editing, I.A.S.d.C., W.D., A.B.R., and S.P.R. All authors have read and agreed to the published version of the manuscript.

**Funding:** This research received no external funding.

**Data Availability Statement:** The codes of the model are available at Supplementary Material.

**Acknowledgments:** S.P.R. acknowledges a grant from the Conselho Nacional de Desenvolvimento Científico e Tecnológico—CNPq, through process 306572/2019-2. A.B.R. acknowledges productivity fund 1B/CNPq. I.A.S.d.C. acknowledges master degree scholarship by Capes/Brazil.

**Conflicts of Interest:** The authors declare no conflict of interest.

## References

1. Ribeiro, S.P.; Castro e Silva, A.; Dáttilo, W.; Reis, A.B.; Góes-Neto, A.; Alcantara, L.C.J.; Giovanetti, M.; Coura-Vital, W.; Fernandes, G.W.; Azevedo, V.A.C. Severe airport sanitarian control could slow down the spreading of COVID-19 pandemics in Brazil. *PeerJ* **2020**, *8*, e9446. [CrossRef] [PubMed]
2. Ribeiro, S.P.; Dáttilo, W.; Barbosa, D.S.; Coura-Vital, W.; Das Chagas, I.A.S.; Dias, C.P.; Silva, A.V.C.D.C.E.; Morais, M.H.F.; Góes-Neto, A.; Azevedo, V.A.C.; et al. Worldwide COVID-19 spreading explained: Traveling numbers as a primary driver for the pandemic. *An. Acad. Bras. Cienc.* **2020**, *92*, 1–10. [CrossRef] [PubMed]
3. Coelho, M.T.P.; Rodrigues, J.F.M.; Medina, A.M.; Scalco, P.; Terribile, L.C.; Vilela, B.; Diniz-Filho, J.A.F.; Dobrovolski, R. Global expansion of COVID-19 pandemic is driven by population size and airport connections. *PeerJ* **2020**, *8*, e9708. [CrossRef]
4. COVID-19 Dashboard by the Center for Systems Science and Engineering (CSSE) at Johns Hopkins University (JHU). Available online: <https://coronavirus.jhu.edu/map.html> (accessed on 20 November 2021).
5. Tkachenko, A.V.; Maslov, S.; Elbanna, A.; Wong, G.N.; Weiner, Z.J.; Goldenfeld, N. Time-dependent heterogeneity leads to transient suppression of the COVID-19 epidemic, not herd immunity. *Proc. Natl. Acad. Sci. USA* **2021**, *118*, e2015972118. [CrossRef] [PubMed]
6. Sanjuán, R.; Domingo-Calap, P. Mechanisms of viral mutation. *Cell. Mol. Life Sci.* **2016**, *73*, 4433–4448. [CrossRef]

7. Latinne, A.; Hu, B.; Olival, K.J.; Zhu, G.; Zhang, L.; Li, H.; Chmura, A.A.; Field, H.E.; Zambrana-Torrel, C.; Epstein, J.H.; et al. Origin and cross-species transmission of bat coronaviruses in China. *Nat. Commun.* **2020**, *11*, 4235. [[CrossRef](#)]
8. Pachetti, M.; Marini, B.; Benedetti, F.; Giudici, F.; Mauro, E.; Storici, P.; Masciovecchio, C.; Angeletti, S.; Ciccozzi, M.; Gallo, R.C.; et al. Emerging SARS-CoV-2 mutation hot spots include a novel RNA-dependent-RNA polymerase variant. *J. Transl. Med.* **2020**, *18*, 1–9. [[CrossRef](#)]
9. SARS-CoV-2 Variant Classifications and Definitions. Available online: <https://www.cdc.gov/coronavirus/2019-ncov/variants/variant-info.html> (accessed on 20 November 2021).
10. Du Plessis, L.; McCrone, J.T.; Zarebski, A.E.; Hill, V.; Ruis, C.; Gutierrez, B.; Raghwan, J.; Ashworth, J.; Colquhoun, R.; Connor, T.R.; et al. Establishment and lineage dynamics of the SARS-CoV-2 epidemic in the UK. *Science* **2021**, *371*, 708–712. [[CrossRef](#)]
11. Mohammadi, M.; Shayestehpour, M.; Mirzaei, H. The impact of spike mutated variants of SARS-CoV2 [Alpha, Beta, Gamma, Delta, and Lambda] on the efficacy of subunit recombinant vaccines. *Braz. J. Infect. Dis.* **2021**, *25*, 101606. [[CrossRef](#)]
12. Farinholt, T.; Doddapaneni, H.; Qin, X.; Menon, V.; Meng, Q.; Metcalf, G.; Chao, H.; Gingras, M.C.; Avadhanula, V.; Farinholt, P.; et al. Transmission event of SARS-CoV-2 delta variant reveals multiple vaccine breakthrough infections. *BMC Med.* **2021**, *19*, 255. [[CrossRef](#)]
13. Saito, A.; Irie, T.; Suzuki, R.; Maemura, T.; Nasser, H.; Uriu, K.; Kosugi, Y.; Shirakawa, K.; Sadamasu, K.; Kimura, I.; et al. Enhanced fusogenicity and pathogenicity of SARS-CoV-2 Delta P681R mutation. *Nature* **2021**, *9*, 1–7. [[CrossRef](#)] [[PubMed](#)]
14. Shuai, H.; Chan, J.F.W.; Hu, B.; Chai, Y.; Yuen, T.T.T.; Yin, F.; Huang, X.; Yoon, C.; Hu, J.C.; Liu, H.; et al. Attenuated replication and pathogenicity of SARS-CoV-2 B.1.1.529 Omicron. *Nature* **2022**. [[CrossRef](#)]
15. Halfmann, P.J.; Iida, S.; Iwatsuki-Horimoto, K.; Maemura, T.; Kiso, M.; Scheaffer, S.M.; Darling, T.L.; Joshi, A.; Loeber, S.; Singh, G.; et al. SARS-CoV-2 Omicron virus causes attenuated disease in mice and hamsters. *Nature* **2022**. [[CrossRef](#)] [[PubMed](#)]
16. Konings, F.; Perkins, M.D.; Kuhn, J.H.; Pallen, M.J.; Alm, E.J.; Archer, B.N.; Barakat, A.; Bedford, T.; Bhiman, J.N.; Caly, L.; et al. SARS-CoV-2 Variants of Interest and Concern naming scheme conducive for global discourse. *Nat. Microbiol.* **2021**, *6*, 821–823. [[CrossRef](#)] [[PubMed](#)]
17. Wang, Z.; Muecksch, F.; Schaefer-Babajew, D.; Finkin, S.; Viant, C.; Gaebler, C.; Hoffmann, H.H.; Barnes, C.O.; Cipolla, M.; Ramos, V.; et al. Naturally enhanced neutralizing breadth against SARS-CoV-2 one year after infection. *Nature* **2021**, *595*, 426–431. [[CrossRef](#)] [[PubMed](#)]
18. Turner, J.S.; Kim, W.; Kalaidina, E.; Goss, C.W.; Raueo, A.M.; Schmitz, A.J.; Hansen, L.; Haile, A.; Klebert, M.K.; Pusic, I.; et al. SARS-CoV-2 infection induces long-lived bone marrow plasma cells in humans. *Nature* **2021**, *595*, 421–425. [[CrossRef](#)]
19. Vitale, J.; Mumoli, N.; Clerici, P.; Paschale, M.; Evangelista, I.; Cei, M.; Mazzone, A. Assessment of SARS-CoV-2 Reinfection 1 Year After Primary Infection in a Population in Lombardy, Italy. *JAMA Intern. Med.* **2021**, *181*, 1407–1409. [[CrossRef](#)] [[PubMed](#)]
20. Ribeiro, S.P.; Reis, A.B.; Dáttilo, W.; Silva, A.V.C.D.C.E.; Barbosa, E.A.G.; Coura-Vital, W.; Góes-Neto, A.; Azevedo, V.A.C.; Fernandes, G.W. From Spanish Flu to Syndemic COVID-19: Long-standing sanitarian vulnerability of Manaus, warnings from the Brazilian rainforest gateway. *An. Acad. Bras. Cienc.* **2021**, *93*, 1–14. [[CrossRef](#)]
21. Sun, K.; Wang, W.; Gao, L.; Wang, Y.; Luo, K.; Ren, L.; Zhan, Z.; Chen, X.; Zhao, S.; Huang, Y.; et al. Transmission heterogeneities, kinetics, and controllability of SARS-CoV-2. *Science* **2021**, *371*, eabe2424. [[CrossRef](#)]
22. Chinazzi, M.; Davis, J.T.; Ajelli, M.; Gioannini, C.; Litvinova, M.; Merler, S.; Pastore y Piontti, A.; Mu, K.; Rossi, L.; Sun, K.; et al. The effect of travel restrictions on the spread of the 2019 novel coronavirus (COVID-19) outbreak. *Science* **2020**, *368*, 395–400. [[CrossRef](#)]
23. Liu, P.; Jiang, J.-Z.; Wan, X.-F.; Hua, Y.; Li, L.; Zhou, J.; Wang, X.; Hou, F.; Chen, J.; Zou, J.; et al. Are pangolins the intermediate host of the 2019 novel coronavirus (SARS-CoV-2)? *PLoS Pathog.* **2020**, *16*, e1008421. [[CrossRef](#)] [[PubMed](#)]
24. Interim Clinical Considerations for Use of COVID-19 Vaccines Currently Approved or Authorized in the United States. Available online: <https://www.cdc.gov/vaccines/covid-19/clinical-considerations/covid-19-vaccines-us.html> (accessed on 20 November 2021).
25. Kermack, W.O.; McKendrick, A.G. A contribution to the mathematical theory of epidemics. *Proc. R. Soc. Lond. A* **1927**, *115*, 700–721. [[CrossRef](#)]
26. Bonabeau, E. Agent-based modeling: Methods and techniques for simulating human systems. *Proc. Natl. Acad. Sci. USA* **2002**, *99*, 7280–7287. [[CrossRef](#)]
27. Chen, Y.-C.; Lu, P.-E.; Chang, C.-S.; Liu, T.-H. A Time-Dependent SIR Model for COVID-19 With Undetectable Infected Persons. *IEEE Trans. Netw. Sci. Eng.* **2020**, *7*, 3279–3294. [[CrossRef](#)]
28. Wangping, J.; Ke, H.; Yang, S.; Wenzhe, C.; Shengshu, W.; Shanshan, Y.; Jianwei, W.; Fuyin, K.; Penggang, T.; Jing, L.; et al. Extended SIR Prediction of the Epidemics Trend of COVID-19 in Italy and Compared with Hunan, China. *Front. Med.* **2020**, *7*, 1–7. [[CrossRef](#)]
29. Fudolig, M.; Howard, R. The local stability of a modified multi-strain SIR model for emerging viral strains. *PLoS ONE* **2020**, *15*, e0243408. [[CrossRef](#)]
30. Rockett, R.J.; Arnott, A.; Lam, C.; Sadsad, R.; Timms, V.; Gray, K.-A.; Eden, J.-S.; Chang, S.; Gall, M.; Draper, J.; et al. Revealing COVID-19 transmission in Australia by SARS-CoV-2 genome sequencing and agent-based modeling. *Nat. Med.* **2020**, *26*, 1398–1404. [[CrossRef](#)]

31. Chang, S.L.; Harding, N.; Zachreson, C.; Cliff, O.M.; Prokopenko, M. Modelling transmission and control of the COVID-19 pandemic in Australia. *Nat. Commun.* **2020**, *11*, 5710. [CrossRef]
32. Kerr, C.C.; Stuart, R.M.; Mistry, D.; Abeysuriya, R.G.; Rosenfeld, K.; Hart, G.R.; Núñez, R.C.; Cohen, J.A.; Selvaraj, P.; Hagedorn, B.; et al. Covasim: An agent-based model of COVID-19 dynamics and interventions. *PLoS Comput. Biol.* **2021**, *17*, e1009149. [CrossRef]
33. Bernardes, A.T.; Ribeiro, L.C. Information, opinion and pandemic. *Phys. A Stat. Mech. Its Appl.* **2021**, *565*, 125586. [CrossRef]
34. Sah, P.; Fitzpatrick, M.C.; Zimmer, C.F.; Abdollahi, E.; Juden-Kelly, L.; Moghadas, S.M.; Singer, B.H.; Galvani, A.P. Asymptomatic SARS-CoV-2 infection: A systematic review and meta-analysis. *Proc. Natl. Acad. Sci. USA* **2021**, *118*, e2109229118. [CrossRef] [PubMed]
35. He, J.; Guo, Y.; Mao, R.; Zhang, J. Proportion of asymptomatic coronavirus disease 2019: A systematic review and meta-analysis. *J. Med. Virol.* **2021**, *93*, 820–830. [CrossRef] [PubMed]
36. Ma, Q.; Liu, J.; Liu, Q.; Kang, L.; Liu, R.; Jing, W.; Wu, Y.; Liu, M. Global Percentage of Asymptomatic SARS-CoV-2 Infections Among the Tested Population and Individuals with Confirmed COVID-19 Diagnosis: A Systematic Review and Meta-analysis. *JAMA Netw. Open* **2021**, *4*, e2137257. [CrossRef]
37. Coutinho, R.M.; Marquitti, F.M.D.; Ferreira, L.S.; Borges, M.E.; da Silva, R.L.P.; Canton, O.; Portella, T.P.; Poloni, S.; Franco, C.; Plucinski, M.M.; et al. Model-based estimation of transmissibility and reinfection of SARS-CoV-2 P.1 variant. *Commun. Med.* **2021**, *1*, 48. [CrossRef]
38. Ioannidis, J.P.A. Infection fatality rate of COVID-19 inferred from seroprevalence data. *Bull. World Health Organ.* **2021**, *99*, 19F–33F. [CrossRef] [PubMed]
39. Johansson, M.A.; Quandelacy, T.M.; Kada, S.; Prasad, P.V.; Steele, M.; Brooks, J.T.; Slayton, R.B.; Biggerstaff, M.; Butler, J.C. SARS-CoV-2 Transmission from People Without COVID-19 Symptoms. *JAMA Netw. Open* **2021**, *4*, e2035057. [CrossRef]
40. Shah, A.S.V.; Gribben, C.; Bishop, J.; Hanlon, P.; Caldwell, D.; Wood, R.; Reid, M.; McMenamin, J.; Goldberg, D.; Stockton, D.; et al. Effect of Vaccination on Transmission of SARS-CoV-2. *N. Engl. J. Med.* **2021**, *385*, 1718–1720. [CrossRef]
41. Instituto Brasileiro de Geografia e Estatística. Available online: <https://www.ibge.gov.br/> (accessed on 20 November 2021).
42. Mathieu, E.; Ritchie, H.; Ortiz-Ospina, E.; Roser, M.; Hasell, J.; Appel, C.; Giattino, C. A global database of COVID-19 vaccinations. *Nat. Hum. Behav.* **2021**, *5*, 1–7. [CrossRef]
43. May, R.M.; Anderson, R.M. Epidemiology and genetics in the coevolution of parasites and hosts. *Proc. R. Soc. Lond. Ser. B* **1983**, *219*, 281–313. [CrossRef]
44. Berngruber, T.W.; Froissart, R.; Choisy, M.; Gandon, S. Evolution of Virulence in Emerging Epidemics. *PLoS Pathog.* **2013**, *9*, e1003209. [CrossRef]
45. Causey, K.; Fullman, N.; Sorensen, R.J.; Galles, N.C.; Zheng, P.; Aravkin, A.; Danovaro-Holliday, M.C.; Martinez-Piedra, R.; Sodha, S.V.; Velandia-González, M.P.; et al. Estimating global and regional disruptions to routine childhood vaccine coverage during the COVID-19 pandemic in 2020: A modelling study. *Lancet* **2021**, *398*, 522–534. [CrossRef]
46. Tang, L.; Zhou, Y.; Wang, L.; Purkayastha, S.; Zhang, L.; He, J.; Wang, F.; Song, P.X.K. A review of multi-compartment infectious disease models. *Int. Stat. Rev.* **2020**, *88*, 462–513. [CrossRef] [PubMed]
47. Moore, S.; Hill, E.M.; Tildesley, M.J.; Dyson, L.; Keeling, M.J. Vaccination and non-pharmaceutical interventions for COVID-19: A mathematical modelling study. *Lancet Infect. Dis.* **2021**, *21*, 793–802. [CrossRef]
48. Foy, B.H.; Wahl, B.; Mehta, K.; Shet, A.; Menon, G.I.; Britto, C. Comparing COVID-19 vaccine allocation strategies in India: A mathematical modelling study. *Int. J. Infect. Dis.* **2021**, *103*, 431–438. [CrossRef]
49. Gharakhanlou, N.M.; Hooshangi, N. Spatio-temporal simulation of the novel coronavirus (COVID-19) outbreak using the agent-based modeling approach (case study: Urmia, Iran). *Inform. Med. Unlocked* **2020**, *20*, 100403. [CrossRef] [PubMed]
50. Ritchie, H.; Mathieu, E.; Rodés-Guirao, L.; Appel, C.; Giattino, C.; Ortiz-Ospina, E.; Hasell, J.; Macdonald, B.; Beltekian, D.; Roser, M. Coronavirus Pandemic (COVID-19). Available online: <https://ourworldindata.org/coronavirus> (accessed on 10 January 2022).
51. Bernardeau-Serra, L.; Nguyen-Huynh, A.; Sponagel, L.; Sernizon Guimarães, N.; Teixeira de Aguiar, R.A.; Soriano Marcolino, M. The COVID-19 Vaccination Strategy in Brazil—A Case Study. *Epidemiologia* **2021**, *2*, 338–359. [CrossRef]
52. Cohn, A.C.; Mahon, B.E.; Walensky, R.P. One Year of COVID-19 Vaccines: A Shot of Hope, a Dose of Reality. *JAMA Netw.* **2022**, *327*, 119–120. [CrossRef]
53. Garrett, R.; Young, S.D. Online misinformation and vaccine hesitancy. *Transl. Behav. Med.* **2021**, *11*, 2194–2199. [CrossRef]
54. Shih, S.F.; Wagner, A.L.; Masters, N.B.; Prosser, L.A.; Lu, Y.; Zikmund-Fisher, B.J. Vaccine Hesitancy and Rejection of a Vaccine for the Novel Coronavirus in the United States. *Front. Immunol.* **2021**, *12*, 558270. [CrossRef]
55. Beleche, T.; Ruhter, J.; Kolbe, A.; Marus, J.; Bush, L.; Sommers, B. *COVID-19 Vaccine Hesitancy: Demographic Factors, Geographic Patterns, and Changes over Time*; Office of the Assistant Secretary for Planning and Evaluation: Washington, DC, USA, 2021.
56. UN News. Available online: <https://news.un.org/en/story/2021/09/1100192> (accessed on 31 January 2022).
57. Troiano, G.; Nardi, A. Vaccine hesitancy in the era of COVID-19. *Public Health* **2021**, *194*, 245–251. [CrossRef]
58. Omer, S.B.; Benjamin, R.M.; Brewer, N.T.; Buttenheim, A.M.; Callaghan, T.; Caplan, A.; Carpiano, R.M.; Clinton, C.; DiResta, R.; Elharake, J.A.; et al. Promoting COVID-19 vaccine acceptance: Recommendations from the Lancet Commission on Vaccine Refusal, Acceptance, and Demand in the USA. *Lancet* **2021**, *398*, 2186–2192. [CrossRef]
59. Bar-On, Y.M.; Goldberg, Y.; Mandel, M.; Bodenheimer, O.; Freedman, L.; Kalkstein, N.; Mizrahi, B.; Alroy-Preis, S.; Ash, N.; Milo, R.; et al. Protection of BNT162b2 vaccine booster against Covid-19 in Israel. *N. Engl. J. Med.* **2021**, *385*, 1393–1400. [CrossRef]

60. Da Fonseca, E.M.; Shadlen, K.C.; Bastos, F.I. The politics of COVID-19 vaccination in middle-income countries: Lessons from Brazil. *Soc. Sci. Med.* **2021**, *281*, 114093. [[CrossRef](#)]
61. Kupek, E. Low COVID-19 vaccination coverage and high COVID-19 mortality rates in Brazilian elderly. *Rev. Bras. Epidemiol.* **2021**, *24*, e210041. [[CrossRef](#)] [[PubMed](#)]
62. Chandan, J.S.; Taylor, J.; Bradbury-Jones, C.; Nirantharakumar, K.; Kane, E.; Bandyopadhyay, S. COVID-19: A public health approach to manage domestic violence is needed. *Lancet Public Health* **2020**, *5*, e309. [[CrossRef](#)]
63. Dunn, C.G.; Kenney, E.; Fleischhacker, S.E.; Bleich, S.N. Feeding low-income children during the Covid-19 pandemic. *N. Engl. J. Med.* **2020**, *382*, e40. [[CrossRef](#)]
64. Brewer, M.; Gardiner, L. The initial impact of COVID-19 and policy responses on household incomes. *Oxf. Rev. Econ. Policy* **2020**, *36*, S187–S199. [[CrossRef](#)]
65. Lopez Bernal, J.; Andrews, N.; Gower, C.; Gallagher, E.; Simmons, R.; Thelwall, S.; Stowe, J.; Tessier, E.; Groves, N.; Dabrera, G.; et al. Effectiveness of Covid-19 vaccines against the B.1.617.2 (Delta) variant. *N. Engl. J. Med.* **2021**, *385*, 585–594. [[CrossRef](#)]
66. Katz, I.T.; Weintraub, R.; Bekker, L.G.; Brandt, A.M. From Vaccine Nationalism to Vaccine Equity—Finding a Path Forward. *N. Engl. J. Med.* **2021**, *384*, 1281–1283. [[CrossRef](#)]
67. Gómez, C.E.; Perdiguero, B.; Esteban, M. Emerging SARS-CoV-2 variants and impact in global vaccination programs against SARS-CoV-2/COVID-19. *Vaccines* **2021**, *9*, 243. [[CrossRef](#)]
68. McIntyre, P.B.; Aggarwal, R.; Jani, I.; Jawad, J.; Kochhar, S.; MacDonald, N.; Madhi, S.A.; Mohsni, E.; Mulholland, K.; Neuzil, K.N.; et al. COVID-19 vaccine strategies must focus on severe disease and global equity. *Lancet* **2022**, *399*, 406. [[CrossRef](#)]
69. Crimmins, E.M. Age-related vulnerability to coronavirus disease 2019 (COVID-19): Biological, contextual, and policy-related factors. *Policy Aging Rep.* **2020**, *30*, 142–146. [[CrossRef](#)] [[PubMed](#)]
70. Matrajt, L.; Eaton, J.; Leung, T.; Brown, E.R. Vaccine optimization for COVID-19: Who to vaccinate first? *Sci. Adv.* **2021**, *7*, eabf1374. [[CrossRef](#)]
71. Sewell, H.F.; Agius, R.M.; Kendrick, D.; Stewart, M. Covid-19 vaccines: Delivering protective immunity. *BMJ* **2020**, *371*, m4838. [[CrossRef](#)] [[PubMed](#)]
72. Jarjour, N.N.; Masopust, D.; Jameson, S.C. T cell memory: Understanding COVID-19. *Immunity* **2021**, *54*, 14–18. [[CrossRef](#)] [[PubMed](#)]
73. Thompson, M.G.; Stenehjem, E.; Grannis, S.; Ball, S.W.; Naleway, A.L.; Ong, T.C.; DeSilva, M.B.; Natarajan, K.; Bozio, C.H.; Lewis, N.; et al. Effectiveness of Covid-19 vaccines in ambulatory and inpatient care settings. *N. Engl. J. Med.* **2021**, *385*, 1355–1371. [[CrossRef](#)]
74. Sadarangani, M.; Raya, B.A.; Conway, J.M.; Iyaniwura, S.A.; Falcao, R.C.; Colijn, C.; Coombs, D.; Gantt, S. Importance of COVID-19 vaccine efficacy in older age groups. *Vaccine* **2021**, *39*, 2020–2023. [[CrossRef](#)]
75. Loembé, M.M.; Nkengasong, J.N. COVID-19 vaccine access in Africa: Global distribution, vaccine platforms, and challenges ahead. *Immunity* **2021**, *54*, 1353–1362. [[CrossRef](#)]
76. Dolgin, E. Omicron thwarts some of the world’s most-used COVID vaccines. *Nature* **2022**, *601*, 311. [[CrossRef](#)]
77. Carreño, J.M.; Alshammery, H.; Tcheou, J.; Singh, G.; Raskin, A.; Kawabata, H.; Sominsky, L.; Clark, J.; Adelsberg, D.C.; Bielak, D.; et al. Activity of convalescent and vaccine serum against SARS-CoV-2 Omicron. *Nature* **2021**, 1–8. [[CrossRef](#)]
78. Anderson, R.M.; May, R.M. Population biology of infectious diseases: Part I. *Nature* **1979**, *280*, 361–367. [[CrossRef](#)] [[PubMed](#)]
79. Ingraham, N.E.; Ingbar, D.H. The omicron variant of SARS-CoV-2: Understanding the known and living with unknowns. *Clin. Transl. Med.* **2021**, *11*, e685. [[CrossRef](#)] [[PubMed](#)]

## 5 CONCLUSION

Recent studies on ecology of zoonotic diseases suggest that simplified and polluted human ecosystems favour few vertebrate species, which are the most likely to transmit new diseases to us. Such conditions prevail in modern cities, but obviously are more harmful to communities experiencing poverty, a condition known as environmental racism. The recent anthropological and ecological findings about Holocene South American, early and late, are in support of a long existence of such contaminated, nutrient-rich environments around human settlements in this continent. From late Holocene on (from 6,000 BP in the southeast coast or 4,000 to 3,000 BP in Marajo Island and Pantanal), the construction of immense mound structures by the Guarani Mbya nations, using debris of all sort, but mainly food wastes, carcasses and burial structures, are clear evidences of much older presence of largely human modified landscapes in the continent.

At any point in history when humans settled, they would start to accumulate waste of all sort, and that is the start of an environmental decaying that actually defines us as a species. Although there are little data about how humans dealt with wastes while living in caves by early Holocene, whatever advantage conditions that a cave life produced (safety from preys, enemies, recognized territory, food predictability in a climatically unstable period), to stand in a same place, to deal with wastes and even their dead ones, might produce ecological scenarios which favour a few, opportunistic, well adapted species to dwell among us. Namely, human modified mounds from the late Holocene, or recorded occupied caves from early Holocene, overlap with present day's geographic distribution of *L. longipalpis*. This neat overlap suggest this is a species which was capable of adapting to conditions we created, jumping from being strictly associated with foxes to survive around humans. There are quite evidence that foxes were from a long time domesticated, tamed or at least tolerated around human settlements in various places in South America. Hence, as the two fox species which are *L. infantum* reservoirs also overlap their territory with those of Holocene humans, the hypothesis that fox-human-*L. longipalpis* association might have existed for a quite long time before European arrival, has to be taken into consideration. No matter how speculative it is at this stage. A similar human-adapted hematophagous insect species, evolved around human settlements by the same period in the Old World is *Aedes aegypti*. These both species are cause of infectious diseases outbreaks of concern, mostly affecting people under poverty worldwide.

This thesis dealt with the human ecosystems and how it favours the evolution of some types of parasites and pathogens. We tend to deteriorate our environments, although technology



has reverted the worst consequences of this fact, creating “hygienic shrines” in many different civilizations. Shrines for few. Still, such shrines based on quality inhabitations, education, and access to recent health science progress, gave us the arrogant idea that we could eradicate infectious diseases.

Indeed, the Technologies that could have produced safer and healthier sedentary communities at the present is ecologically jeopardized. The highly complex worldwide travelling network, global warming, widespread of heavy metal contamination, deforestation, the broadly presence of poverty and lack of access to medicine and environmental services for most of the humanity, have prevented real progress in human health at a populational scale. Many of us, in the parasitological, epidemiological, and ecological aspects of an individual existence, are still inside caves, furthermore, both at the biological and the platonic point of view. In a positive way to face such reality, we must believe we can provide scientific progress for all, this time, for a change.